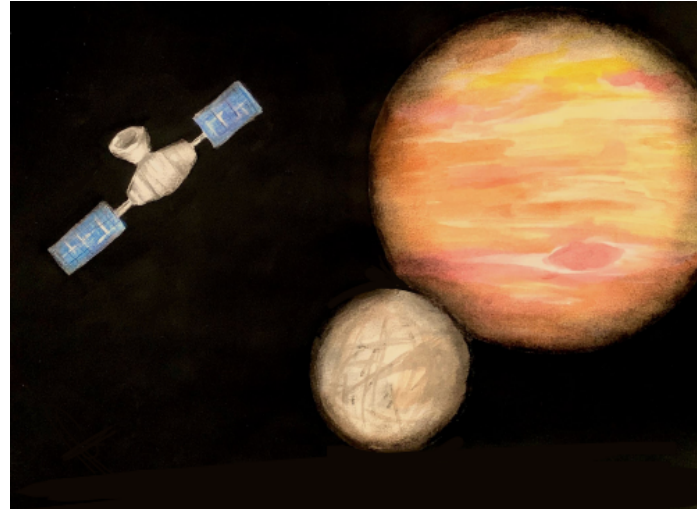


# **Europa Composition and Habitat Observation (ECHO) Lander**

## **Final Design Report**



**MANE 4250 – Space Vehicle Design**  
**Section 1**  
**Design Team 1**

Prepared by:

Joseph Bowers, Katie August, Constantine Childs, Chloe Powell,  
Andrew Olson, Aaryan Sonawane, Mae Tringone

# **1 Executive Summary**

**Prepared by: Constantine Childs**

This final design report outlines the preliminary technical analysis and design considerations for the Europa Composition and Habitat Observation (ECHO) lander. ECHO is part of a large strategic mission by NASA to send a robotic orbiter and lander to the Jupiter system, targeting a landing on Europa by 2037. Scientific experiments will be carried out on the surface for six months. Instruments will study Europa's water-ice surface and the liquid ocean beneath. Europa was chosen as the destination due to its potential to sustain life. Mission objectives and design parameters for key lander project elements were discussed. The key lander project elements were structures, mechanisms and deployables, propulsion, orbital mechanics, attitude determination and control (ADCS), thermal management, power, command and data, and telecommunications. Design trade studies were performed for subsystem component selection.

The ECHO lander module will be composed of an aluminum frame and titanium skin in a hexagonal shape designed to withstand a quasi-static loading of 6 Gs and acoustic loading encountered during launch. Finite element analysis was conducted to analyze the structural integrity under these loads. The lander will use three lander legs and a sample collection suite on Europa, which includes a drill and high-resolution camera. The propulsion system for ECHO is a monomethylhydrazine and nitric oxide bipropellant system. Propellant tanks were sized and selected. Orbital mechanics results indicated a required delta-V of 6.4 km/s after the lander separated from the orbiter in Jupiter orbit. An aerobraking maneuver was also considered for further trajectory optimization. ADCS will use a combination of star trackers, a sun sensor, magnetometer, and an inertial measurement unit for attitude determination. Attitude control is achieved with reaction wheels, magnetic torquers, and monopropellant thrusters using monomethylhydrazine. Thermal management will use a hybrid system including multi-layer insulation, paint, radioisotope heater units, heat pipes, a radiator, and electric heaters. An initial thermal analysis on the lander structure was also conducted. Power for the lander is supplied by a multi-mission radioisotope thermoelectric generator, as well as a lithium-ion battery pack. An onboard command and data system will handle all data processing and storage, supported by the core Flight system software. For lander communications, the X-band will be used for engineering data, and the Ka band will be used for scientific data. A patch antenna will relay signals between the lander and orbiter, which will then transmit the data back to earth.

# Contents

1 Executive Summary.....	2
2 List of Figures.....	6
3 List of Tables.....	7
4 Terms and Definitions.....	8
4.1 Acronyms.....	8
4.2 Decision Matrix Standard.....	9
5 Introduction.....	10
6 Project Scope.....	11
6.1 Mission Objectives.....	11
6.2 Mission Constraints.....	11
6.3 Mission Assumptions.....	12
6.4 Non-Technical Considerations.....	13
6.4.1 Ethical Considerations.....	13
6.4.2 Public Health and Safety.....	13
6.4.3 Cultural Considerations.....	13
6.4.4 Social Considerations.....	13
6.4.5 Environmental Considerations.....	14
6.4.6 Economic Considerations.....	14
6.4.7 Political Considerations.....	14
7 Mission Architecture.....	14
7.1 Launch Vehicle.....	14
7.2 Subsystem Overview.....	15
7.3 Scientific Instrumentation and Sensor Suite.....	16
8 Design Approach.....	18
8.1 Structures.....	18
8.1.1 Definition.....	18
8.1.2 Objectives.....	18
8.1.3 Requirements and Constraints.....	18
8.1.4 Analysis.....	18
8.1.5 Non-Technical Considerations.....	27
8.1.6 Risk Management.....	28
8.1.7 Future Work.....	29
8.2 Mechanisms and Deployables.....	29
8.2.1 Definition.....	29
8.2.2 Objectives.....	30
8.2.3 Requirements and Constraints.....	30
8.2.4 Analysis.....	30

8.2.5 Non-Technical Considerations.....	36
8.2.6 Risk Management.....	36
8.2.7 Future Work.....	38
8.3 Propulsion.....	38
8.3.1 Definition.....	38
8.3.2 Objectives.....	38
8.3.3 Requirements and Constraints.....	38
8.3.4 Analysis.....	39
8.3.5 Non-Technical Considerations.....	47
8.3.5 Risk Management.....	48
8.3.6 Future Work.....	50
8.4 Orbital Mechanics.....	50
8.4.1 Definition.....	50
8.4.2 Objectives.....	51
8.4.3 Requirements and Constraints.....	51
8.4.4 Analysis.....	51
8.4.5 Non-Technical Considerations.....	58
8.4.6 Risk Management.....	59
8.4.7 Future Work.....	62
8.5 Attitude Determination & Control Subsystem (ADCS).....	64
8.5.1 Definition.....	64
8.5.2 Objectives.....	64
8.5.3 Requirements and Constraints.....	64
8.5.4 Analysis.....	65
8.5.5 Non Technical Considerations.....	76
8.5.6 Risk Management.....	76
8.5.7 Future Work.....	77
8.6 Thermal Management.....	78
8.6.1 Definition.....	78
8.6.2 Objectives.....	78
8.6.3 Requirements and Constraints.....	78
8.6.4 Analysis.....	79
8.6.5 Non-Technical Considerations.....	87
8.6.6 Risk Management.....	88
8.6.7 Future Work.....	88
8.7 Power.....	89
8.7.1 Definition.....	89
8.7.2 Objectives.....	89

8.7.3 Requirements and Constraints.....	89
8.7.4 Analysis.....	89
8.7.5 Non-Technical Considerations.....	92
8.7.6 Risk Management.....	93
8.7.7 Future Work.....	93
8.8 Command and Data.....	93
8.8.1 Definition.....	93
8.8.2 Objectives.....	94
8.8.3 Requirements & Constraints.....	94
8.8.4 Analysis.....	94
8.8.5 Non-Technical Considerations.....	97
8.8.6 Risk Management.....	99
8.8.7 Future Work.....	99
8.9 Telecommunication.....	100
8.9.1 Definition.....	100
8.9.2 Objectives.....	100
8.9.3 Requirements & Constraints.....	100
8.9.4 Analysis.....	101
8.9.5 Non-Technical Considerations.....	104
8.9.6 Risk Management.....	105
8.9.7 Future Work.....	105
9 Design Budgets.....	106
9.1 Mass Budget.....	106
9.2 Volume Budget.....	106
9.3 Cost Budget.....	107
10 Sales Pitch.....	108
11 Conclusions.....	108
12 References.....	109
13 Appendix.....	116
13.1: Definition and Assessment of Risk.....	116
13.2: Summary of Non-Technical Considerations.....	116
13.3: Aerobraking Maneuver MATLAB Script.....	117
13.4: Final Optimal Apojoove MATLAB Script.....	127
13.5 Worst-case Temperature Script.....	144
13.6 Landing Leg Transfer Function Generation MATLAB Script.....	145
13.7: Gantt Chart.....	146
13.8: Statement of Work.....	147
13.9: Preliminary Design Review.....	150

## **2 List of Figures**

- Figure 7.1.1: Launch of Europa Clipper on a Falcon Heavy
- Figure 7.3.1: Diagram of the Philae Lander's Scientific Instruments
- Figure 8.1.1: Top and Bottom Panel Structure
- Figure 8.1.2: Side Panel Structure
- Figure 8.1.3: Final Structure
- Figure 8.1.4: Analysis Structure
- Figure 8.1.5: Ball Joint
- Figure 8.1.6: Landing Leg
- Figure 8.1.7: Landing Plate/Ball Joint
- Figure 8.1.8: 6g Quasi Static Result
- Figure 8.1.9: Landing Leg Analysis Results
- Figure 8.1.10: Acoustic Propagation
- Figure 8.1.11: Mode Shape/Stress at 79.48 Hz
- Figure 8.1.12: Mode Shape/Stress at 84.52 Hz
- Figure 8.1.13: Mode Shape/Stress at 77.38 Hz
- Figure 8.1.14: Mode Shape/Stress at 107.54Hz
- Figure 8.2.1: Free-Body Diagram of landing cleats and lander body
- Figure 8.2.2: Typical Non-Pneumatic Linear Actuator
- Figure 8.2.3: Mockup of an SD2-Inspired Sample Drill
- Figure 8.2.4: Moog Type 22 Antenna Pointing Assembly
- Figure 8.3.1: MONARC-1 ADCS Thruster
- Figure 8.3.2: ADCS Thruster layout
- Figure 8.3.3: OST 25/0 Propellant Tank
- Figure 8.3.4: OST 25/3 Propellant Tank
- Figure 8.3.5: OST 31-0 Propellant Tank
- Figure 8.4.1: Orbital mechanics architecture used in PDR calculations
- Figure 8.4.2: Aerobrake Procedure Architecture
- Figure 8.4.3: Aerobrake Trajectory
- Figure 8.4.4:  $\Delta V$  for Transfer Ellipse as a Function of Final Aerobrake Apojove Radius
- Figure 8.4.5: Total  $\Delta V$  vs. Initial Apojove Radius for Hohmann Transfer Architecture
- Figure 8.5.1: Tier list of sensors
- Figure 8.5.2: RedWire Space Pyramid Sun Sensor Assembly
- Figure 8.5.3: Reaction Wheel Pyramid Configuration
- Figure 8.5.4: Framework of ADCS Control law
- Figure 8.5.5: Attitude States of the ECHO Spacecraft
- Figure 8.5.6: System Performance of the ECHO Spacecraft
- Figure 8.5.7: Actuator Performance of the ECHO Spacecraft
- Figure 8.5.8: System Performance of the ECHO Spacecraft
- Figure 8.6.1: Diagram of a variable conductance heat pipe

- Figure 8.6.2: Variable radioisotope heating unit concept**  
**Figure 8.6.3: VRHU diagram used on the Cassini spacecraft**  
**Figure 8.6.4: Temperature distribution simulation result on the lander structure**  
**Figure 8.6.5: Heat flux (in W/mm<sup>2</sup>) on the RTG to the lander's lower body panel**  
**Figure 8.6.6: Galileo entry probe heat shield**  
**Figure 8.8.1: OBC FERMI**  
**Figure 8.8.2: Sample HELIOS Media Tested on the International Space Station**  
**Figure 8.9.1: IQ Spacecom X-Band Antenna**  
**Figure 8.9.2: Printech Ka-Band Antenna**

### **3 List of Tables**

- Table 7.2.1: Mission Objectives and Associated Subsystem(s)**  
**Table 7.3.1: Overview of ECHO's Functional Requirements and Associated Subsystems**  
**Table 8.1.1: Component Specifications**  
**Table 8.1.2: Impact Absorption Decision Matrix**  
**Table 8.1.3: Mesh Element Details**  
**Table 8.1.4: Mesh Element Details for Landing Legs**  
**Table 8.1.5: Structure Non-Technical Considerations**  
**Table 8.1.6: Structure Risk Mitigation Table**  
**Table 8.2.1: Mechanisms and Deployables Non-Technical Considerations**  
**Table 8.2.2: Mechanisms and Deployables Risk Assessment Table**  
**Table 8.3.1: Primary Thruster Selection Matrix**  
**Table 8.3.2: ADCS Thruster Selection Matrix**  
**Table 8.3.3: Propellant Requirements**  
**Table 8.3.4: Lander TWR Analysis**  
**Table 8.3.5: MMH Tank Selection Matrix**  
**Table 8.3.6: MON-3 Tank Selection Matrix**  
**Table 8.3.7: Propulsion Subsystem BOM**  
**Table 8.3.8: Propulsion Non-Technical Considerations**  
**Table 8.3.9: Propulsion Risk Management**  
**Table 8.4.1: ΔV Totals for Aerobraking Maneuver**  
**Table 8.4.2: Non-Technical Considerations for the Orbital Mechanics Subsystem**  
**Table 8.4.3: Orbital Mechanics Risk Mitigation**  
**Table 8.5.1: Star Tracker Model Decision Matrix**  
**Table 8.5.2: Magnetometer Model Decision Matrix**  
**Table 8.5.3: Sun Sensor Model Decision Matrix**  
**Table 8.5.4: IMU Model Decision Matrix**  
**Table 8.5.5: Reaction Wheels Model Decision Matrix**  
**Table 8.5.6: ADCS Total Mass Utilized**  
**Table 8.5.7: ADCS Non-Technical Considerations**  
**Table 8.5.8: ADCS Risk Assessment and Mitigation**  
**Table 8.6.1: List of Temperature Ranges for Specific Lander Components**

- Table 8.6.2: Decision Matrix for Outer MLI Material**
- Table 8.6.3: Decision Matrix for Inner MLI Material**
- Table 8.6.4: Decision Matrix for Interior Coating**
- Table 8.6.5: Summary of Non-Technical Considerations for the Thermal Control System**
- Table 8.6.6: Risk and Mitigation Table for the Thermal Control System**
- Table 8.7.1: Battery Chemistry Decision Matrix**
- Table 8.7.2: Power Scheduling**
- Table 8.7.3: Power Non-Technical Considerations**
- Table 8.7.4: Power Risk Assessment Table**
- Table 8.8.1: On-Board Computing System Decision Matrix**
- Table 8.8.2: Data Storage Unit Decision Matrix**
- Table 8.8.3: Flight Software Decision Matrix**
- Table 8.8.4: Non-Technical Considerations for Command & Data**
- Table 8.8.5: Risk Assessment Table for Command & Data**
- Table 8.9.1: X-Band Antenna Decision Matrix**
- Table 8.9.2: Ka-Band Antenna Decision Matrix**
- Table 8.9.3: Non-Technical Considerations for Telecommunication**
- Table 8.9.4: Risk Assessment Table for Telecommunication**
- Table 9.1.1: Mass Budget by Subsystem**
- Table 9.2.1: Volume Budget by Subsystem**
- Table 9.3.1: Cost Budget**
- Table 13.2.1: Relevance of Non-Technical Factors**

## 4 Terms and Definitions

### 4.1 Acronyms

- ADCS – Attitude Determination and Control System
- APXS – Alpha Particle X-ray Spectrometer
- CAD – Computer Aided Design
- CIVA – Comet Nucleus Infrared and Visible Analyzer
- CONSERT – Comet Nucleus Sounding Experiment by Radio wave Transmission
- COPUOS – Committee on the Peaceful Uses of Outer Space
- COSAC – Cometary Sampling and Composition
- COTS – Commercial Off-The-Shelf
- DSN – Deep Space Network
- ECHO – Europa Habitat and Composition Observation
- FCC – Federal Communications Commission
- FDR – Final Design Review
- FEA – Finite Element Analysis
- HDRM - Hold Down Release Mechanism
- HELIOS – Hardened Extremely Long Life Information Optical Storage
- IMU – Initial Measurement Unit

ISP – Specific Impulse  
JPL - Jet Propulsion Laboratory  
LEO – Low Earth Orbit  
MLI – Multi-Layer Insulation  
OMB – Office of Management and Budget  
OSHA – Occupational Safety & Health Administration  
PDR – Preliminary Design Review  
RCS – Reaction Control System  
RHA – Radiation Hardness Assurance  
RHU – Radioisotope Heating Unit  
ROLIS – Rosetta Lander Imaging System  
ROMAP – Rosetta Lander Magnetometer and Plasma Monitor  
MATLAB - Matrix Laboratory  
MMRTG – Radioisotope Thermoelectric Generator  
SD2 – Sampling Drilling & Distribution System  
SOI – Sphere of Influence  
SSD – Solid State Drive  
TCS – Thermal Control System  
TLC – Triple-Level Cell  
TRL – Technology Readiness Level  
TWR – Thrust to Weight Ratio  
UNOOSA – United Nations Office of Outer Space Affairs  
IADC - Inter-Agency Space Debris Coordination Committee  
 $\Delta V$  - Delta - V (Change in Velocity)  
MLC – Multi-Level Cell  
MMH - Monomethylhydrazine  
MON-3 - Mixed Oxides of Nitrogen with 3 % Nitric oxide  
BOM - Bill of Materials  
SLS - Space Launch System

## 4.2 Decision Matrix Standard

**Prepared by:** Andrew Olson

In the following report, each decision matrix employs the same weighting and scoring approach. Design criteria were established based on customer requirements, with weights assigned to reflect their importance, totaling 10. Higher weights were given to more critical criteria. Each design method was then scored on a scale of 1 to 5 for each criterion, with 5 representing the best performance. These scores were multiplied by their respective weights, and the weighted totals were summed to identify the most suitable design method to pursue.

## 5 Introduction

**Prepared by:** Andrew Olson

Europa is the fourth largest of Jupiter's moons and is one of the most promising candidates for hosting extraterrestrial life in our solar system. Estimated to be 4.5 billion years old, there has been adequate time for life to develop [1]. Additionally, scientists believe Europa possesses the key elements necessary for life, including liquid water, and derives sufficient energy from Jupiter's radiation to support biological processes [2].

While the surface temperature does not rise above minus 260 °F, scientists believe Europa contains twice as much liquid water as earth's oceans [1][2]. In 2013, the Hubble Space Telescope detected water vapor plumes emanating from surface geysers on Europa [1]. Additionally, high resolution images from NASA's Galileo spacecraft showed evidence of "mobile icebergs" on the icy moon [3]. These observations led scientists to believe that there is a liquid ocean underneath the surface – further bolstering the potential for Europa to host life and solidifying its status as a prime candidate for exploration.

While past orbiter missions, including NASA's Juno and Galileo, have provided valuable data, no lander has yet reached the moon's surface. Several missions are planned for the coming decade, such as NASA's recently launched Europa Clipper and ESA's Jupiter Icy Moons Explorer [1], but these will also remain in orbit. To achieve more in-depth analysis of Europa's surface composition and its habitability, a dedicated lander mission is needed.

Design Team 1 is tasked with designing a lander for NASA's Planetary Science Division, aimed at analyzing Europa's surface ice and subsurface water composition, as well as other parameters of its hypothesized subsurface ocean, such as depth. Scheduled to launch in April 2031 aboard SpaceX's Falcon Heavy, ECHO provides a cost-effective and reliable solution for deploying a probe to Europa, designed to operate on the surface for six months. With a mass budget of 1,000 kg, the ECHO lander is designed to maximize mission efficiency and scientific return, while minimizing costs.

Design Team 1 previously completed the Preliminary Design Review (PDR), and this report serves as the team's Final Design Report (FDR) for the ECHO lander. The report will discuss the mission in detail, expanding on technical decisions made in the PDR by including at least one design iteration for each subsystem of the ECHO probe. Additionally, proper risk mitigation and non-technical factors are considered to ensure mission success and adherence to all industry standards.

# **6 Project Scope**

## **6.1 Mission Objectives**

**Prepared by:** Katie August

The ECHO probe has technical and scientific objectives required to complete the mission. The main goal is to understand the composition on Europa to assess its potential for sustaining life. Design Team 1 has developed seven total primary objectives to determine mission success. The technical objectives revolve around getting the ECHO probe to Europa safely while maintaining communication with Earth. These objectives include:

- Starting in a Jupiter orbit, the probe separates from the orbiter and inserts into a Europa parking orbit.
- Achieve a soft landing on the surface of Europa in a safe location.
- Deploy necessary communications and scientific equipment.
- Achieve two-way communication with the Europa Orbiter.
- Survive on the surface of Europa for six months.

The scientific objectives are about determining the composition and conditions on Europa. These objectives include:

- Produce and analyze a sample of Europa's surface ice by using a thermal drill and analysis sensors.
- Measure atmospheric conditions at the surface of Europa.

Secondary objectives are not required to have a successful mission, but they have the potential for further scientific research and knowledge if completed after the primary missions. The secondary objectives include:

- Collect images using a camera suite of Europa's Surface for transmission to Earth.
- Determine the level of geyser activity on Europa.
- Study atmospheric conditions on Jupiter.

## **6.2 Mission Constraints**

**Prepared by:** Katie August & Aaryan Sonawane

Each subsystem has specific design constraints based on the mission objects. These vary based on the timeline of the mission, design choices, and non-technical considerations. These are detailed throughout Section 8. There are mission constraints that apply to the ECHO probe as a whole. These include:

- All subsystems must be designed to operate in extreme temperature fluctuations of the Jovian environment. Temperatures can reach as low as -246 °C (27 K), this is discussed further in Section 8.6.
- There is limited power generation and power storage capacity, affecting the ability to consistently operate all onboard systems simultaneously. This requires an efficient power management strategy, further discussed in Section 8.7.
- The mass budget is constrained due to a majority being dedicated to the propulsions system for providing the power to achieve the necessary orbital maneuvers to safely land on Europa. Mass budget is further discussed in Section 9.1, propulsion specifications in Section 8.3 and orbital maneuvers in Section 8.4.
- The ECHO Probe has a constrained volume budget dictated by the physical dimensions and propulsion capabilities necessary for the mission, which must be adhered to during the design phase to ensure successful deployment and operational functionality. This is discussed further in Section 9.2.
- The ECHO Probe is subject to a constrained budget due to the finite value this mission provides for the customer (discussed further in section 9.3)

## 6.3 Mission Assumptions

**Prepared by: Katie August & Aaryan Sonawane**

Project ECHO is built on several assumptions to ensure feasibility alignment with mission objectives. These assumptions guide the system design and influences mission architecture decisions. The primary mission assumptions are:

- The anticipated mission launch date is April 2031, with approximately five and a half years travel time to Europa. This timeline allows for ample time to solidify subsystem design, subsystem integrations, assembly, and testing.
- It is assumed that the ECHO probe will successfully separate from the Europa orbiter to a stable orbit around Jupiter. A transfer and insertion into a Europa parking orbit shortly follows. The orbiter is expected to provide consistent and effective communication and navigational support during this phase. This is discussed further in Section 8.4.
- Europa's surface is not fully known, but assumed to consist of icy terrain with potential surface irregularities. The landing sequence is designed to account for the irregularities by relying on advanced attitude control and precision landing techniques, which is discussed further in Section 8.2.
- It is assumed that Europa's subsurface contains a liquid ocean beneath layers of icy crust. The goal is drilling and analyzing the surface and shallow subsurface ice. This goal guides the design of sampling instruments and thermal management systems required to operate in that environment. This is discussed further in Section 7.3.

- It is assumed that the ECHO probe will have sufficient power generation from its power source to operate for at least six months, which is discussed further in Section 8.7.
- Communication with the Europa orbiter will be intermittent, requiring robust data storage and transmission mechanisms to function during available communication windows. This is discussed further in Section 8.9.
- It is assumed that Europa's proximity to Jupiter exposes the probe to significant levels of radiation. The lander is equipped with radiation-hardened electronics and shielding to protect sensitive electronic components during the mission. This is discussed further in Section 8.1.
- The design adheres to the mass and cost budgets. The mass budget is 1000 kilograms for the lander and has an allocated budget of \$920,000,000. These constraints guide the selection of subsystems ensuring a balance between performance, reliability and cost effectiveness. This is discussed further in Section 9.
- The design thus far assumes that all design selections are compatible with the orbiter, of which little information is currently known.

## **6.4 Non-Technical Considerations**

### **6.4.1 Ethical Considerations**

**Prepared by:** Katie August

The designers have completed courses in ethics through accredited university Rensselaer Polytechnic Institute. Additionally, all subsystems are built using materials ethically sourced from manufacturers with strong ethical standards.

### **6.4.2 Public Health and Safety**

**Prepared by:** Katie August

The design choices are made to mitigate the risk to public health and safety regardless of mission outcomes. Project ECHO will implement safety measures to ensure the mission will not harm the public. See individual risk assessments throughout Section 8 and Appendix 13.1.

### **6.4.3 Cultural Considerations**

**Prepared by:** Katie August

There are no significant cultural considerations for the design and construction of project ECHO.

### **6.4.4 Social Considerations**

**Prepared by:** Katie August

There are no significant social considerations for the design and construction of project ECHO.

## **6.4.5 Environmental Considerations**

**Prepared by: Chloe Powell**

The ECHO Mission is expected to have minimal, if any, impact on Earth's environment, as the lander will not be conducting any experiments on or near Earth. The mission must adhere to the United Nations Office of Outer Space Affairs' Space Debris Mitigation Guidelines [4]. The guidelines most prevalent to the mission are Guideline 1: limit debris during normal operation, and Guideline 5: minimize potential for post-mission break-ups resulting from stored energy.

## **6.4.6 Economic Considerations**

**Prepared by: Chloe Powell**

The ECHO mission has a cost budget of \$920,000,000. This figure is based on the cost of comparable missions, specifically NASA's Galileo, Juno, and Europa Clipper. The parts required for each subsystem must remain at or under the specified budget throughout the duration of the design process and mission. Each subsystem will be responsible for maintaining a record of all financial transactions, as well as communicating this information to all other subsystems. Keeping detailed records across all subsystems will prevent the ECHO mission from going over its cost budget.

## **6.4.7 Political Considerations**

**Prepared by: Chloe Powell**

The Committee on the Peaceful Uses of Outer Space (COPUOS) has outlined five treaties and five principles that all spacecraft must adhere to [5]. These include, but are not limited to, the Outer Space Treaty, the Liability Convention, the Registration Convention, the Moon Agreement, the Declaration of Legal Principles, and the Benefits Declaration. These are the treaties and principles applicable to the ECHO mission. The lander must also adhere to all United States laws, policies, and regulations related to spaceflight, as stated in Title 51 of the United States Code [6].

# **7 Mission Architecture**

## **7.1 Launch Vehicle**

**Prepared by: Joseph Bowers**

The launch vehicle for this mission has been determined to be the Falcon Heavy. The Falcon Heavy presents numerous advantages to this mission, including its large payload capacity, second among currently operational rockets to the Space Launch System (SLS). Additionally, of currently operational heavy lift launch vehicles, the Falcon Heavy has the longest flight heritage.

The Falcon Heavy also is exceptionally low cost for a vehicle of its size, decreasing the cost for the overall mission.

Understanding the launch vehicle to be utilized is crucial to ensuring mission success. Every launch vehicle has a unique profile of vibration and acceleration forces which the structure of the payload is expected to endure. Additionally, the fairing size and payload capacity of the launch vehicle dictate the maximum volume and mass for the spacecraft. Due to these numerous factors which are specific to a particular vehicle, the design of ECHO has been based specifically for launch on a Falcon Heavy. This allows for maximum payload for the mission, minimizes risk due to flight heritage, and decreases costs for the mission.



**Figure 7.1.1: Launch of Europa Clipper on a Falcon Heavy [17]**

Utilizing the Falcon Heavy provides a final advantage. The Falcon Heavy was also utilized for the Europa Clipper mission. Due to the similarities between the Europa Clipper's mission profile and the profile of the orbiter which will carry ECHO, direct comparisons can be drawn from the mass, volume, and other design constraints on Europa Clipper, which can then be applied to ECHO.

## 7.2 Subsystem Overview

**Prepared by: Chloe Powell**

Each subsystem is responsible for upholding the objectives of the ECHO mission. Table 7.2.1 displays an overview of the mission objectives, as well as the subsystem or subsystems associated with each objective. These mission objectives are expanded on in Section 8: Design Approach.

**Table 7.2.1: Mission Objectives and Associated Subsystem(s)**

Mission Objective	Associated Subsystem(s)
Provide support and safety to all internal components of the lander through the use of a stable and strong structure that can withstand all forces from launch, travel, orbiting, and landing	Structures
Perform a series of precise maneuvers to release the ECHO lander from the orbiter and land on the surface of Europa while maintaining proper pointing accuracy	Orbital Mechanics, Propulsion, Attitude Determination & Control
Anchor to the surface of Europa upon landing and collect samples of the surface ice	Mechanisms & Deployables
Maintain all lander components within an acceptable temperature range, maximizing thermal energy retention	Thermal Management
Reliably provide and store power for all components of the lander and anticipate and provide power at the mission's peak expected load	Power
Store all data collected by the lander and transmit it to the orbiter; receive commands from the orbiter and perform those commands	Command & Data, Telecommunication

## 7.3 Scientific Instrumentation and Sensor Suite

**Prepared by: Mae and Aaryan**

The scientific instrument suite will contain all of the instruments necessary to investigate Europa's surface and subsurface environment. The instrument suite will take heavy inspiration from the Rosetta Mission, in particular the *Philae* lander, due to the flight heritage associated with the mission. To date it is the only space vehicle to successfully land on an icy body and take samples.

A PNI RM3100 Magnetometer will be used in lieu of Philae's ROMAP system. This is described further in Section 8.5.4.1

**Table 7.3.1: Overview of ECHO's Functional Requirements and Associated Subsystems**

Objective	Instruments Used	Relevant Philae Instruments
Sample Collection	Sample Drill	SD2 [105, pp. 2]
Analysis of the elemental and mineralogical composition of Europa	Ice-Penetrating Radar, Mass and Chemical Spectrometer, PNI RM3100 Magnetometer	CONCERT, COSAC, APXS, ROMAP [105, pp. 8-13, 15]
High resolution terrain imaging	High Resolution Camera, Spectral Imager	ROLIS, CIVA [105, pp. 6]

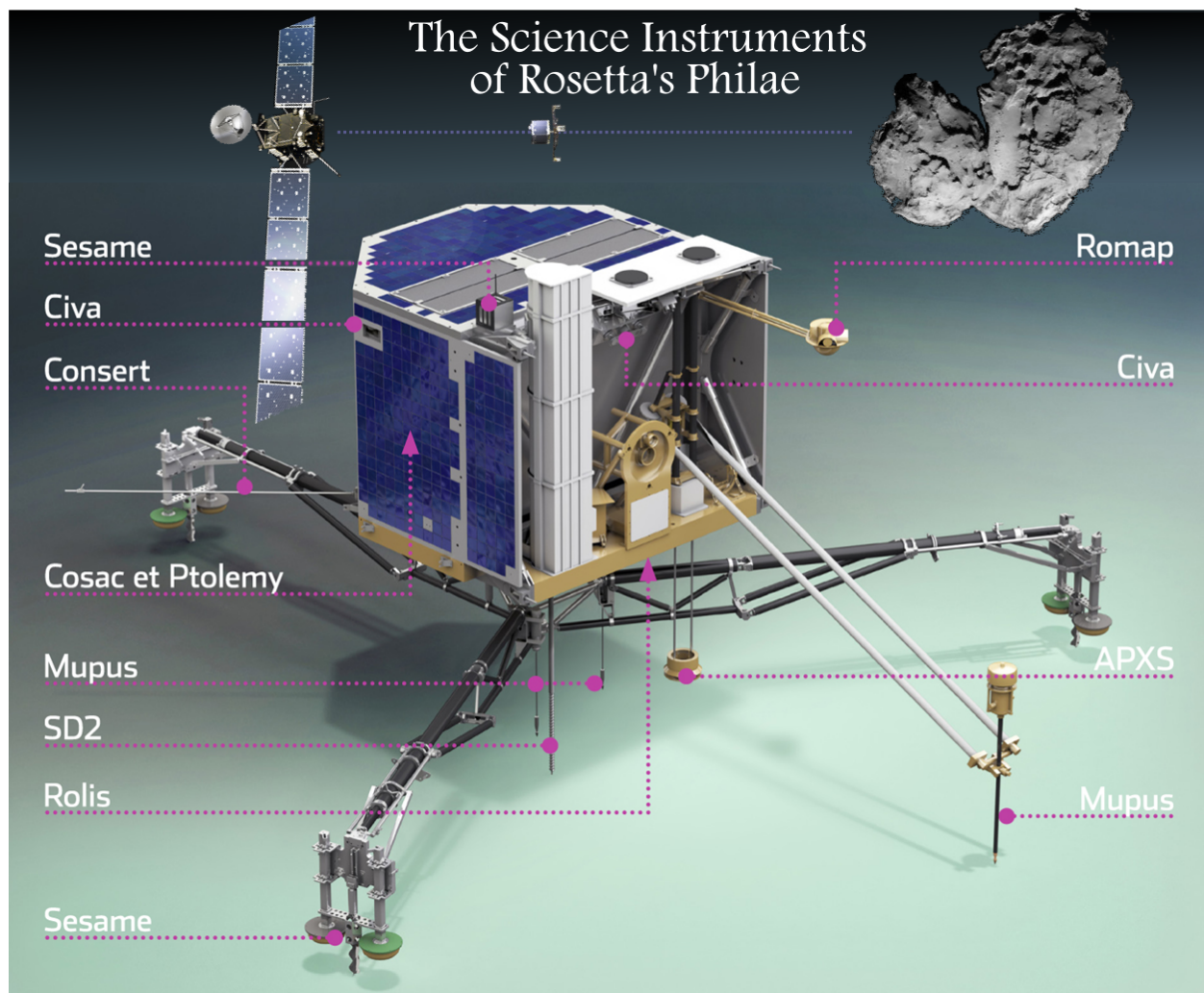


**Figure 7.3.1: Diagram of the *Philae* Lander's Scientific Instruments [105, Fig. 1]**

# **8 Design Approach**

## **8.1 Structures**

**Prepared by: Katie August**

### **8.1.1 Definition**

The structures subsystem is vital for the mission, for it provides support and safety to all the internal components of the spacecraft. It is responsible for all the components that carry any structural load. The spacecraft structure must be able to withstand all the forces it faces during the mission, including launch, travel, and landing. It must protect internal components from the conditions of space and Europa. This involves protection from radiation exposure and temperature conditions. Additionally, it is also designed to minimize cost, mass, and risk while maximizing strength, thermal conductivity, and volume.

### **8.1.2 Objectives**

The main objective for the structures subsystem is to design a stable and strong structure that endures the harsh conditions of space through launch conditions, travel, orbiting, and landing. At launch, the ECHO probe is more protected from the launch vehicle and satellite delivering it to Jupiter. After the satellite safely deploys the probe at Jupiter, it will be subject to the freezing temperatures of space, soon following the orbital maneuvers it will undergo to land on Europa.

### **8.1.3 Requirements and Constraints**

In order to ensure the success of the mission, the structures system must complete the objectives while staying within the constraints. Listed are the requirements and constraints:

- The structure mass budget is 70 kg.
- Minimize mass while maximizing strength and volume.
- Perform quasi-static finite element analysis (FEA) to find maximum stress points.
- Perform dynamic stress analysis for vibrational/acoustic loading.

### **8.1.4 Analysis**

#### **8.1.4.1 Structure Sizing and Specifications**

The main component for determining the size of the structure was housing the internal components. The biggest components are the fuel tanks for the bi-propellants. As mentioned in Section 8.3.4.5, the combined volume for the propellants is 659 liters. The other sizable component is the RTG, sizing to be 64 centimeters in diameter and 66 centimeters tall [7]. After considering the volume of these components, the structure began with an equilateral hexagon for the base with each side being 1 meter. Initial mass analysis proved to exceed the mass budget, so each side was decreased to 0.77 meters. If reduced any further, there would not be enough

volume for the components. The final structural dimensions are 1.4 meters in length and 1.4 meters in width. The height with the landing legs folded is 0.88 meters and 1.8 meters with deployed landing legs. The remaining volume for other components such as ADCS sensors, telecommunication hardware, propellant tubing, deployables and heat insulation is 0.39 cubic meters. The final sizing, material selections, and specifications for the structure components is shown in Table 8.1.1. The total mass does exceed the mass budget, which will be further discussed in Section 8.1.8.

**Table 8.1.1: Component Specifications**

Part	Material	Density (kg/mm <sup>3</sup> )	Young's Modulus (MPa)	Quantity	Mass (kg)
<b>Landing Leg</b>	Aluminum-6061	$2.71 \times 10^{-6}$	68,980	3	29.25
<b>Landing Leg Plate</b>	Aluminum-6061	$2.71 \times 10^{-6}$	68,980	3	11.43
<b>Side Panel Skin</b>	Titanium	$4.46 \times 10^{-6}$	117,270	6	25.68
<b>Side Frame</b>	Aluminum-6061	$2.71 \times 10^{-6}$	68,980	6	32.89
<b>Top Panel Skin</b>	Titanium	$4.46 \times 10^{-6}$	117,270	1	4.35
<b>Top Frame</b>	Aluminum-6061	$2.71 \times 10^{-6}$	68,980	1	8.43
<b>Bottom Panel Skin</b>	Titanium	$4.46 \times 10^{-6}$	117,270	1	4.35
<b>Bottom Frame</b>	Aluminum-6061	$2.71 \times 10^{-6}$	68,980	1	8.43
<b>Total</b>	-	-	-	-	124.81

The hexagon panels consist of aluminum alloy internal framing wrapped in thin titanium alloy skin. The frame is designed to carry most of the loading, while the skin supports structural rigidity and heat retention. Figure 8.1.1 shows the internal framing for the top and bottom panels, and Figure 8.1.2 shows the internal framing for the side panels. The top and bottom panels have both row and column framing, whereas, the side panels just have vertical framing. This is due to the bottom panel having connections to the landing legs and fastening all the internal components. These also require connections to the side panels. The side panels only have vertical fasteners and fasteners at the joints between them. There are frames positioned at an angle to better support the connections at the joints.

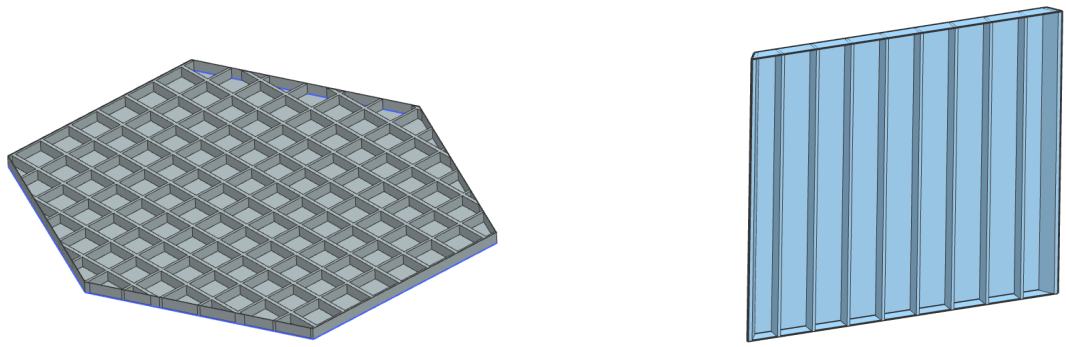


**Figure 8.1.1: Top and Bottom Panel Structure**

**Figure 8.1.2: Side Panel Structure**

An image of the final structure is shown in Figure 8.1.3. To simplify analysis, the internal components were created to represent the volume and weight of the fuel tanks and the RTG.

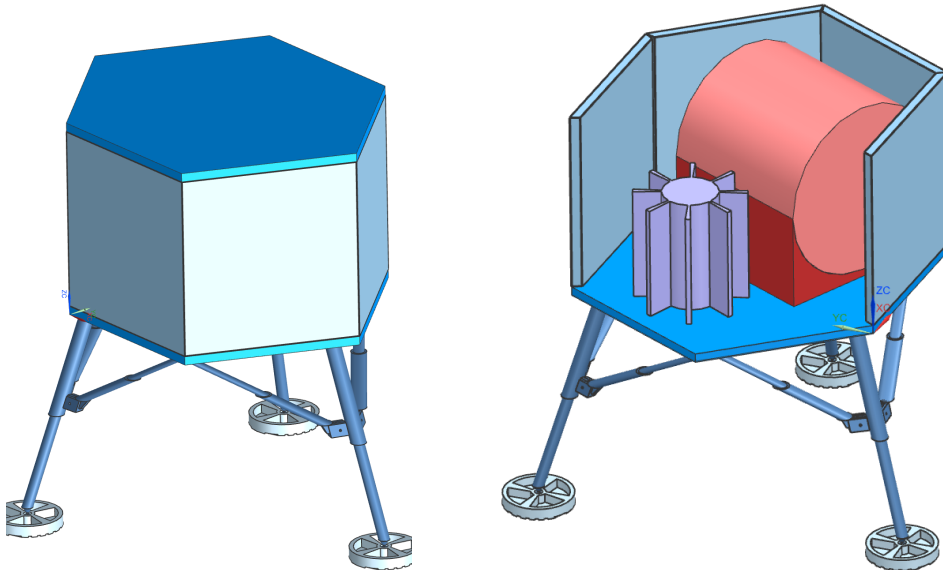


**Figure 8.1.3: Final Structure**

**Figure 8.1.4: Analysis Structure**

### 8.1.4.2 Landing Leg Specifications

The landing legs need to be able to support a potentially harsh landing on uneven ground. The plates on the legs are designed to rotate on rough terrain. The bottom of the main leg has an aluminum ball on the end. The center of the plate provides a friction fit to the aluminum ball, creating a ball joint. Ball joint degrees of freedom and details are shown in Figure 8.1.5, but the fixed constraint is on the ball and output rod rather than the socket since the output rod is fixed to the probe.

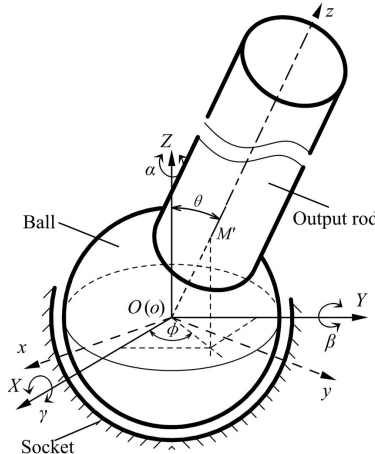


**Figure 8.1.5: Ball Joint [8]**

Additionally, the landing legs must be designed to absorb the impact of landing. Potential impact absorption methods are aluminum foam, thin honeycomb structures, springs, or hydraulics. The decision matrix for these are shown in Table 8.1.2. The criteria for these are stability, weight, manufacturability, and cost [9].

**Table 8.1.2: Impact Absorption Decision Matrix**

Criteria	Weight	Aluminum Foam	Honeycomb	Spring	Hydraulics
Stability	4	4	4	4	5
Weight	3	3	4	5	1
Manufacturability	2	5	2	5	2
Cost	1	3	3	5	1
<b>Total</b>	10	38	35	46	28

The spring was chosen for its lightweight properties and manufacturability. It needs a high spring constant value in order to handle the forces and not have an elastic reaction, which would disrupt the probe's stability. The spring would be located inside larger cylindrical sections.

The final assembly of the landing leg is shown in Figure 8.1.6. A close-up of the ball joint and landing plate is shown in Figure 8.1.7, also showing the traction treads as a slip resistant measure for Europa's icy surface. The legs are folded up during flight and deployed before landing, which is further discussed in Section 8.2.

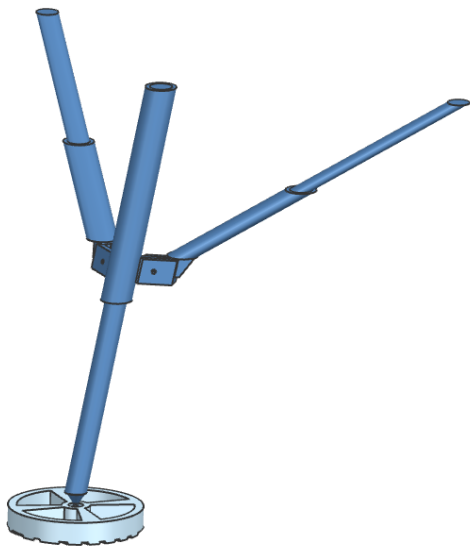


**Figure 8.1.6: Landing Leg**

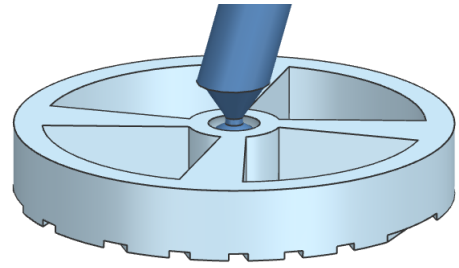


**Figure 8.1.7: Landing Plate/Ball Joint**

### 8.1.4.3 Quasi Static Loading

Quasi-static analysis is a static analysis that assumes the loads are applied slowly over time or constant without any vibration. A spacecraft can experience up to 6 g's of loading during launch [10]. To set up the simulation for 6 g analysis, an idealized part was created, this excluded the side panel skins, for they would be too thin for 3D mesh, creating very large aspect ratios, poor accuracy, and elements exceeding tolerance mesh values [11]. Additionally, the landing legs are not included for this first analysis. Table 8.1.3 displays the detailed specifications for the quasi-static analysis.

**Table 8.1.3: Mesh Element Details**

Part	Element Type	Method	Element Size (mm)	Element Quantity	Node Quantity
<b>Top Panel Skin</b>	CTETRA 4	SOL 1	26.5	38,162	12,133
<b>Top Panel Frame</b>	CTETRA 4	SOL 1	28.1	15,389	8,350
<b>Bottom Panel</b>	CTETRA 4	SOL 1	25.5	40,293	12,568
<b>Bottom Panel Skin</b>	CTETRA 4	SOL 1	27.6	16,735	9,451
<b>Side Panel Frame</b>	CTETRA 4	SOL 1	19.1	5,576	2,820

To finish setting up the simulation, loads, constraints, and contact points need to be defined. A geometric distribution load of 6 g, was applied to the top surface. A fixed constraint was applied to the bottom surface. There were contact points between the frames and top and bottom panels,

between the RTG and bottom panel, and between the fuel tanks and bottom panel. All of these components would be fastened down in the physical structure, so these parts were glued together for the simulation. Figure 8.1.8 displays the results from this.

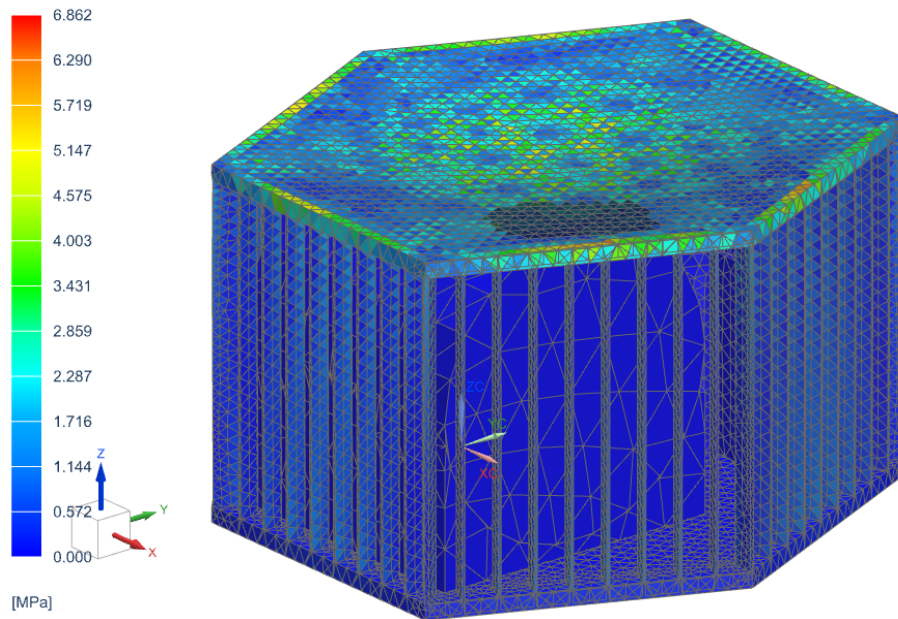


**Figure 8.1.8: 6g Quasi-Static Result**

The maximum stress value is 6.862 MPa, located around the perimeter and at top of the framing. There are no stress values on any of the internal elements, showing that the structure absorbed the load.

The next quasi-static analysis is about the ball joints as they are crucial for the landing impact. A single landing leg with its plate was simulated. The bottom of the plate was fixed, and a downward force of 2,000 kilograms was applied at the top. The mesh element details for this analysis is shown in Figure 8.1.4, and the results are shown in Figure 8.1.9.

**Table 8.1.4: Mesh Element Details for Landing Legs**

Part	Element Type	Method	Element Size (mm)	Element Quantity	Node Quantity
Landing Leg	CTETRA 4	SOL 1	26.3	13,402	3,859
Landing Leg Plate	CTETRA 4	SOL 1	17.4	5,714	1,950

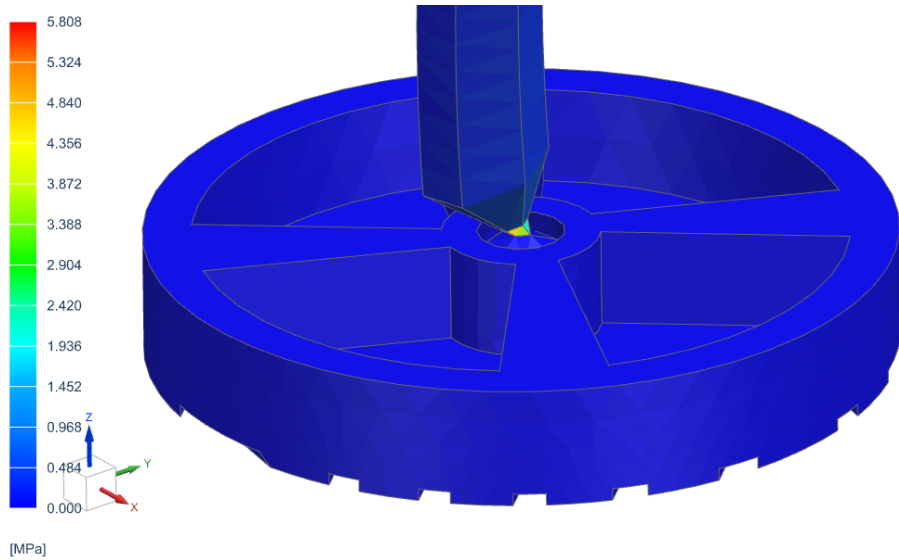


**Figure 8.1.9: Landing Leg Analysis Results**

The maximum stress is 5.808 MPa on the thinnest part of the ball joint. In actuality, the forces would be more distributed among the other two landing legs with support from the spring mechanism. The spring could not be simulated linearly because of the cyclic nature of it.

#### 8.1.4.4 Acoustic Loading

Acoustic loading is a result of engine noise and aerodynamic loading [10]. The rocket boosters create intense vibrations that propagate through the structure. Figure 8.1.10 is a diagram that displays vibration and noise propagation [12].

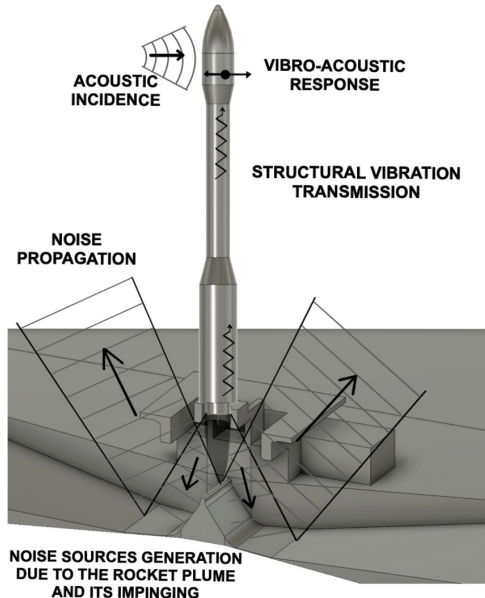


**Figure 8.1.10: Acoustic Propagation [6]**

The panels on spacecraft can act as sounding boards that amplify the experienced vibrations. There are methods to mitigate or dampen the acoustic loading, including internal paneling, foam, and insulation. These protect the structural integrity and internal components. Two simulations were run to find the natural frequencies and mode shapes.

The first test was the side panel skin without any internal framing. The second test was the side panel with the internal framing. This is to test if the internal framing design damps the vibrational loading. Figure 8.1.11 is the side panel skin stress results without internal framing at a natural frequency of 79.48 Hz. Figure 8.1.12 is the side panel skin stress results without internal framing at a natural frequency of 84.52 Hz. These resulted in a maximum stress of 14.16 and 18.40 MPa, respectively. The displacement is exaggerated in order to better see the mode shapes at these frequencies.

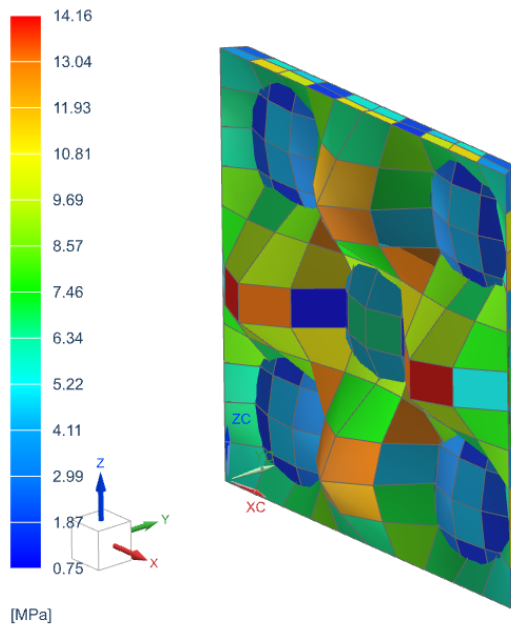


**Figure 8.1.11: Mode Shape/Stress at 79.48 Hz**

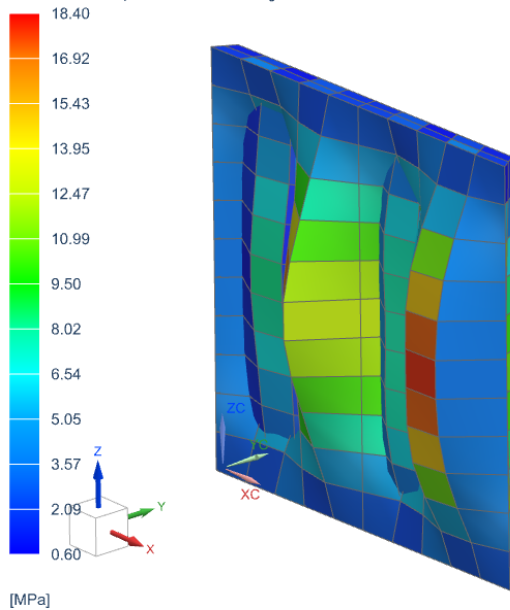


**Figure 8.1.12: Mode Shape/Stress at 84.52 Hz**

Figure 8.1.13 is the side panel stress results with internal framing at a natural frequency of 77.38 Hz. Figure 8.1.14 is the side panel stress results with internal framing at a natural frequency of 107.54 Hz. These resulted in a maximum stress of 7.829 and 11.706 MPa, respectively. The displacement is also exaggerated in order to better see the mode shapes at these frequencies. The maximum stress at these natural frequencies are far less than the maximum stress without the internal framing. There are also fewer maximum stress points due to mode shape differences.

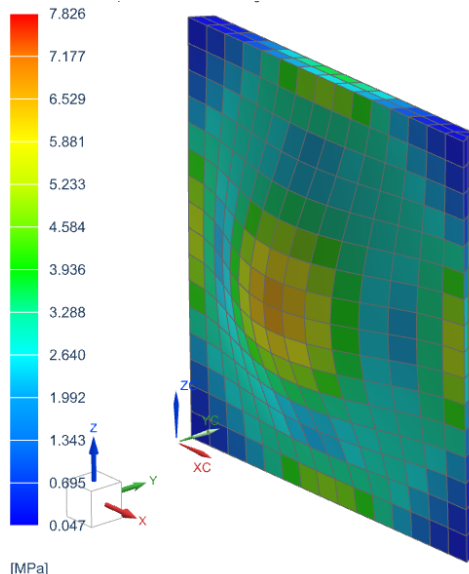


**Figure 8.1.13: Mode Shape/Stress at 77.38 Hz**

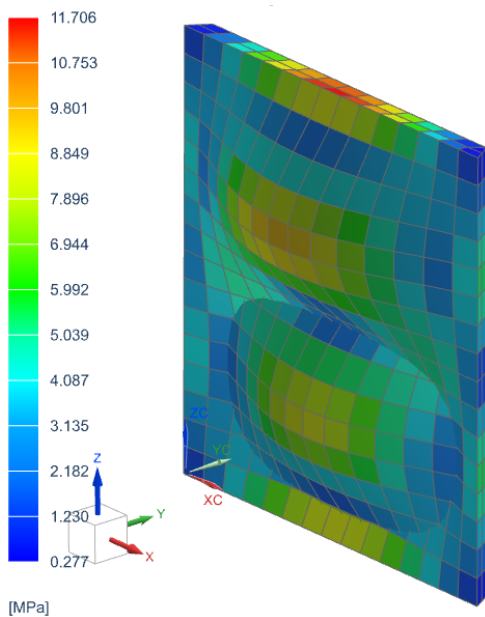


**Figure 8.1.14: Mode Shape/Stress at 107.54Hz**

### 8.1.5 Non-Technical Considerations

Several non-technical considerations influenced the design of the structures subsystem in project ECHO. These include cultural, economic, environmental, ethical, public health and safety, and social considerations.

The structure will undergo extensive digital and physical testing. Finite element analysis (FEA) simulations for general structural configurations and physical testing following successful FEA. The testing ensures that there is no risk to those that are constructing the probe. This leads to economic and environmental considerations, for insufficient FEA testing may result in poor physical testing performances, increasing the amount of resources used and supply costs. All engineers and designers on the ECHO probe and structures team follow ethical standards learned in Rensselaer Polytechnic Institute's ethics courses approved by the Accreditation Board for Engineering and Technology. There is no significant evidence for cultural, global, and social considerations. Table 8.1.5 explains each consideration with respect to the structure subsystem.

**Table 8.1.5: Structure Non-Technical Considerations**

Topic	Consideration
Ethical Responsibility	The designer has completed various college courses in ethics as well as being knowledgeable in the subject areas. Ethical company policies are considered while searching for potential vendors
Public Health & Safety	The intensive structural testing ensures there is no risk to the builders of this probe.
Cultural	N/A - There are no cultural considerations for structures.
Social	N/A - There are no social considerations for structures
Environmental	Structure materials would be purchased from environmentally responsible companies. Computer aided design will be utilized before construction to minimize failures and product waste.
Economic	Materials and parts for the design of the structure can be sourced from various retailers within the project budget. The retailers would benefit from the material and part purchases.

## 8.1.6 Risk Management

The structure subsystem is a key component for mission success because structural failures can lead to complete mission failure. A robust and reliable structure is essential, for structural failures can cause breakdowns in other subsystems. Ensuring that the structure is strong and safe is a top priority. Each design choice was chosen based on the combination of strength, efficiency, and reliability. The structure went under tests to mitigate the risks from structural failures, space debris, landing forces, and radiation exposure. Table 8.1.6 shows these risks and their associated mitigation.

**Table 8.1.6: Structure Risk Mitigation Table**

Hazard	Cause	Effect	Pre-RAT	Mitigation	Verification	Post-RAT
Structure Failure	Improper construction or design or impact with space debris	Loss of spacecraft, loss of mission	1C	Thorough structural analysis of all spacecraft components	Successful testing of load bearing components	3E
Radiation Exposure	Being in proximity of the Jovian radiation belt	Losing contact to the spacecraft, compromises mission	2A	Use of insulation and radiation protective materials	Comparison to successful missions	4B
Landing Leg Point Failure	Harsh landing on Europa	Spacecraft crash landing	2D	Thorough analysis of load bearing joints	Successful testing of the joints	4D

## 8.1.7 Future Work

Future work includes performing FEA to simulate additional scenarios of structural loading during the mission. The FEA performed for this report was limited by the available machinery. Dynamic loading, thermal analysis, and transient responses would all be considered in future design analysis. The thin skin panels were unable to be included in these iterations due to machine incompatibility. The meshed elements of the panel skin are required to be small to meet mesh tolerancing, but the quantity of elements needed for accurate analysis is unachievable without a more efficient machine. Since all simulations proved to be successful, a resizing of the structure can be done to reach the mass budget by making the frames more hollow or smaller. Lastly, the ball joints on the landing legs are a highly concentrated stress point that would be reconstructed to distribute the loads more effectively.

## 8.2 Mechanisms and Deployables

Prepared by: Mae Tringone

### 8.2.1 Definition

The Mechanisms and Deployables subsystem encompasses the mechanical components and moving parts that will aid ECHO in completing its mission. This includes any portion of the lander that relies on robotics or moving parts to achieve design goals. Specifically, this will be encompassed by three main “suites” of mechanisms:

- 1.) The Landing Suite encompasses the parts that allow for the actuation of the landing legs.

- 2.) The Sample Collection Suite encompasses the electromechanical systems that will collect surface and subsurface samples, as well as the mechanisms that facilitate delivery of the samples to onboard sample analysis instruments.
- 3.) The Telecom Tracking Suite encompasses the mechanisms that support the aiming of directional telecommunications equipment.

### **8.2.2 Objectives**

The Mechanisms and Deployables subsystem is involved wherever robotics and moving parts are necessary. Several of ECHO's mission objectives will require the utilization of moving parts. These are as follows:

- Land softly onto the surface of Europa and maintain connection with the ground for the entire duration of the mission.
- Collect surface and subsurface samples from Europa.
- Relay information back to Earth via the mission's orbiter component on subsequent rendezvous with Europa.

### **8.2.3 Requirements and Constraints**

From the previous objectives, the following requirements are as follows:

- ECHO must perform a soft landing, minimizing landing stresses experienced by the lander, using the landing leg system drafted by the Structures subsystem in section 8.1.4.2.
- ECHO must have a durable and capable sample collection system, using a drill that can adequately penetrate the Europian surface and maintain operability for the entire mission.
- ECHO must be able to point its directional telecommunications equipment towards the orbiter when it is within range, and have the mobility required to accurately and autonomously track it through the sky.

### **8.2.4 Analysis**

#### **8.2.4.1.a Landing Suite Deployment Mechanism**

The landing leg triad, further outlined in 8.1.4.2, will consist of three folding, suspended landing legs with gripping cleats at the bottom.

The landing legs will be stowed beneath the lander body until the descent stage is reached, at which point they will be released and pivot outwards on hinges into their final deployed state. Compressive springs inside the leg supports will keep the legs under pressure, and facilitate the rotation of the legs into final design orientation once the release command is given.

Preliminary design ruled out the use of pyrotechnic Hold Down Release Mechanisms due to the risk of explosive shock damage. As such, non-pyrotechnic HDRMs are to be used. There are

many different types of HDRM available on the market. Many of the specifications of these mechanisms are retained under non-disclosure agreement, however their basic mechanics are known. Common types of HDRM include:

- Pin Pullers: A pin connected to a linear actuator, which pulls back on command and releases the attached mechanism [13].
- Thermal Knives: A kevlar restraint draped over a thermal assembly which heats to high temperature on command, degrading the kevlar to failure point and releasing the attached mechanism [14]
- Split-Spool: A threaded connection is held in place via the tensile force of a plunger. When the command is given, the plunger releases, unwinding and releasing the bolt [15].

The exact release times, load limit and power draw vary significantly between manufacturer, however a mechanism can be narrowed down by re-evaluating the exact needs of the landing leg deployment mechanism:

- To minimize propellant and power waste by the ADCS system, it is preferred that all three legs deploy at the same time such that their net moment on the lander body is cancelled out.
- The stresses induced by the spring-loaded landing legs will not be very large: the HDRM does not need to be significantly robust, or capable of handling high loads.
- Lower-power HDRMs are preferred to minimize overhead power cost.

As the legs need to deploy at once, the thermal knife is ruled out; the inability to predict exactly when the kevlar strap will fail means that synchronous deployment cannot be guaranteed. The split spool has many moving parts, and thus has more points of failure, and regardless the load bearing capabilities of threaded design is likely far in excess of what is actually required. Therefore, a relatively simple pin-puller actuator is the preferred choice for the initial design iteration. Three actuators, positioned on the bottom of the craft near the location of the landing leg ends in initial fold-in position, will slot into designated pin locations along the legs, and exert a normal reaction force against the spring. Once pulled, the force imbalance will deploy the legs into landing position.

### **8.2.4.1.b Mathematical Modeling of Impact**

Ideally, the lander will impact the ground at a low speed, with a descent vector mostly orthogonal to the average ground plane. These conditions lend themselves well to analysis via classical control theory.

Analysis starts by modelling the landing legs as a set of mass-spring-damper systems. Ideal springs and dampers are assumed.

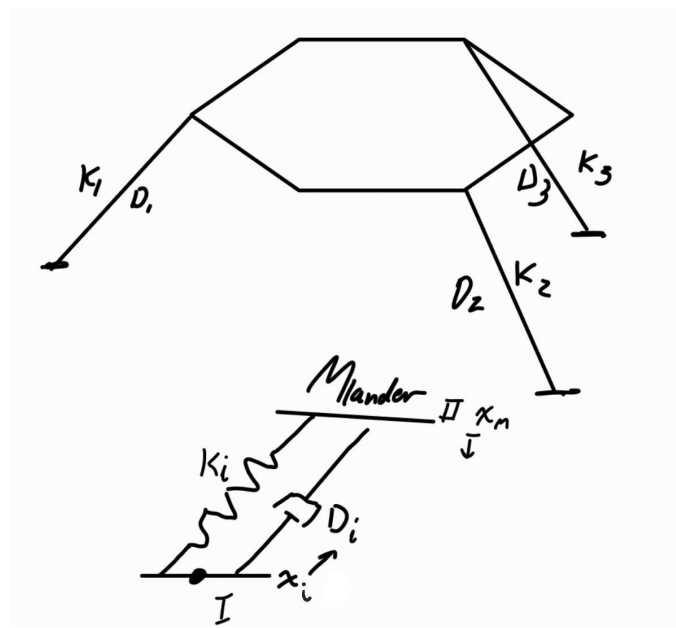


**Fig 8.2.1: Free-Body Diagram of the landing cleats and lander body**

$x_m$  represents the vertical position of the craft (the variable of interest), and  $x_i$  represents the vertical displacement of each of the three landing cleats. From the free body diagram, governing differential equations are determined via a force analysis on all the moving points of the spacecraft. For each of the three landing cleats, the sum of forces is:

$$\sum F_i = K_i(x_m - x_i) + D_i(\dot{x}_m - \dot{x}_i) + F_I = 0 \quad (8.2.1)$$

Where  $F_I$  is the average impact force experienced by the landing cleats upon contact with the ground. Creating another force balance on the body of the craft yields the following:

$$\sum F_m = M\ddot{x}_m = \sum_{i=1}^3 (K_i(x_i - x_m) + D_i(\dot{x}_i - \dot{x}_m)) \quad (8.2.2)$$

Where  $M$  is the payload mass of the lander. The landing cleats are assumed massless compared to the rest of the lander to simplify calculations.

Fully expanded, this analysis yields four linearly independent equations and four unknowns. Applying a laplace transform with zero initial condition assumption, and then solving for the unknowns, yields an 8th order transfer function in terms of the damping and stiffness values for each leg, impact force  $F_I$ , and lander displacement  $x_m$ . Due to the size of the symbolic representation of this equation, a MATLAB script which will generate the equation required for further simulation is provided in appendix 13.6. From this equation, further empirical and simulation data on the expected impact force and environmental conditions can be used to tune the spring and damping coefficients of each of the landing leg's shocks.

### 8.2.4.2 Sample Collection Suite

The primary area of interest of Europa that is readily accessible to the lander is the subsurface regolith. Due to Jupiter's radiation belt, any potential organic matter will exist below a certain threshold of the surface, theorized to be between 0.4-8 inches. [16]

Due to flight heritage, the Philae lander of the Rosetta mission was selected as a benchmark on which all future sample collection iterations are based. To date, this is the only mission to successfully land on an environment relatively similar to Europa's and analyze subsurface samples. Philae's drill was capable of reaching depths of 23 cm, or about 9 inches [14, pp. 1]. In a worst-case landing scenario, in which ECHO is situated where the ionizing Jovian radiation reaches its maximum penetration, this setup still provides barely over an inch of drilling depth past where organic materials are expected to be found.

Public literature on the specific workings of the Philae lander's Sampling, Drilling and Distribution Device (SD2) is limited. Broadly, it is known that it comprises a drill bit, inside which is mounted an extendable sample collection tube. The drill digs into the regolith with a 10 W power supply, and then the tube is extended and forced into the drill site to pack the loose material inside. The drill is then retracted back into the craft body, and a carousel extends to cover the drill path. Once in place, the tube retreats back into the drill bit and the sample drops into the sample carousel. [17, pp. 4-5].

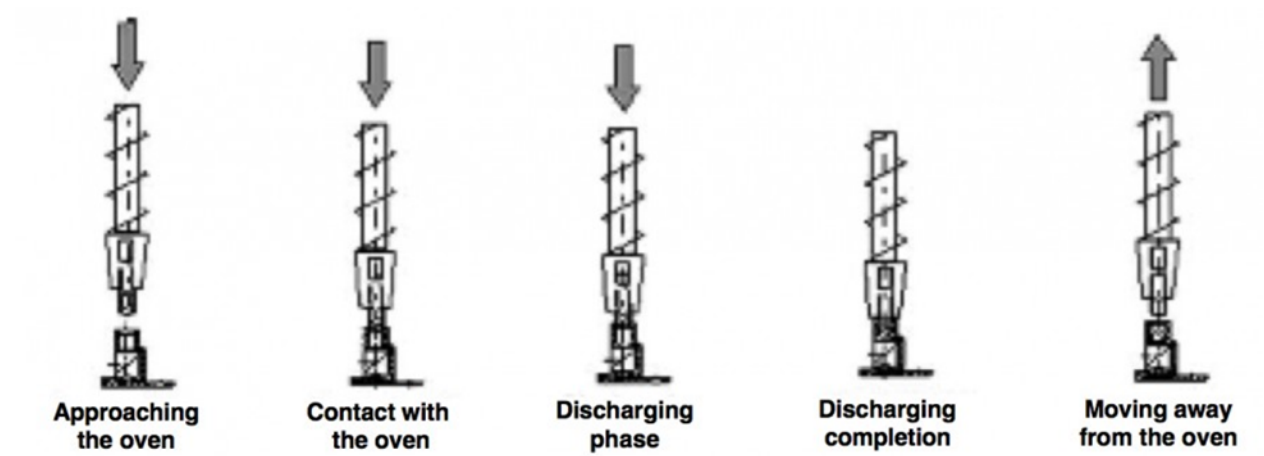


**Fig 8.2.1: Diagram Showcasing the Sampling, Drilling and Distribution Device (SD2) Utilized by the Philae Lander [17, Fig. 3]**

Preliminarily speaking, such an action can be achieved with linear actuators. One supports the main drill housing, allowing it to dig into the soil, and the other is nested inside the drill bit. Power can be delivered to the interior actuator via the use of a slip ring located inside the drill bearing.

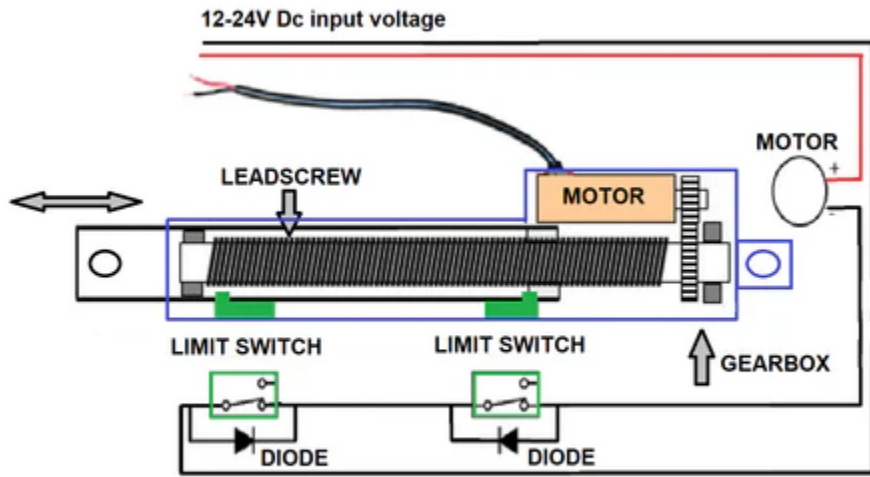


**Figure 8.2.2: Typical Non-Pneumatic Linear Actuator [18, Fig. 4]**

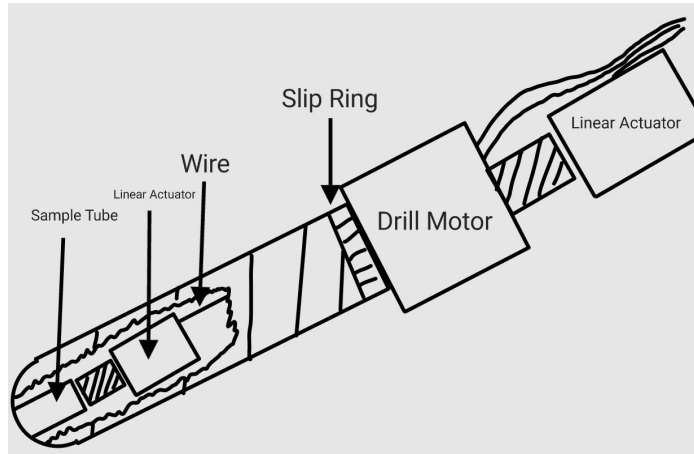


**Figure 8.2.3: Mockup of an SD2-Inspired Sample Drill**

### 8.2.4.3 Telecom Tracking Suite

ECHO will depend on a set of directional high-gain patch antennas to communicate with the associated Europa Orbiter mission, which will serve as a relay station between ECHO and the Deep-Space Network on Earth. A biaxial antenna positioning mechanism, in elevation/azimuth configuration, will orient the antenna in the optimal transmitting position during descent and subsequent fly-bys of the Europa Orbiter.

The market for spacecraft antenna pointing assemblies is vast, and contains many options, from small, cheaper assemblies marketed towards cubesat development, to in-house designs by JPL and other space agencies employed for specific communication and radio astronomy purposes.

However, a few basic aspects that will influence further market research are known. These are as follows:

- The mechanism should be as simple as possible; the communications suite merely needs to support the uplink of engineering and science data and the downlink of instructions. It needs no more accuracy than is required for reasonably efficient transmission to the Europa Orbiter every fly-by, the arc of which can be predicted in advance. Any additional mechanics that may improve the pointing accuracy of the antenna also serve to increase the amount of failure points in the mechanism.
- The low-mass patch antennas utilized by the telecommunications subsystem will not require much power to move and aim. Therefore low-power pointing mechanisms are preferred to optimize the amount of power overhead that can be granted to other subsystems, such as ADCS and propulsion.

As an example, the Moog Type 22 Antenna Pointing Assembly is shown. It is a reasonably capable mechanism, with an output step size of 0.02 degrees and a modest average power draw of 30W when both axes are engaged. Moog's spaceflight heritage makes their low-power pointing system a good baseline for future design iterations.

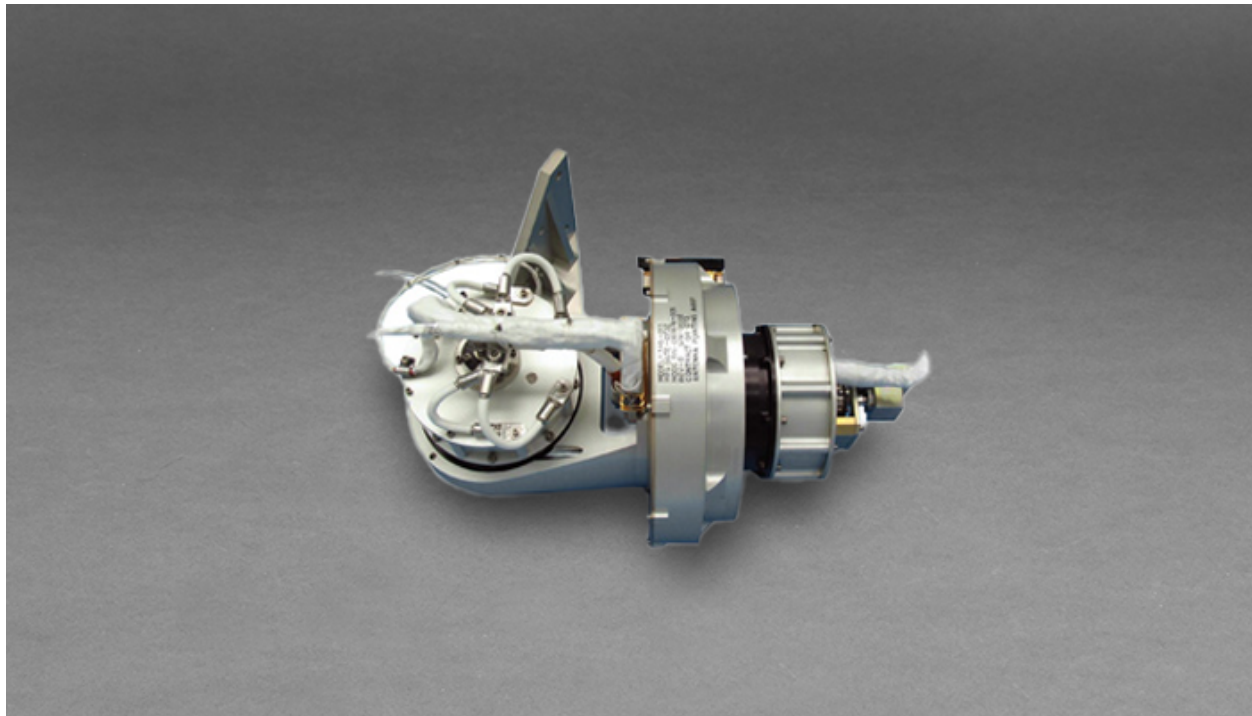


**Figure 8.2.4: Moog Type 22 Antenna Pointing Assembly[19, Fig. 1]**

## 8.2.5 Non-Technical Considerations

While the Mechanisms and Deployables subsystem is mostly concerned with technical requirements, there are several minor non-technical factors to consider.

**Table 8.7.1: Power Non-Technical Considerations**

Non-Technical Factor	Considerations
Ethical Responsibility	The mechanisms and deployables subsystem will ensure all parts are ethically sourced.
Public Health & Safety	The mechanisms and deployables subsystem, despite having occupational hazards, does not pose a threat to the general public's health and safety.
Cultural	The mechanisms and deployables subsystem will not represent or tackle any cultural issues.
Social	The mechanisms and deployables subsystem will not have any social impact.
Environmental	The mechanisms and deployables subsystem will not plan to use any components that represent a substantial risk to the environment.
Economic	There may be economic incentives to use components from specific manufacturers. This must be balanced with the reliability needed from said components during the mission.

## 8.2.6 Risk Management

The landing and communications suites represent single points of failure for the entirety of ECHO if any component of them were to fail, and a failure of the drill rig would cripple ECHO's primary objective of analyzing surface and subsurface regolith. It is imperative that any component facilitating the dynamic movement and deployment of mission-critical components be made to spec for the expected environmental conditions, and that extensive testing on engineering models be performed to ensure reliability.

**Table 8.2.2: Mechanisms and Deployables Risk Assessment Table**

Hazard	Cause	Effect	Pre-RAT	Mitigation	Verification	Post-RAT
Landing legs knocked loose before full deployment	Launch and transfer impulses; excessive maneuvering	shifted center of mass; propellant and energy waste from ADCS corrections; landing leg assembly exposed to supersonic aerodynamic loading during lithobraking	1C	Verification of pin connections; ensuring parts are low tolerance and have minimal play in unintended axes	Adequate sonic and transverse load testing to ensure integrity of deployment mechanism through launch and transit	1E
Drill system failure	damage to electromechanical components during launch stage	Sample analysis component becomes impossible	2C	high tolerance machining and strong supporting materials to ensure minimum flexure of drill assembly or collision with side walls during expected launch impulses	Adequate sonic and transverse load testing to ensure integrity of drilling suite; vetting of the manufacturer for linear actuator and drill motor components	2E
Telecommunications pointing failure	damage to one or more pointing mechanism servos under launch or transit stresses; mechanical impact exceeding shear tolerance of pointing mechanism	Telecommunications becomes significantly more difficult; potential loss of mission	1C	Stowage of antenna assembly in an assembly least likely to subject positioning mechanism to stresses that would lead to expected failure modes	Vetting of the manufacturer of the biaxial pointing mechanism; collaboration with ADCS subsystem to allow for specific landing positioning in the case where azimuth or horizon positioning capability is reduced.	1E

## **8.2.7 Future Work**

Future work in the Mechanisms and Deployables subsystem will revolve primarily around selecting a vendor for the telecom tracking mechanism, as well as further control systems analysis on the suspension setup. Testing and/or simulation will be required to empirically determine the expected impact force in several different landing scenarios, and from there the damping and stiffness coefficient of the landing legs will be tuned to bring the response of the system as close as possible to a critically damped state.

Further collaboration with the European Space Agency will be facilitated to better understand the specific design of the SD2 system utilized on the Rosetta mission. Once a mechanism is finalized, further work will be done to evaluate the anticipated toughness of Europa's regolith, which will influence the specific type of drill bit and motor power required.

## **8.3 Propulsion**

**Prepared by:** Joseph Bowers

### **8.3.1 Definition**

The propulsion subsystem shall include all required components to produce thrust for the spacecraft. This includes both the primary thrusters for orbital maneuvering, as well as ADCS thrusters for attitude control, reaction wheel desaturation, and fine maneuvering. Additionally, this includes propellant storage, plumbing, valves, and thruster assemblies. Within the mission timeline, the scope of propulsion begins in a highly elliptical Jovian orbit upon release of the probe from the orbiter, and concludes upon soft touchdown of the probe on the Europan surface.

### **8.3.2 Objectives**

There are three main objectives of the propulsion subsystem. All objectives are critical for the success of the overall mission.

1. Perform the required orbital maneuvers as described by orbital mechanics to take the probe from a highly elliptical Jupiter orbit to a specified Europa parking orbit over the targeted landing site.
2. De-orbit at Europa and decelerate to perform a soft touchdown on the surface of Europa with near-zero velocity. If required, substantially slow or briefly hover to inspect the landing site and adjust as needed.
3. Perform attitude adjustments prescribed by the ADCS subsystem and as needed to desaturate reaction wheels.

### **8.3.3 Requirements and Constraints**

In order to ensure mission success, the propulsion subsystem must complete its objectives while staying within constraints required for the overall mission's success.

1. Maximize efficiency of the system to minimize propellant mass.
2. Ensure sufficient thrust to land on the Europa surface.
3. Design the system with redundancy to minimize single point failure modes
4. Design for sufficient propellant margins to ensure mission success, accounting for additional propellant needed to adjust for any off-nominal trajectories.

## **8.3.4 Analysis**

### **8.3.4.1 Propellant**

As discussed in the PDR, a hydrazine-derivative bi-propellant has been selected for its mission due to the efficiency of the bi-propellant solution, as well as the shelf stability and flight heritage of hydrazine. With further analysis, the combination of Monomethyl Hydrazine (MMH) and Mixed Oxides of Nitrogen with 3% Nitric oxide (MON-3) has been selected as the ideal bi-propellant for this mission. This is the most commonly utilized hydrazine derivative, and provides the widest selection of available thrusters for the mission. Additionally, the improved thermal stability of MMH when compared to pure Hydrazine will be critical for this mission due to the low temperatures which will be encountered in the deep space environment during transit to Europa.

For the ADCS thrusters, a mono-propellant thruster has been selected, utilizing the same MMH provided for the bi-propellant system. Mono-propellant is utilized due to the lower mass of the thrusters and associated infrastructure. Additionally, as the amount of propellant consumed will be significantly less than the primary thrusters, specific impulse ( $I_{SP}$ ) is a much less significant concern. This will effectively make the overall propulsion system a dual-mode system.

### **8.3.4.2 Thrusters**

For this mission, two types of thrusters must be specified. The spacecraft must have primary thruster(s) to perform all orbital maneuvering, as well as secondary ADCS thrusters to desaturate the reaction wheels.

Four primary factors were considered when selecting a primary thruster. First, maximizing  $I_{SP}$  is important for minimizing fuel mass. Second, by dividing the thrust required across multiple engines, a higher level of redundancy for the design can be achieved, where if a single engine fails the entire mission is not compromised. As such, the desired thrust output for a single thruster is around 120 N, as the hexagonal geometry of the lander lends to utilizing six thrusters. However, a higher powered thruster or lower powered thruster can be utilized at higher or lower quantities. Additionally, the mass of the thruster is a factor, and to account for the differing thrust outputs considered the thrust to weight ratios (TWR) are compared. Finally, flight heritage can be valuable for proving the reliability of a thruster, and is also considered for risk mitigation.

**Table 8.3.1: Primary Thruster Selection Matrix [20][21][22]**

Criteria	Weight	R-1E	R-4D-15	AR-49	25 lbf MMH	200 N Bi-Propellant
Manufacturer		L3 Harris	L3 Harris	L3 Harris	Moog	Ariane Group
<b>Specific Impulse</b>	4	3	5	5	4	2
<b>Thrust Output</b>	3	5	3	5	5	4
<b>TWR</b>	2	2	3	5	2	4
<b>Flight Heritage</b>	1	5	5	2	3	4
<b>Total</b>	10	36	40	47	38	32

The AR-49 thruster produced by L3 Harris is selected for this mission due to its strong  $I_{SP}$  and TWR. While this thruster is not flight proven, it belongs to a family of thrusters with a reported 100% success rate, helping to mitigate thruster failure concerns. This thruster has an  $I_{SP}$  of 317, maximum thrust output of 111 N, and mass of 0.54 kg [20].

The selection of an ADCS thruster is primarily dictated by mass considerations. On a probe of this size, the required thrust magnitude to effectively provide reaction control is minimal, and a relatively small thruster will be sufficient to provide the required torque. The thrusters evaluated range from 0.09 N to 5 N thrust output, with some preference given to thrusters with a larger output. The  $I_{SP}$  of the thrusters is also considered, to ensure efficient use of the propellant which is expended. Finally, the flight heritage of the thruster is an important metric to understand the reliability of the product.

**Table 8.3.2: ADCS Thruster Selection Matrix [23][24][25]**

Criteria	Weight	MONARC-1	MONARC-5	MR-401	MR-103G	1N Monopropellant
Manufacturer		Moog	Moog	L3 Harris	L3 Harris	Ariane Group
<b>Mass</b>	4	4	3	3	4	5
<b>ISP</b>	3	5	5	3	4	4
<b>Thrust</b>	2	4	5	1	4	4
<b>Flight Heritage</b>	1	5	5	5	5	3
<b>Total</b>	10	44	42	28	41	43

The thruster selected to provide ADCS control for this mission is the MONARC-1 produced by Moog. This thruster generates 1 N of thrust, weighs 0.38 kg, and produces a strong  $I_{SP}$  of 235s. These factors combine to make this thruster ideal for this use case.

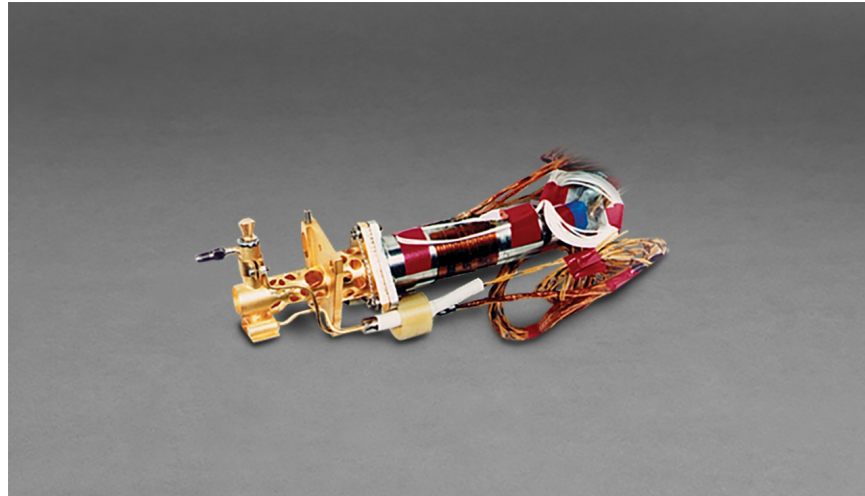


**Figure 8.3.1: MONARC-1 ADCS Thruster [23]**

In order to exert control in both directions across all three axes of motion of the spacecraft, 12 ADCS thrusters will be required. These thrusters will be oriented such that four thrusters are dedicated to each axis, allowing a torque to be exerted on each axis in either direction. The layout of the thrusters may appear similar to Figure 8.3.2.

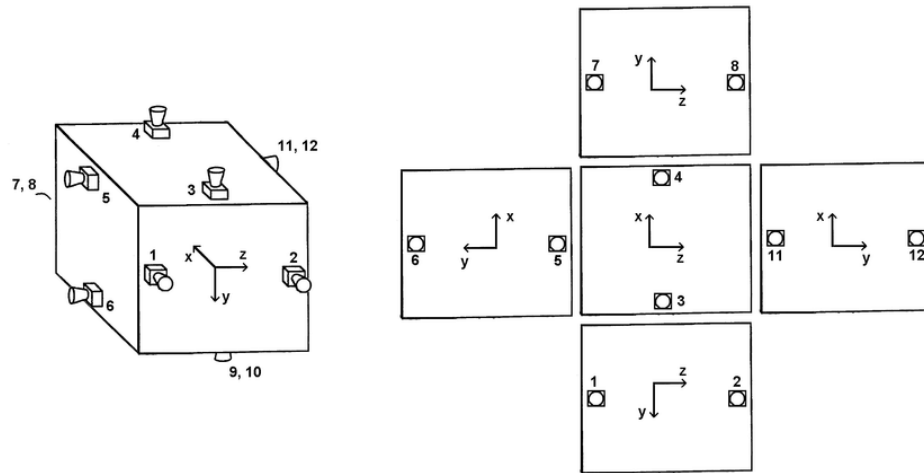


**Figure 8.3.2: ADCS Thruster layout [26]**

### 8.3.4.3 Propellant Budget

Having established the type of propellant and specified a thruster to be utilized, an initial estimate can be generated for the amount of propellant to be utilized. Based on equations from literature [27], and the manufacturer's stated  $I_{SP}$  for the primary thrusters of 317s, the delta-V

(dV) estimates for the spacecraft can be utilized to determine the amount of propellant required for the mission. Table 8.3.3 contains the propellant mass required for each individual burn the craft will be expected to perform, and the overall requirement for the mission.

**Table 8.3.3: Propellant Requirements**

Burn	dV (km/s)	Initial Mass (kg)	Final Mass (kg)	Propellant Expended
Europa Insertion	4.34	1000	247.7	752.3
Parking Orbit Departure	0.18	247.7	234.1	13.6
Landing Burn	1.88	234.1	127.8	106.3
Total	6.40	-	-	872.2

Current analysis for the mission will require 872 kg of propellant to perform the required orbital maneuvers for an initial lander mass of 1000 kg. Additionally, a propellant margin should be added for any anomalies which may be encountered during the mission, as well as any unusable propellant. This margin will be dictated by the overall propellant tank size, where the excess volume becomes the propellant margin for the mission. An intentionally oversized tank shall be selected to ensure this margin is sufficient.

#### 8.3.4.4 Thrust Budget

To ensure sufficient thrust to allow soft touchdown on the surface of Europa, the probe's TWR must be greater than one at the surface of Europa. Utilizing our current understanding of Europa's size and mass, a gravitational acceleration at the surface of the planet can be estimated as  $1.32 \text{ m/s}^2$  [28]. Therefore, considering the 200 kg expected dry mass of the spacecraft, to obtain a TWR of 1 at the surface of Europa requires 264 N of force from the thrusters. To ensure the craft can maintain good control and perform a soft touchdown, a higher TWR is desired. By analyzing other extraplanetary lander missions, the average TWR for these landers/rovers is 2.7. The selected thruster produces 111 N of thrust, and utilizing seven of these thrusters can produce a total thrust of 777 N, for a TWR of 2.9. This allows for some redundancy, where in the unlikely event of a single thruster failure a soft touchdown remains possible.

**Table 8.3.4: Lander TWR Analysis**

Mission	TWR at Landing
Mars Science Laboratory (Curiosity) [29]	3
Mars InSight [30]	2.3
Mars 2020 (Perseverance) [31]	2.8

### 8.3.4.5 Propellant Storage

The MMH and MON-3 propellants must be stored in tanks which minimize leakage, ensure fuel pressure remains high enough to ensure engine function, and are structurally sound enough to survive primary boost and the journey to Europa. In order to select an appropriate propellant tank, first the amount of MMH and MON-3 required for the mission must be evaluated.

First, MMH and MON-3 are not burned at an equal rate. While there is no publicly available mixture ratio for the AR-49, based on review of similar thrusters an expected oxidizer to fuel ratio is approximately 1.63 [28][29], where it is expected to consume (by mass) more MON-3 than MMH. Based on this ratio and the expected overall fuel consumption of 872 kg, 540 kg of MON-3 and 332 kg of MMH are required for this mission. Additionally, MMH will be utilized for ADCS thrusters, and an additional 5 kg of MMH will be added for that purpose.

Reviewing several options for MMH/MON-3 tanks [30][31][32][33], the average MMH/MON-3 tank holds 1.33 kg/L. This estimate will be used for initial tank sizing, which can later be refined utilizing additional information from the manufacturer. Based on this estimate, the MON-3 tank must have a minimum volume of 406 L, and the MMH tank 253 L.

When considering propellant tanks, three main factors were considered. First, the mass relative to capacity is the highest weighted factor, as minimizing mass is critical for the mission's success. Additionally, the overall capacity was considered, as the tank should be close in size to the minimum required propellant metric, with some additional space for propellant margin. Finally, flight heritage was considered for risk mitigation.

**Table 8.3.5: MMH Tank Selection Matrix**

Criteria	Weight	80318-1	OST 25/0	OST 25/3
Manufacturer		Northrop Grumman	Ariane Group	Ariane Group
<b>Mass</b>	5	3	5	5
<b>Capacity</b>	3	3	5	4
<b>Flight Heritage</b>	2	2	5	5
<b>Total</b>	10	28	50	47

For the MON-3 tank, the OST 25/0 manufactured by Ariane Group was selected. This tank, with a volume of 282 L and mass of 21 kg [33] provides a solution for MMH which allows for up to an 11% propellant margin over the calculated requirement.



**Figure 8.3.3: OST 25/0 Propellant Tank [34]**

The selection criteria for the MON-3 tank are largely the same considerations as the MMH tank. However, as there were no readily available single tanks in volumes suitable for the required propellant, tanks of smaller sizes were considered, to be combined in order to achieve the required volume of propellant.

**Table 8.3.6: MON-3 Tank Selection Matrix**

Criteria	Weight	80514-1	OST 25/3	OST 31-0
Manufacturer		Northrop Grumman	Ariane Group	Ariane Group
<b>Mass</b>	5	3	4	5
<b>Capacity</b>	3	4	3	2
<b>Flight Heritage</b>	2	2	5	5
<b>Total</b>	10	31	39	41

As stated, the MON-3 propellant will be split across multiple tanks. Two tanks have been selected, the larger OST 25/3 and smaller OST 31-0, both manufactured by Ariane Group. The larger OST 25/3 has a capacity of 331 L and mass of 22.7 L [33], and the smaller OST 31-0 has a capacity of 120 L and mass of 6.4 kg [32]. The combined volume of the two tanks holds 451 L of propellant, allowing for a 11% propellant margin.



**Figure 8.3.4: OST 25/3 Propellant Tank [34]**

The use of two tanks also provides an additional advantage. The propellant consumed by the initial burn to insert ECHO into a Europa orbit is sufficient to fully deplete the capacity of the large OST 25/3 propellant tank. This allows for the tank to be detached prior to the landing burn at Europa, reducing the weight of the lander and decreasing both the propellant and thrust required to de-orbit and land on the surface. This will leave the OST 31-0 tank to provide the propellant for de-orbit and descent.



**Figure 8.3.5: OST 31-0 Propellant Tank [35]**

#### **8.3.4.6 Bill of Materials and Subsystem Mass Budget**

Compiling the components currently selected to comprise this subsystem, a bill of materials (BOM) has been generated (Table 8.3.7). This BOM is not comprehensive, additional sensors and valves will be required to complete the subsystem, in addition to the plumbing and harness. A COPV will also be required to store pressurized nitrogen gas to maintain pressure within the propellant tanks. However, this BOM reflects the most significant and massive components of the subsystem. An additional 5-10 kg budget for additional propulsion hardware is expected.

**Table 8.3.7: Propulsion Subsystem BOM**

Model	Manufacturer	Unit Mass (kg)	Quantity	Net Mass (kg)
Thrusters				
AR-49	L3 Harris	0.54	7	3.78
MONARC-1	Moog	0.38	12	4.56
Thrusters Total				8.34
Tanks				
OST 25/0	Ariane Group	21	1	21
OST 25/3	Ariane Group	22.7	1	22.7
OST 31-0	Ariane Group	6.5	1	6.5
Tanks Total				50.2
Propellant				
Primary MON-3	-	-	-	540
Primary MMH	-	-	-	332
ADCS MMH	-	-	-	5
Margin MON-3	-	-	-	60
Margin MMH	-	-	-	43
Propellant Total				980
<b>Subsystem Total</b>				1038.54

As reflected by the BOM, the mass requirement for the propulsion subsystem is problematic for the mission outlook. The propellant required consumes essentially the entire mission's mass budget, and the additional components and required infrastructure then exceed the remaining mass. The propellant margins can be reduced to bring the subsystem mass budget below the mission mass budget, however this bears significant risk for the mission's success, and is still insufficient to allow the remaining subsystems to fulfill their requirements.

### 8.3.5 Non-Technical Considerations

Considering non-technical factors will be important for the success of ECHO. Particularly due to the high profile and high cost nature of deep space missions, it is especially important to consider these factors as their effects can have consequences affecting hundreds, thousands, or even millions of people. Table 8.3.8 discusses the specific considerations for the propulsion subsystem of ECHO.

**Table 8.3.8: Propulsion Non-Technical Considerations**

Non-Technical Factor	Considerations
Ethical Responsibility	Ethical concerns include ethical sourcing of materials for the propulsion module. The use of materials such as Inconel is not uncommon for thruster nozzles, and other materials such as aluminum and titanium may be selected for propellant tanks and plumbing. Ensuring materials are ethically sourced with fair labor and environmentally conscious mining practices.
Public Health & Safety	Due to the selection of a Hydrazine derivative bi-propellant for ECHO, health & safety is a major concern. The dangers presented by Hydrazine exposure are numerous and substantial. Hydrazine is caustic, carcinogenic, and contact, ingestion, and inhalation of the chemical can have ranging health consequences. Utilizing industry best practices and proper PPE these risks can be effectively mitigated.
Cultural	There are no significant cultural considerations for the propulsion subsystem.
Social	There are no significant social considerations for the propulsion subsystem.
Environmental	Environmental hazards are a significant concern when working with Hydrazine. As discussed in public health and safety, there are numerous consequences of Hydrazine release into the environment, as a liquid or gas. Ensuring the propellant is properly contained to prevent accidental releases, and utilizing industry standard best practices for storage, testing, and disposal will mitigate these risks.
Economic	The propulsion subsystem may have a substantial cost attached, as thrusters, valves, tanks, and other components can have a significant cost. Selecting components with a lower cost and minimizing the use of custom components will help to minimize cost, without compromising the overall mission.

### 8.3.5 Risk Management

The propulsion subsystem carries a significant amount of risk, both to the mission objectives of ECHO and to the health & safety of the personnel asked to work on its assembly. While the unmitigated risks can be significant, with proper risk mitigation strategies the likelihood of mission success is not significantly affected by these risks. The risks and their mitigation strategies are tabulated in Table 8.3.6. This risk evaluation is not comprehensive but covers the most significant risks associated with this subsystem.

**Table 8.3.9: Propulsion Risk Management**

Hazard	Cause	Effect	Pre-RAT	Mitigation	Verification	Post-RAT
Propellant Leak	-Excessive Valve Leakage Rates -Plumbing Leaks -Propellant Tank Leaks	Severe Limitations on or Loss of Mission	2C	Use of components with flight heritage and substantial qualification testing. Additional valves and redundant seats to prevent single point failures and close off leaky components. Tanks and plumbing are housed within vehicle structure to mitigate risk of on-mission damage. Propellant surplus can accommodate some mild leaks.	Passing Internal & External leakage rate during acceptance testing prior to integration & launch.	2E
Insufficient Thrust	-Primary Thruster Failure -Insufficient Propellant -Propellant Feeding Issues	Loss of Mission	1C	Use of hardware with flight heritage and substantial qualification testing, thrust margin can accommodate multiple thruster failures. Propellant surplus to prevent premature fuel depletion.	Ensure all hardware passes acceptance testing prior to integration and launch.	1E
Exposure of Personnel to Hydrazine	-Improper handling -Leaks in components/test fixturing	Significant health consequences including death	1C	Utilize industry standard best practices for handling Hydrazine, utilize proper PPE	OSHA Exposure Guidelines	1E
Loss of ADCS Control	-Failure of ADCS Thrusters -Insufficient Propellant	Severe limitations on or Loss of Mission	2C	Utilize thrusters with extensive flight heritage, Propellant surplus to prevent premature depletion.	Ensure all hardware passes acceptance testing prior to integration and launch.	2E

### **8.3.6 Future Work**

Additional analysis must be completed to determine the required valves, regulators, transducers and other sensors, and plumbing to complete the propulsion system. Specifications for these components should be developed and appropriate components selected. Once the thruster layout and overall structural layout have been determined the plumbing can be designed to connect the thrusters to the tanks, with intermediate valves and sensors as needed. Additionally, further information regarding the components which have been selected should be obtained from the manufacturer to refine analysis.

The propellant budget for ADCS should be further investigated. The propellant required to desaturate the reaction wheels should be calculated, and the number of desaturations to be accounted for determined. This will further refine the propellant budget to ensure sufficient propellant for ADCS while avoiding excessive propellant margins.

The mass budget for this subsystem presents a substantial issue for the feasibility of this mission. Current analysis shows the propellant subsystem exceeding the mass budget for the entire mission, which is a significant problem. To overcome this, additional analysis should be undertaken to reduce the amount of propellant required to fulfill this mission. This can include reducing the dV required for the mission, adjusting maneuvers to be more propulsion-friendly, or utilizing thrusters with higher  $I_{SP}$ . Additionally, if allowable, an increased mass budget for the mission should be investigated to allow the additional components of this subsystem, including thrusters and propellant tanks, to become a less significant component of the overall mass budget.

## **8.4 Orbital Mechanics**

**Prepared by:** Andrew Olson

### **8.4.1 Definition**

The orbital mechanics subsystem is essential for mission success as it plans the path the ECHO lander will take through space and provides  $\Delta V$  requirements which directly relate to the mass budget. For the ECHO mission, the orbital mechanics team is responsible for designing a reliable and efficient series of transfers to take the ECHO lander from release from the orbiter, to landing on the Europa surface. The orbiter will be placed in its Jovian/Europian orbit using a Mars-Earth gravity assist, but the analysis of these orbital mechanics is left to the orbiter team and considered out of scope for the ECHO mission. Because of the similarity between the ECHO and Galileo missions, as well as the availability of Galileo data, analysis for the ECHO orbital mechanics will be done under the assumption that the orbiter is following the Galileo Jovian tour.

## **8.4.2 Objectives**

The primary objective for the orbital mechanics team is to develop a sequence of precise and efficient maneuvers to guide the ECHO lander from its release from the orbiter to a safe and successful landing on Europa's surface. The maneuvers will be optimized to minimize the required  $\Delta V$ , reducing the fuel and mass needed for the subsystem while maximizing mission efficiency. Another key objective is to ensure compliance with IADC standards by designing trajectories and operations that mitigate the creation of space debris.

## **8.4.3 Requirements and Constraints**

Before developing the orbital mechanics for the ECHO mission, it is essential to establish clear requirements to accurately define the design problem. The following list contains the primary requirements that will be considered throughout the design process:

- Ensure safe delivery of ECHO lander to Europian surface while minimizing environmental stresses during landing
- Minimize  $\Delta V$  during the landing maneuver
- Maintain communication with orbiter during landing maneuver
- Land at target site with optimal accuracy
- Mitigate space debris throughout all maneuvers
- Prevent contamination of Europa

To approach the problem, it is also essential to understand the initial orbit that the ECHO orbiter is in. The orbital mechanics of the orbiter are out of scope for this project, so analysis of similar historical missions was done to pick an initial orbit. Due to the similarity of the missions, NASAs Galileo mission was used as a reference model. In this mission, the probe performed an 11-orbit tour of the Jovian system. The second of these orbits had a perijove of 670,000 km and an apojove of 19,000,000 km [106] and will be the assumed initial orbit for the ECHO orbiter for all analysis conducted.

## **8.4.4 Analysis**

Preliminary  $\Delta V$  calculations were done by analyzing a series of Hohmann transfers to bring the ECHO probe from its initial orbit to a successful landing. In an attempt to improve efficiency, an aerobraking maneuver with Jupiter's atmosphere was investigated. Additionally, further analysis identified potential orbital maneuvers for future study to enhance mission efficiency even more.

### **8.4.4.1 Initial $\Delta V$ estimation**

As shown in the PDR (see Appendix 13.8), initial  $\Delta V$  calculations using the following mission architecture provided a  $\Delta V$  estimation of 6.4 km/s.

1. Orbiter aligns with Europa's SOI when both the orbiter and Europa are at their perigees in their respective orbits around Jupiter.

2. ECHO probe separates from the orbiter and executes a burn to enter a Europan parking orbit
3. ECHO probe executes a burn at apoapsis to exit the Europan parking and enter a Hohmann transfer towards the Europan surface
4. ECHO probe executes a powered descent to perform landing

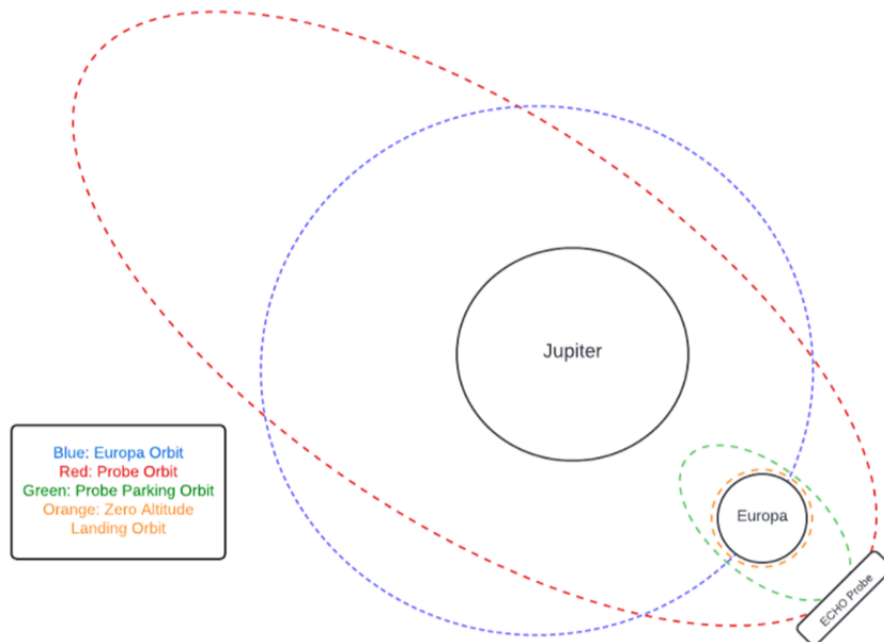


**Figure 8.4.1: Orbital mechanics architecture used in PDR calculations**

#### 8.4.4.2 Aerobraking

In an attempt to reduce the  $\Delta V$  estimation from PDR analysis, an aerobraking maneuver with Jupiter's atmosphere was investigated. The goal of this maneuver is to decrease the relative velocity between the probe and Europa at perijove, which is expected to lower  $\Delta V$  requirements. The architecture for transfer from probe separation to successful landing for this technique is outlined below and shown in Figure 8.4.2.

- **Phase 1 – Separation from orbiter and departure from initial orbit:** The first phase of the flight mechanics for the aerobraking method will involve separating from the orbiter at apojove and performing a perijove-lowering burn to bring the perijove within Jupiter's atmosphere.
- **Phase 2 – Perform aerobrake passes:** Once the perijove has been lowered, the probe will pass through Jupiter's atmosphere each time it reaches perijove. The drag from Jupiter's atmosphere will slow the probe down, lowering apojove with each pass.
- **Phase 3 – Departure from final aerobraked orbit:** After the apojove has been sufficiently lowered, a burn will occur at apojove to enter a Hohmann transfer that will take the probe into the same orbit as Europa.

- **Phase 4 - Insertion into Europen orbit:** At the end of the transfer ellipse, the probe will be located within Europa's SOI, and a burn will occur to insert the probe into the same orbit as Europa. Because the initial apojove of the transfer ellipse will have been lowered via aerobraking, the probe will be moving slower at the end of this transfer. This is intended to reduce the relative velocity between the ECHO probe and Europa at this location and reduce the  $\Delta V$  needed to enter Europa orbit, where most of the  $\Delta V$  arose in preliminary calculations. After this burn, the ECHO probe will be within Europa's SOI, and the relative velocity between the two will be zero.
- **Phase 5 - Ballistic Descent:** Once the probe has entered Europa's SOI, it will begin to experience gravitational acceleration toward the surface. The probe will utilize this to facilitate landing and will perform a final burn near the surface to bring its velocity to zero for landing.

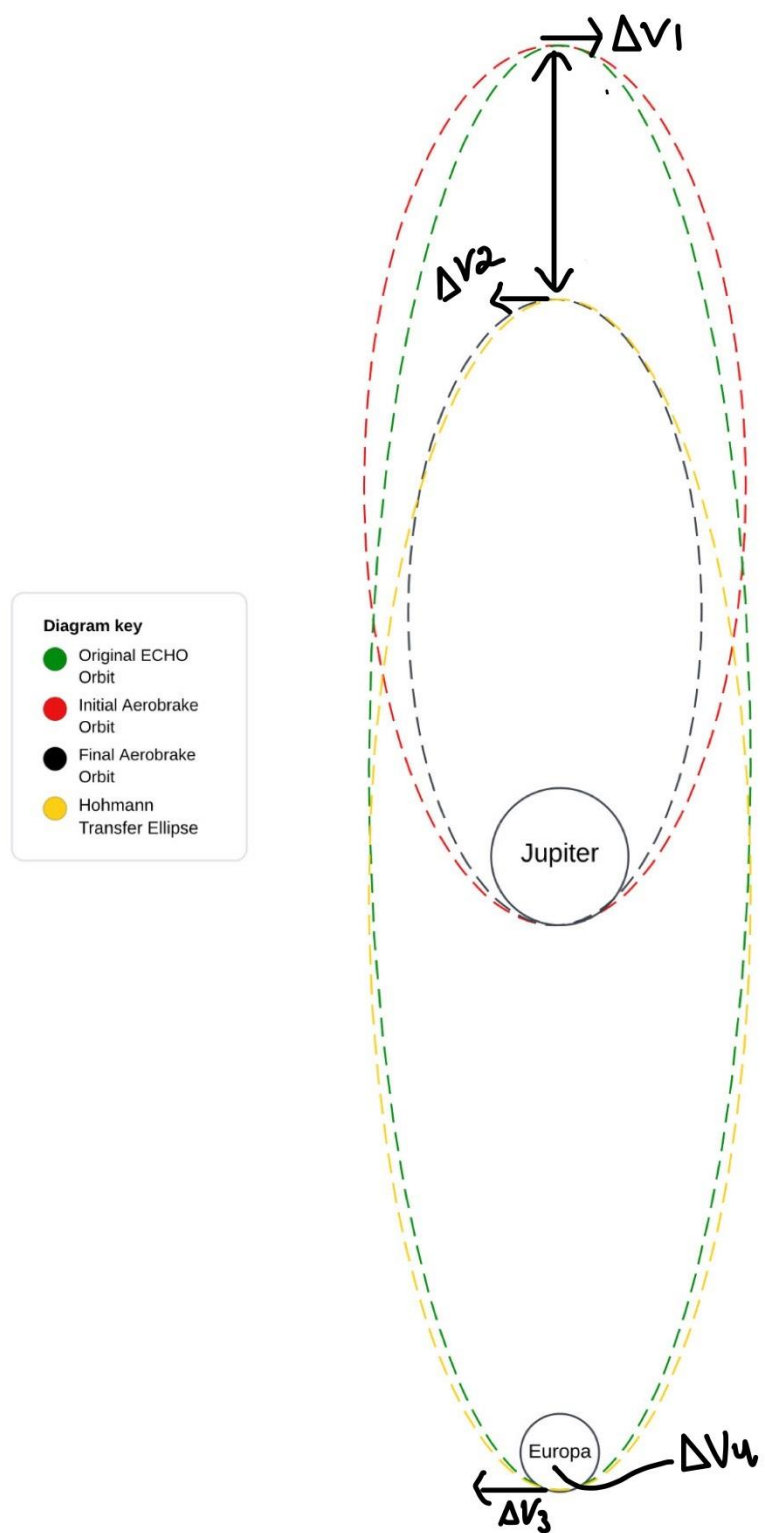
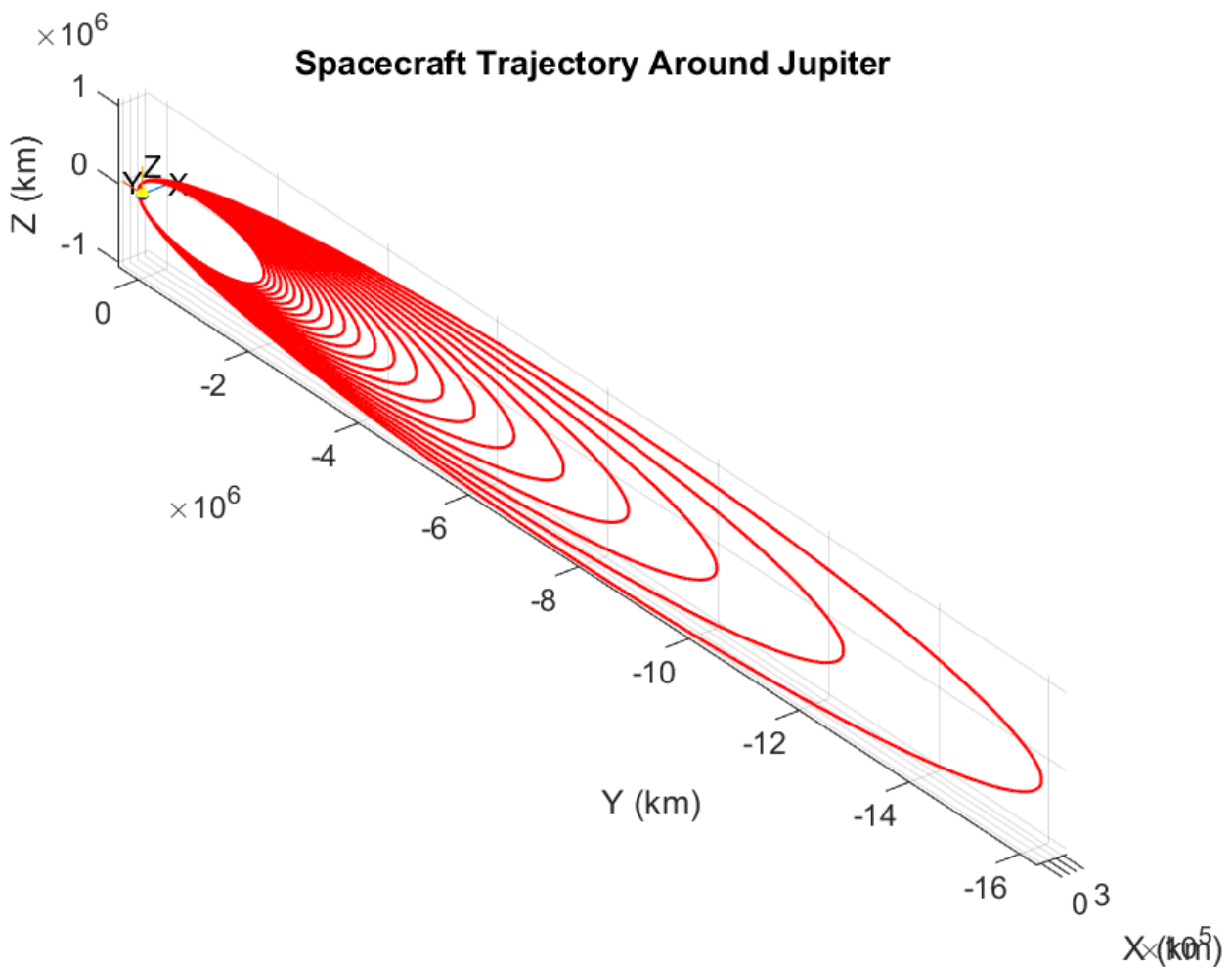


Figure 8.4.2: Aerobraking Procedure Architecture

This architecture contains four burns, and the  $\Delta V$  for each was calculated utilizing a MATLAB script as shown in Appendix 13.3. The aerobrake simulation was conducted by formulating the governing differential equation and using time-stepping methods to compute the state vector at each time step. The code for this portion of the script was adapted from code found in literature [36].

The initial burn reduces the perijove of the ECHO probe's initial orbit so that it resides within Jupiter's atmosphere, facilitating the aerobrake maneuver. For analysis the probe was arbitrarily placed into a 350 km altitude perijove, but future work will investigate optimizing this altitude to mitigate structural stresses and fuel requirements. The  $\Delta V$  required to enter this orbit was found to be 0.4523 km/s.

Once the aerobrake is initiated, each subsequent pass will further reduce the apojove of the orbit, as shown in Figure 8.4.3.



**Figure 8.4.3: Aerobrake Trajectory**

The second burn takes place at the apojove of the final aerobrake orbit to initiate the Hohmann transfer ellipse toward Europa's orbit, while the third burn occurs at the end of this transfer ellipse to insert the probe into Europa's orbit. The  $\Delta V$  for each of these burns depends on the apojove of the final aerobrake orbit, and thus this apojove becomes a design parameter that can be optimized to create the most efficient transfer plan. To discover the most efficient final aerobrake apojove, a second MATLAB script was created (see Appendix 13.4) which utilized equations from literature [37] to calculate the  $\Delta V$  needed for Hohmann transfers. This script calculated the  $\Delta V$  needed for each burn, as well as their sum, as a function of final aerobrake apojove radius. The results are shown in Figure 8.4.4.

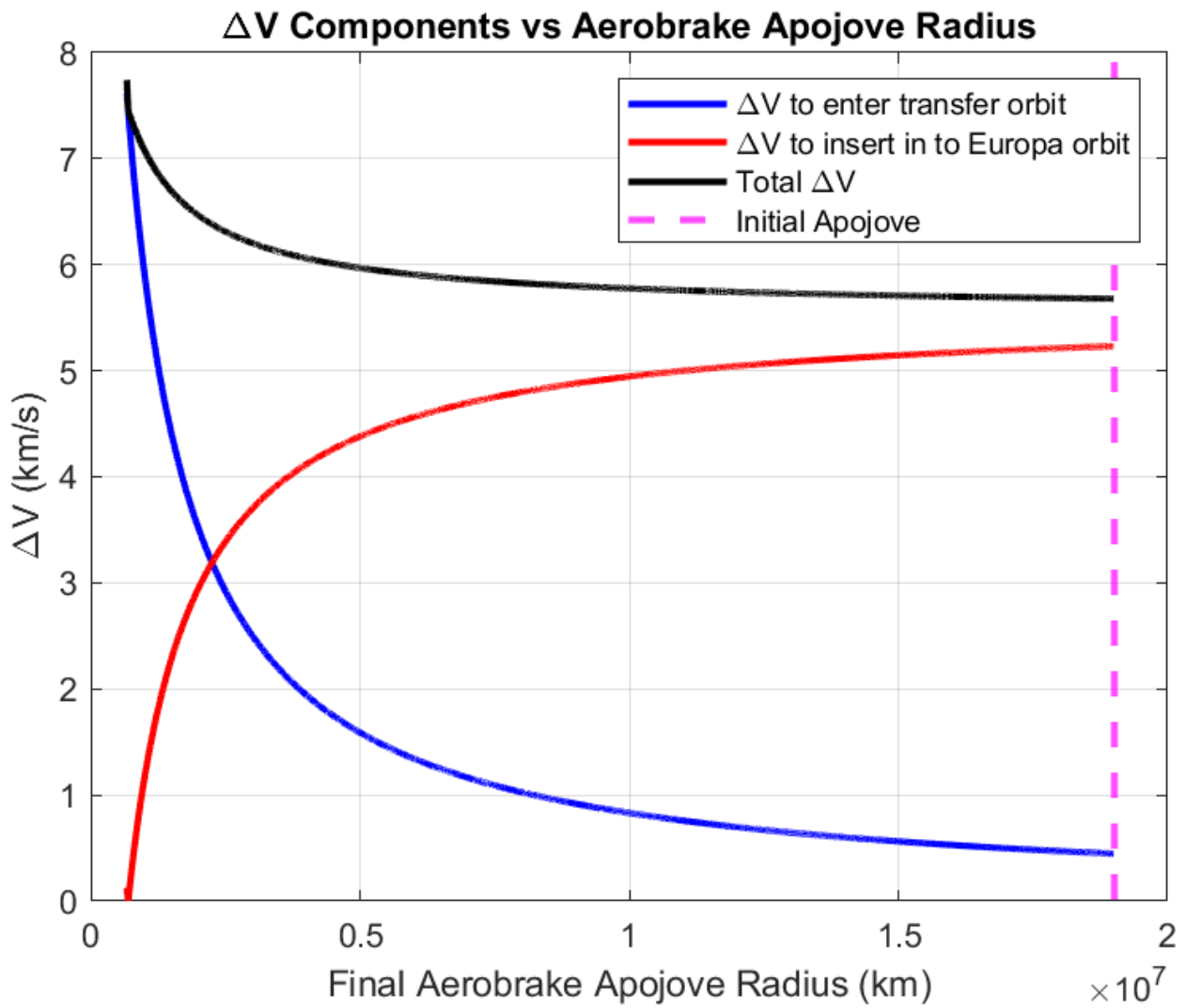


Figure 8.4.4:  $\Delta V$  for Transfer Ellipse as a Function of Final Aerobrake Apojove Radius

Interestingly, the results reveal an inverse relationship between the final radius and the required  $\Delta V$ . Lowering the final radius increases the  $\Delta V$  needed to enter the transfer ellipse, outweighing the corresponding reduction in  $\Delta V$  required for Europian orbit insertion.

The final  $\Delta V$  comes from the burn to bring the ECHO probe to stationary on the surface of Europa. For this segment of the analysis, it was assumed that the probe was positioned at the edge of Europa's SOI when inserted into Europa's orbit, with no tangential velocity relative to Europa at that point. These assumptions reduced this part of the analysis to a two-body problem, and the  $\Delta V$  was calculated for a ballistic descent approach by utilizing the conservation of orbital energy [37]. The  $\Delta V$  calculated corresponds to performing an instantaneous burn directly at the surface of Europa to bring the probe velocity to zero. An instantaneous burn is the most efficient type of burn, but is impossible to perform in practice and therefore the  $\Delta V$  calculated for landing is a slight under-estimation. This  $\Delta V$  was calculated to be 1.857 km/s, and all  $\Delta V$  values for different final aerobrake apojoove radius' are shown in table 8.4.1.

**Table 8.4.1:  $\Delta V$  Totals for Aerobraking Maneuver**

Number of Aerobrake Passes	Final Aerobrake Apojoove Radius (km)	$\Delta V_1$ (km/s)	$\Delta V_2$ (km/s)	$\Delta V_3$ (km/s)	$\Delta V_4$ (km/s)	Total $\Delta V$ (km/s)
0	$1.90 \times 10^7$	0.4523	0.4470	5.2318	1.857	7.9981
1	$1.63 \times 10^7$	0.4523	0.5182	5.1786	1.857	8.0061
2	$1.27 \times 10^7$	0.4523	0.6591	5.0734	1.857	8.0418
3	$1.04 \times 10^7$	0.4523	0.7982	4.9696	1.857	8.0770
4	$8.83 \times 10^6$	0.4523	0.9354	4.8672	1.857	8.1119
5	$7.65 \times 10^6$	0.4523	1.0708	4.7662	1.857	8.1463
6	$6.75 \times 10^6$	0.4523	1.2044	4.6666	1.857	8.1804
7	$6.04 \times 10^6$	0.4523	1.3363	4.5684	1.857	8.2140

Evidently, the aerobraking architecture is less efficient than the original series of Hohmann transfers designed in the PDR, even with the idealized instantaneous burn used for landing in the analysis.

It is worth noting that alternative orbital architectures were explored for transferring to Europa's surface following the aerobrake. One such approach involved aligning the probe with Europa at the final aerobrake apojoove and entering a Europian parking orbit from this point to facilitate landing. This method yielded a  $\Delta V$  of 9.7975 km/s. The second approach involved executing a perijove-raising burn at the conclusion of the aerobraking phase to align the ECHO probe with Europa at perijove. From this position, the probe would enter a Europian parking orbit, enabling a

subsequent landing. The most efficient simulation for this method resulted in a  $\Delta V$  of 7.7354 km/s, which, like the first approach, proved significantly less efficient than the original Hohmann transfer series design.

The inefficiency of the aerobrake maneuver for this mission combined with the added mass it would entail outside of fuel costs - mainly a heat shield - makes it clear that this technique is not a viable option for the ECHO probe.

#### **8.4.5 Non-Technical Considerations**

As with any subsystem, consideration of non-technical issues is an important aspect of designing the spaceflight mechanics subsystem for the ECHO probe. Multiple aerospace industry standards apply directly to the spaceflight mechanics subsystem and will be followed throughout the design process. The most relevant of these is mitigating any potential for space debris, as outlined by the Inter-Agency Space Debris Coordination Committee (IADC) [38]. To do this, future work will analyze the orbits of all known satellites in the Jovian system to ensure the risk of collision with the ECHO orbiter and probe will be mitigated. This will not only prevent any collisions which would cause space debris, but will add to the probability of mission success. While the orbital mechanics of the orbiter are out of scope for this project, communication with the orbiter team will occur to ensure proper disposal of the orbiter once its mission is completed so that any space debris will be prevented.

Additional potential non-technical considerations include ethical responsibility, public health and safety, as well as cultural, social, environmental, and economic factors. Of these, ethical, environmental, and economic are the most applicable to the spaceflight mechanics subsystem.

Environmental concerns center around potential contamination of bodies within the Jovian system as outlined by the NASA Planetary Protection Standard [39]. To mitigate microbial contamination risk, the ECHO probe will be chemically sterilized on Earth prior to launch. Additionally, future work will investigate graveyard trajectories in case of the unlikely event that the ECHO probe strays from its target trajectory. This will prevent an accidental crash landing and contamination on another celestial body.

Economic concerns will be addressed by following NASA's Cost Estimating Handbook [40]. This will ensure efficient use of public funding throughout the design process for the spaceflight mechanics subsystem.

All non-technical considerations for the ECHO probe are summarized in Table 8.4.2.

**Table 8.4.2: Non-Technical Considerations for the Orbital Mechanics Subsystem**

Non-Technical Factor	Considerations
Ethical Responsibility	The spaceflight mechanics system must adhere to all Inter-Agency Space Debris Coordination Committee standards for mitigating space debris. This includes analysis of all Jovian satellites to mitigate risk of collision, as well as communication with the orbiter team to ensure an established plan is in place for disposal of the orbiter once its mission is completed.
Public Health & Safety	The spaceflight mechanics system does not pose any threat to public health and safety as the scope of the project limits the spaceflight mechanics to the maneuvers performed within the Jovian system, much too far away to pose any threat to the public, even in the event of a maneuver failure or crash.
Cultural	The spaceflight mechanics system does not have any cultural considerations.
Social	The spaceflight mechanics system does not have any social considerations.
Environmental	The spaceflight mechanics team must consider potential contamination of both Jupiter and Europa throughout the mission. To mitigate microbial contamination, the probe will undergo rigorous sterilization on Earth prior to launch. Additionally, a graveyard trajectory will be designed for the ECHO probe as a contingency in the event of an unrecoverable deviation from the planned trajectory, ensuring the probe does not collide with any planetary bodies or moons.
Economic	The spaceflight mechanics team must optimize $\Delta V$ to lower the fuel mass required for the propulsion system. Reducing $\Delta V$ directly translates to increased mass budget efficiency and significant cost savings for the ECHO probe.

## 8.4.6 Risk Management

The orbital mechanics subsystem carries significant risks to mission success and the preservation of Europa's environment, including the potential for contamination of the surface and the creation of orbital debris within the Jovian system. While the unmitigated risks can be catastrophic, proper risk mitigation greatly reduces the likelihood of them occurring. The risks for the orbital mechanics subsystem are outlined in Table 8.4.3.

**Table 8.4.3: Orbital Mechanics Risk Mitigation**

Hazard	Cause	Effect	Pre-RAT	Mitigation	Verification	Post-RAT
Contamination of Europa and/or Jupiter	Transfer of microbial life from earth to Jupiter during aerobrake maneuver or Europa during landing	- False identification of microbial life on Europa - Danger to any potential microbial life on Europa	2C	ECHO Probe and orbiter will be chemically sterilized on Earth prior to launch	NASA Planetary Protection Standard Section 3.4 [39]	2E
Contamination of Jovian System Via Space Debris	Collision with Jovian satellites	- Generation of uncharted Jovian satellites creating difficulties for future missions	3D	- Future work will analyze all known orbits of Jovian satellites to prevent collisions - Future work will design graveyard trajectories for the ECHO probe should it deviate catastrophically from its intended path	IADC Space Debris Mitigation Guideline Section 5 [38]	3E

Running out of fuel	Inaccurate $\Delta V$ calculations for the mission	Failure to conduct a safe landing due to insufficient fuel for necessary burns. Loss of Mission.	1B	Future work will include extensive analysis of all maneuver's to ensure $\Delta V$ estimations are accurate so that sufficient fuel is taken on the mission. Additionally, a surplus of 5% above the necessary fuel found from $\Delta V$ calculations will be taken on the mission. This minimal surplus will keep mass as small as possible while allowing for correcting burns to be made throughout the mission.	N/A	1E
Crash landing into Europa Surface	- Poor landing site - Insufficient fuel for landing	Loss of the ECHO probe and mission	1C	- The ECHO probe will wait until the orbiter has made enough passes of Europa to provide sufficient data to select an appropriate landing site - Fuel Surplus will mitigate insufficient fuel concerns	N/A	1E

Trajectory Deviations	- Unexpected gravity perturbations from Jupiter moons	Waste of fuel to re-align trajectory leading to insufficient fuel to complete the mission	1C	- Thorough analysis will establish a flight corridor to keep the spacecraft within throughout the mission - Fuel surplus will mitigate insufficient fuel concerns and allow for correcting burns to keep the spacecraft within the flight corridor	N/A	1E
Timing Errors in Orbital Maneuvers	- Command failure - Unexpected firing rate and acceleration magnitude	- Missed optimal efficiency window increasing $\Delta V$ requirements	1C	- Extensive testing of ADCS and propulsions systems - Fuel surplus will mitigate insufficient fuel concerns	N/A	1E

#### 8.4.7 Future Work

Although a lower initial apojoove resulted in less efficient  $\Delta V$  for the aerobrake architecture, this trend does not hold for the Hohmann transfer based architecture presented in the PDR. Figure 8.4.5 illustrates the relationship between total mission  $\Delta V$  and the initial apojoove radius for the Hohmann transfer architecture detailed in the PDR, assuming the initial perijove is held constant.

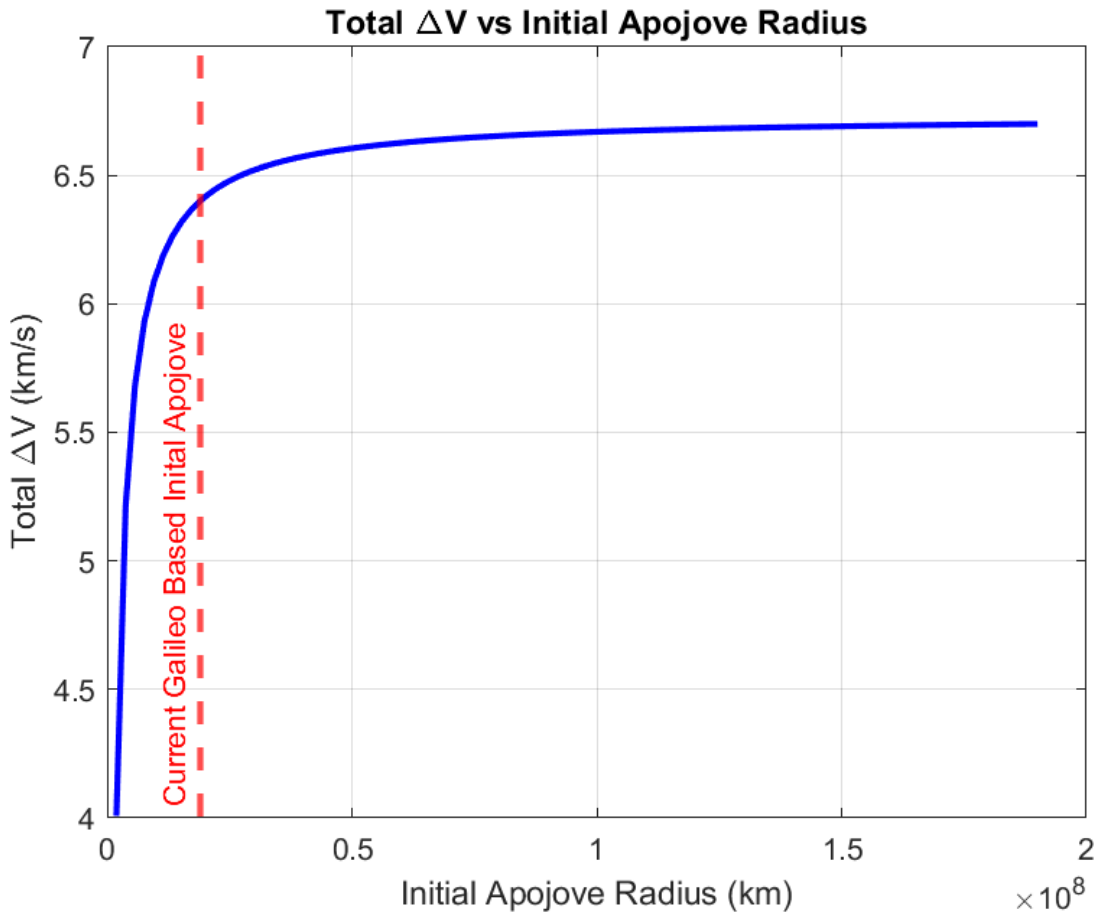


**Figure 8.4.5: Total  $\Delta V$  vs. Initial Apojove Radius for Hohmann Transfer Architecture**

Clearly, lowering the initial orbital apojoove yields a more efficient mission. This results from a decrease in relative velocity between the ECHO probe and Europa at perijove, leading to a more efficient insertion into the Europan parking orbit.

Future work will be focused on decreasing this initial apojoove through alternative methods. The reason that the aerobrake architecture did not yield more efficient results with decreased apojoove was because it required lowering and re-raising the perijove. That being said, future methods investigated will attempt to lower initial apojoove while keeping the perijove relatively unchanged.

One approach to consider is leveraging a gravity assist with one of Jupiter's 95 moons. By guiding the ECHO probe around the leading side of a moon within its SOI, the probe's velocity relative to Jupiter can be reduced due to the moon's gravitational pull. This maneuver would lower the apojoove of the orbit, enabling more efficient Hohmann transfers. Achieving this gravity assist would involve a series of small burns years prior to the maneuver, incurring minimal  $\Delta V$  as the adjustments would occur early in the mission.

Future work will include a comprehensive analysis of this mission architecture, examining the  $\Delta V$  required to position the probe for the gravity assist and the subsequent  $\Delta V$  savings. The study will focus on optimizing the timing, location, and magnitude of the burns and the gravity assist itself. Additionally, the selection of the assisting moon will be investigated, along with the feasibility of performing a sequence of gravity assists with multiple moons to further reduce the initial apojoove.

Additionally, future work will determine a flight corridor that the ECHO probe must be held within throughout its maneuvers for maximum efficiency. Communication ability between the probe and orbiter throughout the mission will also be determined, and efforts will be made to ensure all  $\Delta V$  predictions are accurate.

## **8.5 Attitude Determination & Control Subsystem (ADCS)**

**Prepared by: Aaryan Sonawane**

### **8.5.1 Definition**

As stated in the PDR, the ADCS consists of two different parts: attitude determination and an attitude control system. Attitude determination subsystem will consist of star trackers, sun sensors, magnetometers and an inertial measurement unit (IMU). Whereas, the attitude control system consists of reaction wheels, and traditional reaction control system (RCS) thrusters. The instruments within the two subsystems are bound together via a mathematical control law used for analysis of the performance of the ADCS.

### **8.5.2 Objectives**

The primary objective of the ADCS is to guide the pointing accuracy of the ECHO spacecraft throughout the course of the mission as efficiently as possible. For the purposes of the FDR, a desired angular velocity vector of [0,0,0] rad/s and euler angles of [0,0,0] degrees are used to analyze the performance of the ADCS when dealt with an initial non zero angular velocity and euler angle values.

### **8.5.3 Requirements and Constraints**

It is important to define clear constraints and requirements to complete for the success of the mission. Below are the mission objectives and constraints pertaining to ADCS

- The ECHO spacecraft must be come to a desired steady state of euler angles of [0,0,0] degrees with an angular velocity of [0,0,0] rad/s through the length of the mission
- The total mass budget of ADCS is 15 kg
- Maximize efficiency of the system to minimize energy usage

- Design attitude determination and attitude control subsystems with redundancy to minimize single point failures

## 8.5.4 Analysis

### 8.5.4.1 Attitude Determination

As stated in the PDR, three tiers of sensors were considered for the purposes of the ECHO lander. However, changes have been made since the PDR. The addition of sun sensors was deemed of high importance due to their reliability in tracking the location of the spacecraft. This means that the sensor suite now consists of 2x star trackers, 2x sun sensors, 2x magnetometer, and 2x inertial measurement units (IMUs).

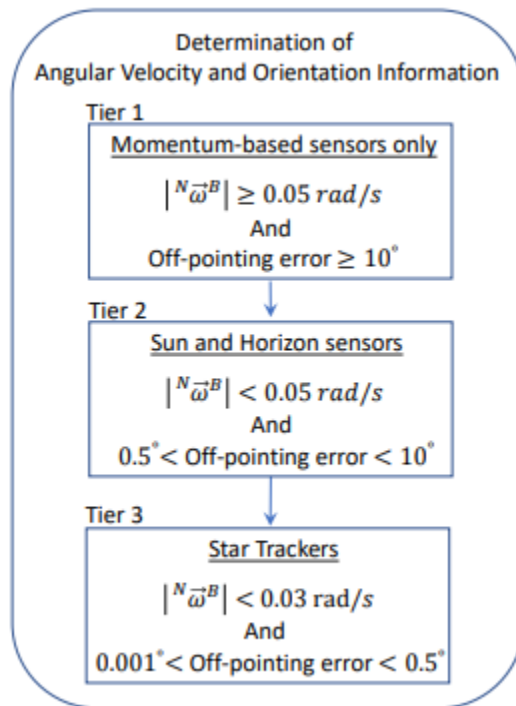


**Figure 8.5.1** Tier list of sensors

The micro-Advanced Stellar Compass ( $\mu$ ASC) from Denmark Technical University (DTU) emerges as the optimal Star tracker for the ECHO mission, offering exceptional performance while minimizing demands. The  $\mu$ ASC design is inspired by the ASC which was a star tracker used on the Juno spacecraft, signifying reliable flight heritage. At just 0.213 kg for a dual-redundant configuration, it weighs significantly less than competing options like the Space Micro STAR series, which range from 1.8 to 3.3 kg [41]. The  $\mu$ ASC's power consumption of 1.9W represents a dramatic improvement over alternatives, requiring less than half the power of even the most efficient Space Micro model (STAR-100M at 5W), and less than a third of the

power needed by the STAR-400M (18W) [42]. In terms of performance, the  $\mu$ ASC matches the best-in-class pointing accuracy of 0.00028 degrees.

While radiation tolerance specifications aren't explicitly stated for the  $\mu$ ASC, the documentation confirms its proven performance in extreme radiation environments including solar storms and the South Atlantic Anomaly, making it well-suited for the intense radiation environment around Europa. And going off the radiation specs for the ASC on which the  $\mu$ ASC is based, it will be able to sustain radiations up to 100krad [43]. For the purposes of the ECHO lander, two of the dual configuration  $\mu$ ASCs will be used.

**Table 8.5.1 Star Tracker Model Decision Matrix**

Manufacturer	Model	Mass (kg)	Power (W)	Radiation Tol (krad)	Pointing Acc (deg)
Space Micro	$\mu$ STAR - 100M	1.8	5	100	0.0014
Space Micro	$\mu$ STAR - 200M	2.1	8-10	100	0.0014
Space Micro	$\mu$ STAR - 200H	2.7	10	100	0.00028
Space Micro	$\mu$ STAR - 400M	3.3	18	100	0.0014
DTU	$\mu$ ASC	0.213	1.9	100	0.00028

The PNI RM3100 (MAGNET) stands out with its exceptional combination of low mass and high radiation tolerance. At less than 3g, it is over 13 times lighter than the flight proven magnetometer, ROMAP. Most importantly, MAGNET's demonstrated radiation tolerance of > 300 krad significantly outperforms other specified devices [44]. The closest competitor, ZARM Technik, only tolerates 50 krad, while others like the NewSpace Systems NMRM and AACCS MM200 fail at just 10 krad and 30 krad respectively. While ROMAP has proven flight heritage from the Philae comet lander mission and comparable power consumption (0.75W), its larger mass and lower radiation tolerance make it less suitable for the purposes of the ECHO lander [45]. MAGNET's digital magneto-inductive technology eliminates radiation-sensitive components like ADCs and amplifiers, contributing to its superior radiation hardness while maintaining low power consumption (<1 W). This combination of minimal mass, proven radiation tolerance, and reasonable power requirements makes it the optimal choice for Europa's challenging radiation environment. In fact, the MAGNET is an ongoing NASA project to build a magnetometer with the purpose of being used for a Europa landing mission. For the purposes of the ECHO spacecraft, two of these devices will be used.

**Table 8.5.2 Magnetometer Model Decision Matrix**

Manufacturer	Model	Mass (g)	Power (W)	Radiation Tolerance (krad)
GomSpace	NanoSense M315	8	Unk	Unk
AAC Clyde Space	MM200	12	0.01	30
NewSpace Systems	NMRRM-Bn25o485	85	0.75	10
ZARM Technik	FGM-A-75	330	0.75	50
TU Braunschweig	ROMAP	40	0.75	Unk
PNI	RM3100 (MAGNET)	<3	<1	100

The Redwire Space Coarse Pyramid Sun Sensor was picked as the top choice due to its high radiation tolerance, wide field of view (FOV), and lower mass. The Redwire Coarse Sun sensor is a pyramidal assembly containing 4 sensors arranged in a pyramid structure. The Pyramid Sun sensors have an extremely high flight heritage, most notably used in NASA's STARDUST mission which travelled to Comet Wild 2 out in deep space [46].

**Table 8.5.3 Sun Sensor Model Decision Matrix [47, 48, 49, 50]**

Manufacturer	Model	FOV (± deg)	Mass (kg)	Power (W)	Pointing Acc (deg)	Radiation Tol (krda)
Redwire Space	Coarse Pyramid Sun Sensor	$2\pi$ coverage	0.13	0	± 1°	> 100
Redwire Space	Digital Sun Sensor	± 64°	1.35	0.5	± 0.25°	100
Redwire Space	Fine Pointing Sun Sensor	± 4.24°	2.03	< 3	± 0.01°	100
Bradford Space	Fine Sun Sensor	± 69°	0.375	0.25	± 0.3°	100
Space Micro	Coarse Sun Sensor	± 60°	0.01	0	5°	100

Arranging two assemblies of this pyramid upside down will allow the ECHO spacecraft a field of view of  $4\pi$  Steradians [51]. This means that the spacecraft has an active field of view along

the entire sphere of space around it. 4 of these assemblies will be used for the ECHO lander in total to incorporate redundancy.



**Figure 8.5.2: RedWire Space Pyramid Sun Sensor Assembly**

Inertial Measurement Units (IMUs) are added to the spacecraft in case of tumbling. Star Tracker and sun sensors help detect the spacecraft's orientation with respect to the fixed location of certain stars and they can be extremely accurate when it comes to pointing. However if the spacecraft is undergoing rapid rotations, the IMU which consists of 3 Gyros and 3 Accelerometers within its assembly work hand in hand to determine the orientation of the spacecraft. The gyros are used to detect the angular velocity whereas accelerometers detect the linear acceleration of the spacecraft. These operate in all 3 axes and nowadays even contain a 3 axis magnetometer included in the assembly. The bias stability measures how much the gyroscope or accelerometer output drifts over time without any input and the ARW/VRW measures the amount of noise in the IMU data measured. The lower these numbers, the higher the accuracy of the IMU is.

**Table 8.5.4 IMU Model Decision Matrix [52, 53, 54, 55]**

Manufacturer	Model	Mass (kg)	Temp range (°C)	Power (W)	Gyros	Accelerometers
Honeywell	HG170 0	0.95	-54° to 85°	3	Bias Stability: 1°/hr ARW: 0.125°/rt(hr)	Bias Stability: 1µg VRW: 0.065 m/s/√Hz
Northrop Grumman	LN-200 S	0.74	-54° to 71°	12	Bias Stability: 1°/hr ARW: 0.07°/rt(hr)	Bias Stability: 1µg VRW: 0.11 m/s/√Hz
Safran	STIM3 77H	0.055	-40° to 85°	2	Bias Stability: 0.3°/hr ARW: 0.15°/rt(hr)	Bias Stability: 0.04 µg VRW: 0.07 m/s/√Hz
VectorNav	VN-110	0.125	-40° to 85°	2.5	Bias Stability: 1°/hr ARW: 0.0833°/rt(hr)	Bias Stability: <10µg VRW: <0.04 m/s/√Hz

For the ECHO mission, the VectorNav VN-110 was chosen due to its low power usage, high temperature function, inclusion of a 3 axis magnetometer and good stability with an extended kalman filter onboard the assembly to mitigate gyro drifts over time. For mission ECHO, the VN-110 would have radiation hardened to 100k krad as there are currently no radiation specs available online. 2 of the VN-110 assemblies will be used for the ECHO spacecraft.

### 8.5.4.2 Attitude Control

For the actuators for the ECHO spacecraft, it was determined that reaction wheels and magnetorquers would be used as per the PDR. However, after feedback and consideration, a set of RCS thrusters have been added to provide optimal control torques and the use of a magnetorquer assembly was not considered further due to the short duration of the mission.

Reaction wheels are designed for the purposes of the mission. For the ECHO lander, high flight heritage momentum + reaction wheel assembly was considered. Moreover, the reaction wheels chosen will still have to be designed to survive in a 100k krad radiation environment. This process is called radiation hardening (RAD HARD). Moreover, a pyramidal configuration was chosen to add redundancy to the design in case one of the reaction wheels fails.

**Table 8.5.5 Reaction Wheels model decision matrix [56, 57]**

Manufacturer	Model	Mass (kg)	Peak Power (W)	Peak Torque (Nm)	Peak Momentum (Nms)
Honeywell	HC7	<4.5	130	0.2	6
Rocket Lab	RW4-0.4	0.77	84	0.1	0.4
NewSpace	NRWA-T065	1.55	1.7	0.02	0.00094
Rockwell	RSI45	<7.7	90	0.075	45
Blue Canyon	RW4	3.2	10	0.25	4

Based on the mass constraints of the mission along with a required max RW torque of 0.6 Nm calculated, the Rocket Lab RW4-0.4 was chosen to be the most optimal choice for the purposes of the ECHO mission. The Blue Canyon RW4 is another strong choice with a higher tolerance for peak torque and peak angular momentum. However, after running its specs in the model control system, it was found that the settling time to 1 degree was 350s compared to a settling time of 337.7s for the RW4-0.4 configuration when the spacecraft is given an initial  $\omega_m = 2.0 * [-1.1, -1.25, -0.33]$  rad/s. The RW4-0.4 has the best peak torque and peak momentum performance per kg. In the design for the ECHO lander, some changes will have to be made to build a configuration suitable for the ECHO lander. Assuming the reaction wheels specs are scaled by a factor of 2, the mass of 1 wheel becomes 1.54kg. Subsequently, the reaction wheel

pyramidal assembly is designed in a  $45^\circ$ ,  $35.26^\circ$  Pyramidal configuration to mitigate a potential single point failure and incorporate redundancy [58].

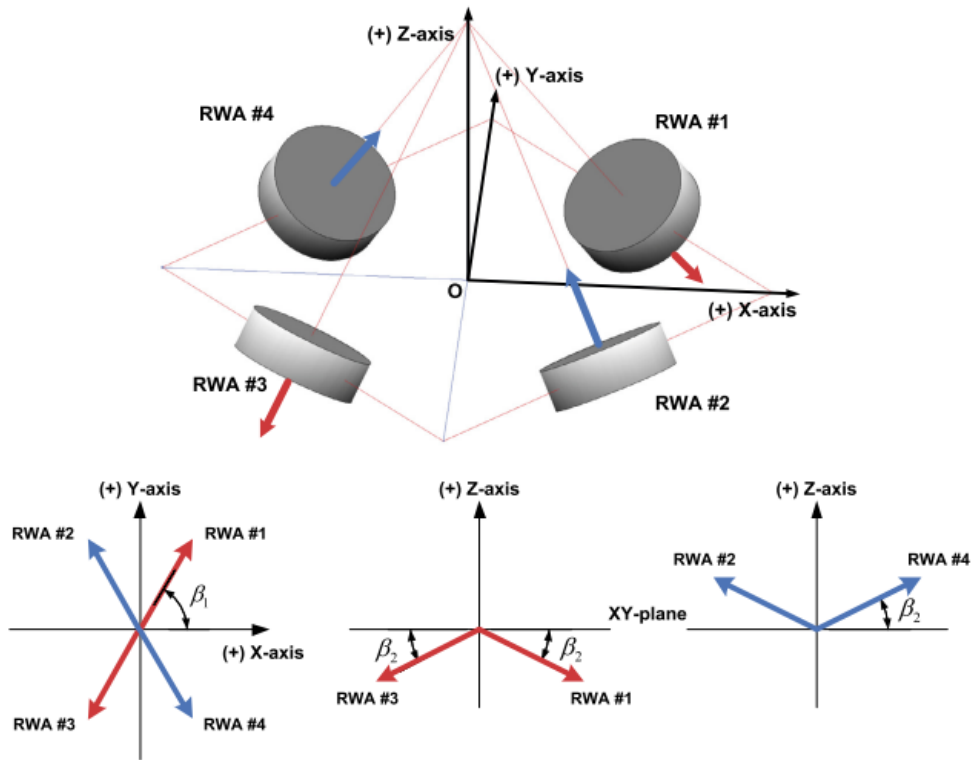


**Fig. 1.** Reaction wheel array in the pyramid configuration.

### Figure 8.5.3: Reaction Wheel Pyramid Configuration

For the sake ECHO lander,  $45^\circ$ ,  $35.26^\circ$  angled pyramid provides a reliable amount of torque around what is called a momentum envelope. Reaction wheels spin in upwards or downwards direction to create control torque. And in a pyramidal configuration, two of the wheels will be spinning up and the other two in a downwards direction.

The layout of the RCS Thrusters selected for the purposes of the mission is detailed in Figure 8.3.2 and follow a 12 unit configuration with 4 thrusters units in each axis providing 1 N of Force.

#### 8.5.4.3 ADCS Simulation

A control system was modelled in MATLAB using the control law given by Professor Kurt Anderson's Space Vehicle Design Primer. The control law is implemented using partly quaternion and partly angular velocity control with different gains associated with traditional PD control. The control law is given by:

$$M_C = -K_q \times qe - K_{om} \times om_{error}$$

Where  $M_C$  is the total control torque being applied,  $K_q$  is the quaternion gain term,  $qe$  is the quaternion error term,  $K_{om}$  is the derivative error term relating to the angular velocity values and  $om_{error}$  is the angular velocity error. The given framework served as a reference to model the ADCS for the ECHO spacecraft.

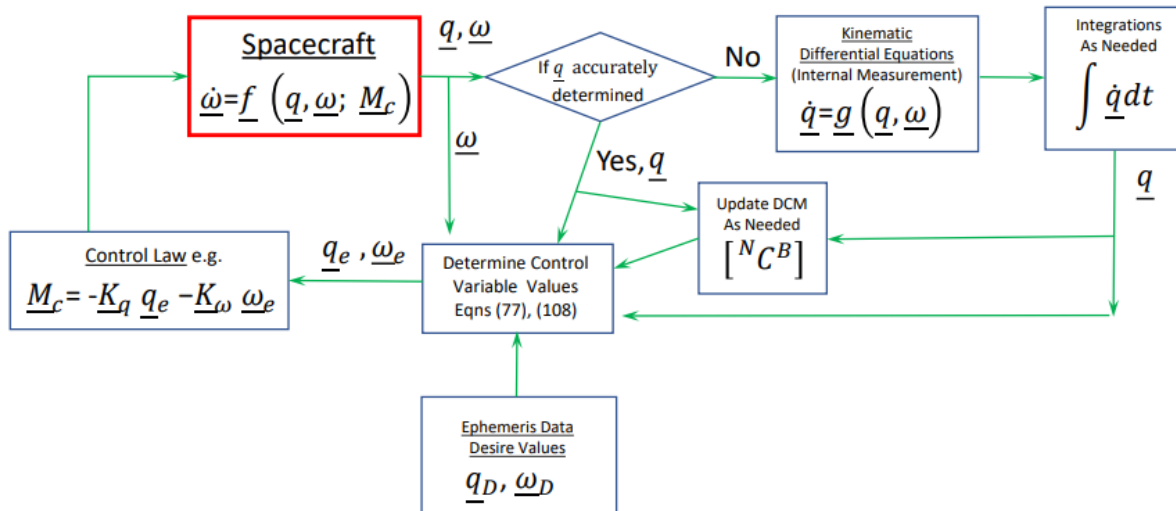


**Figure 8.5.4 Framework of ADCS Control law**

For the sake of the simulation, the sensor suite has been assumed to collect perfect data. The biggest considerations when modelling the ADCS of ECHO were keeping the total control torques applied within saturation limits for each individual reaction wheel along with each thruster unit. The maximum control torque applied by a reaction wheel was assumed to be 0.2 Nm as per the specs of the RW4-0.4 along with the maximum momentum of the wheel equalling 0.8 Nm-s. Maximum thrust torque was equal to 4 Nm in one singular axis. So, combined the thrust torque available is 12 Nm. The goal was to get the spacecraft pointing to a reference angle [0, 0, 0] degrees and [0, 0, 0] rad/s by applying appropriate control measures. Even though Euler Angles are used for visualization, the math used to calculate the errors was done by using the direction cosine matrices and quaternions in order to avoid singularities in calculations. Reaction wheel pyramidal configuration along with the 12 unit thruster design is used to control the orientation of the spacecraft with a given initial angular velocity of  $om = 1.0 * [-1.1, -1.5, -0.33]$  rad/s along with an initial set of euler angles given by  $EA = 0.1 * [-1.0, 10, -2]$  rad. The gain arrays for the spacecraft were predetermined and were given by  $K_q = 100 * [2, 3, 4]$  and  $K_{om} = 600 * [1.5, 2, 2.5]$  and a simulation is run over the course of 500 seconds. The inertia matrix for the spacecraft is given as  $I = [467.4, 390.2, 518.5]$  kg-m<sup>2</sup>. No external disturbance torque was added for the purposes of the ADCS simulation.

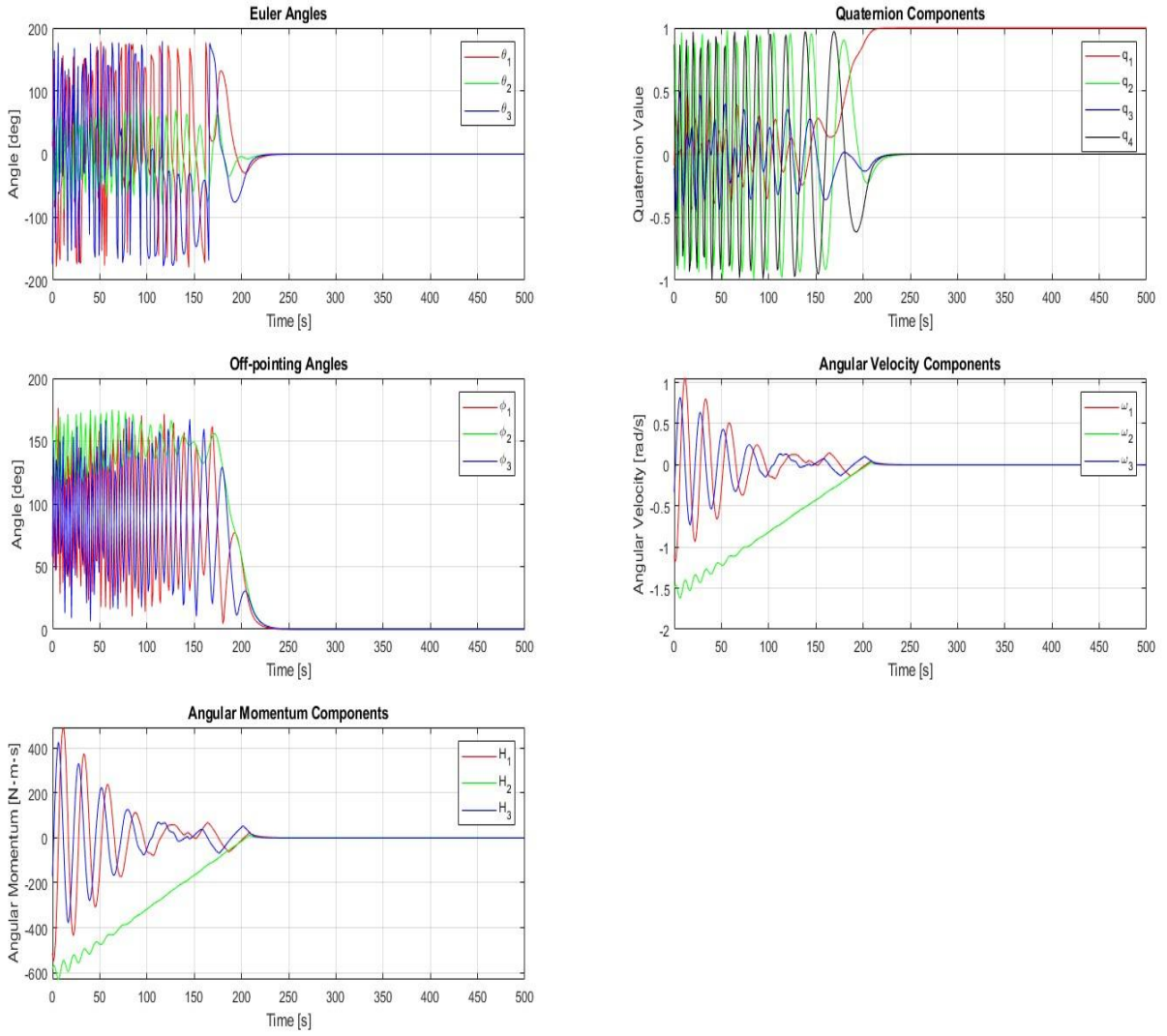


**Figure 8.5.6: Attitude States of the ECHO Spacecraft**

Given the above initial conditions, the simulation was run and state space, actuator specific and system performance data was collected. The settling time for the ADCS subsystem was estimated to be 234.47 s. Now, this might seem like a large number but it is worth remembering that the spacecraft weighs over 1000 kg and not a model point mass. The system starts out with a large angular velocity and angle error oscillating continuously for the first ~200 s of the simulation. The constant oscillation can be visualized through imagining the reaction wheels and thrusters working at full force. The thrusters, by design, are made to handle the majority of the control torque and reaction wheels aid in fine pointing.

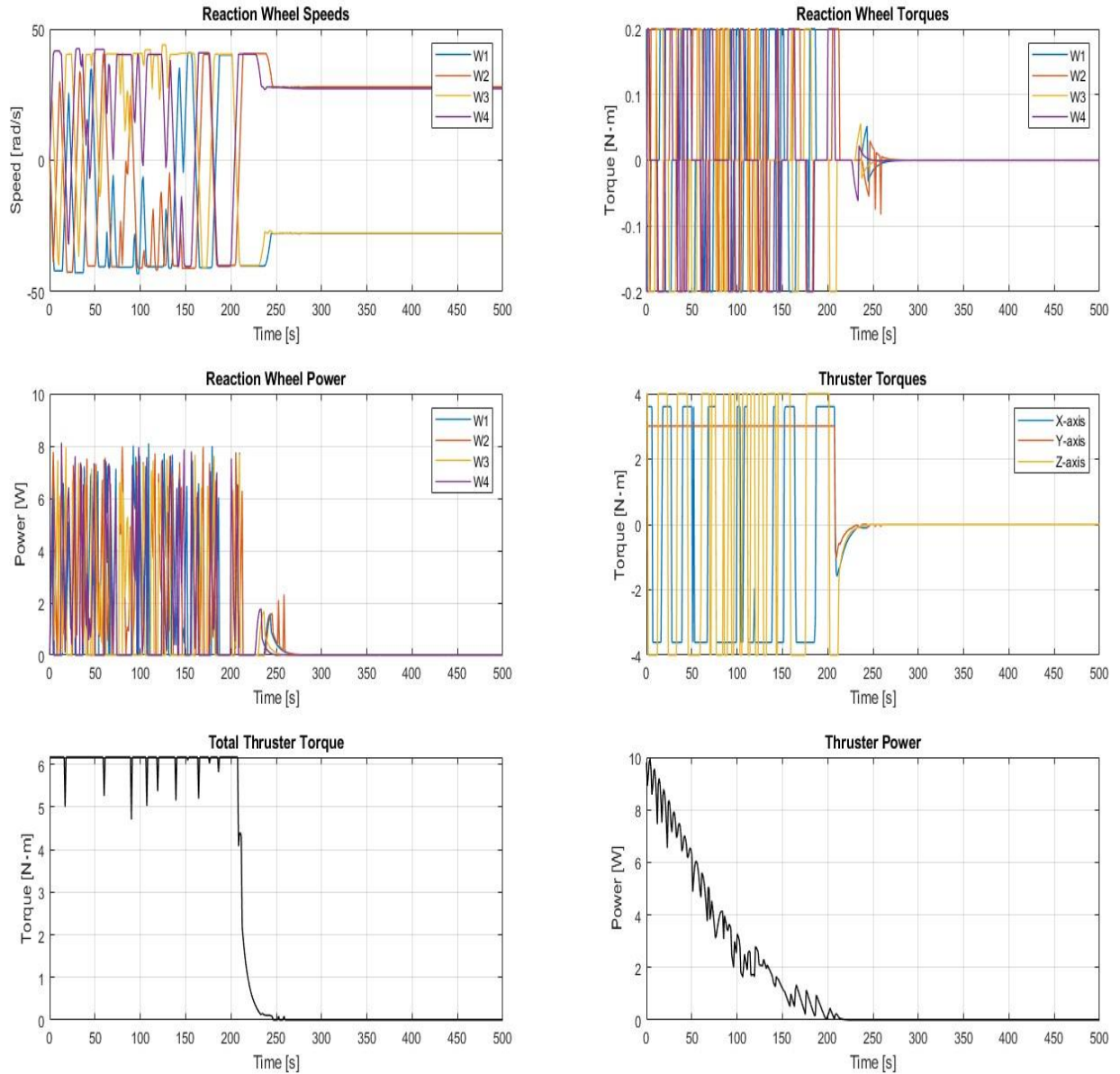


**Figure 8.5.7: Actuator Performance of the ECHO Spacecraft**

The reaction wheels and thrusters constantly operate near saturation. As suggested, the reaction wheels operate in pairs within the pyramid with 2 wheels producing upward torque and 2 producing downward control torque. Whereas, the thrusters operate in a configuration of 4 per axis, where 4 thrusters combine together to produce 1 N of force in their axis. The total power consumed by the actuator assembly came out to be 747.79 Ws, which over the span of a 500 s simulation comes out to 1.5 W power consumed, showing excellent energy efficiency.

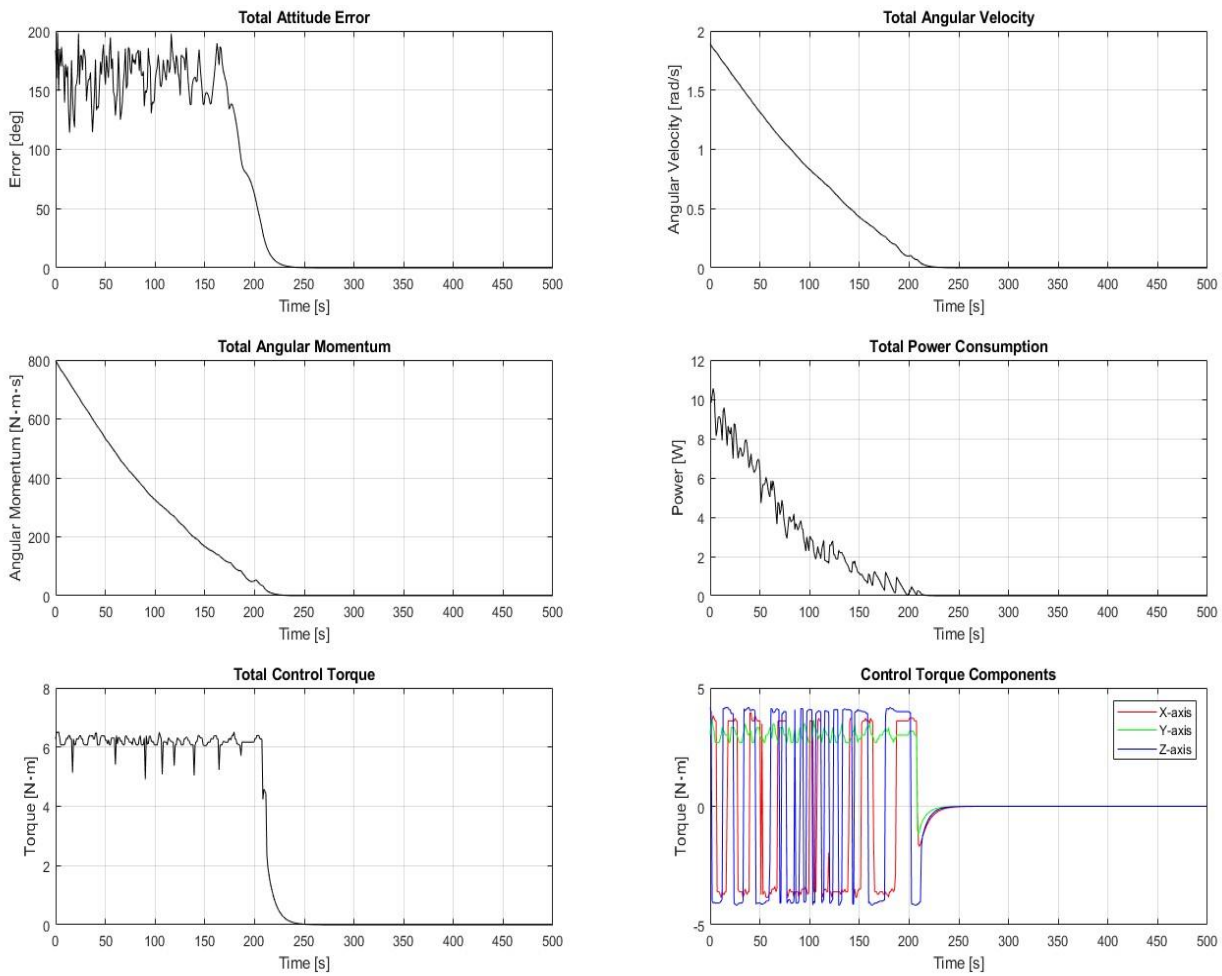


**Figure 8.5.8 System Performance of the ECHO Spacecraft**

The tumbling process is clear to see based on the oscillating nature of the state space variables in Figure 8.5.4. Constant oscillations of the angular velocity of the spacecraft indicate constant tumbling, verified by the euler angle and off pointing angle plots as well. It is worth noting that the total angular velocity and momentum plots are constantly decreasing along with the power consumed, indicating optimal control based on the given ADCS constraints of the problem.

The total ADCS mass is calculated in Table 8.5.6.

**Table 8.5.6: ADCS Total Mass Utilized**

Manufacturer	Model	Type of Instrument	Mass (kg)	Number of Parts	Total Mass (kg)
DTU	$\mu$ ASC	Star Tracker	0.213	2	0.426
PNI	RM3100	Magnetometer (MAGNET)	<0.0003	2	0.0006
Redwire Space	Coarse Pyramid Sun Sensor	Sun Sensor	0.13	4	0.52
VectorNav	VN-110	IMU	0.125	2	0.25
Rocket Lab	RW4-0.4	Reaction Wheels	1.54	4	6.16
					<b>Total Mass: 7.8326 kg</b>

The allocated mass budget for the ADCS was estimated as 15 kg and this design falls much below that design threshold.

## 8.5.5 Non Technical Considerations

Consideration of non technical factors is equally important for the success of the mission. Table 8.5.7 discusses the specific non technical considerations for the ECHO mission for the ADCS.

**Table 8.5.7: ADCS Non-Technical Considerations**

Non-Technical Factor	Considerations
Ethical Responsibility	There has been no attempt by the designer to infringe on any Intellectual Property when suggesting parts pertaining to ADCS for the ECHO lander. Relevant companies will be contacted to further update the design as per the requirements and constraints.
Public Health & Safety	The presence of thrusters and reaction wheels contains highly flammable and quick rotating parts. Special care must be taken by the engineers in charge of this specific hardware.
Cultural	There are no significant cultural considerations for the ADCS subsystem.
Social	There are no significant social considerations for the ADCS subsystem.
Environmental	ADCS thrusters are a significant concern when working with hydrazine. Utilizing industry standard best practices for storage, testing, and disposal will mitigate the biggest risks when it comes to the monopropellant like accidental leaks.
Economic	The customer's return on investment for the project remains at the forefront of all decisions while picking components reliable for the success of the mission.

## 8.5.6 Risk Management

Mitigating risk when it comes to ADCS is crucial for the success of the ECHO mission. Working with monopropellants along with designing instruments for the purposes of the mission is essential for the success of the mission. Some potential hazards and mitigation strategies are detailed in table 8.5.8.

**Table 8.5.8 ADCS Risk Assessment and Mitigation**

Hazard	Cause	Effect	Pre-RAT	Mitigation	Verification	Post-RAT
Star Tracker and Sun Sensor Failure	Radiation exposure, temperature fluctuations	Loss of Primary Attitude determination	2C	Redundancy incorporated so backup sensors are added for each part	Components tested and built for 100k krad environments	1E
IMU Drift	Radiation exposure, temperature fluctuations	Loss of attitude dynamics sensing	1C	Extended Kalman filter incorporated into the IMU assembly + redundancy incorporated	Temperature testing, Components will be tested and built for 100k krad environments	2E
Reaction Wheel Failure	Bearing Wear, radiation exposure	Loss of fine pointing control	1C	Pyramidal configuration allows for single wheel failure without loss of 3-axis control	Life cycle testing of the bearings, Components will be tested and built for 100k krad environments	2E
Control System Failure	Software errors, hardware failure	Loss of Attitude Control commands	2C	Robust flight computer testing, quaternion based control applied to mitigate singularities in calculations	Hardware testing needs to be up to date and software validated	2E
RCS Failure	Propellant Leakage	Loss of Primary Attitude Control	2C	4 units on each axis to provide redundancy, additional valves and redundant seats are added to prevent leakage	Internal & External leakage rate during acceptance testing prior to integration & launch.	2E

## 8.5.7 Future Work

The above simulation is an extremely simplified model at attempting ADCS. However, this simulation offers insight into potential design considerations. Future work in ADCS requires contacting the companies making the selected parts and moving forward with a mission specific design, suitable for high radiation and temperature fluctuating environments. Sensor test data

should also be incorporated through a Kalman filter along with modelling the control system through the use of a Linear Quadratic Regulator where ADCS is modeled through a loss function. Incorporating external torques is also crucial in the next step in building an even more accurate ADCS simulation for the ECHO spacecraft. Along with these considerations, the script will have to be updated with the specifics of the designed actuators that will be used for the purposes of the ECHO mission along with iterating and finding optimal reaction wheel pyramid configuration angles as well.

## 8.6 Thermal Management

Prepared by: Constantine Childs

### 8.6.1 Definition

The thermal control system of ECHO is designed to maintain all lander components within an acceptable temperature range. This ensures continuous operation of components at maximum efficiency throughout all aspects of the flight. A hybrid system, consisting of both passive and active methods as outlined in the PDR, will be implemented. For passive elements, multi-layer insulation (MLI), coatings, heat pipes, and RHUs will be used, with coatings recently added as an additional item. Active elements of the thermal control system will consist of electric heaters and a radiator.

### 8.6.2 Objectives

To address the extreme environment the lander will encounter in Jupiter's orbit and on Europa's surface, the objective of ECHO's thermal control system is to maximize thermal energy retention while effectively regulating the temperature of the lander's components.

### 8.6.3 Requirements and Constraints

The subsystem is required to be efficient in both thermal energy management and the given mass and volume budgets due to limited space. Components must be durable and reliable in order to maintain efficiency over a range of temperatures. Specific operating temperature ranges for each lander component that the thermal control system is responsible for is tabulated in Table 8.6.1. Ranges were taken from Gilmore's *Spacecraft Thermal Control Handbook*, Brown's *Elements of Spacecraft Design*, or from the component's manufacturer if available.

**Table 8.6.1: List of Temperature Ranges for Specific Lander Components**

Component	Temperature Range (°C)
Structures	-46 to 54[59]
Propellant (MON-3/MMH)	-30 to 50[60]
Command (OBC FERMI))	-20 to 50
Battery	0 to 30
IMU	-40 to 85[61]
ADCS Thruster (MONARC-1)	5 to 45
Sun Sensor	-80 to 120
Star Tracker (DTU $\mu$ ASC)	0 to 30
Magnetometer (PNI RM3100)	-40 to 85[62]
Antenna	-30 to 60[63]
Camera	-30 to 40
Sensors	-10 to 55
Electric Heater	-200 to 200

## 8.6.4 Analysis

### 8.6.4.1 Overview

The worst-case cold and hot temperatures are needed to characterize the environment that the lander will experience. The worst-case cold temperature and hot temperature (assuming a spherical spacecraft) are given by Eqs. 8.6.1 and 8.6.2, respectively [64],

$$T_{\text{MAX-S}} = \frac{G_s \alpha_s / 4 + q_{\text{IR}} \epsilon_{\text{IR}} F_{s-j} + G_s a \alpha_s K_a F_{s-j} + Q_w / (\pi D^2)}{\sigma \epsilon_{\text{IR}}}, \quad (8.6.1)$$

$$T_{\text{MIN-S}} = \frac{q_{\text{IR}} \epsilon_{\text{IR}} F_{s-j} + Q_w / (\pi D^2)}{\sigma \epsilon_{\text{IR}}}, \quad (8.6.2)$$

where

$G_s$  = solar constant

$\alpha_s$  = solar absorptivity of sphere

$q_{\text{IR}}$  = Jupiter IR emission

$\epsilon_{\text{IR}}$  = IR emissivity of sphere

$F_{s-j}$  = view factor, sphere to Jupiter

$a$  = albedo

$K_a$  = reflection of collimated incoming solar energy off a spherical Jupiter

$Q_w$  = electrical power dissipation

$D$  = diameter of spherical spacecraft

The worst-case cold temperature is calculated while the lander is in orbit around Jupiter at its initial apogee, and the worst-case hot temperature is calculated at its initial perigee. A MATLAB script used to calculate these temperatures is included in Appendix 13.5. Using Eqs. 8.6.1 and 8.6.2, the maximum temperature is -61°C, and the minimum temperature is -66°C. Both of these temperatures are well below the operating temperature range of many components. As such, MLI, RHUs, and electric heaters will be needed to retain heat in the lander.

#### 8.6.4.2 Thermal Control System Components

##### MLI and Coatings

The selected thermal control surface, as discussed in the PDR, is MLI, with the new addition of paints for the interior lander compartment. MLI is commonly used on both the exterior and interior of spacecraft to prevent heat loss or excessive heating. However, given the temperatures described in Section 8.6.4.1, the MLI blankets are used solely for insulation. The performance of MLI blankets can be characterized by the effective emittance,  $\epsilon^*$ , where smaller values are desired to reduce heat loss from radiation. A list of potential outer MLI materials was taken from the *Spacecraft Thermal Control Handbook*, and a decision matrix was used to select the specific material, as shown in Table 8.6.2.

**Table 8.6.2: Decision Matrix for Outer MLI Material**

Criteria	Weight	Tedlar (reinforced)	Kapton (coated and backed)	Teflon (backed)	Teflon (coated and backed)
Absorptance	2	2.5	3.5	1	1.5
Emittance	3	1	1	2	2
UV Resistance	2	2	3	3	3
Temperature Range	2	1	1	3	1
Mass	1	2	3	3	3
Total	10	16	21	23	20

For scoring, high absorptance and low emittance values received higher scores. Temperature ranges that intersected with the calculated minimum and maximum temperatures, as well as lower mass per unit area values, were also scored higher. Additionally, materials with better resistance to long-term UV exposure received higher scores. Based on the scoring, the selected material for the outer MLI blanket is backed Teflon. For the inner MLI material selection, the list of potential materials was again taken from the *Spacecraft Thermal Control Handbook* and evaluated using a decision matrix, as shown in Table 8.6.3.

**Table 8.6.3: Decision Matrix for Inner MLI Material**

Criteria	Weight	Aluminized Kapton	Goldized Kapton	Aluminized Mylar
Absorptance	2	1	2	1
Emittance	4	3	4	3
Temperature Range	2	4	4	3
Mass	2	3	3	4
<b>Total</b>	<b>10</b>	<b>28</b>	<b>34</b>	<b>28</b>

Scoring for the inner materials follows the same weights and logic as the outer material decision matrix. Based on the results, Goldized Kapton is the best material for the inner MLI blanket. The selected MLI insulation will be applied to every possible exterior surface of the lander. Further analysis is required to determine the number and thickness of layers needed to accurately assess its performance.

The interior compartment of the lander will use white paints to reflect internal radiation and help retain internal warmth. Table 8.6.4 lists potential paints for the interior, prioritizing those with high reflectivity values.

**Table 8.6.4: Decision Matrix for Interior Coating**

Criteria	Weight	GSFC NS74 White	P764-1A White	Z93 White
Reflectivity	7	4	2	3
Emittance	3	1.5	1.5	2
<b>Total</b>	<b>10</b>	<b>32.5</b>	<b>18.5</b>	<b>27</b>

From the decision matrix the GSFC NS74 white paint will be used to cover all bare surfaces inside the lander compartment where the electronics vault and MMRTG are located to help retain radiant heat.

### Heat Pipes and Radiator

Heat pipes offer a simple and passive way to transfer heat. The ECHO lander will use a variable conductance heat pipe (VCHP) due to its adaptability and ability to control the heat transfer rate, compared to constant conductance heat pipes (CCHP) [65]. VCHPs use both a working fluid and a non-condensable gas to transfer large amounts of energy from the evaporator (hot) end to the condenser (cold) end. Figure 8.6.1 shows a VCHP, with the evaporator on the left and the condenser on the right. The working fluid will be ammonia due to its low freezing point and flight heritage, and the heat pipe material will be aluminum, as ammonia is not reactive with it.

Further analysis and testing of the wick design are required, as it is not known how Europan gravity and the orientation of the lander (any slight deviation from the gravity vector could affect performance) will impact the heat pipe system. The heat pipe will be routed throughout the lander to control major components. The evaporator of the VCHP will be located on the MMRTG, as it is the component with the greatest output of waste thermal energy. The condenser location of the VCHP requires further analysis and iterations for potential placement. If it is determined that the VCHP will not be feasible, particularly given the unknown nature of the Europan surface, a CCHP will be used instead.

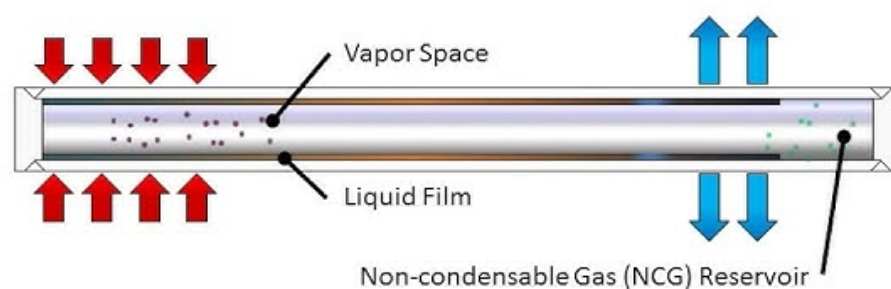


**Figure 8.6.1: Diagram of a variable conductance heat pipe**

The lander's radiator will be mounted on one of the structural side panels and will be made out of 6061-T6 aluminum due to its lightweight and large thermal conductivity. Approximate sizing of the radiator is given by Eq. 8.6.3 [66],

$$Q_w = A_R \sigma \epsilon_{IR} T^4, \quad (8.6.3)$$

where  $A_R$  is the area of the radiator. For a known worst-case value of waste heat that must be removed from the lander and the radiator temperature an initial radiator size can be calculated. For a worst case of 1 kilowatt waste heat using a 6061-T6 aluminum radiator at 294 K, a surface area of  $2.4 \text{ m}^2$  is required for the radiator. Further analysis may be required to determine if any coatings or paints can be applied to the radiator to increase its thermal performance.

### Radioisotope Heating Unit

In addition to the use of the MMRTG for thermal energy control, radioisotope heating units (RHU) will be required to compensate for heat loss to the environment. RHUs have been used in many deep space missions, such as Cassini-Huygens, Galileo, and the Voyager probes [67]. Traditional RHUs use the decay of plutonium-238 to generate thermal energy and output approximately 1 W of power. However, RHUs continuously output this heat and cannot be turned off. As a result, a variable RHU design (VRHU) has been selected for use on the ECHO lander. VRHUs have been used on the Thruster Cluster for the Cassini probe and combine the heating and temperature control into a self-contained unit without requiring any external energy [68]. The VRHU contains up to three RHUs in a rotating cylindrical holder. One side of the

holder is painted white for high emittance, while the other half is covered with MLI for low emittance. Temperature-sensitive springs that are thermally coupled to the hardware control the rotation, allowing for either the low or high emittance side to face the hardware. The springs can be calibrated for different temperatures based on the hardware that the VRHU is attached to, such as the propellant tanks [68]. Figure 8.6.2 illustrates the VRHU concept, which allows for heat to transfer either into the hardware of interest or out into the lander compartment.

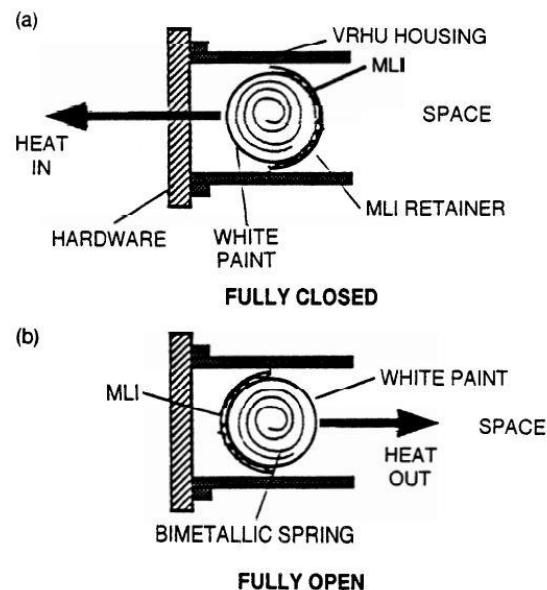


**Figure 8.6.2: Variable radioisotope heating unit concept [68]**

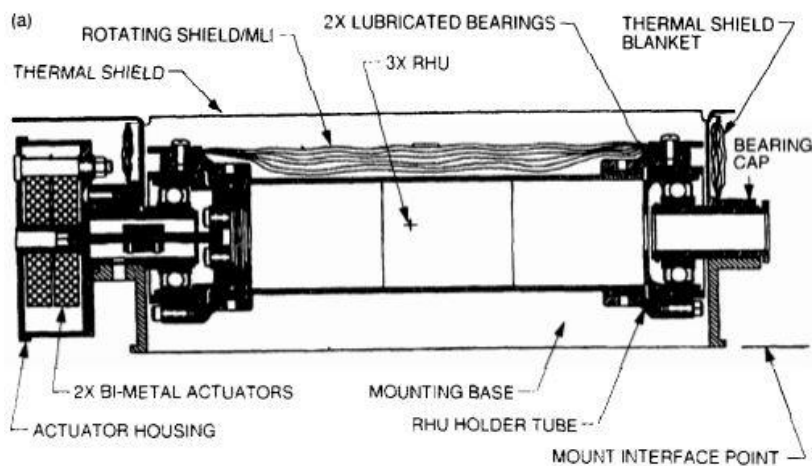


**Figure 8.6.3: VRHU diagram used on the Cassini spacecraft [68]**

Analysis for the number of RHUs required as well as the optimized locations for VRHU assemblies on components must be left for future work.

## Electric Heater

The two most common heaters used in spacecraft are patch heaters and cartridge heaters [69]. Both heater types will be used for the propulsion system. The patch heaters will be mounted on the propellant tank and propellant lines, and a cartridge heater will be used for the propulsion thruster assembly.

Control of the heaters will be controlled by solid-state controllers due to their reliability over a mechanical thermostat and precise temperature control. Due to the importance of maintaining the propellant above its freezing point, redundant heaters will be placed on the tank wired in parallel.

### 8.6.4.3 Thermal Finite Element Preliminary Analysis

A first iteration steady-state thermal finite element analysis of the lander superstructure, including the propellant tank and RTG, was conducted using Autodesk Fusion360 software. The lander structure boundary condition was set to the worst-case cold temperature of -66°C, and the MMRTG was set as a heat source emitting 400 W. The ends of the propellant tank were also set as heat sources at 15 W to simulate 6 RHUs and electric heaters applied to the tank. A 335,769-element mesh was generated, with surface contacts automatically detected using Fusion360 software.

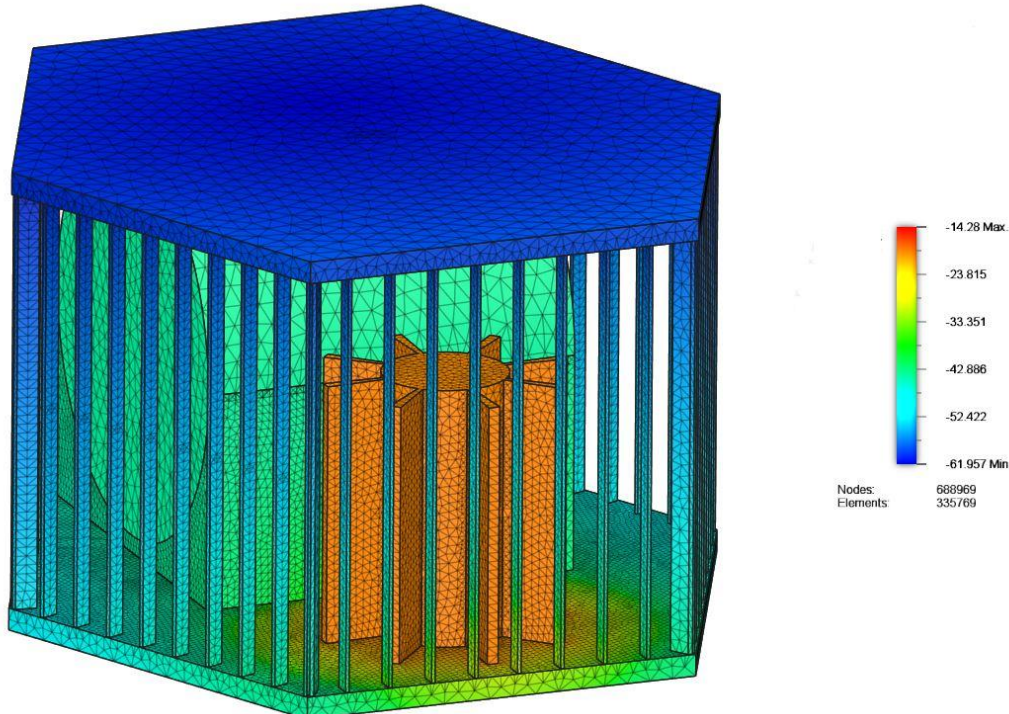


**Figure 8.6.4: Temperature distribution simulation result on the lander structure**

Note that the surface of the propellant tank in Figure 8.6.4 is at -43°C, which is below the required range for the propulsion system, and also does not analyze the temperature with loaded propellant.

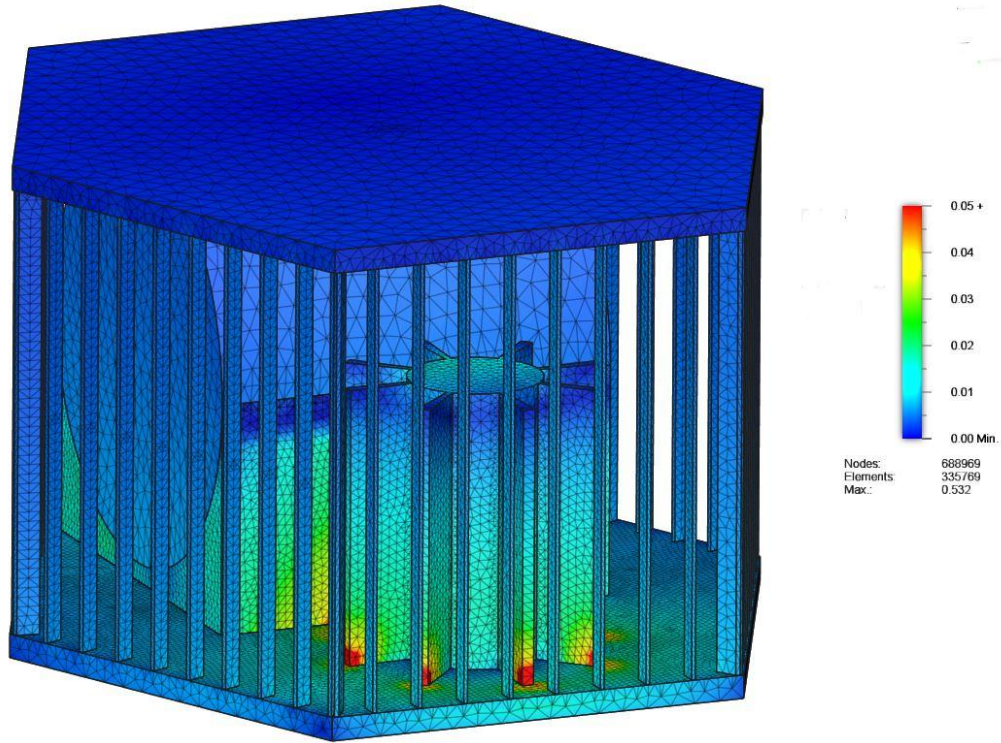


**Figure 8.6.5: Heat flux (in  $\text{W}/\text{mm}^2$ ) on the RTG to the lander's lower body panel**

Further thermal FEA analysis is required for individual components of the lander, as well as for a fully assembled flight configuration model with MLI and coatings, to accurately predict temperatures and fluxes. Iteration on different positions for the electric heaters and RHUs will be necessary to find the optimal locations on the propellant tank and other mission-critical components.

#### 8.6.4.4 Aerobraking Heatshield Preliminary Analysis

As discussed in Section 8.4.4.2 and the PDR, an aerobraking maneuver is being analyzed as a potential maneuver. Due to the extreme entry velocity and the subsequent interaction with the Jupiter atmosphere, a heat shield will be required for this maneuver. Only one other probe, the entry capsule of Galileo, has ever descended into the Jupiter atmosphere with a heat shield. The probe encountered the most extreme heating conditions ever experienced by a planetary entry capsule, with an estimated peak heating of  $35 \text{ kW}/\text{cm}^2$  [70].

From Section 8.4.4.2 an entry velocity of 56,860 m/s at 350 km is expected. However, because the lander is only performing an aerobraking maneuver, the integrated heat load is expected to be

lower than that of the Galileo probe. The heat shield used by Galileo was a 45 degree blunt cone shell made of a high density carbon-phenolic ablative as shown in Figure 8.6.6 [71].

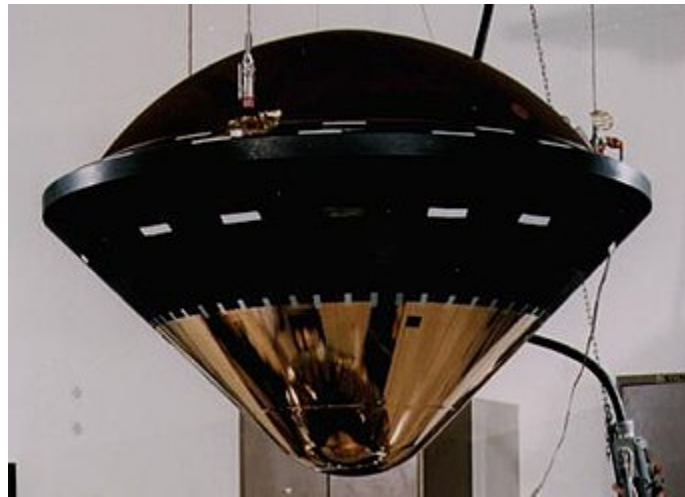


**Figure 8.6.6: Galileo entry probe heat shield [72]**

The ECHO lander will use the same high density carbon-phenolic ablative material and shape as the Galileo entry probe for its heat shield. CFD simulations must be completed to predict the radiative heat flux encountered and model the regression rate of the heat shield, which is outside the scope of this report. An initial case was set up using the open-source OpenFOAM software with the hy2Foam solver; however, due to computational costs and time constraints, results could not be obtained.

## 8.6.5 Non-Technical Considerations

All non-technical considerations are summarized in Table 8.6.5.

**Table 8.6.5: Summary of Non-Technical Considerations for the Thermal Control System**

Non-Technical Factor	Considerations
Ethical Responsibility	The designers of the subsystem have completed college-level courses on thermodynamics and heat transfer. Designs are reviewed by team members and consultants. Thorough technical analysis must be conducted in future work to ensure feasibility.
Public Health & Safety	Radioactive material in the radioisotope heating units (RHU) poses minimal risk to the public. The robust design and stringent handling procedures will minimize the risk of radiation exposure during all aspects of the flight..
Cultural	The thermal control system does not have any cultural considerations.
Social	The thermal control system does not have any social considerations.
Environmental	RHUs contain radioactive material and radiation exposure may pose a risk to the environment. Ammonia used in the heat pipe system also poses a risk if a leak develops. Design of the thermal system will follow the National Environmental Policy Act (NEPA) and safety protocols to reduce risk.
Economic	Thermal components are purchased from potential commercial contractors such as Dunmore, entX Limited, and Advanced Thermal Solutions. The thermal control system must operate within the given mission budget and allocate resources efficiently.

## 8.6.6 Risk Management

Potential hazards and their mitigations are summarized in Table 8.6.6.

**Table 8.6.6: Risk and Mitigation Table for the Thermal Control System**

Hazard	Cause	Effect	Pre-RAT	Mitigation	Verification	Post-RAT
MLI damaged or degradation	High speed debris or UV	Reduced internal temperature and possible component damage	2C	Use UV resistant outer layers	On-Earth testing of MLI performance after degradation simulation	3D
Heat pipe wick structure damaged	Excessive vibrations or forces, improper manufacturing	Disruption of fluid flow and reduced efficiency	2D	Testing of wicking structure and include backups	Use flight-proven hardware and assess performance	3E
Physical damage to the radiator	Launch, micrometeorite impacts	Overheating of lander components	2B	Design for durability and redundancy	Impact testing on radiator	4C
Radiation exposure from RHU/VRHU	Launch vehicle failure, improper handling or assembly	Death or severe personnel injury	1C	Durable containment and handle following safety protocols	Measure and monitor radiation levels	1E
Electric heater failure	Power supply, wiring issue	Freezing of propellant in tank or line	1C	Redundant heaters wired in parallel with multiple circuits	On-Earth testing of part failure and assess redundancy	2E

## 8.6.7 Future Work

Verification of the thermal control system design through simulations must be conducted. Thermal FEA on every component, from circuit boards to the final assembled spacecraft, must be performed for temperature analysis at the system level. Since the aerobraking maneuver, as shown in Section 8.4.4.2, has been determined to be infeasible, no further CFD or heat shield selection is required. The mass of the heat shield alone would have more than tripled the required mass budget of the subsystem, resulting in an overall lander mass that exceeds the allocated budget. The selection of manufacturers and specific component sizing, such as the radiator, variable conductance heat pipe, and electric heaters, must also be completed. Based on current component selections, the subsystem mass is expected to remain within the allocated budget. The

number of RHUs/VRHUs and electric heaters needed for the propellant tanks and other components must be analyzed through an iterative process. Further analysis of the feasibility of a CCHP or VCHP for the Europan surface must also be conducted through surface surveys and on-Earth testing.

## **8.7 Power**

**Prepared by: Mae Tringone**

### **8.7.1 Definition**

ECHO's power subsystem is responsible for providing the power necessary for all other subsystems to function for the entirety of their design life. It will consist of a NASA multi-mission radioisotope thermoelectric generator, paired with a secondary battery array to support loads greater than the RTG can handle.

### **8.7.2 Objectives**

The power subsystem's main and only objective is to supply power as it is needed by the lander's other components throughout the duration of its mission. The power subsystem will additionally ensure enough overhead is given to account for potential emergency situations and increased sustained power draw, for example in the event of necessary prolonged ADCS corrections.

### **8.7.3 Requirements and Constraints**

From the previous objective, the following requirements present themselves:

- The power subsystem must generate, supply, schedule and deliver power to the entire spacecraft for its entire mission life
- Enough nominal power must be generated during the transit stage such that all of the lander's components receive the minimum power required to stay active.

### **8.7.4 Analysis**

#### **8.7.4.1 Power Generation and Storage**

Spacecraft power will be generated singularly by a NASA Multi-Mission Radioisotope Thermoelectric Generator. This RTG weighs 43.6 kg and is capable of supplying 110W at the beginning of its operating life, and contains multiple safety features (including iridium cladding and graphite impact shells) which will protect the surrounding environment, both on Earth and on Europa, in the event of a catastrophic mission failure. [73]

Additionally, a bank of lithium-ion batteries will accompany the generator. This will allow for additional power to be supplied in the event that emergency maneuvering is required. There is not necessarily a limit to how much additional power would be advantageous to have; therefore,

the remaining mass budget of 6.4 kg will be preliminarily allocated to the secondary battery array.

There are many different types of lithium-ion battery chemistries on the market. Each respective chemistry has its own characteristics, and a large variety of advantages and disadvantages. Fully weighing the exact pros and cons of each for the mission would require much greater analysis, and a better understanding of each subsystem's exact power requirements, however the following decision matrix attempts to provide a brief summary of the more important criteria for the mission's secondary battery array, based on available datasheets [74].

**Table 8.7.1: Battery Chemistry Decision Matrix**

Criteria	Weight	Li-Co Oxide	Li-Mn Oxide	Li-Ni-Mn Oxide	Li-Fe Phosphate	Li-Ni-Co-Al Oxide	Li-Ti Oxide
Specific Energy	4	3	2	3	2	5	1
Discharge Rate	3	1	3	2	5	1	4
Cycle Life	2	2	1	3	3	1	5
Full Charge Voltage	1	5	5	5	4	5	3
Total	10	24	24	29	33	30	29

Ultimately, Lithium Iron Phosphate appears to be the best choice initially, due to its excellent discharge characteristics, in particular its ability to deliver up to 50 Amps of current in short discharge cycles [75]. However, it is important to note that it lacks in specific energy capacity, meaning it will not be able to discharge for as long as the other chemistries. It will unfortunately be difficult to further extrapolate on what type, brand and amount of lithium-ion battery will fit the mission best until subsequent design iterations narrow down several more specific requirements, in particular supply voltage, the exact nature of prolonged demand, and the expected achievable operating temperature of the craft.

#### 8.7.4.2 Power Scheduling

Power scheduling is integral to ensuring that all components are adequately powered per what degree of their capabilities is required for mission success. All subsystems will start powered with the bare nominal voltage required for diagnostic checks and status reporting until their full capabilities are needed. Systems will not be shut down until they are no longer required, as more frequent full power cycling runs the risk of damaging components.

The following table is an overview of the expected power delivery requirements from each subsystem during the course of the mission.

**Table 8.7.2: Power Scheduling**

Stage				
Subsystem	Launch	Transit	Descent	Landed
Science Suite (Variable)	Nominal	Nominal	Nominal	Full
Mechanisms (30-40 W)	Nominal	Nominal	Partial (30 W)	Full
Telecommunication (4 W)	Nominal	Nominal	Full	Full
Command & Data (5 W)	Full	Full	Full	Full
Propulsion (50 W)	Nominal	Nominal	Full	Shutdown
ADCS (7.5 W)	Nominal	Nominal	Full	Shutdown
Thermal (25 W)	Full	Full	Full	Full
Total Power Required	30 W	30 W	34 W Marginal, potential peaks of >91.5 W	Average load of 49-89 W, potentially larger peaks during scientific activities

Only Command and Data and thermal will be active for the entire mission, as the former is needed to analyze and compile engineering and diagnostic data during launch and transit, and the latter keeps the entire spacecraft at the correct operating temperature. The payload coupling system will contain a data link allowing the lander to use the orbiter's much more robust broadcasting system for telecom. In the event that this link system fails, arrangements can be made for the lander to autonomously aim and broadcast its engineering data to the orbiter's uplink antenna, requiring only a marginal increase in power consumption (and still well below the constant 110W supplied by the RTG).

The most demanding mission stage for the power subsystem is the landing stage. The craft will have all components except for its science suite fully engaged to allow for precise maneuvering and autonomous descent towards the surface of Europa. While it is not expected for the average peak to consistently max out the supplied power from the RTG, the secondary battery array will provide a safety net in the event that prolonged or rapid maneuvering is required, particularly from the propulsion and ADCS systems.

The power demand of the landing gear deployment mechanism is not considered. This is because the pin-pullers will only have to be actuated once, and will occur after the lithobrake maneuver is performed, but before final Europa descent begins. Since it is expected that nearly 70% of the RTG's total supply as well as the full battery capacity will be available at this stage, the load is not considered an issue at this time.

### 8.7.5 Non-Technical Considerations

Utilizing an RTG for the mission includes bearing the responsibility of ensuring the safe construction, transportation, and launch of radioactive material. A scuttled launch or hard landing could prove disastrous for the surrounding environment and population due to the risk of radiological contamination. While a safe launch is always a priority when planning for spaceflight, every precaution must be taken to ensure that the RTG's protective housing especially does not suffer a loss of structural integrity from launch to final escape from Earth, including minimizing exposure in the unlikely event that the mission must be aborted before leaving the suborbital flight stage.

**Table 8.7.3: Power Non-Technical Considerations**

Non-Technical Factor	Considerations
Ethical Responsibility	The design and construction process of the overall project will be probed regularly to ensure that every precaution is taken for the safety of anyone who must handle, or work within the proximity of, the RTG.
Public Health & Safety	The RTG poses a major threat to life and health if its radiological components are exposed. The RTG will be securely housed in an impact and radiation-resistant housing to ensure minimum exposure to the surroundings.
Cultural	PR will be used to ensure that the general public, especially those who live near the launch site, are well informed of the risks the RTG poses, and more importantly, the rigorous safety precautions that will be put in place to prevent any severe radiological hazard from affecting their health.
Social	There will likely still be opponents to launching a spacecraft with an RTG on board, even after public education is conducted. An empathetic approach is important to ensure cordial proceedings when handling opposing views.
Environmental	The RTG will be securely housed in an impact and radiation-resistant housing. This will ensure minimum exposure of the radioactive components to the surroundings, especially in the event of a scuttled launch.
Economic	The RTG (or the components needed to build one) may be difficult and expensive to procure. Budget will be dynamically allocated to address this as the project develops.

## 8.7.6 Risk Management

Table 8.7.4: Power Risk Assessment Table

Hazard	Cause	Effect	Pre-RAT	Mitigation	Verification	Post-RAT
Loss of power	Frayed wiring or contact damage during launch, transit, or landing	Catastrophic power loss	1D	Wiring secured to anchor points wherever possible; correct soldering practices used	Wiring runs and contacts inspected after each major construction step; extensive testing via multimeter to ensure current flows as expected	1E

## 8.7.7 Future Work

Future work will involve the further analysis of the specific power draw needed by each subsystem at every step of the mission. Particularly of focus is propulsion, ADCS, and telecom. These subsystems will involve short bursts of high power draw, rather than a low, continuous drain, and thus there is room for further optimization of the type of Li-ion battery required. Due to the fact that full power draw still remains below the maximum 110 W from the RTG, except in extreme cases, a less capable battery chemistry may be selected if its qualitative resilience to the space environment or energy density edge out that of Li-Fe Phosphate in a way that would improve mission success.

## 8.8 Command and Data

Prepared by: Chloe Powell

### 8.8.1 Definition

The command & data subsystem consists of an on-board computing system, data storage unit, and dedicated software. It is responsible for storing all data collected by the lander until it is transmitted to the orbiter, as well as data received from the orbiter. Commands that are transmitted are either performed immediately or stored to be performed at a later, specified time. All of these aspects of the subsystem must be low risk parts due to the scope of the ECHO mission and the harsh environment of Europa. Previously, a centralized system was selected for the on-board computing system. The specific computing system as well as the method of data storage and the flight software used must now be selected.

## **8.8.2 Objectives**

Each component of the command & data system has different objectives. The on-board computing system must be able to reliably and accurately process all commands it receives. The data storage unit must be able to store information and commands for prolonged periods of time without experiencing degradation. The flight software must have high performance and be capable of running all required tasks on board the lander.

## **8.8.3 Requirements & Constraints**

There are two physical aspects of the command & data system: the on-board computing system and the data storage unit. The combined mass and volume of these two units must fall within the mass and volume budgets specified in the PDR (see Appendix 13.8). The volume allocated for the command & data system is  $0.2852\text{m}^3$ . All computing systems considered are two to three times smaller than the maximum volume. A specific data storage unit has not been selected at this point in the design process, but the average volume of all data storage types is about three to four times smaller than the maximum volume [76]. The total volume of both pieces of hardware will fall within the volume budget. The mass budget allows for a total mass of 15 kg for the command & data system. Information on the mass of the on-board computing systems was not available for all systems considered. However, they are all either described as lightweight or have a listed mass of 0.3 kg. This will allow the command & data system to fall within the allocated mass budget, as well.

## **8.8.4 Analysis**

### **8.8.4.1 On-Board Computing System**

To select which highly integrated on-board computing systems to consider, NASA's *State-of-the-Art: Command & Data Handling* document was used [77]. Out of all the computing systems listed in the document, five were considered for the ECHO mission: Aitech Systems, Incorporated's SP0-S and SP1-S; Argotec's OBC FERMI and OBC HACK; and SPiN USA's MA61C cPCI serial space. The Europa Clipper mission uses radiation-hardened hardware that is designed to survive between 100 and 300 kilorad (krad) of radiation [78]. Because of this, only on-board computing systems that are designed to withstand at least 100 krad of radiation were considered. To further select the system used, many other criteria were considered. The most heavily weighted was reliability, which was quantified through flight heritage. Power consumed and volume were both weighted equally. There are limited power and volume budgets for the ECHO mission, so minimizing the power needed for the system and the amount of space it consumes within the bus is essential. Finally, Radiation Hardness Assurance (RHA) was considered. Only systems that could withstand a certain level of radiation were considered, so this was not weighed very heavily, as all units considered satisfied this constraint. However, it is still important to maximize the unit's capacity to withstand radiation. A decision matrix is shown

in Table 8.8.1 comparing all units considered. Three of the five on-board computing system options considered had no available information on past flights, so a score of 0 was assigned for reliability.

**Table 8.8.1: On-Board Computing System Decision Matrix**

Criteria	Weight	SP0-S	SP1-S	OBC FERMI	OBC HACK	MA61C cPCI
<b>Reliability</b>	4	5	0	5	0	0
<b>Power Consumed</b>	2.5	3	2	4	3	5
<b>Volume</b>	2.5	2	2	4	4	5
<b>Radiation Hardness Assurance (RHA)</b>	1	3	3	5	5	4
<b>Total</b>	10	35.5	13	45	22.5	29

Based on the criteria described in the decision matrix in Table 8.8.1, Argotec's OBC FERMI was selected to be the highly integrated on-board computing system on the lander. The OBC FERMI has flown in many orbits, including Deep Space flights, making it one of the most reliable options. It is also radiation hardened and falls within the allocated budgets for both volume and power.



**Figure 8.8.1: OBC FERMI [77]**

#### 8.8.4.2 Data Storage

The method of data storage was also considered. In previous deep space missions, solid-state drives (SSDs) have been used. There are two types of SSDs, multi-level cell (MLC) SSDs and

triple-level cell (TLC) SSDs [79]. MLC SSDs can store two bits of data per cell and contain four voltage levels, whereas TLC SSDs can store three bits of data per cell and contain eight voltage levels [80]. Because of their flight heritage, both of these data storage options were considered. A third data storage option, called the Hardened Extremely Long Life In-formation Optical Storage (HELIOS), was also considered, which stores data via optical media [81]. The decision matrix, shown in Table 8.8.2, contains the criteria for selection of data storage. Reliability was the most important criterion, and as such was weighted heavily. This was quantified through flight heritage and testing results. Performance was also heavily weighted in this decision. Should time-sensitive data be sent to the lander, the data storage system must be able to read that information quickly in order to execute it on time. The amount of data stored was criteria in this decision as well. The ability to store large amounts of data until a link can be established with the orbiter is important as the lander has a limited window of link time. The endurance of the data storage method was also considered in this decision, but was not weighed as heavily. The duration of the lander mission is one year on the surface of Europa, so having a data storage method that will survive the entire mission is crucial. SSDs typically have a lifespan of 5 to 7 years, however, so the risk of degradation before the mission is over is low [82]. HELIOS has undergone limited testing and was only in space for a total of 246 days, but the technology used in HELIOS is able to store data for decades, so there is little risk of degradation [81].

**Table 8.8.2: Data Storage Unit Decision Matrix**

Criteria	Weight	TLC SSD [79] [80]	MLC SSD [79] [80]	HELIOS [81]
<b>Reliability</b>	3.5	4	5	3
<b>Performance</b>	3	3	4	5
<b>Amount Stored</b>	2.5	3	2	5
<b>Endurance</b>	1	2	3	5
<b>Total</b>	10	32.5	37.5	43

Based on the decision matrix in Table 8.8.2, HELIOS was selected for data storage method. While the system itself has undergone little testing and has extremely limited flight heritage compared to TLC SSD and MLC SSD, its high performance, storage space, and endurance make this an acceptable tradeoff.

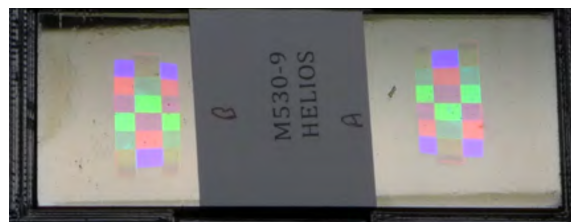


**Figure 8.8.2: Sample HELIOS Media Tested on the International Space Station [81]**

### 8.8.4.3 Flight Software

The software used on board the lander must be robust and high performance. There were several flight software options considered for this. The core Flight System, developed at the Goddard Space Flight Center, was built based on past NASA flight software [83]. F', or F prime, was developed at the Jet Propulsion Laboratory; it is tailored to small-scale systems, but is not limited to use on smaller missions [84]. NanoSat MO, the final flight software considered, was developed at the Graz University of Technology and has been used in several satellite missions [85]. When comparing these options, reliability, flexibility, performance, and deployment rate were considered. Reliability was weighted the heaviest and was quantified through flight heritage. Flexibility and performance were the next two most important criteria. Aspects of each software option are either not applicable to the ECHO mission, or things would need to be added to fully support the mission. As such, flexibility in the software is important in making sure everything that needs to be accomplished, can be. Performance is weighted equally and refers to the amount of computational power needed for each software. The less computationally expensive the software, the faster it can run. The final criterion was portability, though it was not considered as heavily as the other criteria. Portability refers to the software's ability to run on different computing systems. Because all of these software as well as the on-board computing system selected are designed for flight, portability is unlikely to cause any issues.

**Table 8.8.3: Flight Software Decision Matrix**

Criteria	Weight	core Flight System [83]	F' [84]	NanoSat MO [85]
Reliability	3	5	3	2
Flexibility	2.5	5	5	4
Performance	2.5	4	5	4
Portability	2	5	5	3
<b>Total</b>	10	47.5	44	32

Based on the decision matrix shown in Table 8.8.3, the core Flight System was selected for flight software. Its flight heritage is much more extensive than F' and NanoSat MO's, and thus offers the most reliable software option. The cFS also has high flexibility, performance, and portability. This means there is little risk that the software will not run well, or not be able to run at all, since it is compatible with many on-board computing systems and can be modified as needed for the mission.

### 8.8.5 Non-Technical Considerations

In designing the command & data subsystem of the ECHO mission, many non-technical aspects were considered. These include concerns regarding public health & safety, politics, culture,

environmental impact, economic impact, and time. Each of these aspects has been carefully examined, and an explanation of the impacts the subsystem has on each of these aspects is shown in Table 8.8.4.

**Table 8.8.4: Non-Technical Considerations for Command & Data**

Non-Technical Factor	Considerations
Ethical Responsibility	The decisions made regarding the design and use of the command & data subsystem will be clearly communicated to the rest of the design team to ensure accountability.
Public Health & Safety	The command & data system is only used on board the lander, therefore the actual processes done by the command & data system pose no threat to public health and safety. In building, installing, and testing the command & data system, the work conditions, practices, operations, and processes will follow all standards set forth by the Office of Safety & Mission Assurance (OSMA) [86].
Cultural	There are no cultural considerations associated with the command & data system.
Social	There are no social considerations associated with the command & data system.
Environmental	The command & data system will adhere to the United Nations Office of Outer Space Affairs' Space Debris Mitigation Guidelines [89]. The guidelines most prevalent to the mission are Guideline 1: limit debris during normal operation, and Guideline 5: minimize potential for post-mission break-ups resulting from stored energy.
Economic	The command & data system will require the purchase of hardware from external companies. The on-board computing system, data storage unit, and all other hardware required will remain within the budget set by the ECHO team for each subsystem.

## 8.8.6 Risk Management

There are several risks associated with command & data. These can be mitigated by following proper procedures, decreasing the likelihood that one of these risks would occur. The risks and mitigation techniques are displayed in Table 8.8.5.

**Table 8.8.5: Risk Assessment Table for Command & Data**

Hazard	Cause	Effect	Pre-RAT	Mitigation	Verification	Post-RAT
Data degradation	Failure in data storage unit	Modification of information, system damage	1B	Use of reliable data storage unit	Use hardware from vetted sources	1E
Software failure	Use of unauthorized or unvetted software, misconfigured system, logic or implementation errors, instability	Undesirable events, system damage, enabling other threats	2D	Acceptance testing, code walkthroughs, automated code analysis, run-time security monitoring	Run extensive software testing before launch	2E
Data loss	Insufficient storage space, on-board computing system failure	Necessary commands not performed, telemetry and scientific data not received by orbiter	1B	Use of reliable hardware and software, redundancy in data storage units	Use hardware from vetted sources, run extensive software testing before launch	1E
Supply chain failure	Use of software or hardware from non-vetted sources	Delivery interruptions, parts unavailability, counterfeit parts or software	2C	Supply chain confidence, vetted/trusted sources, chain of custody evidence	Thoroughly vet all companies and organizations involved	2E

## 8.8.7 Future Work

The next step in the command & data system is to do further analysis into the lander's data storage needs. This will allow more selections to be made for the data storage unit, modifying the HELIOS unit as needed. Exploring other aspects of a command & data system, such as communications and payload interfaces, would also be done. Finally, determining the method of fully integrating the command & data system into the lander would allow for full control.

## **8.9 Telecommunication**

**Prepared by: Chloe Powell**

### **8.9.1 Definition**

The telecommunication system is responsible for communication between the lander and the orbiter. The lander will transmit scientific data collected from the surface of Europa, as well as engineering data related to the status of the lander itself. This information will be transmitted from the lander to the orbiter when the orbiter is in range for communication, and will then be sent from the orbiter to the ground system on Earth. Any commands from the ground system will be relayed through the orbiter to the lander.

### **8.9.2 Objectives**

The telecommunication system must accurately transmit and receive data. It must do this with minimal delays and loss of information. Some information transmitted to and from the lander, particularly telemetry, is time-sensitive and cannot afford delays. The scientific data, while not being time-sensitive, is the motivation for the entire mission. If the scientific data cannot be transmitted properly, the mission will have failed.

### **8.9.3 Requirements & Constraints**

The telecommunication system for the ECHO lander will utilize X-bands for engineering data and Ka-bands for scientific data. Previously, it was proposed that all data would be communicated through the X-band frequencies. However, this has been modified to include the Ka-band for communication of scientific data as well. This will allow for faster and more clear communication between the lander and the orbiter. This is especially important given the limited window of linkage between the lander and orbiter.

Due to the need for multiple bands of communication, the antennas considered either had to be multi-band (support both X-band and Ka-band) or have a counterpart that supports the other band. Both options require more mass, volume, and power to be allocated to the telecommunication system as opposed to a single band antenna. In looking for Commercial Off-The-Shelf (COTS) options for X-band and Ka-band patch antennas, no multiband antennas were found that satisfied both the mass and volume budgets specified in the PDR (see Appendix 13.8). Because of this, two antennas will be used on the lander: one antenna that supports X-band communication, and one antenna that supports Ka-band communication. The volume of the telecommunication system must be under  $0.2852\text{m}^3$  in order to accommodate all other subsystems. All antennas considered were five to six times smaller than the allotted volume. The overall mass of the lander is 1000 kilograms, 15 of which were provided to the telecommunication system in the mass budget created for the PDR (see Appendix 13.8).

However, the mass of all antennas considered is on the order of magnitude of grams, which is significantly lower than the amount of mass budgeted for the system. Therefore, the increased mass and volume from the two antennas is negligible.

## 8.9.4 Analysis

### 8.9.4.1 Antenna Selection

When looking for the antennas to use on the lander, the most important metrics considered were reliability and power consumed. Reliability refers to how well the antennas typically perform, and was quantified through flight heritage. Because the lander has a limited power budget, power consumed was heavily weighted in the decision matrix as well. The RTGs offer a limited power supply, and even with solar panels and batteries, keeping power consumption low is vital for the mission. The lander also has strict mass and volume budgets, but all units that were considered fall within the allotted mass and volume as described in the PDR (see Appendix 13.8). In the preliminary mass budget, 15 kilograms were allocated to telecom; however, all antennas considered are under 100 grams. This allows for the majority of telecom's mass budget to be redistributed to the other subsystems and for mass to not be weighted heavily in the decision matrix. Volume is similarly weighted due to the small size of all antennas considered. The less volume the antenna takes within the lander, the more space there will be for fuel, scientific equipment, and any other necessary aspects of the other subsystems. All of the units considered fall within the allowable volume range specified in the PDR, so volume was not weighted very highly (see Appendix 13.8). Finally, the gain of the antennas was weighted moderately high in the decision matrix. The gain is the power transmitted in the direction of peak radiation, so it should be high enough that the signal is strong [90]. The lander will not be communicating with Earth, it will be communicating with the orbiter, which then will relay the information to and from Earth. This is a relatively small distance for the data to travel. Due to this shorter distance, the strength of the signal is not compromised as easily as it would be if the signal was travelling to Earth. Therefore, gain was weighted moderately high.

Tables 8.9.1 and 8.9.2 contain the decision matrices for the X-Band and Ka-Band antenna selection, respectively. Due to limited public information being available for these units, some specifications are unknown and as such are assigned a 0 in the decision matrix.

**Table 8.9.1: X-Band Antenna Decision Matrix**

Criteria	Weight	GNSS Patch [91]	Endurosat X-Band [92]	IQ Spacecom [93]	Cubecom XANT [94]
<b>Reliability</b>	3	4	2	5	0
<b>Power Consumed</b>	2.5	5	2	3	2
<b>Gain</b>	2.5	3	3	5	4
<b>Volume</b>	1	0	5	5	3
<b>Mass</b>	1	4	5	3	2
<b>Total</b>	10	36	28.5	43	20

**Table 8.9.2: Ka-Band Antenna Decision Matrix**

Criteria	Weight	Printech [95]	Endurosat K-Band [96]	Sage (Erevant) [97]	Erevant [98]
<b>Reliability</b>	3	2	3	0	0
<b>Power Consumed</b>	2.5	3	2	0	0
<b>Gain</b>	2.5	5	4	5	3
<b>Volume</b>	1	5	0	3	5
<b>Mass</b>	1	5	2	2	3
<b>Total</b>	10	36	26	17.5	15.5

Based on these criteria, the IQ Spacecom antenna was selected for X-band communications and the Printech antenna was selected for Ka-band communications. These are shown in Figure 8.9.1 and Figure 8.9.2 respectively. Both of these antennas provide the highest gain and lowest volume for their respective band frequencies. The IQ Spacecom is also the most reliable option, having been used in multiple Low Earth Orbit (LEO) flights since 2012 [93]. Both of these antennas will provide the ECHO lander reliable, fast communication with the orbiter.

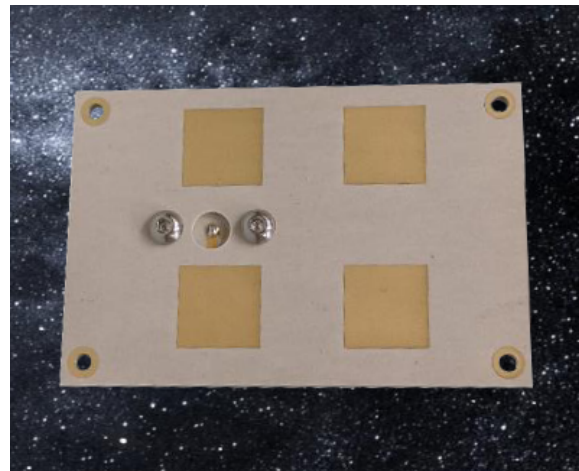


**Figure 8.9.1: IQ Spacecom X-Band Antenna [93]**

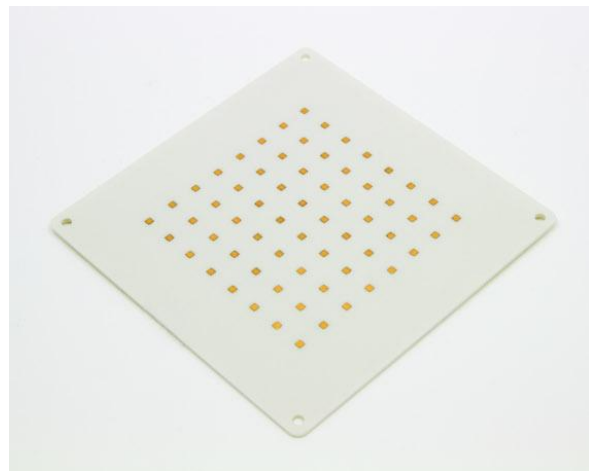


**Figure 8.9.2: Printech Ka-Band Antenna [95]**

## 8.9.5 Non-Technical Considerations

In designing the telecommunication system of the ECHO mission, many non-technical aspects were considered. These include public health & safety, political, cultural, environmental, economic, and time concerns. Each of these aspects have been carefully examined and an explanation of the impacts the two subsystems have on each of these aspects is shown in Table 8.9.3.

**Table 8.9.3: Non-Technical Considerations for Telecommunication**

Non-Technical Factor	Considerations
Ethical Responsibility	The decisions made regarding the design and use of the telecommunication subsystem will be clearly communicated to the rest of the design team to ensure accountability.
Public Health & Safety	The telecommunication system only communicates with the orbiter, therefore the actual communication process poses no threat to public health and safety. In building, installing, and testing the telecommunication system, the work conditions, practices, operations, and processes will follow all standards set forth by the Occupational Safety and Health Administration (OSHA) [99].
Cultural	There are no cultural considerations associated with the telecommunication system.
Social	There are no social considerations associated with the telecommunication system.
Environmental	The telecommunication system will adhere to the United Nations Office of Outer Space Affairs' Space Debris Mitigation Guidelines [102]. The guidelines most prevalent to the mission are Guideline 1: limit debris during normal operation, and Guideline 5: minimize potential for post-mission break-ups resulting from stored energy.
Economic	The telecommunication system will require the purchase of hardware from external companies. The antenna will remain within the budget set by the ECHO team for each subsystem.

## 8.9.6 Risk Management

There are several risks associated with telecommunication. These can be mitigated through following proper procedures, decreasing the likelihood that one of these risks would occur. The risks and mitigation techniques are displayed in Table 8.9.4.

**Table 8.9.4: Risk Assessment Table for Telecommunication**

Hazard	Cause	Effect	Pre-RAT	Mitigation	Verification	Post-RAT
Data corruption	Software failures (bugs, weaknesses), hardware failures	Modification of information, system damage	1B	Data integrity schemes (hashing, check values, digital structures)	Follow all Federal Communications Commission (FCC) and Office of Management and Budget (OMB) guidelines [103] [104]	1E
Ground system loss	Physical or cyber attack on facility, natural disasters	Loss of command, control, and data	1C	Guards, gates, facility design, access control	Follow safety protocols of the ground system facility	1E
Unauthorized access	Lack of authentication	Disruption of operations, system damage	2B	Authorization of commands, access control in control center, no use of open networks	Follow all FCC and OMB guidelines [103] [104]	2E
Supply chain failure	Use of software or hardware from non-vetted sources	Delivery interruptions, parts unavailability, counterfeit parts or software	2C	Supply chain confidence, vetted/trusted sources, chain of custody evidence	Thoroughly vet all companies and organizations involved	2E

## 8.9.7 Future Work

There is limited public information on these antennas. For future work, a more thorough analysis of each option would be performed with all specifications of the antennas used. This analysis would be compared to the needs of the other subsystems, particularly the Command & Data subsystem, to reevaluate the antennas chosen. A simulation of the lander and orbiter in Systems ToolKit (STK) would be made to further analyze the link and a formal link budget report would be formed.

# 9 Design Budgets

## 9.1 Mass Budget

Prepared by: Joseph Bowers

The overall mass budget for ECHO, as set by the PDR, is 1000 kg. The refined mass budget allocations are stated in Table 9.1.1. Additionally, the utilizations of the mass budget by subsystem are stated. Additional information regarding mass budget utilization by subsystem is contained in each individual subsystem section. The utilized mass only represents currently specified components, and may not effectively represent the final mass of the subsystem.

Based on the analysis conducted in the FDR, the mass budget details established in the PDR are not feasible. Additional analysis will be completed to further optimize subsystem mass, and determine any required adjustments to the overall mass budget.

**Table 9.1.1 Mass Budget by Subsystem**

Subsystem	Mass Allocated (kg)	Percentage	Mass Utilized (kg)	Percent Utilized
Structures	70	7.00%	129.91	53.88%
Mechanisms & Deployables	30	3.00%	8.50	352.94%
Propulsion	800	80.00%	1038.50	77.03%
ADCS	15	1.50%	7.83	191.57%
Thermal Management	25	2.50%	25.00	100.00%
Power	50	5.00%	50.00	100.00%
Command & Data	5	0.50%	0.30	1666.67%
Telecomm	5	0.50%	0.03	17241.38%
<b>Total</b>	<b>1000</b>	<b>100.00%</b>	<b>1260.07</b>	<b>19783.48%</b>

## 9.2 Volume Budget

Prepared by: Constantine Childs

The volume of the ECHO lander is based on the total volume of the Europa Clipper (excluding solar arrays) and has not changed since the PDR. The volume of the lander is 25% of the volume of Europa Clipper which results in a volume of 14.26 m<sup>3</sup>. Volume budgets for each subsystem are shown in Table 9.2.1.

**Table 9.2.1 Volume Budget by Subsystem**

Subsystem	Percentage (%)	Volume (m <sup>3</sup> )
Structures	25	3.565
Mechanisms & Deployables	4	0.5704
Propulsion	50	7.13
ADCS	3	0.4278
Thermal Management	4	0.5704
Power	10	1.426
Command & Data	2	0.2852
Telecommunication	2	0.2852
Total	100	14.26

## 9.3 Cost Budget

**Prepared by: Andrew Olson**

The cost budget for the ECHO mission has been established based on an analysis of comparable missions, specifically NASA's Galileo, Juno, and Europa Clipper. To determine an appropriate cost budget, the cost per kilogram of launch mass for each of these missions was calculated and adjusted for inflation, as presented in Table 9.3.1. These values were then averaged, and the resulting average cost per kilogram was multiplied by the estimate of ECHO's mass budget and rounded to the nearest \$10,000,000 to obtain the cost budget.

In the PDR, the predicted mass budget for ECHO was 1,000 kg, resulting in an estimated cost budget of \$920,000,000. FDR analysis has yielded a new mass budget prediction of 1,260.07 kg, resulting in a total budget of \$1,160,000,000 for the ECHO lander, as outlined in Table 9.3.1.

**Table 9.3.1: Cost Budget**

Mission	Cost (Billion \$)	Launch Mass (kg)	Dollar/kg	ECHO Predicted Dry Mass (kg)
Galileo	3.8	2562	1,483,216	1,260.07
Juno	1.52	3625	419,310	
Clipper	5.2	6065	857,378	
Average dollar/kg: 919,968			Predicted ECHO Cost Budget: \$1,160,000,000	

## **10 Sales Pitch**

**Prepared by: Katie August**

Project ECHO holds monumental potential in the scientific and engineering community. This mission can help scientists understand if life can exist beyond Earth and if Europa can sustain it. The historically successful missions of the Mars rovers Perseverance and Curiosity were just the beginning of revolutionary discoveries about extraterrestrial bodies. The Europa Clipper and Juno spacecraft are actively exploring the deep space and Jupiter.

ECHO's primary scientific objectives of sampling the ice and atmospheric conditions on Europa are similar to the missions that have already proven to be successful. This project pushes the boundaries of the knowledge and technology of today and will be a groundbreaking work of science and engineering. The data to be gathered from Europa has the potential to reshape the current understanding of life's existence beyond Earth and open the door to new possibilities of life in the universe.

## **11 Conclusions**

**Prepared by: Chloe Powell**

The ECHO mission objectives are to produce and analyze samples of Europa's surface ice and to measure atmospheric conditions at the surface of Europa. This will be accomplished through the use of a lander on Europa's surface. The lander will descend onto the surface of the moon using a bi-propellant propulsion system and a powered descent. Once it has safely landed, a suite of scientific instruments and sensors will collect data and conduct experiments on samples of surface ice. This suite will include instruments capable of analyzing the elemental, molecular, and mineralogical composition of Europa. Findings from this analysis will be transmitted to the orbiter, which will transmit those findings to Earth. The mission is planned to be six months long, and the lander architecture is designed such that it will survive the duration of the mission, if not longer, with minimal risks. The data collected by ECHO will give valuable insight into Europa's ability to support life.

## 12 References

- [1] Elizabeth Howell, "Europa: Facts About Jupiter's Icy Moon and Its Ocean," *Space.com*, Mar. 22, 2018. <https://www.space.com/15498-europa-sdcmp.html>
- [2] - "Europa: Facts - NASA Science," *Nasa.gov*, Nov. 09, 2017. <https://science.nasa.gov/jupiter/moons/europa/europa-facts/#h-potential-for-life>
- [3] M. H. Carr *et al.*, "Evidence for a subsurface ocean on Europa," *Nature*, vol. 391, no. 6665, pp. 363–365, Jan. 1998, doi: <https://doi.org/10.1038/34857>.
- [4] United Nations, "Space Debris Mitigation Guidelines of the Committee on the Peaceful Uses of Outer Space," United Nations publication, Vienna, 2010.
- [5] United Nations Office for Outer Space Affairs, "Space Law Treaties and Principles," 2017. [Online]. Available: <https://www.unoosa.org/oosa/en/ourwork/spacelaw/treaties.html>.
- [6] United States Code, "TITLE 51—NATIONAL AND COMMERCIAL SPACE PROGRAMS," 2011. [Online]. Available: <https://www.govinfo.gov/content/pkg/USCODE-2011-title51/html/USCODE-2011-title51.htm>.
- [7] NASA, "Multi-Mission Radioisotope Thermoelectric Generator (MMRTG)," NASA, 2020. Accessed: Dec. 04, 2024. [Online]. Available: [https://mars.nasa.gov/internal\\_resources/788/](https://mars.nasa.gov/internal_resources/788/)
- [8] W. Wang, "Schematic Model for the three-degrees-of-freedom (3-DOF) Angular Motions of a Spherical joint," *Research Gate*, Apr. 2019. [https://www.researchgate.net/figure/Schematic-model-for-the-three-degrees-of-freedom-3-DOF-angular-motions-of-a-spherical\\_fig1\\_332696179](https://www.researchgate.net/figure/Schematic-model-for-the-three-degrees-of-freedom-3-DOF-angular-motions-of-a-spherical_fig1_332696179) (accessed Dec. 04, 2024).
- [9] J. Mehta, "Structural Evolution of the TeamIndus Spacecraft That Will Land on the Moon," *Medium*, Feb. 26, 2019. <https://medium.com/teamindus/structural-evolution-of-the-teamindus-spacecraft-that-will-land-on-the-moon-b5aa6bc73ccc> (accessed Dec. 04, 2024).
- [10] Anderson, K. S., "Space Vehicle Systems Engineering," *Spacecraft Design, Dynamics & Control Primer*, RPI, [https://www.rpi.edu/~anderk5/space\\_vehicle\\_systems.pdf](https://www.rpi.edu/~anderk5/space_vehicle_systems.pdf)
- [11] "Mesh Quality | Mesh Visualization Tips | SimScale," *SimScale*, Jul. 30, 2024. <https://simscale.com/docs/simulation-setup/meshing/mesh-quality> (accessed Dec. 04, 2024).
- [12] M. S. Escartí-Guillem, L. M. Garcia-Raffi, and S. Hoyas, "Review of Launcher lift-off Noise Prediction and Mitigation," Aug. 2024, Accessed: Dec. 04, 2024. [Online]. Available: <https://www.sciencedirect.com/science/article/pii/S2590123024009344#br0010>
- [13] N. Nava, M. Collado, and R. Cabás, "New Deployment Mechanisms Based on SMA Technology for Space Applications," 2013.
- [14] A. C. Stewart and J. H. Hair, "Intricacies of Using Kevlar Cord and Thermal Knives in a Deployable Release System: Issues and Solutions," in *Proceedings of the 36th Aerospace Mechanisms Symposium*, Aug. 2013. [Online]. Available: <https://ntrs.nasa.gov/api/citations/20020050204/downloads/20020050204.pdf>
- [15] M. Englund and B. Hamad, *Improved Release Mechanisms for Aerospace Applications*. Uppsala University, 2021.
- [16] NASA, "Radiation Maps of Europa: Key to Future Missions," *NASA's Europa Clipper*, Jul. 23, 2018. Accessed: Dec. 05, 2024. [Online]. Available: <https://europa.nasa.gov/news/17/radiation-maps-of-europa-key-to-future-missions/>
- [17] P. Di Lizia, "Introducing SD2: Philae's Sampling, Drilling and Distribution instrument – Rosetta – ESA's comet chaser," ESA blog navigator. Accessed: Dec. 05, 2024. [Online]. Available:

- <https://blogs.esa.int/rosetta/2014/04/09/introducing-sd2-philaes-sampling-drilling-and-distribution-instrument/>
- [18]Firgelli Automations Team, "Inner Workings of a Linear Actuator," *Firgelli Automations*, Aug. 01, 2018. Accessed: Dec. 05, 2024. [Online]. Available: <https://www.firgelliauto.com/blogs/news/inside-a-linear-actuator-how-a-linear-actuator-works>
- [19]Moog Inc., "Type 22 Antenna Positioning Mechanism," New. Accessed: Dec. 05, 2024. [Online]. Available: <https://www.moog.com/products/space-mechanisms/antenna-pointing-mechanisms/type-22.html>
- [20]"BIPROPELLANT ROCKET ENGINES", Jul. 2024, L3HARRIS. <https://www.l3harris.com/sites/default/files/2024-10/l3harris-ar-bipropellant-rocket-engines-2.pdf>
- [21]"Bipropellant Thruster Datasheet", 2024, Moog Inc. <https://www.moog.com/content/dam/moog/literature/sdg/space/propulsion/moog-bipropellant-thrusters-datasheet.pdf>
- [22]"CHEMICAL BI-PROPELLANT THRUSTER FAMILY", Ariane Group, <https://www.space-propulsion.com/brochures/bipropellant-thrusters/bipropellant-thrusters.pdf>
- [23]"MONOPROPELLANT THRUSTERS", 2024, Moog Inc. <https://www.moog.com/content/dam/moog/literature/sdg/space/propulsion/moog-Monopropellant-Thrusters-Datasheet.pdf>
- [24]"CHEMICAL MONOPROPELLANT THRUSTER FAMILY", Ariane Group, <https://www.space-propulsion.com/brochures/hydrazine-thrusters/hydrazine-thrusters.pdf>
- [25]"MONOPROPELLANT ROCKET ENGINES", Jun. 2023, L3Harris, [https://www.l3harris.com/sites/default/files/2023-07/AJRD-LHX\\_Monopropellant\\_Rocket\\_Engines\\_SpecSheet\\_CMYK\\_061423\\_APPROVED.pdf](https://www.l3harris.com/sites/default/files/2023-07/AJRD-LHX_Monopropellant_Rocket_Engines_SpecSheet_CMYK_061423_APPROVED.pdf)
- [26]W. Gomes dos Santos, "A novel solution for the spacecraft mixed actuators problem based on a multiobjective optimization method," International Symposium on Space Flight Dynamics, Oct. 2015. [https://www.researchgate.net/figure/RCS-setup-for-configuration-with-12-thrusters\\_fig2\\_283291752](https://www.researchgate.net/figure/RCS-setup-for-configuration-with-12-thrusters_fig2_283291752)
- [27]Anderson, K. S., "Space Vehicle Systems Engineering," Spacecraft Design, Dynamics & Control Primer, RPI, [https://www.rpi.edu/~anderk5/space\\_vehicle\\_systems.pdf](https://www.rpi.edu/~anderk5/space_vehicle_systems.pdf)
- [28]"Europa: Facts - NASA Science," NASA.gov, Nov. 09, 2017. <https://science.nasa.gov/jupiter/moons/europa/europa-facts/#h-potential-for-life>
- [29]"Mars Science Laboratory: Curiosity Rover" NASA.gov, <https://science.nasa.gov/mission/msl-curiosity/>
- [30]"InSight Launch Facts" Jet Propulsion Laboratory. [https://www.jpl.nasa.gov/news/press\\_kits/insight/launch/facts/#:~:text=About%201%2C530%20pounds%20](https://www.jpl.nasa.gov/news/press_kits/insight/launch/facts/#:~:text=About%201%2C530%20pounds%20)
- [31]"MSL (Curiosity)", Dec. 01, 2019. WEEBAU SPACE ENCYCLOPEDIA, <https://weebau.com/satplan/msl.htm>
- [32]"Diaphragm Tanks Data Sheets – Sorted by Volume", Northrop Grumman. <https://www.northropgrumman.com/space/diaphragm-tanks-data-sheets-sorted-by-volume>
- [33]"ROLLING METAL DIAPHRAGM PROPULSION TANKS", Moog Inc., 2024. <https://www.moog.com/content/dam/moog/literature/sdg/space/propulsion/moog-rolling-diaphragm-tanks-datasheet.pdf>

- [34]"Hydrazine Propellant Tanks", Ariane Group.  
<https://www.space-propulsion.com/spacecraft-propulsion/hydrazine-tanks/index.html>
- [35]"Bipropellant Tanks", Ariane Group,  
<https://www.space-propulsion.com/spacecraft-propulsion/bipropellant-tanks/index.html>
- [36]N. Bangar and J. Hunter, "Aerobraking Analysis for the Orbit Insertion Around Jupiter a project presented to Master of Science in Aerospace Engineering," 2018. Available:
- [37]H. D. Curtis, *Orbital mechanics for engineering students : revised fourth edition*, 4th ed. Amsterdam: Elsevier, 2021.
- [38]-]"IADC Space Debris Mitigation Guidelines Issued by IADC Steering Group and Working Group 4," 2020. Available:  
<https://orbitaldebris.jsc.nasa.gov/library/iadc-space-debris-guidelines-revision-2.pdf>
- [39]"IMPLEMENTING PLANETARY PROTECTION REQUIREMENTS FOR SPACE FLIGHT," 2022. Available:  
[https://standards.nasa.gov/sites/default/files/standards/NASA/Baseline/0/NASA-STD-871927\\_Baseline.pdf](https://standards.nasa.gov/sites/default/files/standards/NASA/Baseline/0/NASA-STD-871927_Baseline.pdf)
- [40]"NASA Cost Estimating Handbook (CEH) - NASA," NASA, Jun. 23, 2023.  
<https://www.nasa.gov/ocfo/ppc-corner/nasa-cost-estimating-handbook-ceh/>
- [41] NASA Small Spacecraft Systems Virtual Institute, "Guidance, Navigation, and Control - State of the Art," NASA, 2023. [Online]. Available:  
<https://www.nasa.gov/smallsat-institute/sst-soa/guidance-navigation-and-control/#5.2.1>.
- [42] Space Micro, "μSTAR-200M Star Tracker," SatCatalog, 2021. [Online]. Available:  
[https://satcatalog.s3.amazonaws.com/components/303/SatCatalog\\_-\\_Space\\_Micro\\_-\\_%C2%B5TAR-200M\\_-\\_Datasheet.pdf?lastmod=20210708042311](https://satcatalog.s3.amazonaws.com/components/303/SatCatalog_-_Space_Micro_-_%C2%B5TAR-200M_-_Datasheet.pdf?lastmod=20210708042311).
- [43] A. Eisenman and C. C. Liebe, "Operation and Performance of a Second Generation, Solid State, Star Tracker, the ASC," Jet Propulsion Laboratory, California Institute of Technology, Berlin, Germany, 1996. [Online]. Available: <https://hdl.handle.net/2014/27543>.
- [44] L. H. Regoli, H. Matsuura, and G. S. J. Franco, "Testing and validation of magnetometers for extreme environments," *Geoscientific Instrumentation, Methods and Data Systems Discussions*, vol. 9, pp. 499–516, 2020. [Online]. Available: <https://doi.org/10.5194/gi-2020-12>.
- [45] K.-H. Glassmeier, H.-U. Auster, K.-H. Fornacon, *et al.*, "ROMAP: Rosetta magnetometer and plasma monitor," *Space Science Reviews*, vol. 128, no. 1-4, pp. 649–670, 2007. [Online]. Available:  
[https://www.researchgate.net/publication/225019391\\_ROMAP\\_Rosetta\\_magnetometer\\_and\\_plasma\\_monitor](https://www.researchgate.net/publication/225019391_ROMAP_Rosetta_magnetometer_and_plasma_monitor).
- [46] NASA, "Stardust mission overview," NASA Science. [Online]. Available:  
<https://science.nasa.gov/mission/stardust/>.
- [47] Redwire Space, "Digital Sun Sensor ( $\pm 64^\circ$ )," Technical Datasheet V8, May 2021. [Online]. Available: <https://redwirespace.com/>.
- [48] Bradford Engineering BV, "Coarse Sun Sensor," Technical Datasheet, Jan. 2017. [Online]. Available: <https://bradford-space.com/>.
- [49] Bradford Engineering BV, "Fine Sun Sensor," Technical Datasheet, Jan. 2017. [Online]. Available: <https://bradford-space.com/>.
- [50] Redwire Space, "Coarse Sun Sensor Pyramid," Technical Datasheet V5, Apr. 2021. [Online]. Available: <https://redwirespace.com/>.
- [51] "Steradian," Wikipedia. [Online]. Available: <https://en.wikipedia.org/wiki/Steradian>.

- [52] Honeywell Aerospace, "HG1700 Inertial Measurement Unit," Brochure, 2021. [Online]. Available: <https://aerospace.honeywell.com/content/dam/aerobt/en/documents/learn/products/sensors/brochures/N61-1619-000-001-HG1700InertialMeasurementUnit-bro.pdf>.
- [53] Northrop Grumman, "LN-200S Inertial Measurement Unit," Datasheet, SatCatalog, 2021. [Online]. Available: [https://satcatalog.s3.amazonaws.com/components/317/SatCatalog\\_-\\_Northrop\\_Grumman\\_-\\_LN-200S\\_-\\_Datasheet.pdf?lastmod=20210708044025](https://satcatalog.s3.amazonaws.com/components/317/SatCatalog_-_Northrop_Grumman_-_LN-200S_-_Datasheet.pdf?lastmod=20210708044025).
- [54] Safran Sensing Technologies, "STIM377H High-Performance Inertial Measurement Unit," Product Brief, May 2022. [Online]. Available: <https://www.safran-group.com/sites/default/files/2022-05/safran-sensing-technologies-product-brief-stim377h.pdf>.
- [55] VectorNav, "VN-110 Ruggedized IMU/AHRS," Product Brief, 2024. [Online]. Available: [https://www.vectornav.com/docs/default-source/product-brief/vn-110-product-brief.pdf?sfvrsn=b7077cbf\\_2](https://www.vectornav.com/docs/default-source/product-brief/vn-110-product-brief.pdf?sfvrsn=b7077cbf_2).
- [56] Collins Aerospace, "RSI 45-75-60," SatCatalog, 2021. [Online]. Available: [https://satcatalog.s3.amazonaws.com/components/204/SatCatalog\\_-\\_Collins\\_Aerospace\\_-\\_RSI\\_45-75-60\\_-\\_Datasheet.pdf?lastmod=20210708033051](https://satcatalog.s3.amazonaws.com/components/204/SatCatalog_-_Collins_Aerospace_-_RSI_45-75-60_-_Datasheet.pdf?lastmod=20210708033051).
- [57] Blue Canyon Technologies, "RW4," SatCatalog, 2021. [Online]. Available: [https://satcatalog.s3.amazonaws.com/components/176/SatCatalog\\_-\\_Blue\\_Canyon\\_Technologies\\_-\\_RW4\\_-\\_Datasheet.pdf?lastmod=20210708031809](https://satcatalog.s3.amazonaws.com/components/176/SatCatalog_-_Blue_Canyon_Technologies_-_RW4_-_Datasheet.pdf?lastmod=20210708031809).
- [58] H. Yoon, H. H. Seo, and H.-T. Choi, "Optimal uses of reaction wheels in the pyramid configuration using a new minimum infinity-norm solution," *Aerospace Science and Technology*, vol. 39, pp. 109–119, 2014. [Online]. Available: <https://doi.org/10.1016/j.ast.2014.09.002>.
- [59] C. D. Brown, Elements of Spacecraft Design. Reston, VA: American Institute Of Aeronautics And Astronautics, 2002, p. 374.
- [60] H. Trinh, C. Burnside, and H. Williams, "Assessment of MON-25/MMH Propellant System for Deep-Space Engines." Available: <https://ntrs.nasa.gov/api/citations/20190033304/downloads/20190033304.pdf>
- [61] VectorNav, "VN-110 IMU/AHRS Rugged and Miniature Tactical-Grade IMU and AHRS," 2024. [Online]. Available: [https://www.vectornav.com/docs/default-source/product-brief/vn-110-product-brief.pdf?sfvrsn=b7077cbf\\_2](https://www.vectornav.com/docs/default-source/product-brief/vn-110-product-brief.pdf?sfvrsn=b7077cbf_2)
- [62] PNI Sensor, "RM3100 Magneto-Inductive Magnetometer," Pnisensor.com, 2024. <https://www.pnisensor.com/rm3100/>
- [63] IQSpacecom, "DATASHEET X BAND ANTENNA," May 2024. [https://www.iq-spacecom.com/images/Datasheets/IQspacecom\\_X\\_Band\\_Antenna\\_datasheet\\_05.2024.pdf](https://www.iq-spacecom.com/images/Datasheets/IQspacecom_X_Band_Antenna_datasheet_05.2024.pdf)
- [64] C. D. Brown, Elements of Spacecraft Design. Reston, VA: American Institute Of Aeronautics And Astronautics, 2002, p. 398.
- [65] N. Warman, "Variable Conductance Heat Pipes (VCHP): When, How, and Why To Use Them in Space Systems - Advanced Cooling Technologies," Advanced Cooling Technologies, Jan. 23, 2024. [https://www.1-act.com/resources/blog/variable-conductance-heat-pipes-vchp-when-how-and-why-to-use-them-in-space-systems/?srsltid=AfmBOoopQGnQI\\_6xHkUy2xz402b\\_l4x76DWCL2FF\\_FJ1kFieoojovuFC](https://www.1-act.com/resources/blog/variable-conductance-heat-pipes-vchp-when-how-and-why-to-use-them-in-space-systems/?srsltid=AfmBOoopQGnQI_6xHkUy2xz402b_l4x76DWCL2FF_FJ1kFieoojovuFC)

- [66] Anderson, K. S., "Space Vehicle Systems Engineering," Spacecraft Design, Dynamics & Control Primer, RPI, [https://www.rpi.edu/~anderk5/space\\_vehicle\\_systems.pdf](https://www.rpi.edu/~anderk5/space_vehicle_systems.pdf)
- [67]"Thermal: Radioisotope Heater Units," [science.nasa.gov](https://science.nasa.gov/planetary-science/programs/radioisotope-power-systems/thermal-radioisotope-heater-units/).  
<https://science.nasa.gov/planetary-science/programs/radioisotope-power-systems/thermal-radioisotope-heater-units/>
- [68]Lyra, J. and Stultz, J., "The Variable Radioisotope Heater Unit for the Cassini Spacecraft," SAE Technical Paper 941268, 1994, <https://doi.org/10.4271/941268>.
- [69] D. Gilmore, Ed., Spacecraft Thermal Control Handbook, 2nd ed., vol. 1. The Aerospace Press, 2002, pg. 224.
- [70]Laub, B. & Venkatapathy, Ethiraj. (2004). Thermal protection system technology and facility needs for demanding future planetary missions. 544. 239-247.
- [71]L. Santos Fernandes, B. Lopez, M. Lino da Silva; Computational fluid radiative dynamics of the Galileo Jupiter entry. Physics of Fluids 1 October 2019; 31 (10): 106104. <https://doi.org/10.1063/1.5115264>
- [72]Galileo Probe during final assembly. Available: [https://nasa.fandom.com/wiki/Atmospheric\\_entry?file=Galileo\\_probe.jpg](https://nasa.fandom.com/wiki/Atmospheric_entry?file=Galileo_probe.jpg)
- [73]R. Bechtel, "Multi-Mission Radioisotope Thermoelectric Generator (MMRTG," Aug. 2015. [Online]. Available: [https://www.nasa.gov/wp-content/uploads/2015/08/4\\_mars\\_2020\\_mmrtg.pdf?emarc=35c41b](https://www.nasa.gov/wp-content/uploads/2015/08/4_mars_2020_mmrtg.pdf?emarc=35c41b)
- [74]Battery University, "BU-216: Summary Table of Lithium-based Batteries," Battery University. Accessed: Dec. 05, 2024. [Online]. Available: <https://batteryuniversity.com/article/bu-216-summary-table-of-lithium-based-batteries>
- [75]Battery University, "BU-205: Types of Lithium-ion," Battery University. Accessed: Dec. 05, 2024. [Online]. Available: <https://batteryuniversity.com/article/bu-205-types-of-lithium-ion>
- [76] "SSD Form Factors | SNIA," [www.snia.org](http://www.snia.org).  
<https://www.snia.org/forums/cmsi/knowledge/formfactors>
- [77] "8.0 Small Spacecraft Avionics - NASA," NASA, Oct. 16, 2021. <https://www.nasa.gov/smallsat-institute/sst-soa/small-spacecraft-avionics/#8.3>
- [78] "Europa Clipper – NASA's Europa Clipper Mission," NASA, Oct. 13, 2024. <https://blogs.nasa.gov/europaclipper/tag/europa-clipper/>
- [79] "How to Store Data in Outer Space," *Spaceclick*, Jul. 26, 2022. <https://www.spaceclick.com/blog/how-to-store-data-in-outer-space/>
- [80] "MLC vs. TLC: Which Is the Better SSD?," *Pure Storage*, Dec. 21, 2021. <https://blog.purestorage.com/purely-educational/mlc-vs-tlc-which-is-the-better-ssd/>
- [81] R. Solomon, E. Rosenthal, R. Grubbs, and B. Solomon, "Next Generation Big Data Storage For Long Space Missions," Jun. 2021. Available: [https://ntrs.nasa.gov/api/citations/20205007793/downloads/Next%20Generation%20Big%20Data%20Storage%20for%20Long%20Space%20Missions\\_final.pdf](https://ntrs.nasa.gov/api/citations/20205007793/downloads/Next%20Generation%20Big%20Data%20Storage%20for%20Long%20Space%20Missions_final.pdf)
- [82] Mwave Team, "SSD Lifespan: How Long Does an SSD Last?," *Mwave*, Mar. 05, 2024. <https://www.mwave.com.au/blog/how-long-does-an-ssd-last-ssd-lifespan/>
- [83] "Core Flight System," Goddard Engineering and Technology Directorate. <https://cfs.gsfc.nasa.gov/>
- [84] "F' Features," *Flight Software and Embedded Systems Network*, 2020. <https://nasa.github.io/fprime/features.html>
- [85] NanoSat MO Framework, "NanoSat MO Framework," *NanoSat MO Framework*, 2022. <https://nanosat-mo-framework.github.io/>

- [86] “Occupational Safety and Health,” *NASA*, 2023. <https://sma.nasa.gov/sma-disciplines/institutional-safety>
- [87] UNOOSA, “Space Law Treaties and Principles,” *UNOOSA*, 2019. <https://www.unoosa.org/oosa/en/ourwork/spacelaw/treaties.html>
- [88] “U.S.C. Title 51 - NATIONAL AND COMMERCIAL SPACE PROGRAMS,” *U.S. Government Publishing Office*. <https://www.govinfo.gov/content/pkg/USCODE-2011-title51/html/USCODE-2011-title51.htm>
- [89] National Society Of Professional Engineers, “NSPE Code of Ethics for Engineers,” *National Society of Professional Engineers*, Jul. 2019. <https://www.nspe.org/resources/ethics/code-ethics>
- [90] “Antenna Gain,” [www.antenna-theory.com](http://www.antenna-theory.com), 2020. <https://www.antenna-theory.com/basics/gain.php>
- [91] “GNSS Patch Antenna,” *ISISPACE*. <https://www.isispace.nl/product/gnss-patch-antenna/>
- [92] “X-Band Patch Antenna - EnduroSat,” *EnduroSat*, Jul. 02, 2024. <https://www.endurosat.com/products/x-band-patch-antenna/>
- [93] “IQ Spacecom X-Band Antenna,” *IQ Spacecom*, May 2024. [https://www.iq-spacecom.com/images/Datasheets/IQspacecom\\_X\\_Band\\_Antenna\\_datasheet\\_05.2024.pdf](https://www.iq-spacecom.com/images/Datasheets/IQspacecom_X_Band_Antenna_datasheet_05.2024.pdf)
- [94] “XANT X-band Patch Antenna | satsearch,” *satsearch*. <https://satsearch.co/products/cubecom-xant-x-band-patch-antenna>
- [95] “Ka-Band Microstrip Patch Array for Cubesat Systems | satsearch,” *satsearch*, 2024. <https://satsearch.co/products/printech-circuit-laboratories-ka-band-microstrip-patch-array-for-cubesat-systems>
- [96] “K-Band 4×4 Patch Array - EnduroSat,” *EnduroSat*, Jul. 31, 2024. <https://www.endurosat.com/products/k-band-4x4-patch-array/>
- [97] “Ka Band Microstrip Patch Array Antenna, 15.0° x 4.8°,” *Eravant*, 2023. <https://sftp.eravant.com/content/datasheets/SAM-3533532005-KF-L1.pdf>
- [98] “Ka Band Microstrip Patch Array Attenna, 39 Ghz, 6 dBi, 50° x 95°,” *Eravant*, 2023. <https://sftp.eravant.com/content/datasheets/SAM-3934030695-2F-L1-4C.pdf>
- [99] “Occupational Safety and Health Standards: Telecommunications,” *Occupational Safety and Health Administration*. <https://www.osha.gov/laws-regulations/regulations/standardnumber/1910/1910.268>
- [100] UNOOSA, “Space Law Treaties and Principles,” *UNOOSA*, 2019. <https://www.unoosa.org/oosa/en/ourwork/spacelaw/treaties.html>
- [101] “U.S.C. Title 51 - NATIONAL AND COMMERCIAL SPACE PROGRAMS,” *U.S. Government Publishing Office*. <https://www.govinfo.gov/content/pkg/USCODE-2011-title51/html/USCODE-2011-title51.htm>
- [102] National Society Of Professional Engineers, “NSPE Code of Ethics for Engineers,” *National Society of Professional Engineers*, Jul. 2019. <https://www.nspe.org/resources/ethics/code-ethics>
- [103] “Information Quality Guidelines of the FCC,” *Federal Communications Commission*, Feb. 22, 2011. <https://www.fcc.gov/general/information-quality-guidelines-fcc>
- [104] “OMB Guidelines for Ensuring and Maximizing the Quality, Objectivity, Utility, and Integrity of Information Disseminated by Federal Agencies,” *US EEOC*, 2024. <https://www.eeoc.gov/omb-guidelines-ensuring-and-maximizing-quality-objectivity-utility-and-integrity-information>

- [105] T. Reyes, “Scientific instruments of Rosetta’s Philae lander,” Phys.org, Sep. 23, 2014. Accessed: Dec. 06, 2024. [Online]. Available: <https://phys.org/news/2014-09-scientific-instruments-rosetta-philae-lander.html>
- [106] P. Bauduin, “Galileo Orbiter,” Weebau.com, 2024. <https://weebau.com/satplan/galileo.htm> (accessed Oct. 15, 2024).

# **13 Appendix**

## **13.1: Definition and Assessment of Risk**

**Prepared by: Katie August**

Risk is the evaluation of the unfavorable events that could occur and threaten mission success. These events can occur at any point during the mission on varying scales. Project ECHO has taken all necessary design calculations and evaluations to mitigate risk at any point during the mission. Each subsystem has varying levels of risk to overall mission success. Failures in propulsion, orbital mechanics, structures, thermal management, and power risk entire mission collapse. Failures in ADCS, Command and Data, and Telecommunications risk severe mission progress and potential to lead to entire mission collapse.

Project ECHO recognizes the risks that each subsystem holds. Addressing potential failures significantly reduces loss of system or data. The various mitigation solutions maximize mission success and breakthrough discoveries.

## **13.2: Summary of Non-Technical Considerations**

**Prepared by: Andrew Olson**

A summary of non-technical considerations and their relevance to each subsystem for consideration during analysis is presented in Table 13.2.1. The subsystems are labeled corresponding to the section number assigned to them in section 8 of the report as listed below. A “+” indicates that the non – technical factor is considered relevant to the subsystem, and a “-” indicates that it is considered irrelevant.

- 8.1 - Structures
- 8.2 - Mechanisms and Deployables
- 8.3 - Propulsion
- 8.4 - Orbital Mechanics
- 8.5 - ADCS
- 8.6 - Thermal Management
- 8.7 - Power
- 8.8 - Command & Data
- 8.9 - Telecommunication

**Table 13.2.1 Relevance of Non-Technical Factors**

Relevance of Non-Technical Factor to Subsystem										
Applies to Subsystem +										
Does Not Apply to subsystem -										
Non-Technical Factor	Subsystem	8.1	8.2	8.3	8.4	8.5	8.6	8.7	8.8	8.9
Public Health & Safety		+	-	+	-	+	+	+	-	-
Political		-	-	+	-	-	-	+	+	+
Cultural		-	-	-	-	-	-	+	-	-
Environmental		+	-	+	-	-	+	+	-	-
Economic		+	+	+	+	+	+	+	+	+
Social		-	-	-	-	-	-	+	-	-
Ethical		+	+	+	+	+	+	+	+	+

### 13.3: Aerobraking Maneuver MATLAB Script

Prepared by: Andrew Olson

```
%A script for estimating the delta V conservation for performing an
```

```
%aerobraking procedure with Jupiter's atmosphere for the ECHO probe.
```

```
%clear all
```

```
close all
```

```
clc
```

```
%% Define the parameters for the problem
```

```
% Universal gravitational Constant (km^3/kgs^2)
```

```
hr = 3600; %seconds to hr
```

```
G = 6.6743*10^-20;
```

```
Me = 4.79984 * 10^22; % mass of Europa in kg
```

```
Mj = 1.898 * 10^27 ; % mass of Jupiter in kg
```

```

Rj = 69911; % radius of Jupiter

Re = 1560; %radius of europa in km

Per_ht = Rj+350; %Initial orbiter perigee radius km

Per1 = 670000; %initial galileo orbit perigee

Ap1 = 19000000; %Initial orbiter apogee radius in km

R = 671000; %radius between Jupiter and Europa in KM

SOI = R*((Me/Mj)^.4); %sphere of influence of europa

a1 = (Per_ht + Ap1)/2 ; %initial semi major axis

Cd = 2*1.17; %Drag coefficient for heat shield, roughhhh approximatoin (took flat plate for subsonic and doubled it)

A = 9.6; %surface area of the heat shield

mew = Mj*G; %calculate mew for jupiter

mew_eur = Me*G; %calculate mew for europa

pass = 2.9; %number of orbits to simulate

% Calculate the initial state vector

h1 = sqrt(2*mew)*sqrt((Per_ht*Ap1)/(Per_ht+Ap1)); %Initial Orbital Energy of the probe once it is placed in initial aerobrake orbit

T1 = ((2*pi)/sqrt(mew))*(a1^1.5);

e1 = (Ap1-Per_ht)/(Ap1+Per_ht); %initial eccentricity

r1 = (h1^2)/(mew*(1+e1))*[0, 1, 0]; %initial position vector, starting simulation at perigee, theta = 0

VPer1 = h1/Per_ht; % velocity of the probe at perigee of lowered initial orbit

Vap1 = h1/Ap1; %velocity of the probe at the apogee of the lowered initial orbit

V1 = [0, 0, VPer1]; %initial velocity vector at perigee

% calculate orbital velocity of europa around jupiter

EuropaPerigee = 664862; %perigee of europa around jupiter in km

EuropaApogee = 676938; %apogee of europa

a_eur = (EuropaPerigee+EuropaApogee)/2;

hEuropa = sqrt(2*mew)*sqrt((EuropaPerigee*EuropaApogee)/(EuropaPerigee+EuropaApogee)); %angular momentum of europa orbit

VEuropaApogee = hEuropa/EuropaApogee;

%% Set up and call the ODE

```

```

y0 = [r1 V1]'; %initial state vector combining r0 and v0

t0 = 0; % Initial time (s)

tf = pass*T1; % Final time (s) - # orbits times period. consider updating this to change period for each orbit

tspan = linspace(t0, tf, 36000); % Time interval

%% ODE solver

% Tolerance and ode setting adjustment

tol = 1e-12;

options = odeset('RelTol', tol, 'AbsTol', [tol tol tol tol tol tol]);

[t, y] = ode113(@difeq, tspan, y0, options); %this solves the ODE

%pull the position and velocity vectors from solved state vector

r_t = y(:, 1:3)'; % position vector as a function of time

x_t = y(:, 1);

y_t = y(:, 2);

z_t = y(:, 3);

%velocities

v_t = y(:, 4:6)'; %velocity vector as a function of time

vx_t = y(:, 4);

vy_t = y(:, 5);

vz_t = y(:, 6);

r_mag_t = sqrt(x_t.^2 + y_t.^2 + z_t.^2);

v_mag_t = sqrt(vx_t.^2 + vy_t.^2 + vz_t.^2); % Magnitude of velocity vector at each point

plot(r_mag_t)

% Find local maxima and minima in r_mag_t

[max_vals, max_idx] = findpeaks(r_mag_t); %the apogee values and corresponding time index

[min_vals, min_idx] = findpeaks(-r_mag_t); %perigee values and corresponding time index

min_vals = -min_vals; % Convert back to actual values

% Find local maxima and minima in v_mag_t

[max_vals_v, max_idx_v] = findpeaks(v_mag_t); %the apogee values and corresponding time index

[min_vals_v, min_idx_v] = findpeaks(-v_mag_t); %perigee values and corresponding time index

min_vals_v = -min_vals_v; % Convert back to actual values

```

```

% Create figure for apogee (max_vals) evolution

figure;
plot(max_vals, 'r-', 'LineWidth', 2, 'MarkerSize', 8);
grid on;
xlabel('Orbit Number');
ylabel('Radius (km)');
title('Evolution of Apogee Radius');
legend('Apogee Radius');

hold off;

% Create figure for perigee (min_vals) evolution

figure;
plot(min_vals, 'g-', 'LineWidth', 2, 'MarkerSize', 8);
grid on;
xlabel('Orbit Number');
ylabel('Radius (km)');
title('Evolution of Perigee Radius');
legend('Perigee Radius');

hold off;

%plot perigee velo evolution

figure;
plot(max_vals_v, 'r-', 'LineWidth', 2, 'MarkerSize', 8);
grid on;
xlabel('Orbit Number');
ylabel('Perigee Velo (km/s)');
title('Evolution of Perigee Velocity');
legend('Perigee Velocity');

hold off;

%plot apogee velo evolution

figure;
plot(min_vals_v, 'g-', 'LineWidth', 2, 'MarkerSize', 8);

```

```

grid on;

xlabel('Orbit Number');

ylabel('Apogee Velocity (km/s)');

title('Evolution of Apogee Velocity');

legend('Apogee Velocity');

hold off;

% Create a new figure for the spacecraft trajectory around Jupiter

figure; % Create a new figure

% Plot of surface of Jupiter

[xx1,yy1,zz1]=sphere(1000);

surf(Rj*xx1,Rj*yy1,Rj*zz1);

colormap('default');

clim([-Rj/100 Rj/100]);

shading interp;

line([0 5*Rj], [0 0], [0 0]); text(5*Rj,0,0,'X');

line([0 0], [0 5*Rj], [0 0]); text(0,5*Rj,0,'Y');

line([0 0], [0 0], [0 5*Rj]); text(0,0,5*Rj,'Z');

hold on;

% Plot the orbit trajectory

plot3(x_t, y_t, z_t, 'r-', 'LineWidth', 1); % Red line for the orbit path

xlabel('X (km)');

ylabel('Y (km)');

zlabel('Z (km)');

title('Spacecraft Trajectory Around Jupiter');

axis equal; % Makes the scaling equal on all axes

grid on;

%% Calculate all delta V's

% Calculate the delta V needed to enter the lower altitude perigee

h0 = sqrt(2*mew)*sqrt((Per1*Ap1)/(Per1+Ap1)); %orbital ang momentum of the original galileo orbit

VAp0 = h0/Ap1; %initial apogee velo

```

```

%calculate the delta v to transfer to the orbit with lower perigee for

%aerobraking

dv_1 = abs(VAp0-Vap1);

fprintf('The delta - V to enter the lower altitude perigee orbit for aerobraking is %.4f km/s\n', dv_1);

%calculate the desired orbital energy

Enrgy_Eur = (-mew)/(2*a_eur); %this is europas orbital energy, and our desired energy of our last
aerobraking orbit

Enrgy_target = Enrgy_Eur * 1.1; %anderson said slightly higher than the energy of europa orbit

a_target = (-mew)/(2*Enrgy_target); %target semi major axis of final aerobrake orbit

ap_target = (2*a_target)-mean(min_vals(:)); %average perigee of all aerobrake orbits will be what we take
for perigee. this finds our target apogee of last

rap2 = max_vals(end); %final apogee radius

disp('difference between target final aerobrake apogee and actual aerobrake apogee is:')

disp(rap2-ap_target)

%if this is small, then we are meeting the correct apogee

h_transfer = sqrt(2*mew)*sqrt((rap2*R)/(rap2+R)); %the transfer orbit that we will go in to to enter europa
orbit

v_ap_transfer = h_transfer/rap2; %this is the velocity that will be at the apogee of the orbit we are
transferring in to that matches europas energy

%find velocity at apogee of our final aerobraked orbit

hf = sqrt(2*mew)*sqrt((min_vals(end)*max_vals(end))/(min_vals(end)+max_vals(end)));

vf_ap = hf/max_vals(end);

dv_2 = abs(v_ap_transfer-vf_ap); %the delta V needed to enter the transfer orbit to enter europa orbit

fprintf('The delta - V to enter the transfer orbit to match europa orbit is %.4f km/s\n', dv_2);

%now find the delta V to burn to enter europa orbit

v_per_target = h_transfer/R; %velocity at perigee of the transfer orbit

VEuropaPer = hEuropa/EuropaPerigee;

dv_3 = abs(v_per_target-VEuropaPer); % the delta v to enter europa orbit

fprintf('The delta - V to enter the enter Europa orbit is %.4f km/s\n', dv_3);

%now calculate delta v needed for ballistic descent, assuming worst

%case that the probe starts accelerating from the edge of Europa SOI

E = -mew_eur/SOI; %orbital energy once probe has entered Europa SOI

```

```

dv_4 = sqrt(2*(E+(mew_eur/Re))); %velocity at the end of the ballistic descent, and therefor the delta V we
need to

fprintf('The delta - V required for ballistic descent is %.4f km/s\n', dv_4);

%NOW WE ARE GOING SAME VELOCITY AS EUROPA%

%perform burn to enter parking orbit around europa - assume circular for

%now

% v_park = sqrt(mew_eur/SOI); %the velocity of the orbit we want to go in to around europa - this will be
the dv for this burn

% dv_4 = 0;%v_park;

% fprintf('The delta - V to enter the enter Europa parking orbit is %.4f km/s\n', dv_4);

% %

% %

% %now calculate the angular momentum of the transfer ellipse from parking to

% %zero altitude

% hTransfer2 = sqrt(2*mew_eur)*sqrt((SOI*Re)/(SOI+Re)); %this is transfer from apogee of parking orbit -
apogee of parking orbit is at SOI, radius of zero altitude orbit is just radius of europa

% %now calculate velocities of second transfer ellipse

% VTransfer2 = hTransfer2/SOI; %velocity of transfer ellipse to zero altitude orbit at apogee

% %delta v for beginning transfer ellipse that brings us to zero altitude

% %orbit

% dv_5 = 0;%abs(VTransfer2-v_park);

% fprintf('The delta - V to enter the transfer ellipse to surface is %.4f km/s\n', dv_5);

% %now calculate delta v for insertion to 0 altitude parking orbit

% VTransfer2Arrival = hTransfer2/Re; %velocity of transfer orbit 2 once it arrives at zero altitude orbit

% Vzeroalt = sqrt(mew_eur/Re); %velocity of zero altitude circular orbit

% dv_6 = 0;%abs(VTransfer2Arrival-Vzeroalt); %DV for insertion in to zero altitude orbit for transfer 2

% fprintf('The delta - V to enter the zero altitude parking orbit is %.4f km/s\n', dv_6);

% %

% %now add on final DV to go from zero altitude circular orbit to stationary.

% %this is just equal to DV = Vcirc - 0 = Vcirc. or in our case the variable

% %is called Vzeroalt. we will just add this to the end

```

```

% dv_7 = 0;%Vzeroalt;

% fprintf('The delta - V to bring probe to rest is %.4f km/s\n', dv_7);

%sum up for total delta V

dvtotal = dv_1 + dv_2 + dv_3 + dv_4; %total delta V of entire maneuver

fprintf('The total delta - V required to facilitate landing is %.4f km/s\n', dvtotal);

%% Functions section

%Function definitions

% Differential equation

function dfdt = difeq(t,vector) %vector is input vector, in this case it is y0

% Position vector (km)

r = vector(1:3)'; %set position vector as first three entries of state vector

rn = norm(r); %magnitude of position vector

% Velocity vector (km/s)

v = vector(4:6)'; %velocity vector is last three entries of the state vector

% Orbital velocity of Jupiter (rad/s)

wJ = [0;0;1.8268e-04];

% Relative velocity of the spacecraft w.r.t atmosphere (km/s)

vr = v - cross(wJ,r);

% Magnitude of relative velocity (km/s)

vrmag = norm(vr);

% Unit velocity vector

uv = vr/vrmag; %drag will be opposite of this

% Universal gravitational Constant (km^3/kgs^2)

G = 6.6743*10^-20;

% Mass of Jupiter (kg)

msc = 1000; %mass of spacecraft (kg)

Mj = 1.898 * 10^27 ; % mass of Jupiter in kg% Radius of Jupiter (km)

Rj = 69911;

% Mass of the Spacecraft (kg)

mu = G*(Mj);

```

```

% Coefficient of drag for spacecraft
CD =2.2;
% Area of the Spacecraft (m^2)
A = 33.4711;
% Altitude at each position (km)
alt = rn - Rj; %magnitude of the position vector minus the radius of jupiter equals altitude
%disp(alt)
% Density at each altitude (kg/m^3)
rhoJ = atm(alt); %the density is the atmospheric fxn at that altitude
% Components of acceleration due to gravity (km/s^2)
ad = -CD*A/msc*rhoJ*(1000*vrmag)^2/2*uv; %the acceleration due to drag
a = -mu*r/rn^3; %gravitational acceleration
atot = a+ad/1000; %total acceleration
% size_v = size(v);
% size_atot = size(atot);
% disp(['Size of v: ', num2str(size_v)]);
% disp(['Size of atot: ', num2str(size_atot)]);
dfdt = [v atot]';
end
% Density calculation at different altitudes - called by dfdt function
function rhoJ = atm(zz)
% Altitude (km)
% Altitude (km)
z = [-134.7, -118, -98, -78, -58, -38, -18, 0, 2, 22, 42, 62, 82, 102, 122, 142, 162, ...
182, 202, 222, 242, 262, 282, 302, 322, 342, 362, 382, 402, 422, 442, ...
462, 482, 502, 522, 542, 562, 582, 602, 622, 642, 662, 682, 702, ...
722, 742, 762, 782, 802, 822, 842, 862, 871.2, 881, 901, 921, 941, ...
961, 981, 1001, 1021, 1041, 1042, 1043];
% Density at the above altitudes (kg/m^3)
rho_o = [0.07945, 0.003335, 0.009915, 0.03168, 0.001261, 0.000571, 0.0002325, ...

```

```

0.16, 0.000102, 4.98e-5, 2.206e-5, 9.878e-6, 4.41e-6, 2.012e-6, ...
8.713e-7, 3.417e-7, 1.629e-7, 8.251e-8, 3.892e-8, 1.917e-8, ...
1.023e-8, 6.989e-9, 4.27e-9, 3.058e-9, 2.455e-9, 1.937e-9, ...
1.451e-9, 1.114e-9, 9.053e-10, 7.562e-10, 6.39e-10, 5.364e-10, ...
4.506e-10, 3.757e-10, 3.113e-10, 2.567e-10, 2.117e-10, 1.759e-10, ...
1.487e-10, 1.272e-10, 1.101e-10, 9.638e-11, 8.502e-11, 7.539e-11, ...
6.700e-11, 5.948e-11, 5.264e-11, 4.635e-11, 4.057e-11, 3.535e-11, ...
3.082e-11, 2.711e-11, 2.575e-11, 2.4239889*10^-11, 2.31447825*10^-11, ...
1.83882607*10^-11, 1.54317389*10^-11, 1.24752171*10^-11, ...
9.5186953*10^-12, 6.5621735*10^-12, 3.6056517*10^-12, ...
6.491299*10^-13, 0, 0];

% Corresponding scale height, Hs (km) [Hs = (k*T)/(m*g)]
% Corresponding scale height, Hs (km) [Hs = (k*T)/(m*g)]

Hs = [19.01690229, 17.52576982, 18.99334475, 22.29206767, 24.52366002, ...
23.25123718, 24.92816483, 27, 26.20318247, 24.47837484, ...
24.61767988, 24.47794291, 24.27062917, 23.57371192, 23.9013278, ...
27.88221815, 30.70879836, 31.75918808, 37.62505054, 47.78796389, ...
62.20804221, 66.77646033, 83.01818832, 92.91115618, 93.522481, ...
95.94834225, 104.879345, 113.8800791, 118.1323146, 119.5602983, ...
119.8434676, 120.9547474, 122.2195614, 124.6704474, 128.5572063, ...
133.9299006, 140.4993831, 147.1618975, 152.4881568, 156.6924695, ...
159.682461, 161.243726, 161.5055009, 160.9916901, 160.0448426, ...
159.106962, 159.6067468, 158.980608, 160.2980833, 162.6303783, ...
165.23003, 166.5985742, 166.0877434, 166.6, 166, 166, ...
166, 166, 166, 166, 166, 166, 166, ...
166, 166, 166];;

% Out-of-bound altitude adjustments for density calculation

if zz > 1042
zz = 1042;

elseif zz < 0

```

```

zz = 0;
end

% Iterations set-up

for jj = 1:63

if zz >= z(jj) && zz < z(jj+1)

ii = jj;

end

end

if zz == 1042

ii = 63;

end

% Density calculation as exponential function of scale height, altitude,
% and density corresponding to scale height

rhoJ = rho_o(ii)*exp(-(zz - z(ii))/Hs(ii));
end

```

## 13.4: Final Optimal Apojoove MATLAB Script

Prepared by: Andrew Olson

```

%this script calculates delta V to exit the final aerobraked orbit at
%apogee and enter a transfer and then burn to enter the europa orbit. It
%loops over this to find the optimal apogee to leave aerobrake from. the
%perigee of each aerobraked orbit will be assumed to be the average perigee
%from other simulations, this comes to be 7.4001e+04

clear all

close all

per = 7.4001e+04;

G = 6.6743*10^-20;

Me = 4.79984 * 10^22; % mass of eueropa in kg

Mj = 1.898 * 10^27 ; % mass of Jupiter in kg

R = 671000; %radius between Jupiter and Europa in KM

mew = Mj*G; %calculate mew for jupiter

```

```

VEuropaPer = 13.8653;
VEuropaAp = 13.618;
SOI = 9.7251e+03;
Ap1 = 19000000;
%get apogee array from aerobrake script
run('AerobrakeFinal.m')
rap = max_vals; %set apogee from aerobrake script equal to apogee here
h_transfer = zeros(size(rap));
v_ap_transfer = zeros(size(rap));
hf = zeros(size(rap));
vf_ap = zeros(size(rap));
dv_2 = zeros(size(rap));
v_per_target = zeros(size(rap));
dv_3 = zeros(size(rap));
dv_total = zeros(size(rap));
%add on Ap1 so we can calculte delta V for zero passes
rap = [Ap1,rap'];
for i = 1:length(rap)
    h_transfer(i) = sqrt(2*mew)*sqrt((rap(i)*R)/(rap(i)+R));
    v_ap_transfer(i) = h_transfer(i)/rap(i);
    hf(i) = sqrt(2*mew)*sqrt((per*rap(i))/(per+rap(i)));
    vf_ap(i) = hf(i)/rap(i);
    dv_2(i) = abs(v_ap_transfer(i)-vf_ap(i));
    v_per_target(i) = h_transfer(i)/R;
    dv_3(i) = abs(v_per_target(i)-VEuropaPer);
    dv_total(i) = dv_2(i) + dv_3(i);
    fprintf('Apogee Radius: %.2e km\n', rap(i));
    fprintf('ΔV to enter transfer orbit: %.4f km/s\n', dv_2(i));
    fprintf('ΔV to insert into Europa orbit: %.4f km/s\n', dv_3(i));
    fprintf('Total ΔV: %.4f km/s\n', dv_total(i)+.4523 +1.857);

```

```

end

figure;

plot(rap, dv_2, 'b-', 'LineWidth', 2, 'DisplayName', '\DeltaV to enter transfer orbit');

hold on;

plot(rap, dv_3, 'r-', 'LineWidth', 2, 'DisplayName', '\DeltaV to insert in to Europa orbit');

plot(rap, dv_total, 'k-', 'LineWidth', 2, 'DisplayName', 'Total \DeltaV');

% Add vertical line for initial apojoove

xline(Ap1, 'magenta--', 'LineWidth', 2, 'DisplayName', 'Initial Apojoove');

%text(Ap1 - 1e6, max(dv_total)*0.8, 'Initial Apojoove', 'Color', 'black', 'FontSize', 10, 'HorizontalAlignment', 'right');

hold off;

xlabel('Final Aerobrake Apojoove Radius (km)');

ylabel('\DeltaV (km/s)');

grid on;

legend('show');

title('\DeltaV Components vs Aerobrake Apojoove Radius');

% dv_circ = zeros(size(rap));

% %try entering a circular orbit directly at apogee of aerbrake

% for j = 1:length(rap)

%   dv_circ(j) = abs(vf_ap(j)-VEuropaAp);

% end

%

% figure;

% plot(rap, dv_circ, 'b-', 'LineWidth', 2, 'DisplayName', '\DeltaV to enter Europa orbit in one burn at apogee');

% xlabel('Final Aerobrake Apogee Radius (km)');

% ylabel('\DeltaV (km/s)');

```

**ADCS Script for Quaternion + angular velocity based error using Reaction Wheels and Thrusters**

```
clear all; close all; clc
```

```

% Initialize global variables

global I1 I2 I3 K_om K_q EA_d om_d M_sat A_rw rw thr

% Spacecraft inertia properties

I1 = 467.4; %kg*m^2
I2 = 390.2; %kg*m^2
I3 = 518.5; %kg*m^2
I = [I1, 0, 0; 0, I2, 0; 0, 0, I3];

% Optimal configuration angles

beta1 = rad2deg(45); % symmetric angle between x and y axes
beta2 = rad2deg(35.26); % Optimal skew

% Update reaction wheel configuration matrix for asymmetric case

A_rw = [
    cos(beta1)*cos(beta2) -cos(beta1)*cos(beta2) -cos(beta1)*cos(beta2) cos(beta1)*cos(beta2);
    sin(beta1)*cos(beta2) sin(beta1)*cos(beta2) -sin(beta1)*cos(beta2) -sin(beta1)*cos(beta2);
    -sin(beta2) sin(beta2) -sin(beta2) sin(beta2)
];

% RW and thr Design Conditions

rw.max_torque_wheel = 0.2; % N·m (from datasheet)
rw.wheel_inertia = 0.02; % kg·m^2
rw.max_speed = 4000; % rad/s
rw.max_momentum_wheel = .8; % N·m·s (from datasheet)
thr.force = 1.0; % N per thr (from MONARC-1 specs)
thr.min_impulse = 0.01; % seconds
thr.num_per_axis = 4; % 4 thrs per axis
thr.max_torque = 4;
M_sat = thr.max_torque;

% Control gains

K_q = 100 * [2.0; 3.0; 4.0];
K_om = 600 * [1.5; 2.0; 2.5];

% Initial conditions

```

```

om = 1.0*[-1.1; -1.5; -0.33]; % rad/s

EA = 0.1*[-1.0; 10; -2.0]; % rad

% Desired states

om_d = [0.0; 0.0; 0.0];

EA_d = [0.0; 0.0; 0.0];

% Simulation parameters

Tfinal = 500;

tspan = linspace(0, Tfinal, 500);

% Initialize state vector with wheel speeds

initial_DCM = get_DCM_from_EA(EA);

initial_q = get_quaternions_from_DCM(initial_DCM);

initial_w_spd = zeros(4,1);

Y0 = [om; initial_q; initial_w_spd];

% Run simulation

[t, Y] = ode45(@spacecraft_dynamics, tspan, Y0);

% Calculate histories for plotting

n = length(t);

EA1 = zeros(n,1); EA2 = zeros(n,1); EA3 = zeros(n,1);

phi1 = zeros(n,1); phi2 = zeros(n,1); phi3 = zeros(n,1);

M_C_history = zeros(n,3);

rw_torque_history = zeros(n,4);

thr_torque_history = zeros(n,3);

wheel_speed_history = zeros(n,4);

energy_history = zeros(n,1);

H_body = zeros(n,3);

q_history = Y(:,4:7);

for i = 1:n

% Extract states

om = Y(i,1:3)';

q = Y(i,4:7)';

```

```

w_spd = Y(i,8:11)';

% Calculate DCMs and angles
DCM = get_DCM_from_quaternions(q);
[EA1(i), EA2(i), EA3(i)] = calculate_euler_angles(DCM);

% Calculate off-pointing angles
phi1(i) = acos(max(min(DCM(1,1), 1), -1));
phi2(i) = acos(max(min(DCM(2,2), 1), -1));
phi3(i) = acos(max(min(DCM(3,3), 1), -1));

% Calculate control torque
DCM_desired = get_DCM_from_EA(EA_d);
DCM_error = DCM_desired' * DCM;
qe = get_quaternions_from_DCM(DCM_error);
qe = qe(1:3);

om_error = Y(i,1:3)' - om_d;
M_C = -K_q .* qe - K_om .* om_error;

% Split control between RW and thrs
[wheel_torques, M_C_thrs] = distribute_torque_with_desaturation(M_C, w_spd);
M_C_wheels = A_rw * wheel_torques;

% Calculate total angular momentum in body frame
I = diag([I1 I2 I3]);
H_body(i,:) = (I * om + A_rw * (rw.wheel_inertia * w_spd))';

% Store histories
M_C_history(i,:) = (M_C_wheels + M_C_thrs)';

```

```

rw_torque_history(i,:) = wheel_torques';
thr_torque_history(i,:) = M_C_thrs';
wheel_speed_history(i,:) = w_spd';
energy_history(i) = abs(dot(M_C_wheels + M_C_thrs, om));
end

% Calculate M_C_magnitude before plotting
M_C_magnitude = sqrt(sum(M_C_history.^2, 2));
total_torque_magnitude = M_C_magnitude; % They are the same thing

% Performance Analysis
max_torque = max(abs(M_C_history));
mean_torque = mean(abs(M_C_history));
rms_torque = rms(M_C_history);

% Calculate saturation times
rw_saturation = any(abs(wheel_speed_history) >= rw.max_speed-1e-6, 2);
thr_saturation = any(abs(thr_torque_history) >= thr.max_torque-1e-6, 2);
time_saturated_rw = sum(rw_saturation) * (t(2)-t(1));
time_saturated_thrust = sum(thr_saturation) * (t(2)-t(1));

% Calculate settling time
EA_magnitude = sqrt(EA1.^2 + EA2.^2 + EA3.^2);
settling_threshold = deg2rad(1); % 1 degree threshold
settling_idx = find(EA_magnitude(2:end) < settling_threshold, 1, 'first');
if ~isempty(settling_idx)
    settling_time = t(settling_idx);
else
    settling_time = inf;
end

% Calculate other magnitudes
H_magnitude = sqrt(sum(H_body.^2, 2));
omega_magnitude = sqrt(Y(:,1).^2 + Y(:,2).^2 + Y(:,3).^2);
power_wheels = abs(rw_torque_history .* wheel_speed_history);

```

```

% Print analysis results in organized sections

fprintf('\n==== ADCS Performance Analysis ====\n');

% Power Performance Metrics

fprintf('\nPower Performance:\n');

fprintf(' Peak power consumption: %.2f W\n', max(energy_history));
fprintf(' Average power consumption: %.2f W\n', mean(energy_history));
fprintf(' Total energy used: %.2f J\n', trapz(t, energy_history));

fprintf('\nOverall System Performance:\n');

fprintf(' Total control torque applied: %.2f N·m\n', trapz(t, M_C_magnitude));
fprintf(' Total power used: %.2f W·s (%.2f W·hr)\n', trapz(t, energy_history), trapz(t, energy_history)/3600);

% Control Torque Performance Metrics

fprintf('\nControl Torque Performance:\n');

fprintf(' Peak total torque: %.4f N·m\n', max(M_C_magnitude));
fprintf(' Average total torque: %.4f N·m\n', mean(M_C_magnitude));
fprintf(' RMS total torque: %.4f N·m\n', rms(M_C_magnitude));

% Section 2: Actuator Performance

fprintf('\nReaction Wheel Performance:\n');

fprintf(' Maximum wheel speed: %.2f rad/s (Limit: 4000)\n', max(max(abs(wheel_speed_history))));

fprintf(' Maximum wheel torque: %.2f N·m (Limit: 0.2)\n', max(max(abs(rw_torque_history))));

fprintf(' Maximum momentum per wheel: %.2f N·m·s (Limit: 0.8)\n', max(max(abs(wheel_speed_history)) * rw.wheel_inertia));

fprintf(' RMS wheel momentum: %.2f N·m·s\n', rms(max(abs(wheel_speed_history))) * rw.wheel_inertia);

fprintf(' Time at speed saturation: %.2f seconds\n', time_saturated_rw);

fprintf('\nThruster Performance:\n');

fprintf(' Maximum thruster torque: %.2f N·m (Limit: %.2f)\n', max(max(abs(thr_torque_history))), thr.max_torque);

fprintf(' Average thruster usage: %.2f N·m\n', mean(mean(abs(thr_torque_history))));

fprintf(' Time at thrust saturation: %.2f seconds\n', time_saturated_thrust);

% Section 3: State Space Performance

fprintf('\nQuaternion Performance:\n');

```

```

fprintf(' Maximum deviation: [% .4f, % .4f, % .4f, % .4f]\n', max(abs(q_history)));
fprintf(' RMS deviation: [% .4f, % .4f, % .4f, % .4f]\n', rms(q_history));
fprintf('\nEuler Angle Performance:\n');
fprintf(' Maximum angles (deg): [% .2f, % .2f, % .2f]\n', rad2deg(max(abs([EA1, EA2, EA3]))));
fprintf(' RMS angles (deg): [% .2f, % .2f, % .2f]\n', rad2deg(rms([EA1, EA2, EA3])));
fprintf(' Maximum total attitude error: %.2f deg\n', rad2deg(max(EA_magnitude)));
fprintf(' RMS attitude error: %.2f deg\n', rad2deg(rms(EA_magnitude)));
fprintf(' Settling time to 1 deg: %.2f seconds\n', settling_time);
fprintf('\nAngular Motion Performance:\n');
fprintf(' Maximum velocity (rad/s): [% .2f, % .2f, % .2f]\n', max(abs(Y(:,1:3))));
fprintf(' RMS velocity (rad/s): [% .2f, % .2f, % .2f]\n', rms(Y(:,1:3)));
fprintf(' Maximum angular momentum: [% .2f, % .2f, % .2f] N·m·s\n', max(abs(H_body)));
fprintf(' RMS angular momentum: [% .2f, % .2f, % .2f] N·m·s\n', rms(H_body));

% Plot Family 1: Control Torque Performance (6 plots)

figure('Position', [100 100 1500 1000]);
sgtitle('ECHO: System Performance Analysis');

% Plot 1: Total Attitude Error

subplot(3,2,1);

EA_magnitude = sqrt(EA1.^2 + EA2.^2 + EA3.^2);
plot(t, rad2deg(EA_magnitude), 'k', 'LineWidth', 0.1);
title('Total Attitude Error');
xlabel('Time [s]');
ylabel('Error [deg]');
grid on;

% Plot 2: Total Angular Velocity

subplot(3,2,2);

omega_magnitude = sqrt(Y(:,1).^2 + Y(:,2).^2 + Y(:,3).^2);
plot(t, omega_magnitude, 'k', 'LineWidth', 0.1);
title('Total Angular Velocity');
xlabel('Time [s]');

```

```

ylabel('Angular Velocity [rad/s]');
grid on;

% Plot 3: Total Angular Momentum

subplot(3,2,3);
H_magnitude = sqrt(sum(H_body.^2, 2));
plot(t, H_magnitude, 'k', 'LineWidth', 0.1);
title('Total Angular Momentum');
xlabel('Time [s]');
ylabel('Angular Momentum [N·m·s]');
grid on;

% Plot 4: Total Power

subplot(3,2,4);
plot(t, energy_history, 'k', 'LineWidth', 0.1);
title('Total Power Consumption');
xlabel('Time [s]');
ylabel('Power [W]');
grid on;

% Plot 5: Total Control Torque

subplot(3,2,5);
M_C_magnitude = sqrt(sum(M_C_history.^2, 2));
plot(t, M_C_magnitude, 'k', 'LineWidth', 0.1);
title('Total Control Torque');
xlabel('Time [s]');
ylabel('Torque [N·m]');
grid on;

% Plot 6: Control Torque Components

subplot(3,2,6);
plot(t, M_C_history(:,1), 'r', t, M_C_history(:,2), 'g', t, M_C_history(:,3), 'b', 'LineWidth', 0.1);
title('Control Torque Components');
xlabel('Time [s]');

```

```

ylabel('Torque [N·m]');
legend('X-axis', 'Y-axis', 'Z-axis');
grid on;

% Plot Family 2: Actuator Performance (6 plots)

figure('Position', [100 100 1500 1000]);
shtitle('Actuator Performance');

subplot(3,2,1);
plot(t, wheel_speed_history, 'LineWidth', 0.1);
title('Reaction Wheel Speeds');
xlabel('Time [s]');
ylabel('Speed [rad/s]');
legend('W1', 'W2', 'W3', 'W4');
grid on;

subplot(3,2,2);
plot(t, rw_torque_history, 'LineWidth', 0.1);
title('Reaction Wheel Torques');
xlabel('Time [s]');
ylabel('Torque [N·m]');
legend('W1', 'W2', 'W3', 'W4');
grid on;

subplot(3,2,3);
power_wheels = abs(rw_torque_history .* wheel_speed_history);
plot(t, power_wheels, 'LineWidth', 0.1);
title('Reaction Wheel Power');
xlabel('Time [s]');
ylabel('Power [W]');
legend('W1', 'W2', 'W3', 'W4');
grid on;

subplot(3,2,4);
plot(t, thr_torque_history, 'LineWidth', 0.1);

```

```

title('Thruster Torques');

xlabel('Time [s]');

ylabel('Torque [N·m]');

legend('X-axis', 'Y-axis', 'Z-axis');

grid on;

subplot(3,2,5);

thr_magnitude = sqrt(sum(thr_torque_history.^2, 2));

plot(t, thr_magnitude, 'k', 'LineWidth', 0.1);

title('Total Thruster Torque');

xlabel('Time [s]');

ylabel('Torque [N·m]');

grid on;

subplot(3,2,6);

thr_power = abs(sum(thr_torque_history .* Y(:,1:3), 2));

plot(t, thr_power, 'k', 'LineWidth', 0.1);

title('Thruster Power');

xlabel('Time [s]');

ylabel('Power [W]');

grid on;

% Plot Family 3: State Space Performance (5 plots)

figure('Position', [100 100 1500 1000]);

sgtitle('State Space Performance');

subplot(3,2,1);

plot(t, rad2deg(EA1), 'r', t, rad2deg(EA2), 'g', t, rad2deg(EA3), 'b', 'LineWidth', 0.1);

title('Euler Angles');

xlabel('Time [s]');

ylabel('Angle [deg]');

legend('\theta_1', '\theta_2', '\theta_3');

grid on;

subplot(3,2,2);

```

```

plot(t, q_history(:,1), 'r', t, q_history(:,2), 'g', t, q_history(:,3), 'b', t, q_history(:,4), 'k', 'LineWidth', 0.1);
title('Quaternion Components');
xlabel('Time [s]');
ylabel('Quaternion Value');
legend('q_1', 'q_2', 'q_3', 'q_4');
grid on;
subplot(3,2,3);
plot(t, rad2deg(phi1), 'r', t, rad2deg(phi2), 'g', t, rad2deg(phi3), 'b', 'LineWidth', 0.1);
title('Off-pointing Angles');
xlabel('Time [s]');
ylabel('Angle [deg]');
legend('\phi_1', '\phi_2', '\phi_3');
grid on;
subplot(3,2,4);
plot(t, Y(:,1), 'r', t, Y(:,2), 'g', t, Y(:,3), 'b', 'LineWidth', 0.1);
title('Angular Velocity Components');
xlabel('Time [s]');
ylabel('Angular Velocity [rad/s]');
legend('\omega_1', '\omega_2', '\omega_3');
grid on;
subplot(3,2,5);
plot(t, H_body(:,1), 'r', t, H_body(:,2), 'g', t, H_body(:,3), 'b', 'LineWidth', 0.1);
title('Angular Momentum Components');
xlabel('Time [s]');
ylabel('Angular Momentum [N·m·s]');
legend('H_1', 'H_2', 'H_3');
grid on;
% Helper Functions
function [wheel_torques, thr_torques] = distribute_torque_with_desaturation(M_C_desired, w_spd)
    global rw A_rw thr I1 I2 I3

```

```

% Simple pseudo-inverse solution for wheel torques
wheel_torques = pinv(A_rw) * M_C_desired;

% Calculate desaturation torques with asymmetric inertia consideration
desaturation_gains = zeros(4,1);
for i = 1:4
    wheel_momentum = abs(w_spd(i) * rw.wheel_inertia);
    if wheel_momentum > 0.7 * rw.max_momentum_wheel
        % Scale desaturation based on inertia ratio
        inertia_scale = sqrt((I1^2 + I2^2 + I3^2)/(3 * max([I1,I2,I3])^2));
        desaturation_gains(i) = -sign(w_spd(i)) * 0.1 * inertia_scale;
    end
end

% Apply desaturation and enforce limits
wheel_torques = wheel_torques + desaturation_gains;
for i = 1:4
    if abs(wheel_torques(i)) > rw.max_torque_wheel
        wheel_torques(i) = sign(wheel_torques(i)) * rw.max_torque_wheel;
    end
end

% Check predicted momentum
predicted_momentum = abs((w_spd(i) + wheel_torques(i) * 0.01) * rw.wheel_inertia);
if predicted_momentum > rw.max_momentum_wheel && sign(w_spd(i)) == sign(wheel_torques(i))
    wheel_torques(i) = 0;
end
end

% Calculate thruster torques considering asymmetric inertia effects

```

```

M_C_wheels = A_rw * wheel_torques;
thr_torques = M_C_desired - M_C_wheels;

% Enforce thruster limits with inertia-based scaling
inertias = [I1, I2, I3];
max_inertia = max(inertias);

for i = 1:3
    % Scale limit based on axis inertia
    inertia_ratio = inertias(i) / max_inertia;
    axis_limit = thr.max_torque * inertia_ratio;

    if abs(thr_torques(i)) > axis_limit
        thr_torques(i) = sign(thr_torques(i)) * axis_limit;
    end
end

% spacecraft_dynamics function
function dydt = spacecraft_dynamics(t, y)
global I1 I2 I3 K_om K_q EA_d om_d A_rw rw

    % Extract states
    om = y(1:3);
    q = y(4:7);
    w_spd = y(8:11);

    % Calculate errors
    DCM_actual = get_DCM_from_quaternions(q);
    DCM_desired = get_DCM_from_EA(EA_d);
    DCM_error = DCM_desired' * DCM_actual;

```

```

qe = get_quaternions_from_DCM(DCM_error);
qe = qe(1:3);

% Control law
om_error = om - om_d;
M_C_desired = -K_q .* qe - K_om .* om_error;

% Get control torques with desaturation
[wheel_torques, thr_torques] = distribute_torque_with_desaturation(M_C_desired, w_spd);

% Total control torque
M_C = A_rw * wheel_torques + thr_torques;

% Dynamics
I = diag([I1 I2 I3]);
om_dot = I \ (M_C - cross(om, I * om));

% Wheel dynamics
wheel_accelerations = wheel_torques / rw.wheel_inertia;

% Quaternion kinematics
q_dot = 0.5 * [-q(2), -q(3), -q(4);
                q(1), -q(4), q(3);
                q(4), q(1), -q(2);
                -q(3), q(2), q(1)] * om;

dydt = [om_dot; q_dot; wheel_accelerations];
end

function C = get_DCM_from_quaternions(q)
C = [1 - 2*(q(3)^2 + q(4)^2), 2*(q(2)*q(3) - q(4)*q(1)), 2*(q(2)*q(4) + q(3)*q(1));
      2*(q(2)*q(3) + q(4)*q(1)), 1 - 2*(q(2)^2 + q(4)^2), 2*(q(3)*q(4) - q(2)*q(1));
      2*(q(2)*q(4) - q(3)*q(1)), 2*(q(3)*q(4) + q(2)*q(1)), 1 - 2*(q(2)^2 + q(3)^2)];

```

```

2*(q(2)*q(3) + q(4)*q(1)), 1 - 2*(q(2)^2 + q(4)^2), 2*(q(3)*q(4) - q(2)*q(1));
2*(q(2)*q(4) - q(3)*q(1)), 2*(q(3)*q(4) + q(2)*q(1)), 1 - 2*(q(2)^2 + q(3)^2)];
end

function C = get_DCM_from_EA(EA)

EA1 = EA(1); EA2 = EA(2); EA3 = EA(3);

C11 = cos(EA2) * cos(EA3);
C12 = -cos(EA2) * sin(EA3);
C13 = sin(EA2);

C21 = sin(EA1) * sin(EA2) * cos(EA3) + cos(EA1) * sin(EA3);
C22 = -sin(EA1) * sin(EA2) * sin(EA3) + cos(EA1) * cos(EA3);
C23 = -sin(EA1) * cos(EA2);

C31 = -cos(EA1) * sin(EA2) * cos(EA3) + sin(EA1) * sin(EA3);
C32 = cos(EA1) * sin(EA2) * sin(EA3) + sin(EA1) * cos(EA3);
C33 = cos(EA1) * cos(EA2);

C = [C11 C12 C13; C21 C22 C23; C31 C32 C33];

end

function q_vec = get_quaternions_from_DCM(C)

C = real(C);

tr = C(1,1) + C(2,2) + C(3,3);

tr = max(min(tr, 3), -1);

q4 = sqrt(1 + tr) / 2;
q4 = max(q4, 1e-6);

q1 = (C(3,2) - C(2,3)) / (4*q4);
q2 = (C(1,3) - C(3,1)) / (4*q4);
q3 = (C(2,1) - C(1,2)) / (4*q4);

q_vec = [q1; q2; q3; q4];
q_vec = q_vec / norm(q_vec);

```

```

end

function [EA1, EA2, EA3] = calculate_euler_angles(DCM)
    DCM = real(DCM);
    EA2 = asin(max(min(DCM(1,3), 1), -1));

    cosEA2 = cos(EA2);
    if abs(cosEA2) > 1e-10
        EA1 = atan2(-real(DCM(2,3))/cosEA2, real(DCM(3,3))/cosEA2);
        EA3 = atan2(-real(DCM(1,2))/cosEA2, real(DCM(1,1))/cosEA2);
    else
        EA1 = 0;
        EA3 = atan2(real(DCM(2,1)), real(DCM(2,2)));
    end
end

```

## 13.5 Worst-case Temperature Script

```

%Calculating worst-case hot and cold temperatures at Jupiter for a
%spherical spacecraft

Rj = 71300*1000; % Jupiter radius (m)

Hm = 350*1000; %perigee (m)

Hf = 1.9e7*1000; %apogee (m)

Ka = 0.657 + 0.54*(Rj/(Rj+Hm)) - 0.196*(Rj/(Rj+Hm))^2;

Gs = 51; %Direct Solar for Jupiter (W/m^2)

as = 0.1;% solar absorptivity of sphere

q_IR = 13.6; %Jupiter planetary IR (W/m^2)

e_IR = 0.6; %IR emissivity

F_sjmax = 0.5*(1-((Hm^2 + 2*Hm*Rj)^0.5)/(Hm+Rj)); %View factor at perigee

F_sjmin = 0.5*(1-((Hf^2 + 2*Hf*Rj)^0.5)/(Hf+Rj)); %View factor at apogee

a = 0.343; %Jupiter albedo

Qw = 500; %Power dissipation (W) majority from RTG

```

```

sigma = 5.67e-8; %Stefan-Boltzmann
D = 1.6; %sphere diameter (m)
T_MAX = ((Gs*as/4 + q_IR*e_IR*F_sjmax + Gs*a*as*Ka*F_sjmax + Qw/(pi*D^2))/(sigma*e_IR))^0.25 - 273
%in Celsius
T_MIN = ((q_IR*e_IR*F_sjmin + Qw/(pi*D^2))/(sigma*e_IR))^0.25 - 273 %in Celsius

```

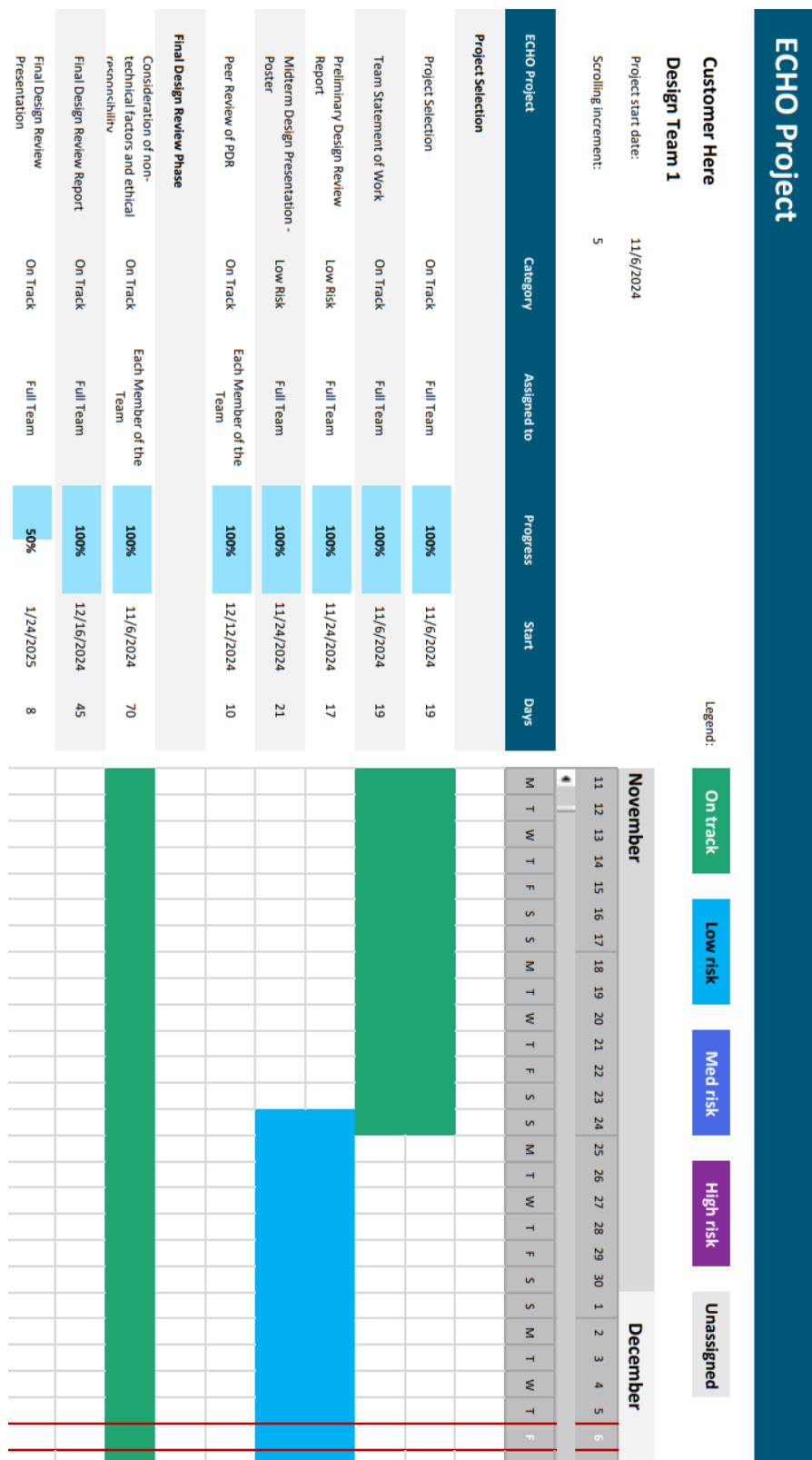
## 13.6 Landing Leg Transfer Function Generation MATLAB Script

```

syms K_1 K_2 K_3 D_1 D_2 D_3 X_m X_1 X_2 X_3 s F_g M_m F_I M_1 M_2 M_3
eqn1 = -M_m*s^2*X_m + K_1*(X_1-X_m) + D_1*(s*X_1 - s*X_m) + K_2*(X_2-X_m) + D_2*(s*X_2 - s*X_m)
+ K_3*(X_3-X_m) + D_3*(s*X_3 - s*X_m)
eqn2 = -M_1*s^2*X_1 + K_1*(X_m-X_1) + D_1*(s*X_m - s*X_1)
eqn3 = -M_2*s^2*X_2 + K_2*(X_m-X_2) + D_2*(s*X_m - s*X_2)
eqn4 = -M_3*s^2*X_3 + K_3*(X_m-X_3) + D_3*(s*X_m - s*X_3)
vars = [X_m, X_1, X_2, X_3]
A = equationsToMatrix([eqn1, eqn2, eqn3, eqn4], vars)
b = [0; F_I; F_I; F_I]
x=A\b
eqnans = x(1) == X_m

```

## 13.7: Gantt Chart



## **13.8: Statement of Work**

# **MANE 4250 - Space Vehicle Design**

## **Statement of Work**

Europa Composition and Habitat Observation (Project ECHO)

---

A Europa Orbiter and Probe Mission

Team 1: Joseph Bowers, Katie August, Mae Tringone, Chloe Powell, Aaryan Sonawane,  
Constantine Childs, Andrew Olson

## **A: Introduction and Background**

Europa, the fourth largest of Jupiter's moons, is one of the most promising candidates for hosting extraterrestrial life in our solar system. Estimated to be 4.5 billion years old, there has been adequate time for life to develop (Howell, 2023). Additionally, scientists believe Europa possesses the key elements necessary for life, including liquid water, and derives sufficient energy from Jupiter's radiation to support biological processes (NASA, n.d.).

While the surface temperature does not rise above minus 260 °F, scientists believe Europa contains twice as much liquid water as earth's oceans (Howell, 2023) and (NASA, n.d.) In 2013, the Hubble Space Telescope detected water vapor plumes emanating from surface geysers on Europa (Howell, 2023). Additionally, high resolution images from NASA's Galileo spacecraft showed evidence of "mobile icebergs" on the icy moon (M. H. Carr, 1998). These observations led scientists to believe that there is a liquid ocean underneath the surface – further bolstering the potential for Europa to host life and making it a prime candidate for exploration and study.

Multiple missions are planned in the next decade to investigate this potential – including both NASA's Europa Clipper and ESA's Jupiter Icy Moons Explorer (Howell, 2023). The Europa Clipper is an orbiter mission designed to perform 44 low-altitude flybys of the moon, beginning in April 2030. Because of the high levels of scientific interest in the composition of Europa's ice and the moon's habitability, it is desired to design a rover to land on the moon for more detailed analysis. Multiple design proposals have been put forth for this mission, including NASA's

## **B: Objectives**

The mission aims to advance our knowledge of Europa's atmosphere and surface composition and assess its potential for sustaining life. The Project ECHO team will put forth a design for a spacecraft that can transit from Earth to a Jupiter-Europa orbit and collect and transmit data about Europa's ice and atmospheric composition back to ground based stations on Earth.

If the primary objectives are achieved, the following secondary objectives will be explored.

- Determination of surface geyser activity levels on Europa.
- Analysis of other moons of Jupiter.
- Analysis of atmospheric conditions on Jupiter.

## **C: Scope of Work**

The Project ECHO team will design a spacecraft/lander system which will travel to Europa and collect data on the surface ice and atmosphere composition. The program team will complete the necessary design and analysis of critical subsystems, including: flight mechanics, structures, attitude determination and control, thermal management, telecommunications, command and

data, propulsion, mechanisms and deployables, and power. The program team will provide the customer with progress updates through Preliminary and Final Design Review reports and presentations.

## D: Requirements

- **Deliverables**

Preliminary Design Review (PDR)

Report

- Define mission objectives and discuss mission overview, identify stakeholders.
- List mission requirements.
- Preliminary design overview with a design trade study for each subsystem utilizing weighted decision matrices to determine which design will be pursued.
- Create concept of operations for mission.
- Risk and hazard analysis with a risk management plan.
- Propose development schedule for mission phases.

Presentation

- General technical overview of preliminary design in the form of a poster, each subsystem lead will discuss components of their respective subsystem.

Ethical & non-technical factors considerations (ENTF) report

- Highlight mission objectives along with considering various ethical and non-technical factors such as public health and safety, cultural issues, social concerns, etc.

Final Design Review (FDR)

Report

- Final spacecraft design overview.
- Comprehensive review of major subsystems with design iteration showcase. At least one design iteration will be done for each subsystem.
- Technical analysis of each subsystem's design and anticipated performance.
- Testing and integration plan.
- Operation and mission plan.
- Risk assessment and mitigation.

## Presentation

- PowerPoint presentation to customer outlining final design, each subsystem lead will discuss technical details of their respective subsystem.
- **Schedule**
  - 01 October 2024: Statement of Work
  - 18 October 2024: PDR Report
  - 22 October 2024: PDR Presentation
  - 12 November 2024: ENTF paper
  - 06 December 2024: FDR Report
  - 09 December 2024: FDR Presentation

## E: References

Gough, E. (2024, April 9). Retrieved from Universe Today: <https://www.universetoday.com/166571/if-europa-has-geysers-theyre-very-faint/#text=In%202013%20the%20Hubble%20Space,the%20moon%20has%20an%20ocean>

Howell, E. (2023, May 3). Retrieved from Space.com: <https://www.space.com/15498-europa-sdcmp.html>

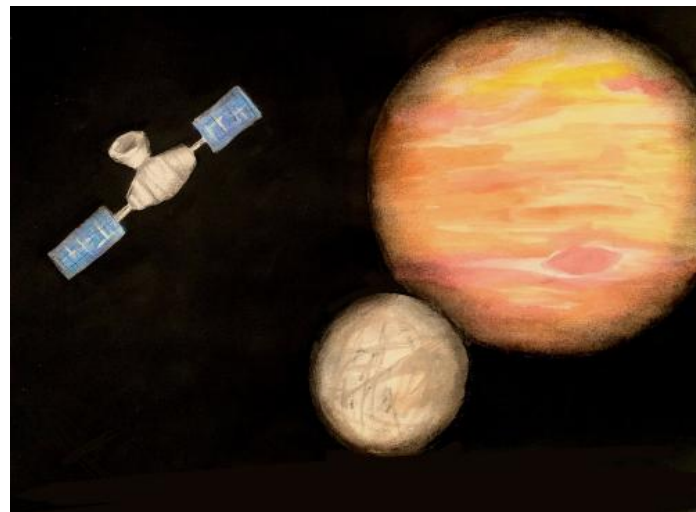
M. H. Carr, M. J. (1998). Evidence for a subsurface ocean on Europa. *Nature*. Retrieved from <https://pubs.usgs.gov/publication/70020620>

NASA. (n.d.). *Europa: Facts*. Retrieved from NASA.gov: <https://science.nasa.gov/jupiter/moons/europa/europa-facts/#h-potential-for-life>

## 13.9: Preliminary Design Review

# **Europa Composition and Habitat Observation (ECHO) Lander**

## **Preliminary Design Report**



**MANE 4250 – Space Vehicle Design**  
**Section 1**  
**Team 1**

**Prepared by:**

**Joseph Bowers, Katie August, Constantine Childs, Chloe Powell,  
Andrew Olson, Aaryan Sonawane, Mae Tringone**

# **1 Executive Summary**

## **Prepared by Constantine Childs**

This preliminary design report outlines the conceptual framework and design considerations for the ECHO lander. ECHO is part of a large strategic mission by NASA to send a robotic orbiter and lander to the Jupiter system, targeting a landing on Europa by 2037. Scientific experiments will be carried out on the surface for two years. Instruments will study Europa's water-ice surface and the liquid ocean beneath. Europa was chosen as the destination due to its potential to sustain life. Mission objectives and design parameters for key lander project elements were discussed. The key lander project elements were structures, mechanisms and deployables, propulsion, orbital mechanics, attitude determination and control, thermal management, power, command and data, and telecommunications. Qualitative design trade studies were performed for subsystem component selection.

The ECHO lander module will be a hexagonal structure comprising aluminum and titanium wrapped in multi-layer insulation. The lander will travel with the orbiter spacecraft and separate once in Jupiter orbit. The lander will enter a parking orbit around Europa before beginning a powered descent using a hypergolic propulsion system. Control of the lander is accomplished through the use of a magnetorquer and reaction wheel. The lander's instrumentation includes a thermal drill, ice-penetrating radar, mass and chemical spectrometers, and a high-resolution camera. The lander will communicate with the orbiter using a patch antenna, which will then relay messages to Earth.

# Contents

1 Executive Summary .....	152
2 List of Figures .....	156
3 List of Tables .....	156
4 Terms and Definitions.....	157
4.1 Acronyms .....	157
4.2 Decision Matrix Standard .....	157
5 Introduction.....	158
6 Project Scope .....	158
6.1 Mission Objectives.....	158
6.2 Mission Constraints .....	159
6.3 Mission Assumptions.....	160
6.4 Non-Technical Considerations.....	161
6.4.1 Environmental Considerations.....	161
6.4.2 Political Considerations .....	161
6.4.3 Cost Considerations .....	161
6.4.4 Time Considerations .....	161
6.4.5 Public Health and Safety.....	162
7 Mission Architecture.....	162
7.1 Launch Vehicle Selection .....	162
7.2 Payload Overview .....	163
7.3 Scientific Instrumentation and Sensor Suite .....	164
8 Design Approach .....	165
8.1 Structures .....	165
8.1.1 Subsystem Definition.....	165
8.1.2 Structure Materials.....	165
8.1.3 Chassis Structure.....	166
8.1.4 Risk Mitigation .....	167
8.1.5 Future Work .....	168
8.2 Mechanisms and Deployables.....	168
8.2.1 Subsystem Definition and Requirements.....	168

8.2.2 Benchmarking Selection .....	168
8.2.3 Risk Assessment .....	170
8.2.4 Future Work .....	171
8.3 Propulsion .....	171
8.3.1 Subsystem Definition and Requirements.....	171
8.3.2 Preliminary Technology Selection.....	171
8.3.3 Risk Assessment .....	173
8.3.4 Future Work .....	174
8.4 Orbital Mechanics.....	174
8.4.1 Definition .....	174
8.4.2 Requirements and Constraints .....	174
8.4.3 Orbital Mechanics Architecture .....	175
8.4.4 Potential Design Solutions.....	176
8.4.5 Preliminary Delta -V Calculations.....	178
8.4.6 Risk Assessment and Mitigation.....	179
8.4.7 Future Work .....	180
8.5 Attitude Determination & Control Subsystem (ADCS) .....	180
8.5.1 Subsystem Definition.....	180
8.5.2 Attitude Determination .....	181
8.5.3 Attitude Control .....	183
8.5.4 ADCS Risk Assessment.....	184
8.5.5 ADCS non-technical considerations .....	185
8.5.6 Plan of procession .....	186
8.6 Thermal Management .....	186
8.6.1 Subsystem Definition and Requirements.....	187
8.6.2 Thermal Environment .....	187
8.6.3 Thermal Control Selection .....	188
8.6.4. Non-Technical Considerations.....	190
8.6.5 Risk Assessment and Mitigation.....	190
8.6.6 Future Work .....	191
8.7 Power .....	191

8.7.1 Subsystem Definition.....	191
8.7.2 Power Generation.....	191
8.7.3 Power Storage .....	191
8.7.4 Risk Assessment and Mitigation.....	192
8.7.5 Future Work .....	192
8.8 Command and Data.....	193
8.8.1 Subsystem Definition.....	193
8.8.2 Computer Architecture.....	193
8.8.3 Risk Assessment .....	194
8.8.4 Future Work .....	194
8.9 Telecommunication.....	194
8.9.1 Subsystem Definition.....	194
8.9.2 Frequency Band Selection .....	195
8.9.3 Antenna Selection .....	195
8.9.4 Risk Assessment and Mitigation.....	196
8.9.5 Future Work .....	196
9 Design Budgets .....	197
9.1 Mass Budget.....	197
9.2 Volume Budget .....	197
9.3 Cost Budget.....	198
10 Sales Pitch.....	199
11 Conclusions.....	199
12 References .....	200
13 Appendix.....	204
13.1: Definition and Assessment of Risk.....	204
13.2: Summary of Non-Technical Considerations.....	205
13.3: Orbital Mechanics Calculations.....	207
13.4: Project Timeline.....	208

## **2 List of Figures**

- Figure 8.1.1: Rectangular FEA  
Figure 8.1.2: Hexagonal FEA  
Figure 8.1.3: Octagonal FEA  
Fig 8.2.2.2: Diagram showcasing the Sampling, Drilling and Distribution Device (SD2) utilized by the Philae Lander.  
Figure 8.4.1: Orbital Mechanics Architecture  
Figure 8.4.2: Europa Parking Orbit  
Figure 8.5.1: Tier-list of Sensors  
Figure 8.6.1: Brightness Temperature of Europa's Surface  
Figure 8.7.3a: Normalized Battery Specification Comparison between lithium-ion and Nickel-metal hydride batteries

## **3 List of Tables**

- Table 7.1.1: Launch Vehicle Decision Matrix  
Table 8.1.1: Materials Decision Matrix  
Table 8.1.2: Chassis Decision Matrix  
Table 8.2.2.1: Decision Matrix for potential landing solutions.  
Table 8.3.1: Propulsion Technology Decision Matrix  
Table 8.4.1: Descent Method Decision Matrix  
Table 8.4.2: Delta –V values for departure from parking orbit  
Table 8.4.3: Delta – V values for insertion into zero-altitude circular orbit  
Table 8.4.4: Total Delta – V values for transfer from Jupiter orbit to landing on Europa  
Table 8.5.2: Attitude Determination Sensor Decision Matrix  
Table 8.5.3: Attitude Control Actuator Decision Matrix  
Table 8.5.5: ADCS Risk Assessment Matrix  
Table 8.5.6: ADCS non-technical factors consideration matrix  
Table 8.6.1: General temperature requirements for Europa ECHO lander  
Table 8.6.2: Decision matrix for thermal control subsystem  
Table 8.6.3: Decision matrix for passive thermal control systems  
Table 8.6.4: Decision matrix for active thermal control systems  
Table 8.6.5: TCS Risk Assessment Matrix  
Table 8.8.1: Decision matrix for computer architecture  
Table 8.9.1: Decision matrix for frequency band  
Table 8.9.2: Decision matrix for antenna type  
Table 9.1.1: Mass Budget by Subsystem  
Table 9.2.1: Volume budget by subsystem  
Table 9.3.1: ECHO Cost Budget  
Table 13.1: Relevance of Non-Technical Factors

## **4 Terms and Definitions**

### **4.1 Acronyms**

ADCS – Attitude Determination and Control System

APXS – Alpha Particle X-ray Spectrometer

CAD – Computer Aided Design

CIVA – Comet Nucleus Infrared and Visible Analyzer

CONCERT – Comet Nucleus Sounding Experiment by Radio wave Transmission

COPUOS – Committee on the Peaceful Uses of Outer Space

COSAC – Cometary Sampling and Composition

DSN – Deep Space Network

ECHO – Europa Habitat and Composition Observation

FDR – Final Design Review

FEA – Finite Element Analysis

IMU – Initial Measurement Unit

ISP – Specific Impulse

MLI – Multi-Layer Insulation

RHU – Radioisotope Heating Unit

ROLIS – Rosetta Lander Imaging System

ROMAP – Rosetta Lander Magnetometer and Plasma Monitor

RTG – Radioisotope Thermoelectric Generator

SD2 – Sampling Drilling & Distribution System

SOI – Sphere of Influence

TCS – Thermal Control System

TRL – Technology Readiness Level

TWR – Thrust to Weight Ratio

UNOOSA – United Nations Office of Outer Space Affairs

### **4.2 Decision Matrix Standard**

**Prepared by Andrew Olson**

In the following report, each decision matrix employs the same weighting and scoring approach. Design criteria were established based on customer requirements, with weights assigned to reflect their importance, totaling 10. Higher weights were given to more critical criteria. Each design method was then scored on a scale of 1 to 5 for each criterion, with 5 representing the best performance. These scores were multiplied by their respective weights, and the weighted totals were summed to identify the most suitable design method to pursue.

## **5 Introduction**

**Prepared by Andrew Olson**

Europa, the fourth largest of Jupiter's moons, is one of the most promising candidates for hosting extraterrestrial life in our solar system. Estimated to be 4.5 billion years old, there has been adequate time for life to develop [1]. Additionally, scientists believe Europa possesses the key elements necessary for life, including liquid water, and derives sufficient energy from Jupiter's radiation to support biological processes [2].

While the surface temperature does not rise above minus 260 °F, scientists believe Europa contains twice as much liquid water as earth's oceans [1,2]. In 2013, the Hubble Space Telescope detected water vapor plumes emanating from surface geysers on Europa [1]. Additionally, high resolution images from NASA's Galileo spacecraft showed evidence of "mobile icebergs" on the icy moon [3]. These observations led scientists to believe that there is a liquid ocean underneath the surface – further bolstering the potential for Europa to host life and solidifying its status as a prime candidate for exploration.

While past orbiter missions, including NASA's Juno and Galileo, have provided valuable data, no lander has yet reached the moon's surface. Several missions are planned for the coming decade, such as NASA's Europa Clipper and ESA's Jupiter Icy Moons Explorer [1], but these will also remain in orbit. To achieve more in-depth analysis of Europa's surface composition and its habitability, a dedicated lander mission is needed.

Space Team 1 is tasked with designing a lander for NASA's Planetary Science Division, aimed at analyzing Europa's surface ice and subsurface water composition, as well as other parameters of its hypothesized subsurface ocean, such as depth. Scheduled to launch in April 2031 aboard SpaceX's Falcon Heavy, the lander, dubbed ECHO, will offer a cost-effective and reliable solution for deploying a probe to Europa. With a mass budget of 1,000 kg, the ECHO lander is designed to maximize mission efficiency and scientific return, while minimizing costs. The following report is the team's Preliminary Design Report for the ECHO lander and will discuss the mission in detail.

## **6 Project Scope**

### **6.1 Mission Objectives**

**Prepared by: Aaryan Sonawane and Mae Tringone**

The ECHO mission has both technical and scientific objectives required for the mission to succeed. The goal is to understand the Europa's potential for sustaining life. The team developed various

objectives to determine this. The technical objectives are for getting to Europa safely while being able to communicate to earth ground stations. The scientific objectives involve the analysis of conditions on Europa. These objectives include:

- Originating from a Jupiter orbit, separate from the orbiter and insert into a Europa parking orbit.
- Achieve a soft landing on the surface of Europa in a safe location.
- Deploy necessary communications and scientific equipment.
- Achieve two-way communication with the Europa Orbiter.
- Survive on the surface of Europa for six months.

The scientific objectives of ECHO are:

- Produce and analyze a sample of Europa's surface ice.
- Measure atmospheric conditions at the surface of Europa.

Secondary objectives are not required to have a successful mission, but they have the potential for further scientific research and knowledge if completed after the primary missions. The secondary objectives include:

- Collect images using a camera suite of Europa's Surface for transmission to Earth.
- Determine the level of geyser activity on Europa.
- Study atmospheric conditions on Jupiter.

## 6.2 Mission Constraints

**Prepared by: Aaryan Sonawane**

Each subsystem has specific design constraints based on mission objectives, context of the mission, traditional design practices along with the consideration of non-technical factors. However, there are certain mission constraints that apply to the ECHO probe as a whole:

- All ECHO Probe subsystems must be designed to operate in the presence of extreme temperature fluctuations typical of the Jovian environment, conditions that can reach as low as -146 °C (127 K) (discussed further in section 8.6).
- The ECHO Probe will have limited power generation and power storage capacity, which will affect the ability to consistently operate all onboard systems, necessitating an efficient power management strategy (discussed further in section 8.7).
- The ECHO Probe has a constrained mass due to the types of propulsion utilized, the amount of fuel on board, and the requirements for achieving the necessary velocity changes to safely land on Europa's surface (discussed further in section 9.1).
- The ECHO Probe has a constrained volume budget dictated by the physical dimensions and propulsion capabilities necessary for the mission, which must be adhered to during the

design phase to ensure successful deployment and operational functionality (discussed further in section 9.2).

- The ECHO Probe is subject to a constrained budget due to the finite value this mission provides for the customer (discussed further in section 9.3)

## 6.3 Mission Assumptions

**Prepared by: Aaryan Sonawane**

The ECHO mission is built on several foundational assumptions to ensure feasibility and alignment with mission objectives. These assumptions guide the overall system design and influence key mission architecture decisions. The following are the primary mission assumptions:

- The mission assumes a launch date in April 2031, with an expected journey of approximately five and a half years to Europa. This timeline allows adequate time for spacecraft assembly, subsystem integration, and testing, ensuring that the ECHO lander lands in Europa by 2037 (discussed further in section 6.4.4).
- It is assumed that the ECHO lander will successfully separate from the orbiter in a stable orbit around Jupiter, followed by a transfer and insertion into a parking orbit around Europa. The orbiter is expected to provide consistent communication and navigational support during this phase (discussed further in section 8.4).
- The surface conditions of Europa, though not precisely known, are assumed to consist of icy terrain with potential surface irregularities. The landing sequence is designed to account for these variables, relying on advanced attitude control and precision landing techniques (discussed further in section 8.2).
- It is assumed that Europa's subsurface contains a liquid ocean beneath its icy crust. The design focuses on drilling, analyzing surface and shallow subsurface ice. This guides the design of sampling instruments and thermal management systems required to operate in such an environment (discussed further in section 7.3).
- It is assumed that the ECHO lander will have sufficient power generation from its onboard power source, allowing the spacecraft to operate for at least six months (discussed further in section 8.7).
- Communication with the Europa orbiter will be intermittent, requiring robust data storage and transmission mechanisms to function during communication windows (discussed further in section 8.9).
- The design assumes that Europa's proximity to Jupiter exposes the lander to significant levels of radiation. As such, the lander is equipped with radiation-hardened electronics and shielding to protect sensitive components over the duration of the mission (discussed further in section 8.1).
- The mission design adheres strictly to mass and cost budgets, with a mass budget of 810 kg for the lander and an allocated budget of \$750 million. These constraints guide the

selection of subsystems, ensuring a balance between performance, reliability, and cost-effectiveness (discussed further in section 9).

- The preliminary design assumes that all design selections are compatible with the orbiter, of which little information is currently known.

## **6.4 Non-Technical Considerations**

### **6.4.1 Environmental Considerations**

**Prepared by: Chloe Powell**

The ECHO Mission is expected to have minimal, if any, impact on Earth's environment, as the lander will not be conducting any experiments on or near Earth. The mission must adhere to UNOOSA's Space Debris Mitigation Guidelines [4,5].

### **6.4.2 Political Considerations**

**Prepared by: Chloe Powell**

The COPUOS has outlined five treaties and five principles that all spacecraft must adhere to [6] stated in Title 51 of the United States Code [7]. These policies will all be followed at risk of legal action being taken against the ECHO team and any related organizations.

### **6.4.3 Cost Considerations**

**Prepared by: Katie August**

The goal of the mission is to keep the monetary budget at a minimum while maximizing the ability to accomplish mission objectives. The team will work on multiple design iterations to find the most efficient values for materials, structural complexity, and scientific instruments. The mission budget was determined by looking at historically similar missions, such as Juno, Galileo, and Europa Clipper. The amount allocated for project ECHO is \$750,000,000 See section 9.3, Cost Budget, for more detailed information.

### **6.4.4 Time Considerations**

**Prepared by: Katie August**

The whole mission, orbiter with lander, has a launch window of twenty days, starting on April 8th, 2031. The orbiter is expected to take approximately five and a half years to arrive based on historically similar missions [8]. Project ECHO plans to spend six months on Europa gathering data, which will be transmitted to the orbiter to be sent back to Earth. The orbiter must maintain a line of sight to receive the data, meaning there will be time periods where no data can be received or sent due to a communication dead zone.

## **6.4.5 Public Health and Safety**

**Prepared by: Katie August**

The design choices are made to mitigate the risk to public health and safety regardless of mission outcomes. Project ECHO will implement safety measures to ensure the mission will not harm the public. See individual risk assessments in section 8, Design Approach, and in Appendix A.

# **7 Mission Architecture**

## **7.1 Launch Vehicle Selection**

**Prepared by: Joseph Bowers**

Understanding the launch vehicle to be utilized by the mission is key to ensuring mission success. The vibrations of the vehicle, acceleration loading, and other vehicle-specific factors effect the design of the structure. Additionally, the fairing size of the vehicle can limit the size of the craft and dictate the overall shape. Finally, the payload capacity of the launch vehicle determines the maximum mass of the spacecraft.

ECHO's mission is initiated upon deployment from an orbiter at Jupiter. However, due to the numerous significant constraints the launch vehicle imposes on the mission, it is important to design the craft for launch on a particular vehicle. As such, a launch vehicle will be selected to utilize for design considerations.

As ECHO is a deep space mission, the payload capacity is a very significant consideration and is weighed heavily in selecting a vehicle. Vehicle readiness, or how soon the vehicle is available for launch is weighted highly, as some vehicles can have extremely long lead times due to their launch cadence, or even longer if still in development. The heritage of the vehicle is also important, as a vehicle that has flown with a strong success rate mitigates the significant risks associated with getting to orbit. The fairing size defines the upper limit of the size of the spacecraft, however from the perspective of ECHO's mission, size is a less important consideration. Finally, the launch cost is considered as certain vehicles may be prohibitively expensive.

**Table 7.1.1: Launch Vehicle Decision Matrix**

Factors	Weight	Space Launch			SpaceX		
		Vulcan	Falcon Heavy	System	Ariane 6	Starship	New Glenn
Payload Capacity	3.5	3	4	5	3	5	4
Vehicle Readiness	2	3	4	2	3	1	3
Flight Heritage	2	3	5	3	2	1	1
Fairing Size	1.5	3	2	4	3	5	4
Launch Cost	1	3	4	1	2	4	5
Score (of 50)	-	30	39	34.5	27	33	33

The SpaceX Falcon Heavy was selected as the launch vehicle for this mission as it performs well in almost all selection criteria. Important, its payload capacity to orbit will enable a larger orbiter, which will in turn allow the lander to have a larger mass. It also has the longest flight heritage of all options considered, decreasing the risks associated with launch.

## 7.2 Payload Overview

**Prepared by: Mae Tringone**

The following is an overview of the base requirements of the payload, and the subsystems that will be principally responsible for achieving and maintaining these objectives. The details of each subsystem's approach are documented further in the following sections.

**Table 7.2.1: Overview of ECHO's Functional Requirements and Associated Subsystems**

Functional Requirement	Associated Subsystem
The structure, instruments, and internal components of ECHO must maintain functionality when subjected to the thermal loads of interplanetary space and the Europa surface.	Thermal Management
ECHO's structure must be able to resist the anticipated conditions of the immediate Jovian System and the Surface/Transient environment of Europa, primarily Jovian radiation and trace surface debris. Additionally, it must maintain integrity through the launch stage and interplanetary transit.	Structures
ECHO must land approximately near the designated landing site. It must maintain maneuverability through the entire landing stage to account for the uncertainty of the environment upon arrival.	ADCS, Spaceflight Mechanics, Propulsion Systems
ECHO must maintain full connectivity to the Europa Orbiter throughout the landing stage. It must be capable of intermittently transmitting/receiving engineering and scientific data on subsequent orbiter rendezvous with Europa	Telecom, Command
ECHO must adequately anchor itself in the surface ice of Europa and maintain stability through the entirety of its mission. All mission-critical infrastructure must be deployed once the landing stage is completed.	Mechanisms & Deployables
ECHO must generate enough power to maintain its mission objectives for its entire design life.	Power

## 7.3 Scientific Instrumentation and Sensor Suite

**Prepared by: Mae Tringone & Aaryan Sonawane**

The main priority of the ECHO mission is to sample and analyze the immediate subsurface ice and regolith of Europa, with the auxiliary goal of supplementing the attached orbiter mission with experimental surface data. The following is a brief overview of the instruments that will support these goals. The relevant example uses from the Philae lander have been used for comparison due to the similarities in the scope of the mission. [Refer to section 4.1 Acronyms for names of the instruments]

**Table 7.3.1: Overview of ECHO's Functional Requirements and Associated Subsystems**

Objective	Instruments Used	Relevant Instruments used in Philae
Drilling a hole in the icy surface of Europa	Thermal Drill attached to the probe	SD2
Analyze the elemental, molecular, and mineralogical composition of Europa	Ice-Penetrating Radar, Mass, and Chemical Spectrometer, Magnetometer	CONCERT, COSAC, APXS, ROMAP
Return high resolution images and terrain information of Europa back to Earth	High Resolution Camera, Spectral Imager	ROLIS, CIVA

## 8 Design Approach

### 8.1 Structures

Prepared by: Katie August

#### 8.1.1 Subsystem Definition

The structures subsystem is responsible for all components of the spacecraft that carry loads. The spacecraft structure must be able to withstand all the forces it faces during the mission, including launch, travel, and landing. It must protect internal components from the conditions of space and Europa. This involves protection from radiation exposure and temperature conditions. Additionally, it is also designed to minimize cost, mass, and risk while maximizing strength, thermal conductivity, and volume.

#### 8.1.2 Structure Materials

There are multiple materials being considered for the main body of the spacecraft. Table 8.1.1 explores the property weighting of each considered material. The decision matrix for material selection prioritizes the strength and stiffness, Young's Modulus, as well as the protection from radiation they provide. These were the most highly rated in order to mitigate structural failures and risk to mission success. Future design ideas will explore and incorporate the top two materials into the structure. [9] [10] [11]

**Table 8.1.1: Material Decision Matrix**

Criteria	Weight	Aluminum	Steel	Beryllium	Carbon Fiber	Titanium
Strength/Stiffness	3	3	5	5	4	4
Radiation Protection	3	4	3	4	3	5
Density	2	4	1	2	3	2
Manufacturability	1.5	5	5	2	2	3
Cost	0.5	5	5	1	2	4
Total		39	36	34.5	31	37.5

Aluminum and titanium were selected to be potential materials. The density strength ratio of aluminum makes it a strong, lightweight material, making it desirable for spacecraft design. Titanium is valued for radiation protection but is a very dense material.

### 8.1.3 Chassis Structure

Three shapes were considered for the base chassis design, rectangular, hexagonal, and octagonal prisms. The chassis will be holding all the necessary equipment to complete the mission. The final shape will be more complex than the geometry here, but this serves as the starting point to determine what is the most suitable based on strength, risk, mass, volume, and manufacturability. Strength and risk are prioritized factors in chassis selection to mitigate risk to the structure and internal components.

**Table 8.1.2: Chassis Decision Matrix**

Criteria	Weight	Rectangular	Hexagonal	Octagonal
Strength	3	2	5	4
Risk for Lander	3	3	5	4
Mass	2	4	5	4
Manufacturability	1	5	4	3
Volume	0.5	3	4	5
Cost	0.5	4	3	2
Total		31.5	47.5	38.5

The numbers in table 8.1.2 came from simple Finite Element Analysis (FEA) simulations and NX Siemens property analyses. Each shape was created to be a hollow shell of aluminum of similar sizes. Based on this decision matrix, the chassis will follow a hexagonal shape. The Von-Mises Elemental stresses are shown in the three figures below. The stress analysis further solidifies the hexagonal design choice.

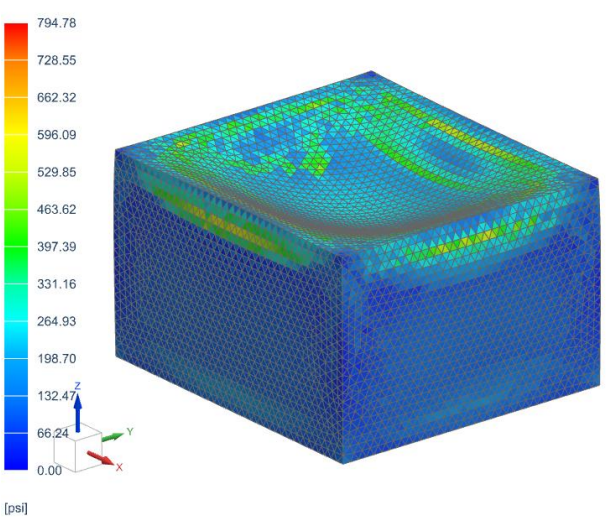


**Figure 8.1.1: Rectangular FEA**

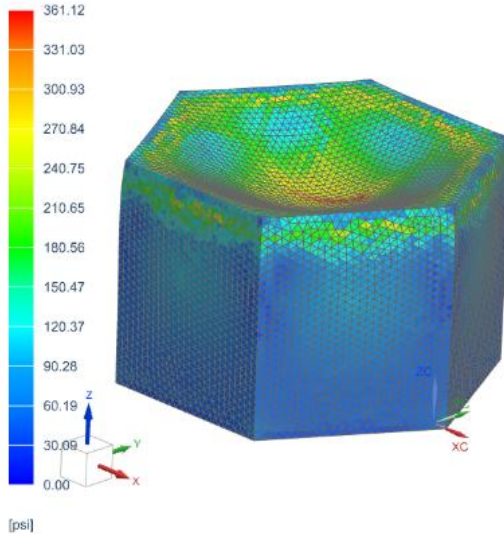


**Figure 8.1.2: Hexagonal FEA**

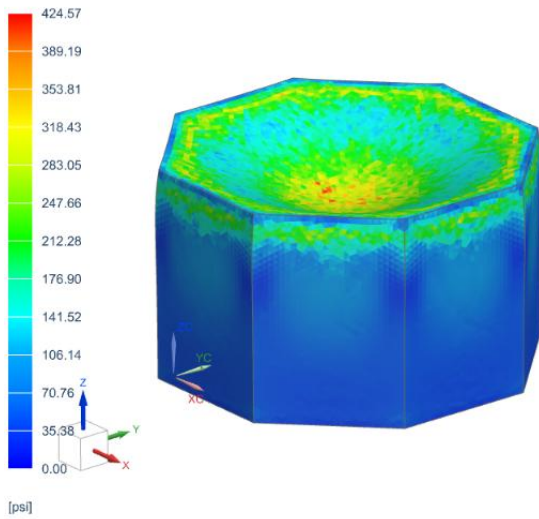


**Figure 8.1.3: Octagonal FEA**

## 8.1.4 Risk Mitigation

The structure subsystem is a key component for mission success because structural failures can lead to complete mission failure. A robust and reliable structure is essential, for structural failures can cause breakdowns in other subsystems. Ensuring that the structure is strong and safe is a top priority. Each design choice will be selected based on the combination of strength, efficiency, and reliability. The design of the structure itself will undergo rigorous testing to find the best configuration for withstanding the harsh environment of space.

## **8.1.5 Future Work**

In the future, a more complex design and its analysis will be explored. A more detailed computer aided design (CAD) model will be created. With this, materials will be applied to various parts of the structure to maximize the strength of each section. Finite element analysis will be used to determine the best part configuration and structural layouts. FEA will also be utilized to determine how the spacecraft will react to the forces it would encounter.

## **8.2 Mechanisms and Deployables**

**Prepared by:** Mae Tringone

### **8.2.1 Subsystem Definition and Requirements**

The Mechanisms and Deployables subsystem encompasses the mechanical components that will aid ECHO in completing its mission. There are three main “suites” of mechanisms that will be required:

1. Landing: Anchoring ECHO to the surface of Europa after its final decent stage.
2. Sample Collection: Facilitating the collection of, and delivery to the Sample Analysis Suite of, surface and subsurface samples.
3. Communication: Facilitating the pointing and tracking of directional communication equipment.

### **8.2.2 Benchmarking Selection**

The following sections detail the analysis of potential designs that would support the goals of each suite.

#### **8.2.2.1 Landing**

The lack of a definitive ability to plan for a specific landing site on the surface of Europa makes it imperative that the lander have a stable landing platform that will support it through the vast majority of its mission life. A particular concern is the anticipated abundance of surface ice and relatively low gravity. While the ADCS and Propulsion subsystems will optimize the conditions in which ECHO will land, the landing suite must account for relatively unknown surface conditions. There are two main methods by which this can be achieved:

1. Landing Gear: a triad or quartet of robust, cleated landing struts that will suspend the chassis of ECHO off the ground and absorb most of the impact shock from landing.
2. Ice Harpoons: Utilizes traditional landing gear as specified above for the landing stage, however relies principally on pyrotechnically administered harpoons deployed into the regolith for stability, rather than a specialized foot.

**Table 8.2.2.1: Decision Matrix for potential landing solutions.**

Design Criteria	Weighting	Landing Gear	Ice Harpoons
Overall Mass	2.5	4	3
Risk to Mission	2.5	5	1
Deployment Reliability	2	3	5
Traction	2	4	5
Flight Heritage	1	5	2
Score (of 50)		41.5	32

Traditional landing struts specially designed for the environment will introduce more points of failure than a comparatively simple harpoon system. In addition, it may require a more expensive model and further testing to ensure it can account for the uncertain conditions of the Europa surface, as it will rely entirely on contact with the surface regolith for support. However, introducing the pyrotechnic loads required to drive the harpoons into the ice could prove challenging for ECHO's lightweight design to withstand. The harpoon linkage, though simple in execution, would have to be mounted onto robust, variable platforms, onto which would be placed the additional responsibility of shielding the rest of the craft from the explosive shock. In addition to all of this, the vast majority of terrestrial space missions, qualitatively, utilize landing legs of some variety. The way they react in unsteady, low-gravity environments is well understood, and the associated flight heritage is invaluable to a successful mission.

### 8.2.2.2 Sample Collection

Anticipating that the majority of Europa's surface composition is ice, the sample collection system will be inspired heavily by that used by the *Philae* lander during the *Rosetta* Mission. This comprises a drill bit, inside which is mounted an extendable sample collection tube that can retrieve sample material at various depths and deposit them into the supporting scientific instrumentation. [12]

There is a relative lack of literature on interplanetary ice sample collection. The only other non-impactor mission besides *Rosetta* to successfully sample and analyze ice is the Mars *Phoenix* lander, however the rasp method utilized by the lander achieved a relatively low, imprecise depth [13]. On the contrary, the area of principle scientific interest on Europa extends to roughly 10 cm below the surface [14]. A precise drilling platform based on the only other mission operating in a relatively similar environment appears to be the only sensible choice.

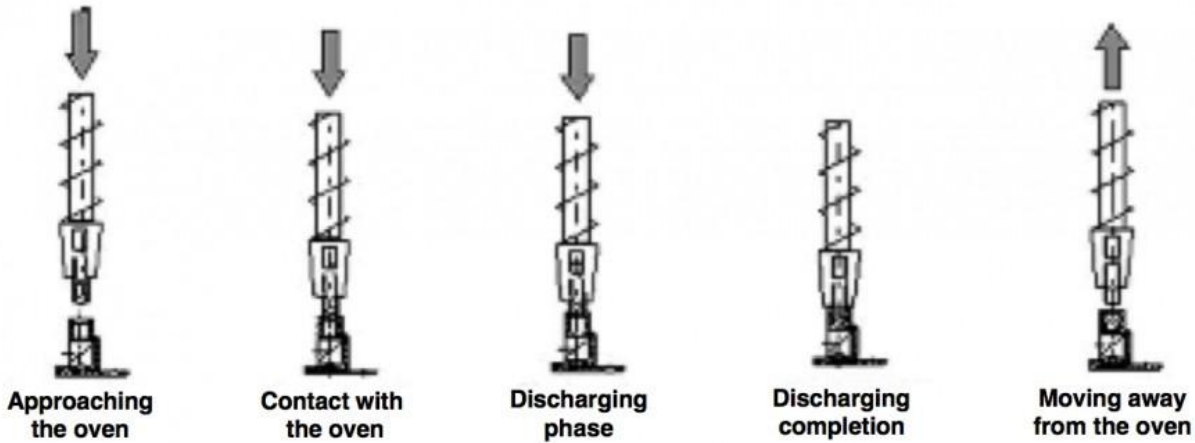


**Fig 8.2.2.2: Diagram showcasing the *Sampling, Drilling and Distribution Device* (SD2) utilized by the *Philae Lander* [13]**

### 8.2.2.3 Communication

As further discussed in Section 8.9, ECHO will depend on a directional high-gain patch antenna to communicate with the associated Europa Orbiter mission, which will serve as a relay station between ECHO and the Deep-Space Network on Earth. A biaxial antenna positioning mechanism, in Elevation/Azimuth configuration, will be used to orient the antenna in the optimal transmitting position during descent and subsequent fly-bys of the Europa Orbiter.

A single-axis servo mechanism, which tracks only the altitude of the orbiter and relies on the physical positioning of ECHO for azimuthal adjustment, would likely be more robust and marginally less expensive than a biaxial gimbal, however uncertainty in the final settled position of ECHO necessitates the existence of marginal pitch adjustment at the very least, and the transient conditions involved in the descent stage of the mission are too uncertain to rely on a single axis for telecommunications pointing during such a critical portion of the mission.

## 8.2.3 Risk Assessment

The main risk associated with this subsystem is with respect to the mission itself; the landing and communications suites represent single points of failure for the entirety of ECHO if any component of them were to fail, and a failure of the drill rig would cripple ECHO's primary objective of analyzing surface and subsurface regolith. It is imperative that any component facilitating the dynamic movement and deployment of mission-critical components be made to spec for the expected environmental conditions, and that extensive testing on engineering models be performed to ensure reliability.

## **8.2.4 Future Work**

The landing stage will be modeled and baseline numerical simulations run in order to narrow down the suspension configuration and optimal number of individual legs. Existing literature on *Philae*'s sample drill will be collected and studied to further develop and eventually finalize ECHO's sample collection system. The telecommunications subsystem will be consulted in order to narrow down a list of flight-tested aerospace grade biaxial antenna positioning mechanisms that would best support the mission requirements.

## **8.3 Propulsion**

**Prepared by:** Joseph Bowers

### **8.3.1 Subsystem Definition and Requirements**

The propulsion subsystem encompasses all components required to generate an external force spacecraft for the purpose of orbital insertion or adjustment, station keeping, and descent. This includes propellant storage, plumbing, valves and thruster assemblies.

The objectives of the primary propulsion system for this mission are centered around taking the probe from deployment in Jupiter Orbit to a successful soft landing on the surface of Europa. The requirements to accomplish this are outlined as:

- Perform a burn to insert into a high Europa orbit from a Jupiter orbit.
- Perform a series of burns to reduce the orbit to a low Europa orbit, including performing any orbital adjustments required to target landing site.
- Perform a de-orbit burn and series of burns along decent to decrease velocity leading to an eventual soft touchdown with near-zero velocity.
- If required, substantially slow descent or briefly hover prior to touchdown to allow inspection of the landing site to ensure viability and adjust as required.

The system must be designed such that all required maneuvers can be accomplished efficiently, where the amount of onboard propellant and size of the thrusters can be minimized to ensure spacecraft mass budgets are met, and maximizing the available mass for equipment supporting the mission objectives on the surface of Europa.

A secondary propulsion system may be required in support of the ADCS subsystem to enable the spacecraft to perform attitude adjustments as required during the orbital insertion and decent portion of the mission. This secondary system would also be capable of performing fine orbital adjustments.

### **8.3.2 Preliminary Technology Selection**

To facilitate a soft landing on the surface of Europa, the primary propulsion system will be required to perform multiple high delta-V burns. There are numerous propulsion technologies which can

be considered for this task. The selection matrix on able 8.3.1 overviews several conservable technologies and their associated benefits.

Experimental propulsion technologies including solar sails and nuclear thermal were not considered due to their TRL greatly increasing risk to the mission. Additionally, the requirement for the primary propulsion system to land the craft on the surface of Europa requires the system to produce a substantial amount of thrust. If it is assumed the mass of the spacecraft on touchdown with Europa is approximately 400kg, a minimum thrust of approximately 550 N will be required to ensure a TWR greater than 1. Therefore, all forms of electric/plasma propulsion were also not considered, as high-power models are only capable of thrust on the order of 5 N [8]. Due to the relatively small mass budget, the mass of the system was considered heavily in the decision, both as the overall mass of the system, including thruster assemblies, tanks, and propellant, as well as the TWR of the thruster. Additionally, risk and stability of the propellant were considered important factors, particularly when considering the duration of the mission. The ability to throttle precisely will be important to a smooth landing and this is taken into account. The ISP of the engine is also considered, as a more efficient engine will require less propellant. Finally, non-technical factors related to each solution are considered.

**Table 8.3.1: Propulsion Technology Decision Matrix**

Design Criteria	Weighting	Solid	Cold Gas	Monopropellant	Bipropellant	Dual-Mode
Overall Mass	2.5	1	5	5	4	3
Risk to Mission	2.5	2	5	5	4	3
TWR	1.5	4	2	3	5	4
Propellant Stability	1.5	5	1	4	4	4
Throttling	1	1	3	3	4	5
ISP	0.75	2	1	3	5	5
Non-Technical	0.25	4	5	3	3	3
Score (of 50)	-	24.5	34.5	41.5	42	36.5

Based on the parameters, a bipropellant system was selected. Bipropellant has great efficiency due to its high ISP and is also capable of a substantial thrust output. A bipropellant system does add significant complexity and therefore mass, however the added efficiency and thrust compensate for this. Monopropellant is also a strong option due to its simplicity and reliability, however its decreased efficiency is a significant factor due to the mission profile, as the already

large propellant requirement would be increased further. When only considering the primary propulsion system, the added precision and versatility of a dual-mode adds unnecessary weight and further complexity. However, if thrusters are required for ADCS a dual mode system may be advantageous. Cold gas has advantages due to its simplicity and minimal infrastructure, however its poor efficiency and storage make it non-ideal for this use case. Solid fuel was also considered due to its simplicity; however, the added weight and lack of control make it problematic for this mission.

While there are a wide variety of available options for bipropellants, due to the mission duration and other mission constraints it is reasonable to eliminate any cryogenic propellants due to their poor long-term stability and added weight due for tank insulation, as well as larger volume tanks. Hypercolic propellants are also advantageous as they do not require an ignition source, eliminating a point of failure for thruster ignition. Hydrazine and dinitrogen tetroxide is a logical bipropellant for this mission due to its long flight heritage. While some bipropellants have much higher ISP (455 for LOx-LH<sub>2</sub> vs 335 for hydrazine bipropellant) [21], the stability and space efficiency of hydrazine make it advantageous for this mission. Further investigation into exactly what form of hydrazine and selection of a primary thruster will be completed as requirements are further specified for the FDR.

### **8.3.3 Risk Assessment**

Due to the high cost and complexity of ECHO's mission, minimizing risk wherever possible is generally beneficial. However, to achieve the necessary performance to achieve mission objectives within the mission constraints, some risks will have to be accepted and mitigated. The considerations outlined are not comprehensive and require deeper analysis regarding the extent of the risks and effectiveness of mitigation strategies.

Bipropellant systems add significant complexity compared to monopropellant or cold-gas systems. With this added complexity comes additional risk, as each individual component adds new failure modes. These risks can be mitigated utilizing hardware with built-in redundancy, as well as having multiple smaller thrusters in leu of a single large thruster. Additionally, utilizing hardware with proven flight heritage is a strong risk mitigation strategy. Due to the prevalence of hydrazine bipropellant thrusters in spaceflight, selecting flight proven hardware is not a significant obstacle.

Finally, the hydrazine itself presents a notable risk to personal interaction with the ECHO prior to launch. Hydrazine is extremely toxic, making it dangerous to humans in several ways. Special care must be taken to prevent harm to individuals working with the craft. Due to the prevalence of hydrazine in spaceflight, required safety measures are well known and if implemented properly mitigate risks substantially.

### **8.3.4 Future Work**

As the mission profile is further refined and more accurate delta-V specifications delivered, the required maneuvers and associated burns can be determined. With the consideration of an aerobraking maneuver, delta-V requirements could change substantially from the current estimates. Once the sequence of maneuvers has been determined, an engine will be selected, and the quantity of engines determined. The amount of propellant will also be calculated, and fuel tanks sized appropriately. Further measures including staging may also be considered.

Additional considerations around the type of propellant will be made, particularly with concern to thermal management of the hydrazine, as thermal stability varies significantly across the commonly utilized hydrazine derivatives. Thermal management considerations will be required to ensure propellant maintains stable temperatures while in transit.

The exact configuration and layout of fuel tanks, thrusters, and other associated components will continue to develop as the mission requirements are more clearly defined, basic structure determined, and ADCS needs determined.

## **8.4 Orbital Mechanics**

**Prepared by:** Andrew Olson

### **8.4.1 Definition**

The orbital mechanics subsystem is essential for mission success and requires preliminary analysis as it provides key delta-V calculations that are critical for other subsystem analyses. For the ECHO mission, the orbital mechanics team is responsible for designing a reliable and efficient series of transfers to take the ECHO lander from release from the orbiter, to landing on the Europa surface. The orbiter will be placed in its Jovian/Europian orbit using a Mars-Earth gravity assist [16], but the analysis of these orbital mechanics is left to the orbiter team and considered out of scope for the ECHO mission. Because of the similarity between the ECHO and Galileo missions, as well as the availability of Galileo data, analysis for the ECHO orbital mechanics will be done under the assumption that the orbiter is following the Galileo Jovian tour.

### **8.4.2 Requirements and Constraints**

Before designing the orbital mechanics for the ECHO mission, design requirements require consideration to clearly define the design problem. The following list are the primary requirements that will be considered during the design process:

- Ensure safe delivery of ECHO lander to Europian surface while minimizing environmental stresses during landing
- Minimize delta-V during the landing maneuver
- Maintain communication with orbiter during landing maneuver

- Land at target cite with optimal accuracy

To approach the problem, it is also essential to understand the initial orbit that the ECHO orbiter is in. The orbital mechanics of the orbiter are out of scope for this project, so analysis of similar historical missions was done to pick a potential initial orbit. Due to the similarity of the missions, NASAs Galileo mission was used as a reference model. In this mission, the probe performed an 11-orbit tour of the Jovian system. The second of these orbits had a perijove of 670,000 km and an apojove of 19,000,000 km [17] and will be the assumed initial orbit for the ECHO orbiter for the analysis conducted in the PDR.

### **8.4.3 Orbital Mechanics Architecture**

The overall flight mechanics from the initial orbit to landing must adhere to a specific mission architecture, allowing for different design solutions at each phase. The planned mission consists of three main phases, detailed below and depicted in figure 8.4.1:

- **Phase 1 – Departure from Jovian Orbit and Orbiter:** The first phase of the flight mechanics involves separating from the orbiter and departing from the Jovian orbit.
- **Phase 2 – Insertion into Parking Orbit:** Upon departure from the orbiter, the lander will be placed into a stable Europan parking orbit. This will reduce analysis to a two-body problem between the lander and Europa and allow for the initiation of descent towards the surface while mitigating delta-V requirements.
- **Phase 3 – Descent to Surface:** The final stage involves departing from the parking orbit at an optimal time to minimize delta-V and executing a controlled descent to the surface of Europa. This descent may involve additional parking orbits and different descent methods, and detailed analysis of this process will be presented in the Final Design Review.

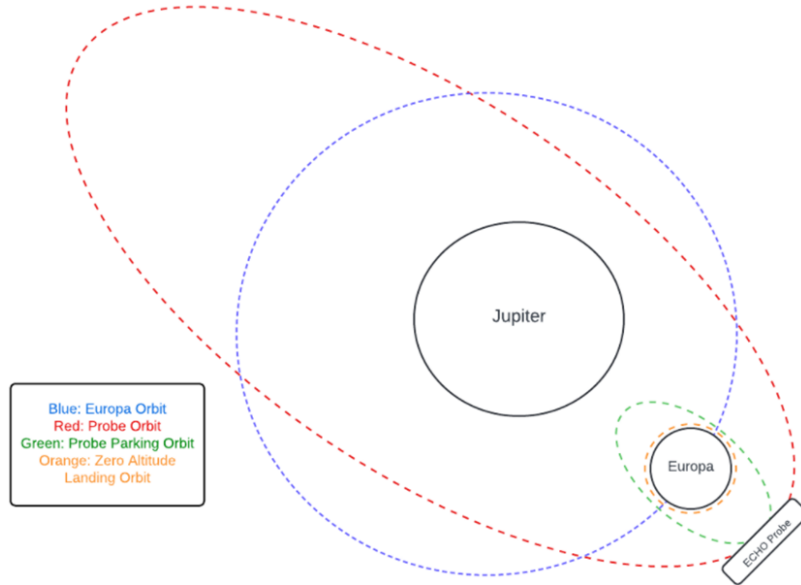


**Figure 8.4.1: Orbital Mechanics Architecture**

#### 8.4.4 Potential Design Solutions

It is planned to use a Hohmann transfer to transition from the Jovian orbit to the parking orbit above Europa. This requires that the parking and Jovian orbits be in the same orbital plane and provides the most efficient two-impulse solution for the transfer between the two. For the descent to the surface, multiple orbital mechanics techniques are feasible. To select the type of descent maneuver to analyze further, multiple options were considered and scored based on performance categories generated from customer requirements.

- **Ballistic Descent:** From the initial Europan parking orbit, the lander executes a burn to slow its velocity and transition to a free-fall trajectory, using the gravity of Europa to descend toward the surface. Braking is accomplished through high-impulse engine burns as the lander approaches the surface, providing a safe touchdown. The use of a short, high impulse burn tends to mitigate delta-V requirements.
- **Powered Descent:** From the initial Europan parking orbit, the lander executes a series of controlled burns to gradually decrease its velocity and adjust its trajectory as it descends toward the surface, potentially entering additional lower-altitude parking orbits. The descent profile can be optimized based on real-time sensor data and environmental conditions, increasing the odds of a safe landing by minimizing the risk of impact damage and maintaining stability during the final approach.
- **Aerobraking Descent:** From the initial Europan parking orbit, the lander executes a burn to adjust its trajectory towards the surface. During descent, the lander would deploy a parachute and utilize aerodynamic drag to slow its velocity in assistance with engine burns. This utilization of atmospheric drag would reduce the fuel-based delta-V requirements for landing.

A decision matrix on table 8.4.1 was developed to select the most suitable descent method for further analysis. Design criteria were established based on customer requirements and assigned weights, with the total weighting adding up to 10. Higher weights were given to more critical criteria. Each descent method was then scored on a scale from 1 to 5 for each criterion, with 5 indicating the best performance. The scores were multiplied by their respective weights, and the totals were summed to determine the best descent method to pursue.

As shown in the matrix, risk was selected as a design criterion and assigned the highest weighting. In the context of the orbital mechanics subsystem, this risk refers to potential damage to the lander during orbital maneuvers, which, in the worst-case scenario, could lead to the catastrophic loss of the mission. Mitigating this risk corresponds to a high likelihood of assuring lander safety, so descent methods with a high-risk score are anticipated to provide the best chance of a safe touchdown.

**Table 8.4.1: Descent Method Decision Matrix.**

Design Criteria	Weighting	Descent Method		
		Ballistic Descent	Powered Descent	Aerobraking
Feasibility of Method for Europa Landing	3	4	5	1
Risk (Lander Safety)	3	1	5	3
Delta- V Magnitude	2	5	3	5
Communication Ability with Orbiter	1.5	3	4	3
Landing Site Accuracy	0.5	2	5	3
Technical Complexity	0.5	3	3	3
Score	-	32	46	29.5

As shown in the matrix, powered descent emerged as the top choice, scoring the highest overall score. This method will be further analyzed in the FDR, as the ECHO team believes it offers the best chance for a safe touchdown, which remains the mission's top priority.

### 8.4.5 Preliminary Delta -V Calculations

To provide the other subsystem design teams with an initial delta-V estimate for their analysis, a MATLAB script (see appendix 13.3) was developed. Since the system being analyzed is conservative, the calculated delta-V will be similar across all descent methods. Therefore, preliminary calculations were made assuming a controlled Hohmann transfer from parking orbit to surface landing, providing a reasonable estimate of the required delta-V.

Europa orbits Jupiter with an apojoove of 676,938 km and a perijove of 664,862 km [18], which is close to the orbiter's perijove of 670,000 km. Therefor, the analysis begins inside Europa's SOI, which was calculated to be 9,725.15 km using equations found in literature [19]. Calculations were done under the assumption that the orbiter team designed the orbit to align the orbiter and Europa at perijove.

To begin the analysis, the velocities of Europa and the ECHO orbiter at perijove were calculated to be 13.8653 km/s and 19.1119 km/s, respectively. This yielded a relative velocity between the two bodies of 5.2465 km/s.

Next, an elliptical parking orbit around Europa was designed (Figure 8.4.2), with the apojoove radius set to the SOI and the perijove radius equal to the distance between the orbiter and Europa at perijove. Utilizing a Hohmann transfer, the delta – V required to insert the probe into this orbit was calculated to be 4.3432 km/s.

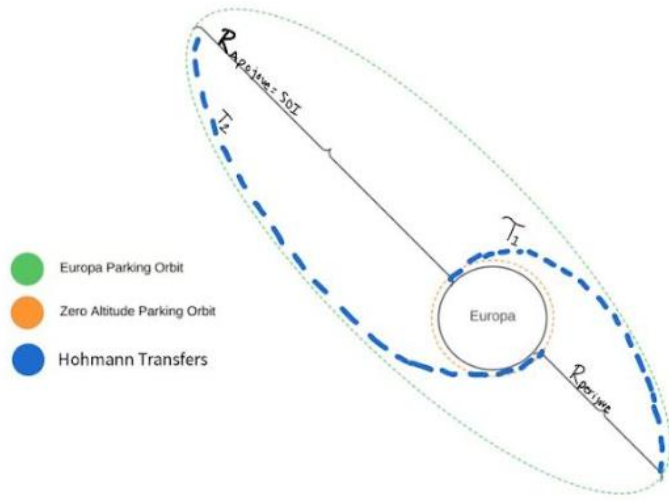


Figure 8.4.2: Europa Parking Orbit.

Following this, Hohmann transfer ellipses (see Figure 8.4.2) were investigated to bring the lander from the parking orbit to a zero-altitude circular orbit about Europa, effectively facilitating the

landing. The calculated delta-V values for transfers from the apogee and perigee of the parking orbit are displayed in table 8.4.2:

**Table 8.4.2: Delta –V values for departure from parking orbit.**

Departure Location	Delta – V (km/s)
Perigee (T1)	0.3644
Apogee (T2)	0.1754

The delta-V required to insert into the zero-altitude circular orbit for each Hohmann transfer ellipse is displayed in table 8.4.3:

**Table 8.4.3: Delta - V values for insertion into zero-altitude circular orbit.**

Transfer Ellipse	Delta – V (km/s)
T1	0.3420
T2	0.4483

Finally, the delta – V required to bring the probe from a zero-altitude circular orbit to stationary on the surface was calculated to be 1.433 km/s. The overall delta – V values for both transfer ellipses are shown in table 8.4.4, providing a preliminary estimate for the total mission delta-V. While this analysis suggests that the Europa parking orbit should be left at apogee, more detailed analysis of departure location, as well as other orbital maneuvers, will be conducted in the FDR.

**Table 8.4.4: Total Delta – V values for transfer from Jupiter orbit to landing on Europa.**

Transfer Ellipse	Total Delta – V (km/s)
T1	6.4826
T2	6.400

## 8.4.6 Risk Assessment and Mitigation

For the orbital mechanics of the ECHO mission, the primary risk is the probe failing to sufficiently reduce its velocity during landing, leading to a hard impact and crash landing that could result in the complete loss of the probe. This risk has been mitigated through the decision matrix, as the lander safety was given a high priority, and a powered descent was selected. Powered descent is considered a relatively safe landing method since it allows for complete control throughout the landing process. It also has a proven track record, with missions such as Apollo, Curiosity, and Viking 1 and 2 successfully using some form of powered descent to land on celestial bodies. Another significant risk is the lander ending up in the wrong orientation upon landing, such as upside down, again leading to complete loss of the probe. The selected powered descent method mitigates this risk as well, allowing for continuous adjustments using propulsion and ADCS

systems to maintain the correct orientation with the surface throughout the descent. Finally, using too much fuel during early-stage delta-V maneuvers could leave insufficient fuel for landing. To address this, detailed analysis of the required fuel for early stage Hohmann transfers, along with mass budgeting, will ensure there is enough fuel for a successful landing.

### **8.4.7 Future Work**

Future work will include a detailed technical analysis of each stage of the orbital mechanics architecture, with the goal of minimizing delta-V requirements to conserve mass for the mass budget. The powered descent will be optimized to find a fuel-efficient sequence of maneuvers to successfully land the probe. Considerations such as orbit departure locations, additional intermediate parking orbits, and specific type of powered descent will be examined. Moreover, alternative orbital maneuvers, such as utilizing Jupiter's atmosphere for aerobraking to mitigate fuel-based delta- V, may be considered. Finally, communication ability between the probe and orbiter throughout the landing process will be determined. All findings will be presented in a final orbital mechanics plan in the FDR, with at least one iteration of an overall orbital mechanic's mission architecture designed and investigated.

## **8.5 Attitude Determination & Control Subsystem (ADCS)**

**Prepared by:** Aaryan Sonawane

### **8.5.1 Subsystem Definition**

The Attitude Determination and Control Subsystem (ADCS) is responsible for maintaining the position and orientation of a spacecraft. Accurate control of orientation in space is essential for reliable two-way communication and seamless data transfer between Earth and the high gain antenna on the ECHO probe [20].

To determine the spacecraft's position and orientation relative to a fixed celestial body, various sensors are employed. This process, called attitude determination, is one of the three main duties of the ADCS. Where attitude determination is used to measure the exact orientation and position of the spacecraft, attitude control is used to mitigate differences between the sensor-measured value and the expected attitude and position. Actuators are used to control the position and orientation of a spacecraft. These two are bound together by an appropriate control law and a control system to map the spacecraft's path. The ADCS must quantify the mission's pointing requirements and develop a suitable control system to ensure the spacecraft stays on course, even if it deviates from its intended path. A well-designed control law appropriately models the forces acting on a spacecraft and determines their effects on the spacecraft's intended trajectory over time. Thus, it is necessary that the equations of motions that control the spacecraft's attitude and location

are accurately represented in the time domain. Additionally, to compute all the forces together, it is essential that reference frame for these control measures be in the universal 'N' basis [21].

## 8.5.2 Attitude Determination

Sensors will be used to determine the spacecraft's orientation with respect to known celestial bodies. To improve accuracy, multiple sensors will be used to verify the orientation of the spacecraft. The harsh conditions within the Jovian atmosphere along with heavy magnetic fields are going to affect the accuracy of a sensor. This adds complexity in determining the current state (location & orientation) of the spacecraft. For example, star tracker data will be noisy while the spacecraft is within the high radiation zone around the Jovian orbit. Another example being methods that use GPS will be rendered useless for the ECHO probe due to the distance away from the earth. Mass constraints also play a huge role in determining the type of sensors we can use, and which group of sensors fit best for the ECHO probe. The current allocated mass budget for the entire ADCS is 25kg.

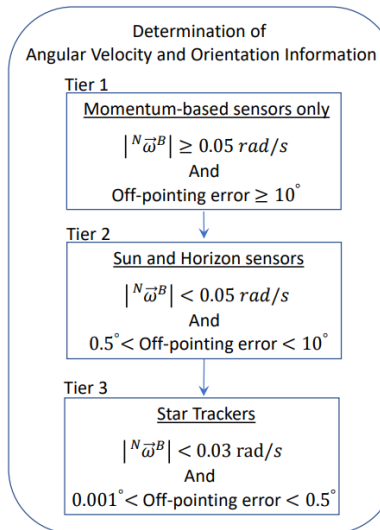


Figure 8.5.1: Tier-list of Sensors [21]

Figure 8.5.1 displays different tiers of sensors and the angular velocities they best operate at.  $N\vec{\omega}^B$  is the measured angular velocity vector of spacecraft body 'B' in the universal space reference frame 'N.' Off pointing error is calculated by subtracting measured angle of orientation from the expected angle of orientation of the spacecraft. These two factors were used to rank the sensors into a tier system with each tier of sensors presenting its own advantages. Without a momentum-based sensor present on a spacecraft, the spacecraft dynamics will not be accurate. For example, angular velocities over 0.05 rad/s can be tracked by neither Sun Sensors nor Star Tracker despite being the most accurate pointing sensors. Keeping this in mind, three types of sensors were selected for the mission: the star tracker, magnetometer, and inertial measurement unit (IMU). The star tracker is a small camera with an attached computer that uses various known stars as reference points to accurately determine the spacecraft's attitude and location. It will serve as the primary

sensor to determine the position and orientation of the spacecraft. The star tracker in context of the ECHO probe will be appropriately designed to filter out noise within the data created by the intense radiation in the Jovian orbit. As demonstrated in the Juno probe, star trackers could filter out the noise from these pictures [22]. Magnetometers were chosen to compliment the star tracker in attitude determination. Magnetometers have been proven to accurately measure strength and direction of magnetic fields. The direction and strength of the magnetic field data collected near the Jovian orbit can be used to infer the exact orientation and location of the spacecraft [23]. Apart from attitude, magnetometers have also been proven to provide crucial data about the presence of the ocean beneath the icy crust of Europa. If there is an ocean present under the icy surface of Europa, its induced magnetic field will be different to what Europa would be if it was just an icy body. Magnetometer measurements are crucial to track these differences [24]. To round out the suite, the IMU will be employed. While not as accurate as the star tracker or magnetometer, the IMU is particularly valuable for measuring high angular velocities, allowing for responsive maneuvering during complex flight dynamics. It contains a ring laser gyro to measure angular velocities and an accelerometer to measure acceleration tracking delta-v changes [25].

**Table 8.5.2: Attitude Determination Sensor Decision Matrix**

Design Criteria	Weighting (1-5)	Sun Sensor	Star Tracker	Magnetometer	IMU	Horizon Sensor
Mass	0.15	5	4	4	3	4
Power	0.15	4	4	4	3	4
Accuracy	0.1	2	5	4	3	2
Risk	0.3	3	3	4	3	3
Effectiveness	0.2	2	5	4	4	2
Cost	0.1	3	3	3	4	3
Score	1	3.15	<b>3.9</b>	<b>3.9</b>	<b>3.3</b>	3.0

As seen in the decision matrix on table 8.5.2, mass, risk, and effectiveness remain critical factors for the success of the mission. The environmental conditions near Jupiter are extremely challenging and therefore, considering risk in this environment coupled with the effectiveness of the sensors as a unit are crucial for the success of the ECHO lander probe. With only 25kg allocated for the ADCS, sensors must optimize performance while adhering to strict weight constraints. Certain sensors were not selected for this mission based on their limitations in the context of deep space exploration. The sun sensor was not preferred due to its dependency on the Sun as a reference frame, possessing significant challenges beyond Jupiter's orbit. In deep space, especially when navigating around Jupiter and its moons, sun sensors can face massive operation errors due to potential occlusion by Jupiter itself in line of sight to the Sun, leading to inconsistent attitude and location data. A horizon sensor was considered but ultimately rejected, as its effectiveness

diminishes in a deep space context where consistent referencing to a planetary body, mostly Earth, is not efficient for tracking orientation and location of the spacecraft. Given the vast distances and potential lack of clear horizon references while in the Jupiter system, these sensors may struggle to provide accurate data. Horizon sensors may be more accurate than IMUs on their own but collectively, the package of Star trackers, Magnetometers, and IMU is a much more effective combination in the context of this mission.

### 8.5.3 Attitude Control

Attitude control is achieved through the use of actuators. Actuators act as correcting agents in case the data measured by the sensors does not match with the expected data of the attitude and position of the spacecraft. After determining the numerical error between the data points, control measures must be undertaken to mitigate this error. Like the sensors there will be tiers of actuators depending on the need for accuracy throughout the mission. As such, primary actuators provide a greater degree of freedom when it comes to correcting the attitude in all three dimensions.

Reaction wheels and magnetorquers were finalized as the best options for the primary actuator and secondary actuators for the probe's mission to Europa. Reaction wheels are small cylindrical wheels attached to each axis of the spacecraft's body. Reaction wheels control attitude error by spinning around their axes using motors, generating a proportional counter-rotational torque on the main body of the spacecraft due to the conservation of angular momentum. This process is used as a control mechanism in case the spacecraft is measured to be off its intended track [26]. Magnetorquers, on the other hand, utilize magnetic fields to create torque, allowing for efficient attitude adjustments without adding significant moving parts to the spacecraft. Due to the presence of a strong magnetic field around Jupiter and magnetometers aboard the spacecraft, data transfer to the magnetorquers will be seamless. This way, magnetorquers can produce the necessary torques quicker by precisely adjusting current in specific coils within [27].

**Table 8.5.3: Attitude Control Actuator Decision Matrix**

Design Criteria	Weighting	Reaction Wheels	CMG	Solar Sails	Magnetorquers	Small Ion Thrusters
Mass	0.2	4	2	5	4	3
Power efficiency	0.05	4	4	5	5	3
Accuracy	0.15	4	5	2	4	4
Operation Speed	0.15	4	4	1	4	5
Risk	0.2	4	4	4	4	3
Effectiveness	0.15	5	3	2	4	3
Cost	0.1	3	3	4	4	5
Total	1	4.05	3.5	3.2	4.05	3.65

As detailed in the decision matrix on table 8.5.3, mass, risk, accuracy, speed of operation, and effectiveness rank almost equally and it is the combination of these factors that make up an effective actuator solution. Like the sensors, the harsh conditions within the Jovian orbit pose severe safety risks to the success of the actuators and incorporating and mitigating this risk is crucial for the success of the ECHO probe. Several potential actuator solutions were considered but ultimately failed to align with the goals of the mission. Control Moment Gyros (CMGs), while offering high precision and responsiveness, were eliminated due to their increased mass and complexity. Solar Sails, despite being power-efficient, are dependent on solar radiation, making them impractical for the low light conditions near Jupiter [28]. Small ion thrusters capable of providing excellent thrust were heavily considered but ultimately would not be as efficient near Jupiter due to their dependence on Solar power [29].

#### 8.5.4 ADCS Risk Assessment

The primary risk associated with the ADCS is part failure. Part failure has many reasons such as wear & tear, exposition to intense radiation, saturation of attached motors, etc. The parts used to handle ADCS of the ECHO probe are divided into two categories. They are the sensor suite and the actuator suite. The sensor suite consists of Star Trackers, magnetometers, and IMU whereas the actuator suite consists of Reaction Wheels and Magnetorquers. Backups and redundancy are never harmful in the case of ADCS and provide critical support in case of part failure. Picking the right number of parts is crucial to keep in line with the limited and strict mass budget of the mission.

The risks associated with the different parts of the ADCS in relation to the context of the mission are highlighted in further detail in table 8.5.5.

**Table 8.5.5: ADCS Risk Assessment Matrix**

Instrument Name	Risk	Cause	Mitigation
Star Tracker	Part Failure	Fatigue	Incorporate redundancy by adding a backup Star Tracker along with periodic calibration tests
		Intense radiation	Protective Design measures taken to filter out data noise caused by intense radiation
IMU	Drift in readings	Fatigue	Incorporate redundancy by adding a backup IMU along with periodic calibration tests
Reaction Wheel	Mechanical Failure	Part Saturation	Magnetorquers added to provide appropriate desaturation torque
Magnetorquers	Part Failure	Electrical & Mechanical Failure	Incorporate redundancy by adding a backup Magnetorquer

Based on the risk factors and possible mitigations for them listed in table 8.5.5, the preliminary number of ADCS parts used on the ECHO probe will be

- (2x) Star Tracker: 1.5kg each
- (1x) Magnetometer: 1kg each
- (2x) IMU: 2kg each
- (4x) Reaction Wheels: 2kg each
- (2x) Magnetorquers: 1.5kg each

Total mass allocated for these parts is 25kg and it is imperative to remain within this strict mass budget for the success of the mission. As such, the total mass used by ADCS parts comes out roughly around 19kg [20]. This is simply a preliminary estimate based on potential options looked at for the usage of the mission.

## 8.5.5 ADCS non-technical considerations

The following non-technical factors were also considered for the ADCS of the ECHO mission:

**Table 8.5.5: ADCS non-technical factors consideration matrix**

<b>Topic</b>	<b>Consideration</b>
Public Health & Safety	Reaction wheels contain extremely precise fast-moving parts which present risks to the engineers during manufacturing, handling, and installation. Appropriate safety measures should be taken to ensure the well-being of engineers
Global	N/A - The selection of the ADCS design does not have significant global considerations
Cultural	N/A - The selection of the ADCS design does not have significant cultural considerations
Social	N/A - The selection of the ADCS design does not have significant social considerations
Environmental	N/A - The selection of the ADCS design does not have significant Environmental considerations
Ethical	The selection of ADCS parts is purely for the customer's and the scientific community's best interest. All solutions, assumptions, and considerations are based on the full knowledge of the engineering team and are reviewed closely by a secondary lead
Economic	Even though ADCS is not a huge constituent of the economic budget, the ADCS design is built for efficient use of finite resources on hand

## 8.5.6 Plan of procession

The forces around the body should be quantified. Forces like Solar Pressure, gravitational variance, magnetic fields along with external and internal disturbances will be quantified in the universal 'N' basis. This will help determine the equations of motion for the spacecraft and accordingly control equations will be modelled to make up a recurring closed loop control system. The forces will be quantified as functions of time and appropriate control torques will be applied based on sensor data and the error between the intended and measured orientation and location. Once the forces have been quantified, different control models will be compared to make specific determination of parts most relevant to the mission.

## 8.6 Thermal Management

Prepared by: Constantine Childs

## 8.6.1 Subsystem Definition and Requirements

The TCS of ECHO ensures that all components of the lander are within a suitable temperature range for all aspects of the flight. The allowable temperature ranges for each major lander component are tabulated in table 8.6.1. Based on mission requirements to keep mass as low as possible, the subsystem must account for no more than 2.5% (25 kg) of the overall lander mass [30]. Individual sensors and cameras have a variety of temperature ranges and their own respective thermal control systems. Thermal control of the lander during launch and interplanetary travel is controlled by the Europa orbiter and thus not discussed in this report.

**Table 8.6.1: General temperature requirements for Europa ECHO lander [31]**

	Allowable Flight Temperatures (°C)	
Assembly	Min	Max
Vault	-20	50
Propulsion Module	0	35
RF Antennas	-135	105
Batteries	0	30

## 8.6.2 Thermal Environment

Jupiter and Europa's distance from the sun is 5.2 AU [32]. At this distance the ECHO lander will be subject to extreme cold, as the solar flux is proportional to the inverse square of distance. This results in a direct solar flux of  $51 \text{ W/m}^2$ , and the planetary IR from Jupiter is  $13.6 \text{ W/m}^2$  and its albedo is 0.343 [32]. This results in a worst-case to best-case temperature range of 27 K to <sup>105</sup><sub>46</sub> in orbit around Jupiter. At the surface of Europa, the mean surface temperature at its equator is 96 K and drops to 46 K at its poles [33]. Figure 8.6.1 shows a thermal observation of Europa's surface temperature based on brightness and potential landing zones based strictly on temperature. Europa does not have any meaningful atmosphere and as a result no heat shield is required for the descent from orbit.

---

<sup>1</sup> Temperatures calculated using simplified assumptions of eqns. 7.37 and 7.36 from Charles Brown's Elements of Spacecraft Design

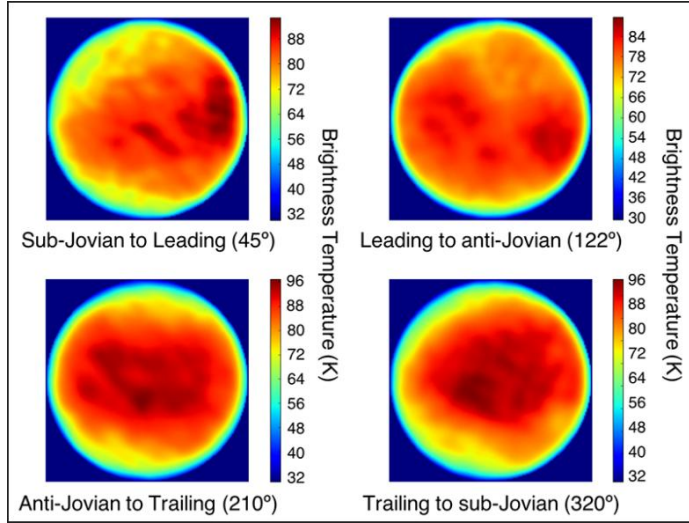


**Figure 8.6.1: Brightness Temperature of Europa's Surface [34]**

Since the temperatures in the flight regime are well below the allowable flight temperatures and never exceed 174 K, heat retention, generation, and distribution are the primary focus of the TCS. In addition, the short but frequent Europan eclipses block the direct solar flux and increases heat loss from the lander.

### 8.6.3 Thermal Control Selection

The lander thermal control subsystems can be classified as active or passive. As described in section 8.6.2, the Jupiter/Europa environment is a harsh and extremely cold environment. Based on the importance of the subsystem, risk to mission is an important factor that must be considered for each type of TCS selection. This criterion is based on the impact on the overall lander performance if the subsystem were to suffer a failure mode. A hybrid system consisting of both active and passive components was selected for flexibility and effective thermal performance. A decision matrix for each possible subsystem option is shown in table 8.6.2.

**Table 8.6.2: Decision matrix for thermal control subsystem**

Design Criteria	Weighting	Passive	Active	Hybrid
Overall Mass	1	4	3	3
Cost	0.5	4	3	3
Risk to Mission	2.5	3	2	3
Power Usage	2	5	1	3
Reliability	2	4	3	4
Thermal Performance	2	3	5	5
	SCORE	37.5	27.5	36

Ideally a passive system is used in cases requiring low power usage and where mass budgets are tight. However, due to the extreme temperature that the lander will encounter and the required temperature ranges for certain components demands the use of an active system as well. Potential passive systems are listed and selected for future consideration in table 8.6.3.

**Table 8.6.3: Decision matrix for passive thermal control systems**

Design Criteria	Weighting	MLI	Coatings	Heat Pipes	RHU
Overall Mass	2	4	4	3	4
Temperature Control	2.5	3	3	5	4
Reliability	2	4	4	4	5
Risk to Mission	2.5	3	3	2	1
Radiation Resistance	1	2	1	3	5
	SCORE	22.5	23.5	25.5	30.5

MLI and heat pipes are particularly of interest despite having the lowest scores of the three selections as they are more environmentally friendly compared to RHUs. MLI is an effective insulator in vacuum, is lightweight, and can be wrapped around virtually any component. Heat pipes can transfer large amounts of heat without using any electrical power. In the context of this mission heat pipes can be used to transfer power dissipation from the electronics vault and heat from the RTG to the propellant storage tanks and battery packs. The RHU was selected if more heat generation is required and for their small packing volume and mass.

**Table 8.6.4: Decision matrix for active thermal control systems**

Design Criteria	Weighting	Electric Heaters	Fluid Loops	Radiators
Overall Mass	1	4	2	3
Temperature Control	2.5	5	3	3
Reliability	1	4	3	4
Power Consumption	2	3	2	4
Risk to Mission	2.5	3	2	3
Radiation Resistance	1	3	3	4
	SCORE	34.5	25	36.5

The active TCS will prevent any component from falling below its operating temperature using electric heaters and provide precise localized temperatures. Components that have a narrower temperature operating range such as the propellant storage tanks and batteries will be prioritized by the placement of these heaters. The selected propellant, hydrazine, has a freezing point at 1.5 °C and requires special consideration from the TCS to stay above this point [35]. A small radiator

may be placed on the outside of the lander for heat rejection if there is any excess power generation, although it may not be included if the mass budget becomes too constrained.

### 8.6.4. Non-Technical Considerations

In addition to qualitative technical considerations discussed previously, the following non-technical considerations were weighed in preliminary design of the TCS:

Public health and safety – The use of RHUs in the thermal subsystem may pose a threat to the public. Compliance with safety standards will mitigate hazards at all stages of the design life.

Environmental – Certain materials in the heat pipes and RHUs such as ammonia or radioactive or other environmentally harmful materials. Safety protocols and environmental regulations will be followed when designing and handling these materials.

Economic – Partnership with companies that produce system components will generate revenue and affect stock value, resulting in a small impact on the overall economy.

### 8.6.5 Risk Assessment and Mitigation

The TCS is essential in keeping vital lander components within their operating temperatures to guarantee optimum performance. If the temperature drops below a component's allowable flight temperature it can lead to that component failing and jeopardizing mission requirements. A non-comprehensive list of potential risks and their mitigation is documented in table 8.6.5.

**Table 8.6.5: TCS Risk Assessment Matrix**

Risk	Cause	Effect	Pre-RAC	Mitigation	Post-RAC
MLI damaged or degradation [36]	High speed debris or UV	Reduced insulation of the lander, reducing internal temperature and damaging components	2C	Use UV resistant outer layers on MLI	3D
Electric heater failure	Power supply, wiring issue	Freezing of component or fuel freezing	1C	Extensive testing of system and vetting process	2E
Radiation exposure from RHU	Launch vehicle failure, improper handling	Death or severe personnel injury	1C	Robust containment features and handle following safety protocols	1E

## **8.6.6 Future Work**

Future work will include thermal analysis of the subsystem to provide preliminary quantitative results as a future basis for component sizing. As refinements are made to the design, mass budget, and power dissipation a more constrained analysis will determine the performance requirements of each subsystem component. An aerobraking maneuver is being evaluated and if chosen, an analysis of the interaction between the lander and Jupiter atmosphere must be done for heat shield consideration. An exhaust plume shield may also be necessary to install on the nadir of the lander to protect the lander structure from ejecta and exhaust gases.

## **8.7 Power**

**Prepared by: Mae Tringone**

### **8.7.1 Subsystem Definition**

ECHO's power subsystem is responsible for providing the power necessary for all other subsystems to function for the entirety of their design life. It must:

1. Provide nominal power to keep ECHO continuously and reliably powered on for the duration of its mission.
2. Be able to anticipate and provide power at the mission's expected peak load.

### **8.7.2 Power Generation**

The environment of Europa presents a challenge when it comes to persistent power generation; the tidally locked nature of the moon, its periodic eclipse by Jupiter, and the distance of the Jovian system from the Sun make utilizing solar power on the surface of the moon particularly difficult. While exclusive primary battery power would be a comparatively simple solution, the desire to continue transmitting long-term observations of the general Europian surface and subsurface environment makes in-situ power recovery a hard requirement. Thus, the utilization of a Radioisotope Thermoelectric Generator is the likely solution. This solution has the added benefit of providing a lot of waste heat, which can be used to keep the rest of the lander at adequate operating temperature.

RTGs are typically designed for the mission they are to be launched on. NASA has standardized a model of RTG for its missions, the MMRTG, which can provide 110 W of power at the beginning of its mission life. Its mass falls within mass budget allotted to the power subsystem, at 43.6 Kg [37].

### **8.7.3 Power Storage**

Limited mass budget means that the lander will have to function on the nominal voltage supplied by the onboard RTG, without room for much else. However, to ensure that unforeseen peak loads do not lead to a mission failure, a secondary battery array should be considered.

The *Philae* comet lander, which several aspects of this mission are using as a benchmark, functioned on 8 W of photovoltaic power generation and relied principally on primary battery power for much of its scientific suite [38]. The solar panels were not actually able to draw in enough power to keep the lander operational, and thus the long-term performance of *Philae*'s secondary batteries in a cold environment has not been determined.

The majority of rechargeable spacecrafts with ongoing missions are powered by whatever rechargeable battery technology was available at the time of launch, be it nickel-metal hydride or lithium-ion. The vast gulf in battery capacity and efficiency between these two technologies, combined with the need to optimize for mass wherever possible, makes lithium-ion the clear choice.

**Figure 8.7.3a: Normalized Battery Specification Comparison between lithium-ion and Nickel-metal hydride batteries [39]**

	Ni-MH	Li-ion
Cell Voltage (V)	1.2	3.6
Specific Energy (Wh/kg)	1 – 80	3 – 100
Specific Power (W/kg)	<200	100 – 1000
Energy Density (kWh/m <sup>3</sup> )	70 – 100	80 – 200
Power Density (MW/m <sup>3</sup> )	1.5 – 4	0.4 – 2
Efficiency (%)	81	99

## 8.7.4 Risk Assessment and Mitigation

Utilizing an RTG for the mission includes bearing the responsibility of ensuring the safe construction, transportation, and launch of radioactive material. A scuttled launch or hard landing could prove disastrous for the surrounding environment and population due to the risk of radiological contamination. While a safe launch is always a priority when planning for spaceflight, every precaution must be taken to ensure that the RTG's protective housing especially does not suffer a loss of structural integrity from launch to final escape from Earth, including minimizing exposure in the unlikely event that the mission must be aborted before leaving the suborbital flight stage.

## 8.7.5 Future Work

Where possible, the mass budget allocation will be optimized to allow for a previously developed RTG, plus supporting secondary batteries, to be included in the final design. In the event that this becomes impossible, an empirical relationship between prior RTG designs and their associated masses will be computed and used to estimate the power output of an RTG custom-fit for ECHO.

The lack of previously attempted lander missions in an environment like Europa, coupled with the lander's low mass constraints, additionally makes estimating the expected draw of ECHO's instrumentation a challenge. Further analysis will be performed on each individual subsystem to estimate a nominal and peak power draw by the time the design is close to being finalized, which will then be used to further refine the selection of an RTG and possible secondary battery array for the mission.

## **8.8 Command and Data**

**Prepared by: Chloe Powell**

### **8.8.1 Subsystem Definition**

The command and data subsystem is responsible for receiving commands from the orbiter and performing those commands at the specified time. To do this, a computer system is integrated into the lander. This computer has enough memory to store commands and data [41]. This way, a command can be sent to the lander prior to when it needs to be acted on and will be performed when a specific state is reached or at a certain time.

### **8.8.2 Computer Architecture**

The computer architecture of the command and data subsystem can be represented in one of three ways: centralized, decentralized, and distributed. A centralized architecture has a single point of control of one main server with multiple connected servers used for smaller computational tasks. A decentralized architecture has multiple main servers, each with their own subset of servers for smaller computational tasks. A distributed architecture has many servers connected through a network, all communicating and working towards the same goal [41, 42]. Table 8.8.1 contains the decision matrix for computer architecture.

**Table 8.8.1 Decision Matrix for Computer Architecture [40]**

Design Criteria	Weight	Centralized	Decentralized	Distributed
Risk	2.5	2	4	5
Mass	2.5	4	3	2
Power Consumption	2	4	4	2
Performance	1.5	4	3	5
Volume	1.5	5	3	2
Total	10	36.5	34.5	32

### **8.8.3 Risk Assessment**

Hardware or software failure is the most prevalent risk associated with command and data. These failures could come from a malfunction in the system itself or an outside force affecting the system. With a centralized computer architecture and a single point of control, the impacts of this risk increase. Testing of the system prior to launch will make any problems evident and can be fixed early on. An adequate protective structure outside the computer architecture will protect it from the harsh conditions of Europa and will mitigate the risk of damage to the system.

### **8.8.4 Future Work**

Future work will include selecting a computer system to use in the lander. As more details are confirmed for other subsystems in the lander, a more informed decision can be made regarding the computer system to be used.

## **8.9 Telecommunication**

**Prepared by: Chloe Powell**

### **8.9.1 Subsystem Definition**

The telecommunication system is responsible for maintaining communication between the lander and the orbiter. The lander will not have direct communication with Earth, and the orbiter's telecommunication system will relay information from the ground station to the lander and vice versa as needed. The uplink, from the orbiter to the lander, will be used to relay information from

the ground station. The downlink, from the lander to the orbiter, will be used to transmit data collected from experiments done on Europa's surface, as well as telemetry data [43].

## 8.9.2 Frequency Band Selection

An appropriate frequency band to communicate with must be selected. The most important metric is the reliability of communication over the band [48]. The mission objective is to perform experiments on the surface of Europa, so data collected by the lander must be accurately transmitted to the orbiter for the mission to be successful. Power consumption is also an important factor and must be minimized as much as possible. The range of the frequency band and the speed were also considered, but were not weighted as heavily, as the lander will not be far from the orbiter while the orbiter is in range for communication. Table 8.9.1 displays the decision matrix used to determine which frequency band should be used.

**Table 8.9.1 Decision Matrix for Frequency Band**

Design Criteria	Weight	X-Band	S-Band	Ka-Band	UHF
Risk [46]	3	3	4	2	5
Power Consumption [47] [48]	2.5	4	3	5	2
Range [44]	1.5	5	3	5	2
Speed [44]	1	5	4	5	2
Total		41.5	35	41	29

Based on the decision matrix shown in table 8.9.1, the X-band is the best frequency band to use for communication with the orbiter. There is a tradeoff with lower power consumption and lower reliability. However, many deep-space vehicles use the X-band frequency band, so it has been proven to be reliable enough for this type of mission [44, 45].

## 8.9.3 Antenna Selection

The type of antenna used by the lander must be selected as well. The antenna must be highly directional and have low mass and power consumption. A high directionality increases signal strength and reduces interference from other signals. The signal will be traveling from the lander to the orbiter, not to Earth, so the strength of the signal is more important than the range. As gain increases, signal strength, or directionality, and range increase [49]. Directionality was chosen as design criteria as opposed to gain because the range does not need to be considered. The decision matrix for selecting an antenna is shown in table 8.9.2.

**Table 8.9.2 Decision Matrix for Antenna Type**

Design Criteria	Weight	Parabolic Grid [52, 54]	Parabolic Dish [52, 54]	Yagi-Uda [53, 51, 55]	Patch [56]	Sector [50]
Risk	3	3	3	2	4	2
Directionality	3	4	5	5	5	3
Power Consumption	2	3	3	2	4	4
Mass	2	2	2	5	5	4
Total	10	31	34	35	45	31

## 8.9.4 Risk Assessment and Mitigation

The risk most likely to occur within the telecommunication system is a software or hardware failure. While a failure could be catastrophic to the mission and result in loss of communication with the orbiter, there are steps that can be taken to mitigate this. Extensive vetting of the companies used will help confirm the integrity of the technology used. Testing of both the hardware and software will lead to identifying any issues before launch. Redundancy of aspects of the system where possible will offer a backup should something stop working during the mission. Other issues that are less likely to occur are physical damage to the ground facility and unauthorized access to the radio frequency used. Security measures such as security cameras and an alarm system, as well as gates and other protective architecture, will decrease the likelihood of damage to a ground facility from an attack or a natural disaster. Unauthorized access can be prevented by encrypting data and using authentication for anyone attempting to access information going to or from the ground facility.

## 8.9.5 Future Work

Future work will include a detailed analysis of the telecommunication system using the frequency band and the selection of an antenna model. The system's anticipated performance will be evaluated, and the design will adjust accordingly.

# **9 Design Budgets**

## **9.1 Mass Budget**

**Prepared by: Joseph Bowers**

The preliminary mass budget for ECHO has been based on the mass of the Europa Clipper, as both missions are destined to Jupiter and launched by a Falcon Heavy. It is reasonable that the mass budget of ECHO would be 30% of the dry mass of Europa Clipper. As such, the overall mass budget of ECHO is 1000 kg (wet mass). A preliminary subsystem mass budget has been outlined in Table 9.1.1. The distribution of mass to the various subsystems is expected to change with additional analysis.

**Table 9.1.1 Mass Budget by Subsystem**

Subsystem	Percentage	Mass (kg)
Structures	8.0%	80
Mechanisms & Deployables	4.0%	40
Propulsion	75.0%	750
ADCS	2.5%	25
Thermal Management	2.5%	25
Power	5.0%	50
Command & Data	1.5%	15
Telecomm	1.5%	15
Totals	100.0%	1000

## **9.2 Volume Budget**

**Prepared by: Constantine Childs**

A preliminary estimate of the volume of the ECHO lander is based on the total volume of the Europa Clipper (excluding solar arrays). The volume of the lander is 25% of the volume of Europa Clipper which results in a volume of 14.26 m<sup>3</sup>. Volume budgets for each subsystem are shown in table 9.2.1.

**Table 9.2.1: Volume budget by subsystem**

Subsystem	Percentage	Volume (m <sup>3</sup> )
Structures	25.0%	3.565
Mechanisms & Deployables	4.0%	0.5704
Propulsion	50.0%	7.13
ADCS	3.0%	0.4278
Thermal Management	4.0%	0.5704
Power	10.0%	1.426
Command & Data	2.0%	0.2852
Telecomm	2.0%	0.2852
Totals	100.0%	14.26

## 9.3 Cost Budget

**Prepared by Andrew Olson**

The preliminary cost budget for the ECHO mission has been established based on an analysis of comparable missions, specifically NASA's Galileo, Juno, and Europa Clipper. To determine an appropriate mass budget, the cost per kilogram of launch mass for each of these missions was calculated and adjusted for inflation, as presented in Table 9.3.1. These values were then averaged, and the resulting average cost per kilogram was multiplied by the current estimate of ECHO's mass budget. This calculation produced a cost budget, which was subsequently rounded to the nearest \$10,000,000, resulting in a total budget of \$920,000,000 for the ECHO lander.

**Table 9.3.1 ECHO Cost Budget**

Mission	Cost (Billion \$)	Launch Mass (kg)	Dollar/kg	ECHO Predicted Dry Mass (Kg)
Galileo	\$3.80	2,562	1,483,216	1,000
Juno	\$1.52	3,625	419,310	
Clipper	\$5.20	6,065	857,378	
Average dollar/kg: 919,968				Predicted ECHO Cost Budget \$ 920,000,000

## 10 Sales Pitch

**Prepared by: Katie August**

Project ECHO holds monumental potential in the scientific and engineering community. This mission can help scientists understand if life can exist beyond Earth and if Europa can sustain it. There have been historically successful missions of rovers exploring extraterrestrial bodies such as Mars rovers Perseverance and Curiosity. These two rovers made countless scientific discoveries that challenged the way scientists and engineers can explore the universe.

ECHO's primary missions of sampling the ice and atmospheric conditions on Europa are similar to missions that have already proven to be successful. This project pushes the boundaries of current knowledge and technologies and will prove to be a groundbreaking work of science and engineering. The data gathered from Europa has the potential to reshape the current understanding of life's existence beyond Earth and open new possibilities of life in the universe.

## 11 Conclusions

**Prepared by: Chloe Powell**

The ECHO mission objectives are to produce and analyze a sample of Europa's surface ice and to measure atmospheric conditions at the surface of Europa. This will be accomplished through the use of a lander on Europa's surface. The lander will descend onto the surface of the moon using a bi-propellant propulsion system and a powered descent. Once it has safely landed, a suite of scientific instruments and sensors will collect data and conduct experiments on samples of surface ice. Findings from this analysis will be transmitted to the orbiter, which will transmit those findings to Earth. The mission is planned to be six months long, and the lander architecture is designed such that it will survive the duration of the mission, if not longer, with minimal risks. The data collected by ECHO will give valuable insight into Europa's ability to support life.

## 12 References

- [1] Elizabeth Howell, "Europa: Facts About Jupiter's Icy Moon and Its Ocean," Space.com, Mar. 22, 2018. <https://www.space.com/15498-europa-sdcmp.html>
- [2] "Europa: Facts - NASA Science," Nasa.gov, Nov. 09, 2017. <https://science.nasa.gov/jupiter/moons/europa/europa-facts/#h-potential-for-life>
- [3] M. H. Carr et al., "Evidence for a subsurface ocean on Europa," Nature, vol. 391, no. 6665, pp. 363–365, Jan. 1998, doi: <https://doi.org/10.1038/34857>
- [4] United Nations, "Space Debris Mitigation Guidelines of the Committee on the Peaceful Uses of Outer Space," United Nations publication, Vienna, 2010.
- [5] NASA, "Europa: Facts," [Online]. Available: <https://science.nasa.gov/jupiter/moons/europa/europa-facts/#h-potential-for-life>. [Accessed 2024].
- [6] United Nations Office for Outer Space Affairs, "Space Law Treaties and Principles," 2017. [Online]. Available: <https://www.unoosa.org/oosa/en/ourwork/spacelaw/treaties.html>. [Accessed October 2024].
- [7] United States Code, "TITLE 51—NATIONAL AND COMMERCIAL SPACE PROGRAMS," 2011. [Online]. Available: <https://www.govinfo.gov/content/pkg/USCODE-2011-title51/html/USCODE-2011-title51.htm>. [Accessed October 2024].
- [8] NASA, "Europa Clipper Launch Windows," [Online]. Available: <https://science.nasa.gov/mission/europa-clipper/launch-windows/>. [Accessed 2024 October].
- [9] Anderson, K. S., "Space Vehicle Systems Engineering," Spacecraft Design, Dynamics & Control Primer, RPI, [https://www.rpi.edu/~anderk5/space\\_vehicle\\_systems.pdf](https://www.rpi.edu/~anderk5/space_vehicle_systems.pdf)
- [10] "Materials database." <https://tpsx.arc.nasa.gov/MaterialsDatabase>
- [11] Editor Engineeringtoolbox, "Young's Modulus, Tensile Strength and Yield Strength Values for some Materials," Aug. 20, 2024. [https://www.engineeringtoolbox.com/young-modulus-d\\_417.html](https://www.engineeringtoolbox.com/young-modulus-d_417.html)
- [12] P. Magnani *et al.*, "ROSETTA PHILAE SD2 DRILL SYSTEM AND ITS OPERATION ON 67P/CHURYUMOV-GERASIMENKO." Available: [https://robotics.estec.esa.int/ASTRA/Astra2015/Papers/Session%203A/95631\\_Magnani.pdf](https://robotics.estec.esa.int/ASTRA/Astra2015/Papers/Session%203A/95631_Magnani.pdf)
- [13] "Introducing SD2: Philae's Sampling, Drilling and Distribution instrument – Rosetta – ESA's comet chaser," *Esa.int*, 2014. <https://blogs.esa.int/rosetta/2014/04/09/introducing-sd2-philae-sampling-drilling-and-distribution-instrument/> (accessed Oct. 17, 2024).

- [14] A. Johnson *et al.*, "First Ice Cores from Mars A report from the NASA Mars Ice Core Working Group," 2021. Available: [https://www.nasa.gov/wp-content/uploads/2021/12/mars\\_ice\\_core\\_working\\_group\\_report\\_final\\_feb2021.pdf](https://www.nasa.gov/wp-content/uploads/2021/12/mars_ice_core_working_group_report_final_feb2021.pdf)
- [15] "Europa Lander," [www.jpl.nasa.gov](http://www.jpl.nasa.gov). <https://www.jpl.nasa.gov/missions/europa-lander/>
- [16] "Europa Clipper's Trajectory to Jupiter – NASA's Europa Clipper," *NASA's Europa Clipper*, 2024. <https://europa.nasa.gov/resources/533/europa-clippers-trajectory-to-jupiter/>
- [17] P. Bauduin, "Galileo Orbiter," *Weebau.com*, 2024. <https://weebau.com/satplan/galileo.htm> (accessed Oct. 15, 2024).
- [18] Wikipedia Contributors, "Europa (moon)," *Wikipedia*, Mar. 10, 2019. [https://en.wikipedia.org/wiki/Europa\\_\(moon\)](https://en.wikipedia.org/wiki/Europa_(moon))
- [19] H. D. Curtis, *Orbital mechanics for engineering students : revised fourth edition*. Amsterdam: Elsevier, 2021
- [20] NASA, "Guidance, Navigation, and Control for Small Satellites," <https://www.nasa.gov/smallsat-institute/sst-soa/guidance-navigation-and-control/#5.2.1>
- [21] Anderson, K. S., "Space Vehicle Systems Engineering," *Spacecraft Design, Dynamics & Control Primer*, RPI, [https://www.rpi.edu/~anderk5/space\\_vehicle\\_systems.pdf](https://www.rpi.edu/~anderk5/space_vehicle_systems.pdf)
- [22] NASA, "Mission Dispatch: Star Tracker Integration," Europa Clipper, <https://europa.nasa.gov/resources/344/star-tracker-integration/>
- [23] NASA, "Danish Instrument Helps NASA's Juno Spacecraft See Radiation," NASA, <https://www.jpl.nasa.gov/news/danish-instrument-helps-nasas-juno-spacecraft-see-radiation/>
- [24] NASA, "NASA's Magnetometer for Europa Clipper," Europa Clipper, <https://science.nasa.gov/mission/cassini/spacecraft/cassini-orbiter/magnetometer/mag-technical-write-up/>
- [25] NASA, "Magnetometer Technical Overview," Europa Clipper, <https://ntrs.nasa.gov/api/citations/20200000353/downloads/20200000353.pdf>
- [26] NASA, "Reaction Wheels for Deep Space Travel," Europa Clipper, <https://www.nasa.gov/news/nasas-europa-clipper-spacecraft-kicks-assembly-into-high-gear>
- [27] Radar-based Navigation and Orientation in Deep Space, Michigan Technological University, <https://digitalcommons.mtu.edu/cgi/viewcontent.cgi?referer=&httpsredir=1&article=1895&context=etds>
- [28] NASA, "Solar Power and Actuators for Deep Space Missions," Europa Clipper, <https://www.lpi.usra.edu/opag/JJSDTNASAReport.pdf>

- [29] NASA, "Small Ion Thrusters for Spacecraft,"  
<https://ntrs.nasa.gov/api/citations/20050041919/downloads/20050041919.pdf>
- [30] C. D. Brown, Elements of Spacecraft Design. Reston, VA: American Institute Of Aeronautics And Astronautics, 2002, p. 373.
- [31] H. Ochoa, J. Hua, R. Lee, A. Mastropietro, and P. Bhandari, "Europa Clipper Thermal Control Design," 2018.
- [32] D. Gilmore, Ed., Spacecraft Thermal Control Handbook, 2nd ed., vol. 1. The Aerospace Press, 2002, p. 49-60.
- [33] Y. Ashkenazy, "The surface temperature of Europa," Oct. 2016.
- [34] S. Trumbo, M. Brown, and B. Butler, Comparison of ALMA Images with model images. 2018.
- [35] NOAA, "Hydrazine (HDZ)," CAMEO Chemicals, [Online]. Available:  
<https://cameochemicals.noaa.gov/chris/HDZ.pdf>.
- [36] M. Finckenor, "Multilayer Insulation Material Guidelines," 1999. Available:  
<https://ntrs.nasa.gov/api/citations/19990047691/downloads/19990047691.pdf>
- [37] R. Bechtel, "Multi-Mission Radioisotope Thermoelectric Generator (MMRTG) Space and Defense Power Systems Radioisotope Missions- Collectively 200+ Years\* of Space Science." Available: [https://www.nasa.gov/wp-content/uploads/2015/08/4\\_mars\\_2020\\_mmrtg.pdf?emrc=35c41b](https://www.nasa.gov/wp-content/uploads/2015/08/4_mars_2020_mmrtg.pdf?emrc=35c41b)
- [38] T. Reyes, "Scientific instruments of Rosetta's Philae lander," Phys.org, Sep. 23, 2014.  
<https://phys.org/news/2014-09-scientific-instruments-rosetta-philae-lander.html> (accessed Oct. 17, 2024).
- [39] "Lithium vs NiMH Battery Packs - Cost Effective Battery Pack Designs,"  
[www.epectec.com](http://www.epectec.com). <https://www.epectec.com/batteries/lithium-vs-nimh-battery-packs.html>
- [40] "Comparison - Centralized, Decentralized and Distributed Systems," *GeeksforGeeks*, Dec. 24, 2018. <https://www.geeksforgeeks.org/comparison-centralized-decentralized-and-distributed-systems/>
- [41] "Architectures of Onboard Data Systems," [www.esa.int](http://www.esa.int).  
[https://www.esa.int/Enabling\\_Support/Space\\_Engineering\\_Technology/Onboard\\_Computers\\_and\\_Data\\_Handling/Architectures\\_of\\_Onboard\\_Data\\_Systems](https://www.esa.int/Enabling_Support/Space_Engineering_Technology/Onboard_Computers_and_Data_Handling/Architectures_of_Onboard_Data_Systems)
- [42] "Spotlight: a guide to Command and Data Handling (CDH) systems for space missions - with Alén Space," *satsearch blog*, Aug. 31, 2022. <https://blog.satsearch.co/2022-08-31-spotlight-a-guide-to-command-and-data-handling-cdh-systems-for-space-missions-with-alen-space>

- [43] “9.0 Communications - NASA,” *NASA*, Feb. 12, 2024. <https://www.nasa.gov/smallsat-institute/sst-soa/soa-communications/>
- [44] “Telecom - NASA Science,” *science.nasa.gov*. <https://science.nasa.gov/learn/basics-of-space-flight/chapter10-1/>
- [45] “Deep Space Network 201 Frequency and Channel Assignments,” 2014. Available: <https://deepspace.jpl.nasa.gov/dsndocs/810-005/201/201C.pdf>
- [46] “Chapter 6: Electromagnetics - NASA Science,” *science.nasa.gov*. <https://science.nasa.gov/learn/basics-of-space-flight/chapter6-5/>
- [47] N. Bobrinsky, P. Maldari, K.-J. Schulz, G. Sessler, and Íñigo Mascaraque, “ESA’s Space Communication Architecture and Ground Station Evolution,” *SpaceOps 2008 Conference*, May 2008, doi: <https://doi.org/10.2514/6.2008-3237>.
- [48] “Identifying Key Characteristics of Bands for Commercial Deployments and Applications Subcommittee Final Report and Recommendations,” Nov. 17, 2017. [https://www.ntia.doc.gov/files/ntia/publications/key\\_characteristics\\_subcommittee\\_final\\_report\\_nov\\_17\\_2017.pdf](https://www.ntia.doc.gov/files/ntia/publications/key_characteristics_subcommittee_final_report_nov_17_2017.pdf)
- [49] H. Hemmati *et al.*, “Comparative Study of Optical and Radio-Frequency Communication Systems for a Deep-Space Mission,” Feb. 15, 1997. <https://ntrs.nasa.gov/api/citations/20040191349/downloads/20040191349.pdf>
- [50] “S-band Communication Subsystem,” [www.esa.int](https://www.esa.int/Education/ESEO/S-band_Communication_Subsystem). [https://www.esa.int/Education/ESEO/S-band\\_Communication\\_Subsystem](https://www.esa.int/Education/ESEO/S-band_Communication_Subsystem)
- [51] “Directional Antennas: Longer Range / High Gain by narrowing the beam,” *Data-alliance.net*. <https://www.data-alliance.net/blog/directional-antennas-longer-range-high-gain-by-narrowing-the-beam/>
- [52] “What is a Sector Antenna?,” *Sanny Telecom*, Mar. 10, 2024. <https://www.sannytelecom.com/what-is-a-sector-antenna/>
- [53] “What is a Yagi Antenna?,” *Sanny Telecom*, Mar. 14, 2024. <https://www.sannytelecom.com/what-is-a-yagi-antenna/>
- [54] “Parabolic Grid Antenna vs Parabolic Dish Antenna: How to Choose?,” *Sanny Telecom*, Apr. 20, 2024. <https://www.sannytelecom.com/parabolic-grid-antenna-vs-parabolic-dish-antenna-how-to-choose/>
- [55] “Advantages and Disadvantages of Yagi Antenna,” [www.facebook.com/Theantennaexperts](https://www.facebook.com/Theantennaexperts). <https://www.antennaexperts.co/blog/advantages-and-disadvantages-of-yagi-antenna>

[56] GeeksforGeeks, “Microstrip Patch Antenna,” *GeeksforGeeks*, Nov. 29, 2023.  
<https://www.geeksforgeeks.org/microstrip-patch-antenna/#advantages-and-disadvantages-of-microstrip-patch-antenna>

## 13 Appendix

### 13.1: Definition and Assessment of Risk

#### Prepared by: All

Risk is the evaluation of the unfavorable events that could occur and threaten mission success. These events can occur at any point during the mission on varying scales. Project ECHO is taking necessary design calculations and evaluations to mitigate risk at any point during the mission. Each subsystem has varying levels of risk to overall mission success. Failures in propulsion, orbital mechanics, structures, thermal management, and power risk entire mission collapse. Failures in ADCS, Command and Data, and Telecommunications risk severe mission progress and potential to lead to entire mission collapse.

A propulsion failure risks hard landing on Europa where the probe becomes severely damaged or destroyed. Propulsion leaks or valve errors can also cause a complete mission loss. To mitigate this, additional hardware, such as multiple thrusters, are implemented so a failure of one thruster does not result in a loss of propulsion. An orbital mechanics failure risks a crash landing from insufficient reduction of velocity or poor landing. To mitigate this, a decision matrix is utilized to select the best descent method backed by historically successful missions. A failure in structures risks a cascading breakdown of other subsystems. To mitigate this, decision matrices are utilized to select the safest arrangement of systems and materials backed by finite element analysis. Thermal management risks include a component failure that results in the loss of thermal control over the probe. Without thermal control, the probe is unable to function to complete the mission. Table 8.6.5 highlights components that mitigate the risks of thermal management. The primary risk for power is an RTG power failure with radiological contamination. Keeping the RTG housing safe and strong will mitigate this.

An ADCS risk is failure of certain components. For example, losing reactor wheels inhibits movement of the probe in one of the three axes, which results in loss of data. To mitigate this, component backups will be installed. The primary risk of command and data is hardware or software failure of the computer, resulting in loss of data. Testing of the computer will take place as well as a protective structure surrounding the computer architecture will mitigate this risk. Similarly, telecommunications risk is a failure in hardware or software. Confirming the integrity of the technology used, encrypting data, and enabling user authentication will mitigate this risk. The main risk to mechanisms and deployables is inability to complete mission objectives. The main objective of ECHO is to drill into the ice, and a failure to deploy the drill makes this objective unfeasible. Extensive testing on the models will mitigate this risk.

Project ECHO recognizes the risks that each subsystem holds. Addressing potential failures significantly reduces loss of system or data. The various mitigation solutions maximize mission success and breakthrough discoveries.

## 13.2: Summary of Non-Technical Considerations

**Prepared by:** Andrew Olson

A summary of non-technical considerations and their relevance to each subsystem for consideration during analysis is presented in Table 13.1. The subsystems are labeled corresponding to the section number assigned to them in section 8 of the report as listed below. A “+” indicates that the non – technical factor is considered relevant to the subsystem, and a “-” indicates that it is considered irrelevant.

- 8.1 - Structures
- 8.2 - Mechanisms and Deployables
- 8.3 - Propulsion
- 8.4 - Orbital Mechanics
- 8.5 - ADCS
- 8.6 - Thermal Management
- 8.7 - Power
- 8.8 - Command & Data
- 8.9 - Telecommunication

**Table 13.1 Relevance of Non-Technical Factors**

Relevance of Non-Technical Factor to Subsystem										
Applies to Subsystem +										
Does Not Apply to subsystem -										
Non-Technical Factor	Subsystem	8.1	8.2	8.3	8.4	8.5	8.6	8.7	8.8	8.9
<b>Public Health &amp; Safety</b>		+	-	+	-	+	+	+	-	-
<b>Political</b>		-	-	+	-	-	-	+	+	+
<b>Cultural</b>		-	-	+	-	-	-	+	-	-
<b>Environmental</b>		+	-	+	-	-	+	+	-	-
<b>Economic</b>		+	+	+	+	+	+	+	+	+

## 13.3: Orbital Mechanics Calculations

### Contents

- Problem Parameters
- Calculate orbital angular momentums and velocities

```
%This script employs a Hohman transfer calculation to calculate the
%required delta V to bring a lander from an orbiter to the surface of
%Europa. It makes the following assumptions:
% - The orbiter is on Europa Clippers Ganymede 3G3 orbit, with parameters of Ra =
%   18.2*Rj km, and Rp = 45.9*Rj km wrt to Jupiter
% - Europa and the ECHO probe align at perigee within Europas sphere of
% influence, delta V before this point will be approximated as zero and
% analysis will begin here

clear all
close all
clc
```

### Problem Parameters

```
M_e = 4.79984 * 10^22; % mass of europa in kg
M_j = 1.898 * 10^27 ; % mass of jupiter in kg
R = 671000; %radius between Jupiter and Europa in KM
SOI = R*((Me/Mj)^.4); %sphere of influence of europa
Rj = 69911; %radius of jupiter
G = 6.6743*10^-20 ; %gravitational constant parameter, km^3/kgs^2
Re = 1560; %europa radius in km
RPer_Jup = 670000; %orbiter perigee radius km
RAp_Jup = 19000000; %orbiter apogee radius in km
new_eur = Me*G; %calculate new for europa
new_jup = Mj*G; %calculate new for jupiter

E_Europa = .089;
EuropaPerigee = 664862; %perigee of europa around jupiter in km
EuropaApogee = 676938; %apogee of europa
EuropaAverageRadius = 670900; % average orbital radius of europa

%Define circular parking orbit parameter, arbitrary 500000 km altitude for now
RCirc = Re+10000;
```

### Calculate orbital angular momentums and velocities

```
%Europa
hEuropa = sqrt(2*new_jup)*sqrt((EuropaPerigee*EuropaApogee)/(EuropaPerigee+EuropaApogee)); %angular momentum of europa orbit
VEuropaPerigee = hEuropa/EuropaPerigee;

%Probe
hProbe = sqrt(2*new_jup)*sqrt((RPer_Jup*RAp_Jup)/(RPer_Jup+RAp_Jup)); %orbital energy of the probe
VPprobePerigee = hProbe/RPer_Jup; %velocity of the probe at perigee

%Calculate relative velocity when probe and europa are at perigee
V1 = abs(VProbePerigee-VEuropaPerigee);

%Now calculate elliptical parking orbit parameters
%set apogee of parking orbit to radius of SOI of europa for optimization
ParkingOrbitPerigee = RPer_Jup-EuropaPerigee;
hParkingOrbit = sqrt(2*new_eur)*sqrt((SOI*ParkingOrbitPerigee)/(SOI+ParkingOrbitPerigee));
%calculate velocity at perigee of parking orbit
VParkingPerigee = hParkingOrbit/ParkingOrbitPerigee;

%calculate first delta V as difference between velocity at perigee of
%hyperbolic orbit (V1) and velocity at perigee of parking orbit
%(VParkingPerigee)

DV1 = abs(V1-VParkingPerigee);

%Now I should investigate transferring to a zero altitude europa orbit from
%both apogee and perigee
%find velocity of elliptical parking orbit at apogee
VParkingApogee = hParkingOrbit/SOI; %setting apogee to edge of SOI for most efficient
```

```

%Now calculate the angular momenutm of the transfer ellipse from parking to
%zero altitude
hTransfer2 = sqrt(2*mew_eur)*sqrt((SOI*Re)/(SOI+Re)); %this is transfer from apogee of parking orbit
hTransfer2Prime = sqrt(2*mew_eur)*sqrt((ParkingOrbitPerigee*Re)/(ParkingOrbitPerigee+Re)); %this is transfer from apogee of parking orbit

%Now calculate velocites of second transfer ellipse
VTransfer2 = hTransfer2/SOI; %velocity of transfer 2 at apogee
VTransfer2Prime = hTransfer2Prime/ParkingOrbitPerigee; %velocity of transfer 2' ellipse at perigee

%Now calculate potential delta Vs for transfer 2 and transfer 2 prime
DV2 = abs(VTransfer2-VParkingApogee);
DV2Prime = abs(VTransfer2Prime-VParkingPerigee);

%Now calculate delta Vs for insertion in to circular zero altitude orbit
VTransfer2Arrival = hTransfer2/Re; %velocity of transfer orbit 2 once it arrives at zero altitude orbit
VTransfer2PrimeArrival = hTransfer2Prime/Re; %velocity of transfer orbit 2 prime once it arrives at zero altitude orbit

%Now calculate velocity of zero altitude orbit
Vzeroalt = sqrt(mew_eur/Re); %velocity of zero altitude circular orbit
DVTransfer2Arrival = abs(VTransfer2Arrival-Vzeroalt); %DV for insertion in to zero altitude orbit for transfer 2
DVTransfer2PrimeArrival = abs(VTransfer2PrimeArrival-Vzeroalt); %DV for insertion in to zero altitude orbit for transafer 2 prime

%Now add on final DV to go from zero altitude circular orbit to stationary.
%this is just equal to DV = Vcirc - 0 = Vcirc. or in our case the variable
%is called Vzeroalt. we will just add this to the end

%Calculate overall Delta Vs
DVT2overall = DV1 + DV2 + DVTransfer2Arrival + Vzeroalt;
DVT2PrimeOverall = DV1 + DV2Prime + DVTransfer2PrimeArrival + Vzeroalt;

% Print the total delta V for each transfer orbit
fprintf('The total delta V for transfer orbit from apogee of parking orbit is: %.4f km/s\n', DVT2overall - Vzeroalt);
fprintf('The total delta V for transfer orbit from perigee of parking orbit is is: %.4f km/s\n', DVT2PrimeOverall - Vzeroalt);

% Print the overall delta V for each transfer orbit
fprintf('The overall delta V for transfer orbit from apogee of parking orbit (including surface to orbit) is: %.4f km/s\n', DVT2overall);
fprintf('The overall delta V for transfer orbit from perigee of parking orbit (including surface to orbit) is: %.4f km/s\n', DVT2PrimeOverall);

```

## 13.4: Project Timeline

